

**COMMUNITY ASSEMBLY IN HOST-ASSOCIATED AND  
ENVIRONMENTAL MICROBIOMES**

A Dissertation  
Presented to  
The Academic Faculty

by

Ana Gabriel Clavere-Graciette

In Partial Fulfillment  
of the Requirements for the Degree  
Doctor of Philosophy in Biology in the  
School of Biological Sciences

Georgia Institute of Technology  
May 2021

**COPYRIGHT © 2021 BY ANA GABRIEL CLAVERE-GRACIETTE,  
2021**

# COMMUNITY ASSEMBLY IN HOST-ASSOCIATED AND ENVIRONMENTAL MICROBIOMES

Approved by:

Dr. Stewart, Advisor  
School of Biological Sciences  
*Georgia Institute of Technology*

Dr. Taillefert  
School of Earth and Atmospheric  
Sciences  
*Georgia Institute of Technology*

Dr. Hammer  
School of Biological Sciences  
*Georgia Institute of Technology*

Dr. Hoopes  
Director of Research, Conservation and  
Nutrition  
*Georgia Aquarium*

Dr. Kostka  
School of Biological Sciences  
*Georgia Institute of Technology*

Date Approved: April 22, 2021



## **ACKNOWLEDGEMENTS**

I would like to thank my mother, Cecilia Jaimes, and my grandmother, Agripina Amado for their unconditional love and support. I would like to thank my boyfriend, Carlos Ruiz for loving me, encouraging me, and keeping me sane throughout this journey. I would also like to thank my extended family and friends who have supported me, and always being there during difficult times.

I will forever be grateful to my PhD advisor, Dr. Frank Stewart, for his constant support, guidance, and mentorship throughout this experience. I would also like to thank all the members of the Stewart lab for the advice, feedback, and support they have given me towards the completion of my PhD.

Finally, I would like to thank my PhD committee members, Dr. Brian Hammer, Dr. Martial Tallefert, Dr. Joel Kostka, and Dr. Lisa Hoopes for contributing to the completion of this dissertation and for their guidance during this journey as a scientist.

## TABLE OF CONTENTS

<b>ACKNOWLEDGEMENTS</b>	<b>iii</b>
<b>LIST OF TABLES</b>	<b>vii</b>
<b>LIST OF FIGURES</b>	<b>xi</b>
<b>LIST OF SYMBOLS AND ABBREVIATIONS</b>	<b>xvii</b>
<b>SUMMARY</b>	<b>xxi</b>
<b>CHAPTER 1. Drivers of microbial community assembly, and how environmental change and captivity affect host-associated microbiomes</b>	<b>1</b>
1.1 Drivers of microbial community assembly	1
1.2 Differences between free living and host associated microbial community assembly	6
1.3 Effects of environmental change on host-associated microbiomes	13
1.4 Effect of captivity on microbiomes	22
1.5 Current tools for studying microbial community assembly	31
1.6 Conclusion	37
<b>CHAPTER 2. Microbiome differences between wild and captive spotted eagle rays (<i>Aetobatus narinari</i>)</b>	<b>39</b>
2.1 Abstract	40
2.2 Background	41
2.3 Materials and methods	43
2.3.1 Sample collection	43
2.3.2 Illumina data processing	48
2.3.3 Statistical analysis	48
2.4 Results	50
2.4.1 Differences in microbial composition according to captivity status	50
2.4.2 Differences in microbial composition according to body site niche	53
2.4.3 Taxonomic composition of the microbiome of spotted eagle rays and cownose rays	54
2.4.4 Potential spotted eagle rays' core microbiome	55
2.5 Discussion	57
2.5.1 Environmental influence (Captive vs. Wild)	57
2.5.2 Species influence (Eagle ray vs. cownose ray)	60
2.5.3 Physiology influence (skin vs. gills vs. cloaca)	61
2.5.4 Potential pathogens	63
2.6 Conclusion	64

<b>CHAPTER 3. The microbiome of the African penguin (<i>Spheniscus demersus</i>) reflects their lifestyle between land and sea</b>	<b>66</b>
<b>3.1 Abstract</b>	<b>67</b>
<b>3.2 Background</b>	<b>68</b>
<b>3.3 Materials and methods</b>	<b>71</b>
3.3.1 Sample collection	71
3.3.2 DNA extraction and sequencing	74
3.3.3 Illumina data processing	75
3.3.4 Statistical analysis	76
<b>3.4 Results</b>	<b>78</b>
3.4.1 Microbiome samples	78
3.4.2 The penguin oral microbiome is similar to those of marine mammals	78
3.4.3 The penguin fecal microbiome is most similar to those of other kids	83
3.4.4 Penguin microbiomes from external body sites are similar to those of the environment	86
<b>3.5 Discussion</b>	<b>89</b>
3.5.1 Influence of phylogeny (cloaca vs. oral cavity)	89
3.5.2 Differences in microbial composition according to body site niche	91
3.5.3 Uniqueness of the African penguin microbiome	92
<b>3.6 Conclusion</b>	<b>93</b>
 <b>CHAPTER 4. Water column and sediment core depth drive spatial decoupling of sediment microbial communities in the Northern Gulf of Mexico</b>	 <b>95</b>
<b>4.1 Abstract</b>	<b>96</b>
<b>4.2 Introduction</b>	<b>97</b>
<b>4.3 Materials and methods</b>	<b>101</b>
4.3.1 Station locations and core descriptions	101
4.3.2 Sediment collection, voltammetric profiling, and pore water analyses	103
4.3.3 Nucleic acids extraction and Illumina sequencing	106
4.3.4 Quality sequence processing analyses	107
4.3.5 Phylogenetic inference	108
4.3.6 Multivariate analyses	108
<b>4.4 Results</b>	<b>109</b>
4.4.1 Mississippi river discharge and visual sediment characteristics	109
4.4.2 Bottom water oxygen concentrations and oxygen penetration depths in the sediment	111
4.4.3 DIC, $\text{NH}_4^+$ , $\Sigma\text{PO}_4^{3-}$ and pH profiles	111
4.4.4 Main sedimentary redox processes in the LCS	114
4.4.5 Abiotic factors influencing microbial community structure in the Northern GoM	118
4.4.6 Universal prokaryotic primers vs. Archaea specific primers	120
4.4.7 Microbial community composition along the Northern GoM shelf and slope	121
<b>4.5 Discussion</b>	<b>125</b>
4.5.1 Water column depth and sediment core depth represent major drivers of microbial community composition	125

4.5.2	Shelf sediments are characterized by intense carbon remineralization and sulfur cycling	127
4.5.3	Slope sediments are characterized by metal reduction and nitrogen-related microbial processes	131
4.5.4	Possible cryptic sulfur cycling in shelf and slope sediments	133
<b>4.6</b>	<b>Conclusions</b>	<b>135</b>
<b>CHAPTER 5.</b>	<b>Conclusions and suggestions</b>	<b>137</b>
<b>5.1</b>	<b>Effect of body site niche</b>	<b>137</b>
<b>5.2</b>	<b>Relative effect of phylogeny and uniqueness of the microbiome</b>	<b>139</b>
<b>5.3</b>	<b>Sediment biogeography</b>	<b>140</b>
<b>5.4</b>	<b>Final remarks</b>	<b>140</b>
<b>APPENDIX A.</b>	<b>Supplementary information for chapter 2: Microbiome differences between wild and captive spotted eagle rays (<i>Aetobatus narinari</i>)</b>	<b>142</b>
<b>APPENDIX B.</b>	<b>Supplementary information for chapter 3: The microbiome of the African penguin (<i>Spheniscus demersus</i>) reflects its lifestyle between land and sea</b>	<b>165</b>
<b>APPENDIX C.</b>	<b>Supplementary information for chapter 4: Water column and sediment core depth drive spatial decoupling of sediment microbial communities in the Northern Gulf of Mexico</b>	<b>184</b>
<b>REFERENCES</b>		<b>198</b>

## LIST OF TABLES

Table 2.1	Summary of the number of samples collected and the number of individuals sampled according to body site, ray species, and captivity status	44
Table 3.1	Table 3.1. Summary of the number of samples and ASVs associated with each sample type from the African <i>penguin</i> ( <i>Spheniscus demersus</i> ) and from the Georgia Aquarium penguin exhibit. These ASV numbers include ASVs shared between body sites, and <b>environmental samples</b> .	74
Table 3.2	Summary of the proportion of each host species oral microbiome represented by unique or unassigned ASVs. Unique ASVs corresponded to ASVs not shared with any other host species, and unassigned ASVs corresponded to ASVs that could not be classified beyond the kingdom level	83
Table 3.3	Summary of the proportion of each host species fecal microbiome represented by unique or unassigned ASVs. Unique ASVs corresponded to ASVs not shared with any other host species, and unassigned ASVs corresponded to ASVs that could not be classified beyond the kingdom level	86
Table 4.1	Station location, depth and corresponding bottom water oxygen concentrations, salinities and temperatures	103
Table A.1	Metadata for all samples, including captive and wild spotted eagle rays, and cownose rays	143
Table A.2	Pairwise results for a one way analysis of variance (Kruskal-Wallis) for all $\alpha$ -diversity metrics between captive cownose ( <i>Rhinoptera bonasus</i> ) and spotted eagle ( <i>Aetobatus narinari</i> ) rays, and wild spotted eagle rays ( <i>Aetobatus narinari</i> ) for different body sites.* indicates a significant difference $p \leq 0.05$ , ** indicates $p \leq 0.01$ , *** indicates $p \leq 0.001$ , **** indicates $p \leq 0.0001$ , and NS indicates not significant ( $p > 0.05$ ). NA indicates no possible comparison. $\alpha$ -diversity metrics include Observed ASVs, Shannon diversity index, Pielou's evenness, and Faith's Phylogenetic Diversity	153
Table A.3	Pairwise results for all permutational multivariate analysis of variance (PERMANOVA) for all $\beta$ -diversity <i>metrics between</i> captive cownose ( <i>Rhinoptera bonasus</i> ) <i>and</i> spotted eagle ( <i>Aetobatus narinari</i> ) rays, and <i>wild spotted</i> eagle rays ( <i>Aetobatus narinari</i> ) for different body sites. * indicates a significant difference $p \leq 0.05$ , **	153

indicates  $p \leq 0.01$ , \*\*\* indicates  $p \leq 0.001$ , \*\*\*\* indicates  $p \leq 0.0001$ , and NS indicates not significant ( $p > 0.05$ ). NA indicates no possible.  $\beta$ -diversity metrics include Bray-Curtis, Weighted UniFrac, and Unweighted UniFrac

Table A.4	Pairwise results for all permutational multivariate analysis of dispersion (PERMDISP) for all $\beta$ -diversity metrics and body sites for spotted eagle rays ( <i>Aetobatus narinari</i> ) and cownose rays ( <i>Rhinoptera bonasus</i> ). * indicates a significant difference $p \leq 0.05$ , ** indicates $p \leq 0.01$ , *** indicates $p \leq 0.001$ , **** indicates $p \leq 0.0001$ , and NS indicates not significant ( $p > 0.05$ ). NA indicates no possible comparison. $\beta$ -diversity metrics include Bray-Curtis, Weighted UniFrac, and Unweighted UniFrac	154
Table A.5	Pairwise results for a one way analysis of variance (Kruskal-Wallis) for all $\alpha$ -diversity metrics between different body sites for cownose ( <i>Rhinoptera bonasus</i> ), and captive and wild spotted eagle rays ( <i>Aetobatus narinari</i> ). * indicates a significant difference $p \leq 0.05$ , ** indicates $p \leq 0.01$ , *** indicates $p \leq 0.001$ , **** indicates $p \leq 0.0001$ , and NS indicates not significant ( $p > 0.05$ ). NA indicates no possible comparison. $\alpha$ -diversity metrics include Observed ASVs, Shannon diversity index, Pielou's evenness, and Faith's Phylogenetic Diversity	154
Table A.6	Pairwise results for all permutational multivariate analysis of variance (PERMANOVA) for all $\beta$ -diversity metrics between different body sites for cownose ( <i>Rhinoptera bonasus</i> ), and captive and wild spotted eagle rays ( <i>Aetobatus narinari</i> ). * indicates a significant difference $p \leq 0.05$ , ** indicates $p \leq 0.01$ , *** indicates $p \leq 0.001$ , **** indicates $p \leq 0.0001$ , and NS indicates not significant ( $p > 0.05$ ). NA indicates no possible. $\beta$ -diversity metrics include Bray-Curtis, Weighted UniFrac, and Unweighted UniFrac	155
Table A.7	Number of ASVs shared between captive and wild spotted eagle rays ( <i>Aetobatus narinari</i> ), and captive cownose rays ( <i>Rhinoptera bonasus</i> ) for each body site. Proportion refers to the percentage shared out of the total microbial community of each body site. Relative abundance refers to the average relative abundance represented by shared ASVs for each body site	156
Table A.8	Number of ASVs shared between different body sites for wild and captive spotted eagle rays ( <i>Aetobatus narinari</i> ), and captive cownose rays ( <i>Rhinoptera bonasus</i> ). Proportion refers to the percentage shared out of the total microbial community of each body site. Relative abundance refers to the average relative abundance represented by shared ASVs for each body site	157

Table A.9	List of common fish pathogens, and number of ASVs and average relative abundance of those found in wild and captive spotted eagle rays ( <i>Aetobatus narinari</i> ), and cownose rays ( <i>Rhinoptera bonasus</i> )	158
Table B.1	Metadata for all samples collected, including penguin ( <i>Spheniscus demersus</i> ) and environmental samples	166
Table B.2	Summary of the number of samples and ASVs associated with the oral microbiome for each host species. These ASV numbers include ASVs shared between body sites, and environmental samples	171
Table B.3	Summary of the number of samples and ASVs associated with the fecal microbiome for each host species. These ASV numbers include ASVs shared between body sites, and environmental samples	172
Table B.4	Summary of penguin's oral microbiome unique sequences (ASVs not shared with any other vertebrate host) with a relative abundance > 1 %	173
Table B.5	Summary of penguin's fecal microbiome unique sequences (ASVs not shared with any other vertebrate host) with a relative abundance > 1 %	174
Table B.6	Pairwise results for all permutational multivariate analysis of variance (PERMANOVA) for weighted UniFrac distances between penguin body sites and environmental samples. * indicates $p \leq 0.05$ , and NS indicates not significant	175
Table B.7	Summary of the number of ASVs shared between <i>each</i> penguin ( <i>Spheniscus demersus</i> ) body site and the environment, and of the number of unique ASVs (not shared with environmental samples) for each penguin body site, as well as their associated proportion	178
Table B.8	Summary of the number of ASVs unique to <i>each</i> penguin ( <i>Spheniscus demersus</i> ) body sites, including the taxonomic assignment. Unique ASVs correspond to ASVs only present in one body site and not shared with either other penguin body sites or environmental samples of the penguin exhibit	179
Table B.9	List of pathogens, number of ASVs, and relative abundance (%) present in penguin body sites	180
Table C.1	Results of test of significance of environmental variables for Canonical Correspondence Analysis on both the prokaryotic and Archaea specific datasets. * indicates a significant difference $p \leq 0.05$ , ** indicates $p \leq 0.01$ , *** indicates $p \leq 0.001$ , **** indicates $p \leq 0.0001$ , and NS indicates not significant ( $p > 0.05$ )	185

Table C.2	Phylogenetic approximation of Bathyarchaeal ASVs inferred by comparing those sequences to the Bathyarchaeota database from Zhou, Pan et al. (2018) using BLASTN (97 % similarity cutoff). ASVs included correspond to those presented in the heatmap (Figure C.10)	186
-----------	--	-----



## LIST OF FIGURES

Figure 2.1	Pictures demonstrating sample collection for wild spotted eagle rays ( <i>Aetobatus narinari</i> ): a) a spotted eagle ray in the water bath after being brought on board the ship, b) cloaca sampling, c) gill sampling, d) skin sampling. All samples were collected by gently rubbing sterile swabs along the target body site.	47
Figure 2.2	$\alpha$ -diversity metrics a) observed ASVs, and b) Shannon diversity index, for different body sites (cloaca, gill, and skin) of captive and wild spotted eagle rays ( <i>Aetobatus narinari</i> ), along with their respective water samples. Captive spotted eagle rays have lower diversity for all body sites compared to wild spotted eagle rays.	51
Figure 2.3	Principal coordinate analysis (PCoA) of $\beta$ -diversity comparison using Bray-Curtis distances between wild spotted eagle rays ( <i>Aetobatus narinari</i> ), and captive spotted eagle rays ( <i>Aetobatus narinari</i> ) for a) cloaca, b) gill, and c) skin samples. Note that wild spotted eagle rays harbor different microbial communities than captive spotted eagle rays, and both captive and wild spotted eagle rays harbor microbial communities that differ from the surrounding water for all body sites. Interestingly, cloaca samples show higher overlap, suggesting higher similarities compared to more external body sites (gill and skin)	52
Figure 2.4	Principal coordinate analysis (PCoA) based upon Bray-Curtis dissimilarity matrices between cloaca, gill, skin, and water for a) captive spotted eagle rays ( <i>Aetobatus narinari</i> ), and b) wild spotted eagle rays. Note that different body sites have different microbial community structures that differ from the surrounding water, as indicated by the separate clustering. In captive spotted eagle rays, the gills appear more similar to the surrounding water, while the skin is more similar to the surrounding water in wild spotted eagle rays	53
Figure 3.1	Principal coordinate analysis (PCoA) of $\beta$ -diversity comparisons using weighted Unifrac distances between the oral microbiome of various vertebrate hosts including birds, reptiles, and mammals	79
Figure 3.2	Bar plots indicating the average relative abundance of taxa composing the oral microbiome of various vertebrate hosts (birds, reptiles, and mammals). A) at the phyla level, B) at the genus level. Only the 4 most abundant genera for each host species are included	81

Figure 3.3	Principal coordinate analysis (PCoA) of $\beta$ -diversity comparisons using weighted Unifrac distances between the fecal microbiome of various vertebrate hosts including birds, reptiles, and mammals A) includes poultry samples, B) does not include poultry samples	84
Figure 3.4	Bar plots indicating the average relative abundance of taxa composing the fecal microbiome of various vertebrate hosts (birds, reptiles, and mammals). A) at the phyla level, B) at the genus level. Only the 4 most abundant genera for each host species are included	85
Figure 3.5	A) Schematic of the penguin ( <i>Spheniscus demersus</i> ) body sites sampling locations and B) Principal coordinate analysis (PCoA) of $\beta$ -diversity comparisons using weighted Unifrac distances between the microbiome of various penguin body sites and from environmental samples of the penguin exhibit	87
Figure 3.6	Bar plots indicating the average relative abundance of taxa composing the penguin ( <i>Spheniscus demersus</i> ) microbiome at different body sites and of environmental samples collected from the penguin exhibit . A) at the phyla level, B) at the genus level. Only the 4 most abundant genera for each host species are included	88
Figure 4.1	Map of the locations across the Louisiana shelf and slope in the northern Gulf of Mexico where sediment cores were collected during a research cruise in late July- early August of 2016. Water depths (D, m) and bottom water oxygen concentrations measured from CTD profiles ( $O_2$ , $\mu M$ kg <sup>-1</sup> ) are provided for reference. Depth contours (m) indicate ocean bathymetry. Mississippi and Atchafalaya Rivers are labeled.	102
Figure 4.2	Pore water geochemistry (a-c) and bacterial (d) and archaeal (e) populations at the family level ( including the 10 most abundant families of each sample) at: a) St. 6; b) St. 2; and c) St. 11. Sediment-water interface (SWI) indicated by the dashed line. The pH data was not available at St. 2. Mn and Fe signals overloaded between 40 and 80 mm at St. 2 and are not provided. Note the change in scale for voltammetric $Mn^{2+}$ , $Fe^{2+}$ and org- $Fe(III)$ measurements, as well as Mnd, $Fe^{2+}$ (St. 6), and $\Sigma PO_4^{3-}$ (St. 2) concentrations to better display trends at each station.	110
Figure 4.3	Dissolved inorganic carbon (DIC, mM), $NO_x = NO_2^- + NO_3^-$ ( $\mu M$ ), orthophosphate ( $PO_4^{3-}$ , $\mu M$ ), ammonium ( $NH_4^+$ , $\mu M$ ), total dissolved Mn (Mnd, $\mu M$ ), sulfate ( $SO_4^{2-}$ , mM), and total dissolved Fe (Fed, $\mu M$ ) measured in the pore waters along with dissolved sulfide ( $\Sigma H_2S$ , $\mu M$ ) and aqueous FeS (FeS, nA)	113

measured by voltammetric microelectrodes as a function of depth at each station using a heat map. The map of station locations is included for reference (bottom right). Black dots on each plot represent actual measurement locations. Color contours from red to purple represent high to low concentrations indicated by the scale to the right of each panel. Plots created in Ocean Data View (ODV) software.

Figure 4.4	Ordination plots of Canonical Correspondence Analysis (CCA) obtained with: a) universal primers; and b) archaeal specific primers to explore the relationship between prokaryotic communities at each station and significant environmental variables (p-value<0.01). Only samples with measurements of all geochemical parameters were included in analysis (i.e. NH <sub>4</sub> <sup>+</sup> data not available for C6C and ΣPO <sub>43</sub> - data not available for 5B)	119
Figure 4.5	Interaction networks of sediment microbial community members. ASVs are depicted as circles, and sized and colored based on betweenness centrality values (the larger this value, the larger the size of the circle, and the warmer the color). Cluster 1 is composed by ASVs with higher relative abundances on the slope, cluster 2 is composed by ASVs with higher relative abundances on the shelf, and clusters 3 and 4 are composed by ASVs particularly abundant in deeper layers of the sediment. For this analysis, only ASVs with a relative abundance ≥ 0.0002 %, and only interactions with a p-value ≤ 0.01 were included.	123
Figure A.1	Bar plots representing the relative abundance of microbes associated with a) the cloaca, b) the gills, and c) the skin of captive cownose rays ( <i>Rhinoptera bonasus</i> ), captive spotted eagle rays ( <i>Aetobatus narinari</i> ), and wild spotted eagle rays. Skin communities appear highly distinct between captive and wild spotted eagle rays, while cloaca samples are more similar. Taxa are classified to the species level where possible	161
Figure A.2	Principal coordinate analysis (PCoA) based upon a Bray-Curtis dissimilarity matrix between a) cloaca, b) gill, and c) skin samples for wild and captive spotted eagle rays ( <i>Aetobatus narinari</i> ) and captive cownose rays ( <i>Rhinoptera bonasus</i> ). Wild spotted eagle rays harbor different microbial communities than captive spotted eagle rays, as indicated by the separate clustering, and microbial communities from cow-nose rays appear more similar to captive spotted eagle rays (as opposed those from the wild)	162
Figure A.3	α-diversity metrics a) observed amplicon sequence variants (ASVs), and b) Shannon diversity index, for <i>all</i> body sites (cloaca, gill, and skin) of <i>captive</i> cownose rays ( <i>Rhinoptera bonasus</i> ),	163

captive and wild spotted eagle rays (*Aetobatus narinari*), as well as the surrounding water column. Cloaca microbiome had lower diversity compared to other body sites

Figure A.4	Principal coordinate analysis (PCoA) based upon a Bray-Curtis dissimilarity matrix between cloaca, gill, skin, and water samples for captive cownose rays ( <i>Rhinoptera bonasus</i> ). Microbial communities associated with all body sites cluster separately from the surrounding water, but do not differentiate according to body site	163
Figure A.5	Bar plots representing the relative abundance of microbes associated with a) the cloaca, b) the gills, and c) the skin of captive cownose rays ( <i>Rhinoptera bonasus</i> ), captive spotted eagle rays ( <i>Aetobatus narinari</i> ), and wild spotted eagle rays. Skin communities appear highly distinct between captive and wild spotted eagle rays, while cloaca samples are more similar. Taxa are classified to the species level where possible	164
Figure B.1	Box plots representing differences in $\alpha$ -diversity (Observed ASVs, and the Shannon index) between the oral microbiome of various vertebrate hosts including birds, reptiles, and mammals	181
Figure B.2	Box plots representing differences in $\alpha$ -diversity (Observed ASVs, and the Shannon index) between the fecal microbiome of various vertebrate hosts including birds, reptiles, and mammals	181
Figure B.3	Box plots representing differences in $\alpha$ -diversity (Observed ASVs, and the Shannon index) between different penguin ( <i>Spheniscus demersus</i> ) body sites and environmental samples from their exhibit	182
Figure B.4	Heat map showing the relative abundances of Tenericutes in penguins ( <i>Spheniscus demersus</i> )' food, oral and cloaca samples at the ASV level. Hierarchical clustering of the samples is represented by the dendrogram on the left, while ASVs are organized following Bray Curtis distances	183
Figure C.1	Mississippi River Discharge data (cm <sup>3</sup> s <sup>-1</sup> ) at the Belle Chasse, LA monitoring station (USGS Station #07374525). Date in Month: Year format (MM:YY)	188
Figure C.2	Pictures of the cores showing variations in sediment color and stratification at the different locations. Thin, medium, and thick white and black lines represent depth intervals of 1, 2, and 5 cm respectively. The inset picture of the St. MK sediment core	189

provides a better contrast of the top 14 cm. A picture of the sediment core from St. 13 was not available (NA)

Figure C.3	Depth microprofiles at St. C6C of O <sub>2</sub> , Mn <sup>2+</sup> , Fe <sup>2+</sup> , H <sub>2</sub> S, org-Fe(III) complexes and FeSaq (first and second panel) as well as pH (second panel) obtained with voltammetric and potentiometric microelectrodes. Depth profiles of pore water species DIC, NH <sub>4</sub> <sup>+</sup> (third panel), Fe <sup>2+</sup> , Fe(III) <sub>d</sub> , Mnd (fourth panel), NO <sub>3</sub> <sup>-</sup> , NO <sub>2</sub> <sup>-</sup> , and SO <sub>4</sub> <sup>2-</sup> (fifth panel). pH and NH <sub>4</sub> <sup>+</sup> data were not available (NA)	190
Figure C.4	Depth microprofiles at St. 5B of O <sub>2</sub> , Mn <sup>2+</sup> , Fe <sup>2+</sup> , H <sub>2</sub> S, org-Fe(III) complexes and FeSaq (first and second panel) as well as pH (second panel) obtained with voltammetric and potentiometric microelectrodes. Depth profiles of pore water species DIC, NH <sub>4</sub> <sup>+</sup> (third panel), Fe <sup>2+</sup> , Fe(III) <sub>d</sub> , Mnd (fourth panel), NO <sub>3</sub> <sup>-</sup> , NO <sub>2</sub> <sup>-</sup> , and SO <sub>4</sub> <sup>2-</sup> (fifth panel). ΣPO <sub>4</sub> <sup>3-</sup> data were not available (NA)	191
Figure C.5	Depth microprofiles at St. MK of O <sub>2</sub> , Mn <sup>2+</sup> , Fe <sup>2+</sup> , H <sub>2</sub> S, org-Fe(III) complexes and FeSaq (first and second panel) as well as pH (second panel) obtained with voltammetric and potentiometric microelectrodes. Depth profiles of pore water species DIC, NH <sub>4</sub> <sup>+</sup> (third panel), Fe <sup>2+</sup> , Fe(III) <sub>d</sub> , Mnd (fourth panel), NO <sub>3</sub> <sup>-</sup> , NO <sub>2</sub> <sup>-</sup> , and SO <sub>4</sub> <sup>2-</sup> (fifth panel)	192
Figure C.6	Depth microprofiles at St. 10 of Mn <sup>2+</sup> , Fe <sup>2+</sup> , H <sub>2</sub> S, S <sub>2</sub> O <sub>3</sub> <sup>-</sup> , org-Fe(III) complexes and FeSaq (first and second panel) as well as pH (second panel) obtained with voltammetric and potentiometric microelectrodes. Depth profiles of pore water species DIC, NH <sub>4</sub> <sup>+</sup> (third panel), Fe <sup>2+</sup> , Fe(III) <sub>d</sub> , Mnd (fourth panel), NO <sub>3</sub> <sup>-</sup> , NO <sub>2</sub> <sup>-</sup> , and SO <sub>4</sub> <sup>2-</sup> (fifth panel). Voltammetric O <sub>2</sub> profiles were not available (NA)Depth microprofiles at St. 10 of Mn <sup>2+</sup> , Fe <sup>2+</sup> , H <sub>2</sub> S, S <sub>2</sub> O <sub>3</sub> <sup>-</sup> , org-Fe(III) complexes and FeSaq (first and second panel) as well as pH (second panel) obtained with voltammetric and potentiometric microelectrodes. Depth profiles of pore water species DIC, NH <sub>4</sub> <sup>+</sup> (third panel), Fe <sup>2+</sup> , Fe(III) <sub>d</sub> , Mnd (fourth panel), NO <sub>3</sub> <sup>-</sup> , NO <sub>2</sub> <sup>-</sup> , and SO <sub>4</sub> <sup>2-</sup> (fifth panel). Voltammetric O <sub>2</sub> profiles were not available (NA)	193
Figure C.7	Depth microprofiles at St. 3 of O <sub>2</sub> , Mn <sup>2+</sup> , Fe <sup>2+</sup> , H <sub>2</sub> S, org-Fe(III) complexes and FeSaq (first and second panel) as well as pH (second panel) obtained with voltammetric and potentiometric microelectrodes. Depth profiles of pore water species DIC, NH <sub>4</sub> <sup>+</sup> (third panel), Fe <sup>2+</sup> , Fe(III) <sub>d</sub> , Mnd (fourth panel), NO <sub>3</sub> <sup>-</sup> , NO <sub>2</sub> <sup>-</sup> , and SO <sub>4</sub> <sup>2-</sup> (fifth panel)	194

Figure C.8	Depth microprofiles at St. 13 of O <sub>2</sub> , Mn <sup>2+</sup> , Fe <sup>2+</sup> , H <sub>2</sub> S, S <sub>2</sub> O <sub>3</sub> <sup>-</sup> , org-Fe(III) complexes and FeSaq (first and second panel) as well as pH (second panel) obtained with voltammetric and potentiometric microelectrodes. Depth profiles of pore water species DIC, NH <sub>4</sub> <sup>+</sup> (third panel), Fe <sup>2+</sup> , Fe(III) <sub>d</sub> , Mnd (fourth panel), NO <sub>3</sub> <sup>-</sup> , NO <sub>2</sub> <sup>-</sup> , and SO <sub>4</sub> <sup>2-</sup> (fifth panel). ΣPO <sub>4</sub> <sup>3-</sup> data were not available (NA)	195
Figure C.9	α-diversity metrics A) and B) Faith phylogenetic index (Faith-pd), and C) and D) Shannon diversity index, of shelf and slope sediments according to sediment core depth.	196
Figure C.10	Heat map showing the relative abundances of Bathyarchaeota in shelf and slope sediments. Hierarchical clustering of the samples is represented by the dendrogram on the left, while ASVs are organized following Bray Curtis distances	197

## LIST OF SYMBOLS AND ABBREVIATIONS

DNA	Deoxyribonucleic acid
GIT	Gastrointestinal tract
16S rRNA	Small subunit ribosomal RNA
GoM	Gulf of Mexico
MARS	Mississippi and Atchafalaya River
HGT	Horizontal gene transfer
OMZ	Oxygen minimum zone
<i>Bd</i>	Batrachochytrium dendrobatidis
PCR	Polymerase chain reaction
RNA	Ribonucleic acid
FISH	Fluorescent in situ hybridization
Nano-SIMS	Nanoscale secondary ion mass spectrometry
ichip	Isolation chip
IUCN	International union for conservation of nature
OV	Ocean voyager exhibit at Georgia Aquarium
BSA	Bovine serum albumin
ASV	Amplicon sequence variant
PCoA	Principal coordinates analysis
QIIME	Quantitative insights into microbial ecology
PERMANOVA	Permutational multivariate analysis of variance
PERMDISP	Permutational analyses of multivariate dispersions
PRIMER	Plymouth routines in multivariate ecological research

DESEQ	Differential expression analysis for sequence count data
GA	Georgia
U.S.A	United States of America
LSS	Life support system
PSK	Protein skimmer
OZC	Ozone contactor
IACUC	Institutional animal care and use committee
EDTA	Ethylenediamine tetraacetic acid
N.Y	New York
MAFFT	Multiple alignment using fast Fourier transform
O <sub>2</sub>	Oxygen
Mn <sup>2+</sup>	Manganese (II)
Fe <sup>2+</sup>	Iron (II)
org-Fe(III)	Organic-Fe(III) complexes
FeS <sub>aq</sub>	Iron sulfide
ΣH <sub>2</sub> S	Hydrogen sulfide
Ag	silver
AgCl	Silver chloride
Pt	platinum
Au	Gold
Hg	Mercury
AIS	Analytical Instrument Systems
CCA	Canonical correspondence analysis
nGoM	Northern Gulf of mexico
LCS	Louisiana continental shelf



R/V	Research vessel
St	Station
CTD	Conductivity, temperature, depth probe
LSV	Linear sweep voltammetry
pH	Potential of hydrogen
TRIS	Tris(Hydroxymethyl)aminomethane
MnCl <sub>2</sub>	Manganse (II) chloride
CSW	Cathodic square wave voltammetry
NaCl	Sodium chloride
N <sub>2</sub>	Nitrogen
Fe <sup>2+</sup> <sub>d</sub>	Dissolved Fe(II)
ΣPO <sub>4</sub> <sup>3-</sup>	Orthophosphates
DIC	Dissolved inorganic carbon
Fe <sub>tot</sub>	Total dissolved iron
Fe(III) <sub>d</sub>	Dissolved Fe(III)
Mn <sub>d</sub>	Dissolved manganese
NH <sub>4</sub> <sup>+</sup>	Ammonium
HPLC	High performance liquid chromatography
NaCO <sub>3</sub>	Sodium carbonate
NaHCO <sub>3</sub>	Sodium bicarbonate
Cl <sup>-</sup>	Chlorine
Br <sup>-</sup>	Bromine
SO <sub>4</sub> <sup>2-</sup>	Sulfate
NO <sub>2</sub> <sup>-</sup>	Nitrite
NO <sub>3</sub> <sup>-</sup>	Nitrate

BLASTN	Basic nucleotide local alignment search tool
ANOVA	Analysis of variance
MCL	Markov clustering method
SparCC	Sparse correlations for compositional data
NO <sub>x</sub>	Nitrate plus Nitrite
$\alpha$	Alpha
$\beta$	Beta

## SUMMARY

Microbes play ecological and biogeochemical roles in all environments, including in host-associated systems. They are central providers of ecosystem services, notably by transforming matter and energy (Kowalchuk, Jones et al. 2008). They also engage in social interactions that directly affect the health, development, and behavior of animals and plants (Das, Lyla et al. 2006, Van Der Heijden, Bardgett et al. 2008, Steffan, Chikaraishi et al. 2015). Identifying the factors that influence community taxonomic assembly in microbiomes - i.e., which microbes are present and in what abundance - is necessary to predict how microbiomes might influence an ecosystem's diversity, functional services, and overall health.

Many studies have investigated the factors shaping microbial distributions and community diversity. Despite a wealth of data on the topic, it has been challenging to identify universal principles of microbiome assembly across diverse systems. For host-associated microbiomes, for instance, it is often hard to quantify the relative contributions of host physiology versus environmental conditions in shaping microbiomes. This dissertation explores these challenges in both host-associated and free-living microbiomes that are subjected to distinct organizing factors. In Chapter 2, I sample across a diverse set of host-associated niches to understand how the microbiome of wild spotted eagle rays (*Aetobatus narinari*) differs from that of individuals housed at Georgia Aquarium. In Chapter 3, I provide the first assessment of the microbiomes of African penguins (*Spheniscus demersus*), focusing the analysis on the variation among body site niches and one of the first characterizations of the oral microbiome of birds. Finally, in a collaborative

study that couples electrochemical measurements of redox substrates with analysis of both bacterial and archaeal microbiomes, I explore the role of environmental substrate availability in shaping community assembly.

In Chapter 1 of this dissertation, I review the drivers of community taxonomic assembly in host-associated microbiomes. My review explores how processes such as dispersal, drift, diversification, and selection (Vellend 2010) shape the interplay between an animal and its microbiome and how these might differ under environmental change, including the transition from wild to captive environments for animals. I argue that characterizing the host microbiome's "biogeography" among various body site niches, particularly over gradients of environmental change or host health, is essential for establishing baseline knowledge of what constitutes a stable or 'core' microbiome and identifying microbial taxa most likely to influence host health, negatively or positively. However, most host-associated microbiome studies have focused on humans, terrestrial mammals, model organisms, and commercially relevant species, leaving many microbiome-host relationships unexplored. These include diverse animals and plants in marine systems, which can be difficult to access and often require specific equipment and resources to sample. As an alternative, captive animals in zoos and aquariums can be accessed relatively easily and are typically maintained under controlled environmental conditions with low variability. While captivity has been shown to modify microbiome composition and richness, changes are often host species-specific and difficult to link to host health. I argue that studying captive animal microbiomes compared to those of wild populations is essential for distinguishing a natural versus unbalanced (or 'dysbiotic')

microbiome and can potentially help identify disease progression and enhance conservation strategies.

In **Chapter 2**, I build on this theme by studying how the microbiome of a charismatic marine fish, the spotted eagle ray (*Aetobatus narinari*), differs between wild and captive individuals. This comparison, which was made possible by a collaboration with scientists at Mote Marine Laboratory and Georgia Aquarium, allowed me to explore the potential for environmental change to reshape animal microbiomes. This study also explored differences in taxonomic assembly among body niches, including the skin, gill, and cloaca. Microbiomes of captive eagle rays were also compared to those of cownose rays (*Rhinoptera bonasus*) in the same exhibit, allowing me to explore the effect of host identity on the ray microbiome. The results suggest that while captivity is associated with shifts in the spotted eagle ray microbiome, this restructuring is not absolutely determined by environmental conditions, as the microbiome remains distinct from that of other ray species and that of the surrounding water. Further, this restructuring does not appear associated with poor health, suggesting that the host can tolerate some amount of variability in community taxonomic assembly.

Following a similar approach, in **Chapter 3**, I characterize the microbiome of African penguins (*Spheniscus demersus*) in captivity at Georgia Aquarium, focusing on variation among body niches and relative to patterns in the surrounding environment and in other vertebrates. My results suggest that the penguin microbiome is unique and contains high proportions of potentially novel microbes. Comparisons with other vertebrate hosts indicated that the oral microbiome of *Spheniscus demersus* is more similar to that of marine mammals, suggesting a potential role for shared diet in shaping this microbiome niche. In

contrast, the cloaca microbiome is more similar to that of other birds, which indicates a differential effect of host identity on these two body sites. As for *Aetobatus narinari*, long term veterinary monitoring showed that the captive penguins were healthy, again suggesting that potential microbiome differences relative to wild populations are not associated with disease. These results highlight the need to continue monitoring these microbiomes to establish a baseline for a healthy microbiome and potentially identify biomarkers indicative of host health.

Finally, in **Chapter 4**, I characterized the 'free-living' microbiomes of marine sediments relative to surrounding geochemical conditions in the northern Gulf of Mexico. I compared sediment microbiomes - focusing independently on both the archaeal and bacterial communities - among sites that span a gradient of water depth (continental shelf versus slope) and influx of organic matter. In contrast to the host-associated studies, taxonomic assembly in sediment microbiomes could be strongly linked to environmental parameters. Shelf sediment microbiomes are characterized by taxa suggestive of sulfate reduction, organic matter degradation, and methane cycling, while slope sediment microbiomes are enriched in dissimilatory nitrogen cycling taxa, including those potentially linked to nitrate and metal reduction. This study provides insight into the strong role of environmental redox conditions in microbiome assembly. These conditions are undeniably shaped by regional patterns in biological activity and nutrient loading influenced by the Mississippi and Atchafalaya River systems. The region is influenced by both natural and anthropogenic disturbances, as well as by seasonal variation. Such variation highlights a need to understand the potential effects of environmental change on

microbial processes, while also suggesting the system as a model for teasing apart the drivers of microbiome assembly.

Together, these studies advance our knowledge of how and why microbiomes change. Exploring microbiomes across environmental and host-associated systems is necessary for understanding the full spectrum of nature's microbial diversity and its relationship to ecosystem health.

# **CHAPTER 1. DRIVERS OF MICROBIAL COMMUNITY ASSEMBLY, AND HOW ENVIRONMENTAL CHANGE AND CAPTIVITY AFFECT HOST-ASSOCIATED MICROBIOMES**

## **1.1 Drivers of microbial community assembly**

Microbes are both abundant and globally distributed, representing a large portion of the global genetic diversity. They are involved in all biogeochemical and elemental cycles on earth, are highly metabolically diverse, and appear to be capable of using almost every energy source presented to them (Kowalchuk, Jones et al. 2008). Moreover, microbes can serve as a food source or form symbiotic associations with other organisms, including plants and animals. These relationships directly affect these organisms' health, development, and behavior, therefore contributing to ecosystem productivity and diversity (Das, Lyla et al. 2006, Van Der Heijden, Bardgett et al. 2008, Steffan, Chikaraishi et al. 2015). Due to the central role of microorganisms as drivers of ecosystem function, understanding the factors that determine microbial community assembly is key to establishing general principles governing the structure, productivity, and diversity of these environments. In addition, establishing a conceptual framework of how microbes interact with each other, with other organisms, and their surroundings, can help predict how these communities change when confronted by external disturbances. Such knowledge is necessary to better preserve or engineer ecosystem services and resources in response to changes caused by increased anthropogenic pressure and climate change (Wallenstein and Hall 2012, De Vries and Shade 2013).



Most factors shaping microbial communities also structure macrobial communities. These factors include niche assembly and dispersal assembly rules, as well as ecological drift (Hubbell 2001, Nemergut, Schmidt et al. 2013, Stegen, Lin et al. 2013). However, microbes possess specific characteristics that differentiate them from their macrobial counterparts, and that may affect assembly processes. Compared to larger organisms, the small size of microbes allows them to be easily transported over greater distances through passive mechanisms such as air and water currents (Finlay and Clarke 1999, Finlay 2002, Wilkinson, Koumoutsaris et al. 2012). Moreover, they can also associate with macrobial hosts that can act as vectors (Troussellier, Escalas et al. 2017), and contribute to their dispersal potential, which is higher than for larger organisms. Besides their phylogenetically widespread capability to stay dormant or modulate their activity in response to stressful conditions (Lennon and Jones 2011), microorganisms have additional response mechanisms that allow them to adapt more efficiently to environmental disturbances. These include high genetic diversity within species (Achtman and Wagner 2008), the capacity to use a large variety of energy sources (Kowalchuk, Jones et al. 2008), the ability to horizontally exchange genetic material (Ochman, Lawrence et al. 2000), as well as short generation times. Such traits impact microbial ecology and evolution, ultimately influencing the relative effect of factors involved in community assembly.

To better characterize microbial biogeographic patterns, and the forces shaping their communities, several hypotheses on the nature and relative effect of variables involved in microbial community assembly have been proposed. These mainly diverge on the weight given to deterministic versus stochastic factors. The Baas-Becking hypothesis claims that “everything is everywhere – the environment selects” (Baas-Becking 1934), which

highlights the importance of deterministic factors such as selection. In contrast, another hypothesis considers that past events, including dispersal limitation and past environmental conditions, are the main drivers of microbial community assembly, underlining the importance of stochastic processes (Hao, Zhao et al. 2016). Finally, a third alternative contemplates that processes from both these hypotheses influence microbial distributions. Their relative importance may vary at different stages of community assembly and across different systems and different microbial groups, or depend on the scales and metrics considered (Martiny, Bohannan et al. 2006, Nemergut, Schmidt et al. 2013, Li and Ma 2016).

Vellend's microbial community assembly framework divides deterministic and stochastic processes into four categories: diversification, dispersal, selection, and drift (Vellend 2010). Diversification plays a central role in microbial community ecology (Rainey and Travisano 1998) and can be generated rapidly through mutation or horizontal gene transfer (HGT). While mechanisms leading to diversification can be difficult to measure, new genetic variations are subject to selection, which can profoundly affect community composition and function (Burke, Steinberg et al. 2011). Dispersal, on the other hand, is an essential process that governs the spatial movement of microorganisms and can affect microbial community assembly through migration and order of colonization, which can further affect microbial assembly (Nemergut, Schmidt et al. 2013). However, it is also difficult to quantify as current methods do not permit us to rule out that an organism that was not encountered, was not simply missed by the method used.

Some studies hypothesize that microbes do not experience “dispersal limitation,” an idea supported by the presence of “unlikely inhabitants,” identified as microorganisms

found in environments that are not favorable to their metabolism (Finlay 2002, Fenchel and Finlay 2004, Hubert, Loy et al. 2009). However, spatial and temporal heterogeneity in microbial diversity reflects differences in dispersal patterns (Lindström and Östman 2011). Selection in response to both abiotic and biotic factors, including interactions with a host, is an important force structuring microbial communities (Martiny, Bohannan et al. 2006). While there is no consensus as to how selection relates to phylogenetic structure (Horner-Devine and Bohannan 2006, Philippot, Andersson et al. 2010, Shapiro, Friedman et al. 2012), dormant microbes, which can represent over 90% of certain communities (Locey 2010), are capable of evading unfavorable external conditions, which can weaken the impact of selection on community composition. Finally, drift appears to be more critical when selection is weak, and both genetic diversity and the total number of community members are low; rare microbes being more strongly affected. Such conditions can be common for microbes in certain host-associated environments (Shafquat, Joice et al. 2014, Adair and Douglas 2017), while selection, diversification, and dispersal may play a larger role for “free-living” microbes. However, quantitative estimations of the simultaneous effect of these processes on community assembly remain elusive in many environments. Moreover, natural systems are subject to environmental fluctuations, adding another level of difficulty to tracking the relative influence of these factors over time (Nemergut, Schmidt et al. 2013, Stegen, Lin et al. 2013).

Vellend’s conceptual theory allows us to consider community assembly in a relevant ecological framework. While microbial communities generally follow global organizational patterns observed in macroorganismal communities (Martiny, Bohannan et al. 2006, Astorga, Oksanen et al. 2012), exceptions exist. For example, in line with

macroecological principles, microbial communities follow the species-area relationship, the species-time relationship, and the distance-decay relationship. The species-area relationship establishes that larger areas usually support higher richness due to the presence of more niches, larger targets for dispersal, and the possibility to accommodate larger populations (Green, Holmes et al. 2004, Horner-Devine, Lage et al. 2004). The species-time relationship and the distance-decay relationship state that richness increases over time (Adler and Lauenroth 2003), and that community dissimilarity increases as geographical distance increases (Bryant, Lamanna et al. 2008, King, Freeman et al. 2010), respectively. However, relationships established between macroorganismal diversity and longitude, latitude, and altitude do not apply to microbial communities (Green and Bohannan 2006, McGill, Etienne et al. 2007, Hubert, Loy et al. 2009, Wang, Meier et al. 2017). While still unresolved, these disparities may be related to differences in the spatial scale over which chemical and physical factors influence microbes versus larger organisms, or be the result of differences in assembly dynamics between macrobial and microbial communities (Nemergut, Schmidt et al. 2013). Moreover, similarly to macro-organismal assemblages, microbial communities are usually composed of a limited number of dominant species, often considered as “ecosystem engineers,” while most members are found in low proportions. Indeed, these dominant species often have stronger interactions with the surrounding environment, and may be more affected by deterministic factors resulting from environmental change (Griffin and Wells 2017). In contrast, low abundance microbes may be more sensitive to stochastic drivers, such as drift. However, these “rare” members may play a more significant role than in macroorganismal systems, as they may be initially dormant and become active under environmental stress, facilitating community adaptation

(Szabó, Itor et al. 2007). As differences in microbial community composition and diversity profoundly affect ecosystem functioning, better understanding the relative importance of deterministic versus stochastic factors on different members of the community, and how these factors affect microbial community assembly and function is key to preserve ecosystem services under ongoing environmental change.

## **1.2 Differences between free living and host associated microbial community assembly**

It is now widely recognized that the microbiome is essential for all living organisms and plays a critical role in host fitness. It can directly affect host health by inhibiting pathogen colonization or interacting with the digestive, immune and neurological systems affecting host metabolism, development, and behavior (Hooper, Littman et al. 2012, Brestoff and Artis 2013, Kamada, Chen et al. 2013, Archie and Tung 2015). Characterizing microbiomes within an ecological framework is necessary to determine what constitutes a “healthy microbiome” and understand how this microbiome responds to external disturbances, such as infectious agents, and the holobiont (Costello, Stagaman et al. 2012). Doing so would be useful for enhancing treatment methods in human medicine (Costello, Stagaman et al. 2012), and for improving conservation strategies of wild fauna and their associated ecosystems (Trevelline, Fontaine et al. 2019, Banerjee, Cornejo et al. 2020).

In addition to the previously discussed ecological and evolutionary processes that also apply to host-associated microbial systems (Vellend 2010, Shafquat, Joice et al. 2014), the close interplay of the microbiome with the host and its surrounding environment can have a profound effect on the dynamics and the relative importance of

these factors on community assembly. For example, high inter-individual variability in microbiome structure, illustrated by the relatively low (50% or less) proportion of genera shared between closely related individuals (Turnbaugh, Hamady et al. 2009) and strong temporal variability across developmental stages, have been observed in host-associated systems (Koenig, Spor et al. 2011). This variation suggests that certain functions, rather than taxa, may be more informative metrics of a “healthy microbiome.” This hypothesis, reinforced by high rates of HGT within body sites (Smillie, Smith et al. 2011, Huttenhower, Gevers et al. 2012), may involve important functions associated with less abundant or transient species (Shafquat, Joice et al. 2014). Moreover, deterministic processes, including host genetics, developmental shifts in immunity, or diet, contribute to microbiome variation. Indeed, host genetics influences microbiome assembly by imposing body site-specific physicochemical conditions (e.g., temperature, pH, humidity, oxygen concentration, nutrient availability) that act as filters for microbes and limit colonization (Costello, Stagaman et al. 2012).

While changes in the relative importance of these processes affect microbiome assembly, none of them act in isolation. It is the interaction among these drivers and the different pools of microbes in an ecosystem that ultimately determines local microbiome assembly. Different microbial pools interact with each other through dispersal and are influenced by pairwise microbe-microbe and microbe-host interactions (Leibold, Holyoak et al. 2004). In comparison to certain processes that affect only within-host assemblies, dispersal and drift are also important at the metacommunity level (Adair and Douglas 2017). Specific host behaviors or other characteristics can increase/decrease the transmission of certain microorganisms (Bright and Bulgheresi

2010). For example, while dispersal is in part influenced by the intrinsic capability of each microbe to disperse, contact or proximity between hosts can modulate this process, substantially affecting inter-host microbiome variation (Burns, Miller et al. 2017). Moreover, commensal and symbiotic microbial species may vary in their fitness during non-host associated stages accounting for differences in transmission and assembly dynamics. This underscores the importance of host to host interactions on microbiome transmission (Costello, Stagaman et al. 2012), and in some microbe-host partnerships, the importance of vertically transmitted microorganisms in maintaining consistency of microbiome composition (Bright and Bulgheresi 2010, Adair and Douglas 2017). Host effects on dispersal can also interact with diversification. For example, periodic dispersal of microbes between host-associated pools can be a source of diversity by providing new species that may facilitate adaptation. These incoming species may then be subjected to other modes of microbiome transmission that operate within the host, e.g., mother to offspring transmission that subsequently purges diversity or reshapes composition (Fukami, Beaumont et al. 2007, Urban, Leibold et al. 2008). Microbial dispersal can also be affected by the surrounding environment, and hence, host microbiome assembly. However, the level of exposure can specify body site microbiome composition (Zhou, Gao et al. 2013). Indeed, the level of exposure to external conditions creates a fundamental divide between microbial communities living on surface areas compared to those present in more internal sites. Therefore, understanding the biogeography of the host-associated microbiota through space and time is key to determine what a healthy microbiome looks like taking into account body site-specificity, and better identify early disease states.

The inherent differences in microbial structure and other biotic and abiotic factors associated with different body sites make them more or less susceptible to invasion by other microbes. These invaders could include pathogens but also potential therapeutic microorganisms from transplants that may, therefore, have varying levels of success (Costello, Lauber et al. 2009). For example fecal microbiota transplants have been used to treat certain gut dysbiosis successfully. This type of transplantation can help recover from recurrent *Clostridium difficile* infections, despite the mechanisms not been fully understood (Seekatz, Aas et al. 2014). However, microbiota transplants from other body sites are not as common and remain poorly understood. For instance, the first human skin microbiota transplantation with *Roseomonas mucosa* was recently successful in treating atopic dermatitis. Nonetheless, a combination of factors, including environmental ones such as topical products used, might have altered the effectiveness of this procedure (Myles, Earland et al. 2018). Indeed, while microbiome transplantation appears as a promising therapy to treat dysbiosis, the relative effect of other factors can influence microbial community composition and the capacity of incoming microorganisms to establish themselves efficiently. Therefore, it is important to consider shifts in microbiome composition associated with differences in exposure, e.g., the introduction of the host into a new environment, versus microbiome shifts associated with changes in host health and ecology, caused by changes in diet, behavior, metabolism, and physiology. Such changes can differently alter microbe-microbe and host-microbe interactions depending on the body site.

In summary, the combined effects and relative importance of stochastic and deterministic processes would, therefore, result in high intrinsic variation in host-



associated microbiomes. This multi-factorial phenomenon highlights the need to consider host-associated microbial community assembly in light of a meta-community framework. This framework should consider the physiology, behavior, and ecological state of the host, as well as those of free-living and host-associated microbial communities (e.g., in different body-site niches), and environmental and other external factors (Spor, Koren et al. 2011, Adair and Douglas 2017). A prime example of a microbiome studied under a meta-community framework is the gut microbiome. Often the largest in the body, it is involved in key metabolic processes (Turnbaugh, Hamady et al. 2009), plays a central role in harvesting energy from food by processing non-digestible compounds, and modulates gut transit and energy expenditure. The gut microbiota is also involved in host metabolism, physiology, immune system function, and even behavioral traits (Flint, Scott et al. 2012). Therefore, gut dysbiosis can have significant consequences not only on digestive capacity and gut health but also on the overall protection against infection and disease. Indeed, an altered gut microbiome has been related to chronic digestive conditions, e.g., Chron's disease (Lewis, Chen et al. 2015), immunometabolism in which immune cells respond differently to stimuli depending on the host metabolic and physiological state (Belizário, Faintuch et al. 2018), and psychopathologies, e.g., anxiety, panic, depression, psychosis, and delirium (Sternbach and State 1997).

As one of the major modulators of gut microbial structure, diet can largely influence gut and host health. Turnbaugh and collaborators showed in 2009 that switching from a plant-based, low-fat diet to a high-fat, high-sugar diet significantly modified gut microbial communities of gnotobiotic mice that had received human fecal

transfers, within a day (Turnbaugh, Hamady et al. 2009). This change altered community structure, the relative importance of certain metabolic pathways, gene expression, and increased mice adiposity, highlighting the predominant effect of diet on the gut microbiota and its repercussions on host metabolism and physiology (Turnbaugh, Hamady et al. 2009). Similar to the assembly in free-living communities, the order of colonization coupled with microbe-microbe interaction effects can also alter microbial community assembly and ultimately affect host health (Gomez de Agüero, Ganai-Vonarburg et al. 2016). Microbe-microbe interactions can modulate microbiome composition and influence colonization by external microbes or the pathogenicity of existing ones (Ramsey, Freire et al. 2016, Zhang, Derrien et al. 2016). For example, *Staphylococcus aureus* pathogenicity can decrease when *Corynebacterium spp.* is also present (Ramsey, Freire et al. 2016), and the establishment of certain foodborne microbes such as *Lactococcus lactis* is highly dependent on the microbial community structure already present in the gut (Zhang, Derrien et al. 2016).

The effect of stochastic processes is also crucial in driving microbial community assembly at earlier developmental stages and linked to the maternal environment (Wen, Ley et al. 2008, Gomez de Agüero, Ganai-Vonarburg et al. 2016). While several hosts receive their first microorganisms from the mother, the rearing environment can significantly influence microbiome assembly (Orcutt, Gianni et al. 1987, Lucas and Heeb 2005). For example, a study on the cloaca microbiome of blue and great tit nestlings showed that nestlings of different species raised in the same nest harbored a more similar microbiome compared to their biological siblings raised in a different nest, underlining the impact of the rearing environment, particularly in early life stages

(Lucas and Heeb 2005). Gene mutation, transfer, and genetic drift also participate in shaping host-associated microbial community assembly. Gene mutations have been associated with changes in diversity that can translate into a disease state (Levy, Thaiss et al. 2015). For example, a mutation in the gene *MEFV* that encodes pyrin alters the gut microbiota and causes familial Mediterranean fever (Khachatryan, Ktsoyan et al. 2008). Gene flow also affects microbiome assembly processes and varies based on the body site niche. For example, HGT may be more common among microbes sharing the same body site (environmental niche) (Smillie, Smith et al. 2011), and may also be modulated by phage interactions (Wang, Gao et al. 2016). Finally, the influence of genetic drift can vary among body sites based on differences in population size and connectivity to external microbial/gene pools. Indeed, systems that involve the repeated elimination of microbes (i.e., the gastrointestinal tract) may be more sensitive to drift by recurrently decreasing the relative abundance of community members (McKenney, Koelle et al. 2018).

Finally, the essential role of the microbiome as a driver of host health has triggered an increasing effort to characterize host-associated microbial communities, their variation, and the different factors determining community assembly. Due to the potential for microbiome studies to enhance medical treatment strategies, such interest has been mostly concentrated on mammals and humans. However, studying microbiomes of non-model organisms is essential to identifying unifying processes of assembly that extrapolate across systems. Such studies can be used to improve or develop new conservation strategies at the ecosystem level. This research is currently

critically needed as increasing climate change and anthropogenic disturbances continue to undermine ecosystems' diversity and function.

### **1.3 Effects of environmental change on host-associated microbiomes**

Currently, climate change and anthropogenic activities are drastically altering ecosystem diversity by causing species relocation or extinction, destroying habitats, and changing trophic structures (Dunne and Williams 2009, Doney, Ruckelshaus et al. 2011). Despite the faster adaptation rate of microorganisms compared to larger animals, environmental changes also affect microbial communities, either by changing the surrounding physicochemical properties, or by modifying the interactions between different microbial pools (e.g., host-host or host-environment). Such changes can create disturbances that affect ecosystem-level processes. For example, increased temperature and atmospheric CO<sub>2</sub> concentrations, along with increases in other pollutants, are expected to increase primary plant production, and therefore carbon sequestration (Vitousek, Aber et al. 1997, Ainsworth and Long 2005). However, the resulting increases in organic carbon derived from plant biomass are predicted to modify microbial community structure and intensify microbial respiration. Organic matter turnover would consequently increase and result in a net release of carbon to the atmosphere, creating a positive feedback loop that would intensify climate change processes (Blagodatskaya and Kuzyakov 2008, Sayer, Heard et al. 2011). As another example, in marine systems, ocean warming coupled with enhanced nutrient influx has resulted in the expansion of hypoxic (low oxygen) and anoxic ocean waters. These so-called “oxygen minimum zones” (OMZs) are dominated by a microbial community that is taxonomically and functionally distinct from that in oxygen-rich waters. Notably, microbes in OMZs play active roles in pathways of sea-to-

atmosphere nitrogen loss through the metabolic processes of denitrification and anaerobic ammonium oxidation. Expansion of OMZs due to continued environmental change, therefore, alters the nitrogen budget of the ocean, resulting in potentially significant effects on marine productivity (Ulloa, Canfield et al. 2012, Bertagnolli and Stewart 2018).

In addition to free-living microbes, host-associated communities also play a critical role in maintaining ecosystem balance by modulating macroorganisms' health and their function within these systems (Hooper, Littman et al. 2012, Brestoff and Artis 2013, Kamada, Chen et al. 2013, Archie and Tung 2015). However, disruptions to the equilibrium between the host and its microbiome can exacerbate potential adverse effects on host metabolism, development, and behavior due to environmental stress, and therefore accelerate extinction (Qiu, Coleman et al. 2019, van Oppen and Blackall 2019). For example, similarly to corals, warming and acidification cause bleaching and tissue degradation of kelp, a habitat-forming species. This bleaching has been related to an altered associated microbiota and a higher abundance of potential pathogens such as *Nautella sp.* and *Aquamarina sp.* (Marzinelli, Campbell et al. 2015). Moreover, changes in host-microbial communities (e.g., increased pathogen load) can also affect microbial diversity in the surrounding environment and vice versa, further modifying microbial environmental processes or dispersal dynamics (King, Hure et al. 2002, Ylitalo, Stein et al. 2005, Rosenberg, Koren et al. 2007, Hess, Wenger et al. 2015, Jiménez and Sommer 2017). However, most research has focused on free-living microbial communities, and less have explored host-associated systems. A composite understanding of how host microbiomes respond to environmental change requires sampling across different body sites as external (e.g., skin) and internal (e.g., gastrointestinal) sites differ in their physicochemical

conditions and exposure to external factors. These differences cause such sites to be composed of a variety of microbes with differing dispersal dynamics, dormancy potential, physiology, growth rates, and temperature sensitivity, all of which ultimately affect how disturbances impact each community. Finally, due to the strong interconnectivity between the host and its microbiome, factors such as diet, developmental stage, or immune status can create high interindividual variability that makes it hard to draw unifying patterns and predictions (Costello, Stagaman et al. 2012). Nonetheless, the paramount importance of host microbiomes in maintaining host and ecosystem function demands that we study these communities, their interactions with the host, the surrounding environment, and other microbial pools, to fully characterize the effects of environmental disturbances at the ecosystem level.

As an example, coral reef ecosystems play a major role in sustaining diversity and productivity in the ocean (Sebens 1994). They have received significant attention as research targets for understanding marine ecosystems and microbiome responses to environmental change. Indeed, while coral reefs are naturally exposed to frequent perturbations, climate change and human-related activities, including warming temperatures, ocean acidification, overfishing, eutrophication, and disease (Bellwood, Hughes et al. 2004, Hughes, Kerry et al. 2017, Hughes, Kerry et al. 2018) greatly affect these systems. As coastal environments, coral reefs are near and immediately affected by human activities. Tropical corals, indispensable components of coral reefs, often live on the edge of their temperature range and can be highly sensitive to elevated temperatures. Despite being invertebrates, corals are complex organisms that also harbor a highly diverse and dynamic microbiome that includes dinoflagellates, bacteria, archaea, viruses, and fungi

that vary with time (developmental stage) and space (body site), can largely affect host health and are differentially impacted by external changes (van Oppen and Blackall 2019). Therefore, coral reefs, and particularly corals have become the “canary in the coal mine” when trying to understand the effects of climate change and other anthropogenic disturbances on marine organisms and habitats (Sebens 1994, Pandolfi, Connolly et al. 2011, Frieler, Meinshausen et al. 2013). Coral microbiome structure and dynamism, their high sensitivity to environmental change, and the large amount of information that exists compared to other animal’s microbiomes, highlights the advantage of drawing parallels between coral microbiome studies and other biological systems. Ultimately, this approach could enhance our understanding of wild microbiomes, and bring insight into how current and future climate change and human-related disturbances may impact other ecosystems.

As ecosystem engineers, corals form reefs that act as diversity hotspots supporting a wide range of invertebrate and fish species, including those of commercial value (Moberg and Folke 1999). Recent studies have shown that corals harbor a microbiome involved in core metabolic processes, including nutrition, settlement, protection against pathogens, and overall resilience to environmental stress (Blackall, Wilson et al. 2015, Hernandez-Agreda, Gates et al. 2017). Cell densities in coral microbiomes have been estimated at  $10^2$  to  $10^6$  cells per square centimeter of host tissue (Garren and Azam 2012), and are usually species-specific (Morrow, Moss et al. 2012) and stable across geographical and environmental conditions (Sunagawa, Woodley et al. 2010). However, similar to the microbiomes of other animals, microbiome composition can vary spatially and temporally within a host, changing for example in response to coral physiology and health (Mouchka, Hewson et al. 2010), the specific location within the coral structure (mucus, tissue, skeleton, etc.),

developmental stage (Ainsworth, Thurber et al. 2010), and degree of interaction with the surrounding environment (Rohwer, Seguritan et al. 2002).

Diverse environmental stressors impact the coral microbiome. Increasing stresses related to ocean warming and other anthropogenic disturbances have caused a sharp decrease in coral cover of about 80% in the Caribbean and 50% in the Pacific (Hughes, Kerry et al. 2017, Hughes, Kerry et al. 2018). One of the major and most studied processes leading to such decline has been coral bleaching caused by a disruption of the symbiotic relationship between zooxanthellae (*Symbiodinium spp.*) and the coral host. This bleaching allows a shift in microbiome composition and colonization by opportunistic pathogens including *Vibrio spp.* (Thurber, Willner-Hall et al. 2009, Littman, Willis et al. 2011), although the exact mechanisms leading to this infection are not fully understood. In addition to affecting coral calcification, ocean acidification can also modify microbiome composition, including a loss in potentially beneficial bacteria such as *Endozoicomonas spp.* (Morrow, Bourne et al. 2015), and an increase in potentially pathogenic groups such as *Vibrionaceae* and *Alteromonadaceae* (Meron, Atias et al. 2011). Finally, eutrophication and increased sedimentation of organic matter can promote phytoplankton and algal growth that results in seawater and coral tissue anoxia through an increase in bacterial respiration (Dinsdale, Edwards et al. 2008, Kelly, Williams et al. 2014). These changes in the physicochemical properties of the surrounding environment and the coral tissue can drastically alter microbial growth and community composition in coral tissues, potentially leading to coral death (Weber, De Beer et al. 2012). While different human and climate change-induced disturbances cause distinct responses from the coral holobiont, these factors do not act in isolation and often have cumulative or synergistic effects (Dinsdale,



Edwards et al. 2008, Kelly, Williams et al. 2014). The cumulative impacts of warming temperatures, ocean acidification, eutrophication, and other environmental changes, e.g., herbivore loss due to overfishing, induce coral disease and death, while simultaneously stimulating algal growth (Bourne, Morrow et al. 2016). Indeed, as corals disappear, reefs often become dominated by seaweed, which further exacerbates coral loss and microbiome alteration, for example by producing allelochemicals that are toxic to the coral holobiont, or by exuding sugars that fuel microbial (including pathogen) growth. The latter potentially resulting in localized coral hypoxia (Nelson, Goldberg et al. 2013, Pratte, Longo et al. 2018).

While it is now becoming clear that the coral microbiome plays an important role in maintaining host health and is largely affected by environmental changes, the mechanisms leading to these shifts in microbial composition and their effects on the coral host are still unclear. Therefore, whether shifts in microbial composition caused by stressful conditions lead to a disease state, or whether an unhealthy host causes such changes as a protection mechanism is still unknown (Foster, Schluter et al. 2017). Moreover, because most ecosystems are now affected by climate change and human activities, establishing a baseline of what a “healthy microbiome” looks like is near impossible. Due to the rapid response of microbes compared to the host when faced with environmental perturbation, the coral microbiome has been hypothesized to intensify or potentially mitigate harmful effects. For example, microbiome changes often representing a dysbiotic state seem to precede bleaching (Bourne, Iida et al. 2008). However, a relationship between nitrogen availability and bleaching has also been observed, and an increase in nitrogen-fixing microbes in stressed corals suggests that they potentially help mitigate coral starvation

induced by bleaching (Wooldridge 2013). While correlations between stressful conditions, diseased states, and microbiome variations have been observed, the mechanisms and causality of such changes are still largely unknown. A baseline of what represents a healthy microbiome, and to what extent different microhabitats within the holobiont are affected by environmental change, are still unknown. Similarly to other species, the coral microbiome is considered highly diverse, dynamic, and composed by a core microbiome and resident microbes that show high interindividual variability (Hernandez-Agreda, Gates et al. 2017). Despite recent technological and computational advances allowing researchers to increase and streamline microbiome sampling and analysis, these questions remain unanswered for many wild organisms. Extrapolating the large amount of information on corals, and their response to environmental disturbances to other host-associated systems can help identify specific microbial taxa, functions or interactions that are important to maintain a healthy microbiome and host health.

Recent insight into animal microbiomes, including corals, have allowed the identification of a core microbiome shared across phylogenetically- or geographically-related host individuals. This shared core microbiome would allow the identification of microbial members that may be particularly important to host health or responsive to environmental conditions (Ainsworth, Krause et al. 2015, Hernandez-Agreda, Gates et al. 2017). In addition, more recent studies identified core microbial functions and potentially important compounds that microbes might release to protect the host. Indeed, function and metabolic pathways, rather than taxonomy, seem to be the main trait upon which microbes are selected (Louca, Parfrey et al. 2016). Consequently, studies exploring function along with taxonomy are necessary to characterize microbial community assembly processes and

drivers. Moreover identifying microbial exudates, for example by coupling taxonomic and genomic analysis with metabolomics, may ultimately bring insight into the biochemical mechanisms that unite diverse members to form the holobiont, and identify microbes or microbial functions that could be used as indexes of health status (Thurber, Willner-Hall et al. 2009, Hay, Beatty et al. 2017). Ultimately, such studies may be crucial to formulating strategies to protect and conserve keystone or habitat-structuring organisms, like corals, and the ecosystems they support.

The microbiomes of individual animal or plant species ultimately reside in an ecosystem composed of a multitude of microbe-associated hosts that vary in physiology, life-history traits, sensitivity to stress, and in the nature of the relationship with their associated microbiome. Hence, to fully understand how environmental change may alter ecosystem function and services, it is necessary to characterize microbiomes, including their dynamics and functional properties, across diverse hosts. For example, marine mammals and predatory fish are sentinels of ecosystem health and are increasingly targeted as subjects for microbiome research (Reddy, Dierauf et al. 2001, Wells, Rhinehart et al. 2004), due to their longer lifespans, key roles in food webs, and their propensity for accumulating toxins in tissues and fat. Previous studies have shown that, for some of these species, the microbiome can rapidly respond to environmental perturbations, reflect the presence of pollutants or toxic compounds, and carry potentially pathogenic microbes that can affect both human and environmental health (King, Hure et al. 2002, Ylitalo, Stein et al. 2005, Fackelmann and Sommer 2019). Exposure to microplastics has been linked to gut dysbiosis and mechanical damage to the intestinal tract, facilitating the insertion of pathogens or other toxins (Fackelmann and Sommer 2019). As another example, California

sea lions are more prone to urogenital cancer related to the presence of a virus (OtHV-1) (King, Hure et al. 2002), whose invasion is facilitated by immune suppression that can be caused by environmental pollutants such as organochlorines (Ylitalo, Stein et al. 2005). Similarly, marine birds that spend significant time both on land and at sea are research targets for exploring how microbiomes may respond to both terrestrial and marine disturbances. However, the large ranges of such organisms and their sensitivities to potential stresses associated with handling, present logistical challenges. In addition, because many species are now endangered, disturbing these animals even for scientific purposes can be problematic.

Consequently, most microbiome studies have focused on model organisms, with the resulting findings then used to make predictions for wild species. However, research has shown that captivity, and its associated environmental/ecological changes, can drastically alter animal microbiomes. This suggests that studies based on model organisms, the vast majority of which do not test how microbiomes respond to biotic interactions among diverse hosts, may not apply in the wild (Clayton, Vangay et al. 2016, Hird 2017, McKenzie, Song et al. 2017). Nonetheless, microbiome studies from captive animals are invaluable as they enable hypotheses about core microbial species or functions relevant to host health. Moreover, comparing microbiome composition between captive and wild individuals of the same species can help establish a baseline for what a healthy microbiome looks like, and help determine which portion of the microbiome remains constant and which members are affected by captivity and environmental change. Ultimately, characterizing the microbiome of a larger variety of hosts, and combining captive and wild studies, can help elucidate how climate change and anthropogenic disturbances are

affecting host-associated microbial communities, and how these changes relate to host health. This information is particularly valuable to not only protect specific species that may be facing extinction, but also to preserve entire ecosystems.

#### **1.4 Effect of captivity on microbiomes**

Climate change and human activities have resulted in major diversity losses, with 31,000 species now threatened with extinction (IUCN 2019). Maintaining animals in captivity has been widely applied to help conserve declining or rare species (Rahbek 1993). However, a transition to captivity involves substantial environmental and ecological changes, many of which may alter the structure and function of an animal's microbiome (Redford, Segre et al. 2012, McKenzie, Song et al. 2017). Considering the importance of the microbiome in regulating host metabolism, development, behavior, and overall health (Hooper, Littman et al. 2012, Brestoff and Artis 2013, Kamada, Chen et al. 2013, Archie and Tung 2015), understanding how captivity affects microbiomes is key to maintaining the health of captive animals and potentially increasing the likelihood of successful reintroduction (Redford, Segre et al. 2012). Moreover, captive environments are relatively simple (few variables compared to the wild), and the health of captive animals is often rigorously monitored. Therefore, captive animals provide a framework for identifying microbial players that may be strongly related to host metabolism and health, potentially important parameters influencing microbiome assembly, and baseline knowledge of what a "healthy microbiome" may look like. In particular, determining what characterizes a healthy versus dysbiotic state may help identify and address disease progression and predict whether specific stressors may be altering microbiomes in the wild (Potter 2013). Ultimately, this information can be used to enhance conservation strategies and establish

if and how animal-associated microbiomes can be used as an index of environmental change (Ainsworth and Gates 2016, Pace, Dipineto et al. 2019).

Compared to wild individuals, captive animals experience controlled and artificial conditions, dietary changes or restrictions, limited exposure to other fauna and flora or habitat types, freedom from predation and certain diseases, and increased exposure to medical care and humans (Redford, Segre et al. 2012, McKenzie, Song et al. 2017). Indeed, studies have shown that captivity can alter microbiomes in a wide variety of animals ranging from amphibians to primates (Dhanasiri, Brunvold et al. 2011, Eigeland, Lanyon et al. 2012, Loudon, Woodhams et al. 2014, Clayton, Vangay et al. 2016, Delport, Power et al. 2016, Eichmiller, Hamilton et al. 2016, McKenzie, Song et al. 2017, Metcalf, Song et al. 2017, Song, Wang et al. 2017, Jia, Zhao et al. 2018). While most comparisons between wild and captive animals report changes in gut diversity, there is limited consistency across studies and host species. In some species, including primates, carnivores, and equids, gut microbiome diversity (alpha) decreased with captivity (Eigeland, Lanyon et al. 2012, Clayton, Vangay et al. 2016, Stumpf, Gomez et al. 2016, Borbón-García, Reyes et al. 2017, McKenzie, Song et al. 2017, Metcalf, Song et al. 2017). In other species, diversity either increased (Becker, Richards-Zawacki et al. 2014, Xie, Xia et al. 2016, Bletz, Vences et al. 2017, McKenzie, Song et al. 2017) or showed no significant change (Alfano, Courtiol et al. 2015, Flechas, Blasco-Zúñiga et al. 2017, McKenzie, Song et al. 2017).

Microbial community composition ( $\beta$ -diversity) often significantly shifts with captivity, even if  $\alpha$ -diversity is not impacted. In mammals, microbes that vary the most with captivity include phyla that are common in the gut, such as Bacteroidetes, Firmicutes,

and Proteobacteria (McKenzie, Song et al. 2017). Notably, captive Old World Monkeys harbor lower relative abundances of *Prevotella*, and higher abundances of *Bacteroidales* S24-7 (McKenzie, Song et al. 2017). Both *Prevotella* and *Bacteroidales* S24-7 degrade protein and carbohydrates and seem to compete for niche space in the gut (Serino, Luche et al. 2012, Evans, LePard et al. 2014, Ormerod, Wood et al. 2016, McKenzie, Song et al. 2017). In humans higher proportions of *Prevotella* have been linked to individuals eating a more plant-based diet, suggesting that a shift to a higher protein diet in captive animals may cause a decrease in *Prevotella* relative abundance (Wu, Chen et al. 2011, Serino, Luche et al. 2012). In addition, McKenzie and collaborators observed that the abundance of known nitrogen reducers belonging to Alpha- and Betaproteobacteria increased in wild terrestrial mammals, coincident with higher decaying *Cyanobacteria*, reinforcing the idea that a more protein-rich diet in captivity may be responsible for these differences. Bacteria associated with gut dysbiosis in horses, including lactate-producing bacteria such as *Streptococcus luteciae*, are also more abundant in captive terrestrial mammals (Biddle, Black et al. 2013, McKenzie, Song et al. 2017). In contrast, captive primates have been shown to have higher proportions of certain microorganisms, such as members of the *Christensenellaceae*, important in maintaining gut health in humans (Biagi, Franceschi et al. 2016). It is hypothesized that because other beneficial microbes, such as *Prevotella*, decrease in abundance in captive individuals, *Christensenellaceae* may increase to compensate this loss (McKenzie, Song et al. 2017). These and other studies implicate diet shifts and the use of antibiotics (Antwis, Haworth et al. 2014, Clayton, Vangay et al. 2016, Stumpf, Gomez et al. 2016, Jiang, Ma et al. 2017, Metcalf, Song et al. 2017, West, Waite et al. 2019) as a major driver of microbiome change in captivity. The transition from a

relatively complex, fiber-rich diet in the wild to a simpler, more protein-rich diet in captivity are potentially most pronounced in animals such as herbivores that require certain microbes to efficiently digest certain plant components or toxins (Amato, Yeoman et al. 2013, West, Waite et al. 2019). These examples illustrate the complexity of delivering a diet in captivity that properly mimics what the animals consume in the wild, which is necessary to preserve microbiome diversity and function.

The inconsistent effects that captivity can have on animal's microbiome, which is influenced by the relative importance of different factors that affect microbial assembly (host action versus environment), and can be highly dependent on the species considered, makes it challenging to identify specific factors related to captive environments that can be generalized. Moreover, captive environmental conditions including diet, medical care, and exhibit characteristics can be highly variable with some more similar to wild habitats. This increases the number of confounding factors and could partially explain differences in studies comparing changes in diversity associated with captivity. Therefore, captive microbiome variability could reflect real variability in the associated microbiota of these organisms or differences in captivity conditions. Captivity is often also associated with increased human interaction, and medical care that contribute to microbiome change, but the effects of such changes are still poorly understood. While increased care, including the use of antibiotics, can enhance the health of captive hosts compared to their wild counterparts (by directly affecting the associated microbiota or by modulating host physiology), increased handling by caretakers can promote the transfer of human commensals (or potentially pathogens); reported in primates and marine mammals (Clayton, Vangay et al. 2016, Chiarello, Villéger et al. 2017). Moreover, the use of



antibiotics can also promote dysbiosis by inducing taxonomical and functional loss, which can facilitate pathogen infections and antimicrobial resistance (Lange, Buerger et al. 2016). For example, captive cheetahs' gut microbiome harbors higher abundances of pathogenic taxa and metabolic pathways associated with disease, which have been related to increased mortality in captivity due to infections (Terio, Munson et al. 2005, Menke, Melzheimer et al. 2017). As another example, the use of antibiotics on koalas to treat *Chlamydia* infections decreases gut microbial diversity and the abundance of tannin-detoxifying bacteria that play a key role in koala's nutrition, which can lead to poor health and ultimately death (Dahlhausen, Doroud et al. 2018). While the effect of this "humanization" of the animal microbiome is poorly understood and may be species-specific, capturing the extent of these microbiome shifts in a larger variety of animals, and their possible consequences on host health and fitness in the wild is key to certain management decisions, including those about reintroduction (Redford, Segre et al. 2012, West, Waite et al. 2019). For example, the reintroduction of animals with an altered microbiome into the wild may facilitate the transfer of pathogenic strains or antibiotic-resistant microbes into natural ecosystems, which may not be harmful to the initial host but may cause unintended modifications to wild populations (Power, Emery et al. 2013, Delport, Harcourt et al. 2015).

Other aspects of captivity-associated environmental change have been shown to significantly affect the microbiome structure. A study from commercial pig farms showed that solely changing the raising environment (presence or absence of deep bedding of straw) can alter the gut microbiota (Kubasova, Davidova-Gerzova et al. 2017). Hyde and collaborators showed that the oral and skin microbiomes of Komodo dragons were similar to those collected from the surfaces of exhibits (Hyde, Navas-Molina et al. 2016).

Similarly, (Eichmiller, Hamilton et al. 2016) showed that the gut microbiome of common carps differed between river and lake environments, despite similarities in diets. These and other studies suggest that environmental factors, which may be diverse in nature and potentially challenging to quantify, modulate microbiome discrepancies.

Microbial communities from different body sites likely differ in the extent to which they respond to environmental change associated with captivity. While the gut microbiota may be most sensitive to shifts in diet, microbiomes in external body niches, such as the skin, may be more sensitive to habitat modifications. This variation adds another level of complexity when trying to relate conclusions based on microbiomes analysis of a single body site to specific environmental or dietary alterations. For example, a comparison of the microbiome of captive African penguins with that of other vertebrates (including marine mammals, other birds, reptiles, and humans), showed that while the cloacal microbiome of captive penguins was more similar to that of other birds, the oral microbiome was more similar to that of other marine mammals sharing a similar diet (Clavere-Graciette, in preparation). These results suggest that while the phylogenetic relationship among hosts may be important in shaping cloacal microbiomes, diet may play a more important role in shaping the oral microbiome. In this study, the microbiome of penguin skin was highly similar to that collected from exhibit surfaces, supporting the prediction that the surrounding environment primarily shapes the skin microbiome (at least in penguins) compared to more internal body sites (e.g., cloaca, oral cavity). Similarly, a comparison between wild and captive spotted eagle rays showed microbiome body site specificity as well as large differences in cloaca, skin and gill samples between captive and wild samples (Clavere-Graciette et al., in preparation). Interestingly, while cloaca samples of captive

spotted eagle rays were more similar to those of wild eagle rays, gill and skin microbiomes of captive eagle rays were similar to those of cownose eagle rays co-occurring in the same exhibit. In contrast, the cloacal microbiomes differed between these two host species while in captivity; instead, the spotted eagle ray cloacal microbiome was most similar to that of wild eagle rays. These observations suggest that phylogeny is a major driver of cloacal community composition, whereas gill and skin microbiomes, like those of the penguins, seem more readily influenced by environmental parameters. The variability in the relative influence of intrinsic and extrinsic factors such as diet, phylogeny, and other environmental parameters in driving microbial community assembly among different species, and different body sites within a species, highlights the complexity of host-associated microbial systems, the need to explore the microbiome associated with a larger number of species, and the benefit of sampling a variety of body sites and comparing both captive and wild individuals to better understand how and to what extent environmental change may be driving community composition.

Indeed, it is often difficult to relate microbiome shifts to a specific factor (diet, antibiotic use, habitat modification, decreased social interaction). Despite the tight relationship between the microbiome, host metabolism, and immune system function, in many cases, it is difficult to determine if captive microbiomes represent a healthy alternative state or if they may negatively affect host health or hamper reintroduction efforts. Altered captive microbiomes may facilitate cardiac, respiratory, gastrointestinal, and skin anomalies (Amato, Yeoman et al. 2013, Becker, Richards-Zawacki et al. 2014, Wan, Ruan et al. 2016, McKenzie, Song et al. 2017, Hale, Tan et al. 2018), and have been related to disease in a certain number of species (Amato, Metcalf et al. 2016, Wan, Ruan

et al. 2016, Xie, Xia et al. 2016). For example, crocodile lizards seem to be prone to disease in captivity and to harbor certain skin infections not observed in the wild (Jiang, Ma et al. 2017). A study comparing the gut microbiome of captive and wild individuals showed that microbiomes of wild individuals contained higher relative abundances of *Deinococcus-Thermus*, *Mycoplasma*, and *Helicobacter*. However, the function of these taxa within the gut and their potential connection to host health are still poorly understood (Jiang, Ma et al. 2017). Shifts in diet played a major role in shaping these microbial communities, with differences observed in captive individuals following either an earthworm or a loach-based diet. In particular, the earthworm diet led to an enrichment of the genus *Fusobacterium*, a taxon commonly found in diseased reptiles and also associated with pathogenicity in humans and other animals (Stewart 1990, Signat, Roques et al. 2011). Potential pathogens such as *Halomonas* and *Salmonella* (Kim, Lee et al. 2013, Murphy and Oshin 2015) were also enriched on the loach-based diet. While these results suggest that captivity conditions and diet modifications can be potentially harmful to the health and conservation of a species, it is difficult to directly link specific microbial community changes to disease. This difficulty also exists when determining if and to what extent specific captive conditions are causing these changes, and if such changes reflect a consequence of disease, or a response from the host as a protection mechanism (West, Waite et al. 2019).

The increasing interest in wild microbiomes and comparing them to captive ones has allowed researchers to identify key microbial players and encouraged the use of dietary supplements, prebiotics, and probiotics to enhance health, survival, and reintroduction success of captive species (West, Waite et al. 2019). The use of probiotics and prebiotics has been mostly used on commercial species with positive results. Indeed, the use of

probiotics has enhanced weight gain in sheep and dairy calves (Schofield, Lachner et al. 2018) and has also conferred protection against pathogens in poultry (Khan and Naz 2013). In wild animals, the use of probiotics is still being explored but seems promising. For example, two plant fermenting strains of *Lactobacillus* that also exhibited antibacterial activity against pathogenic *Escherichia coli*, were found in the gut microbiome of a population of wild gorillas and were proposed as potential probiotic for captive individuals (Tsuchida, Kakooza et al. 2018). As another example, captive boreal toads that exhibit higher levels of *Batrachochytrium dendrobatidis* (*Bd*) on their skin associated with the loss of beneficial skin bacteria can be treated with anti-*Bd* probiotic bacteria (Kueneman, Woodhams et al. 2016). However, wild microbiomes remain largely understudied. To bypass this issue, microbiome research has relied on captive organisms, and on comparisons between captive and wild individuals. Zoos and aquaria provide the possibility to monitor the evolution of host health and its associated microbiota in a detailed manner through significant periods of time, taking into account any subtle changes in the surrounding environment or handling of the animals. Therefore, microbiome studies of fauna in the wild and captive environments provide fewer confounding factors and a vast number of additional metadata that can help identify specific changes associated with disease or increased vulnerability, and what specific habitat modifications or management strategies may be enacted to bring about such changes. While several of these comparisons have focused on terrestrial mammals and their gut microbiota, many other groups such as aquatic organisms remain largely unexplored. For these understudied species, high-end captive facilities such as the Georgia Aquarium provide an opportunity to explore their microbiota and how it compares to those from wild populations. This could help reduce

the gap between host health and microbiome composition, by identify microbial indexes, e.g., taxa or genes, that could be used as biomarkers of host and environmental health and develop prebiotic or probiotic treatments to enhance survival and fitness in both captive and wild environments.

### **1.5 Current tools for studying microbial community assembly**

Due to the central role of microbes in all biogeochemical cycles, as well as their effect on host metabolism, behavior, and health, microbiome research is inherently multidisciplinary (Das, Lyla et al. 2006, Kowalchuk, Jones et al. 2008, Van Der Heijden, Bardgett et al. 2008, Steffan, Chikaraishi et al. 2015). This characteristic has served as an advantage, and microbiome research has benefited from technological advancements in a variety of fields, including microbiology, synthetic biology, engineered biomaterials, bioinformatics, and environmental sampling and instrumentation (Arnold, Roach et al. 2016). Such advancements have allowed researchers to expand the type and body site location of host-associated samples and have greatly enhanced the ability to characterize complex microbial communities taxonomically and functionally, as well as to better understand microbe to microbe and host to microbe interactions.

Early studies of host-associated microbes heavily relied on monoculture and co-culture cultivation techniques (Parker and Snyder 1961, Gibbons, Socransky et al. 1964). While these methods are still relevant and vital to understanding the mechanisms behind microbial interactions, only about 1% of microorganisms are currently culturable (Torsvik and Øvreås 2002, Schmeisser, Steele et al. 2007), limiting the characterization of microbial assemblages at the community level. A decrease in sequencing costs, along with an increase in publicly available data and analytical advances, has not only facilitated the

characterization of complex microbial communities but also provides the possibility to establish new standards to contextualize and compare different microbial studies and systems (Sinha, Abnet et al. 2015, Knight, Vrbanc et al. 2018). The 16S rRNA gene sequencing coupled with polymerase chain reaction (PCR)-based techniques and deep-sequencing of PCR amplicons is now widely used to taxonomically characterize microbial communities (Blaut, Collins et al. 2002, Sogin, Morrison et al. 2006, Huber, Mark Welch et al. 2007). Indeed, the use of these methods allows us to capture microbial diversity at high resolution, including species with very low abundances in these communities (Arnold, Roach et al. 2016). These advances in sequencing technologies, coupled with new bioinformatics and statistical methods for the analysis of highly multi-factorial datasets, has allowed us to widely characterize microbial communities and their relationship to experimental or environmental conditions in a simpler, cost- and time-effective way (Rhodes, Urbanc et al. 1998, Knight, Vrbanc et al. 2018). The near-universal use of high throughput sequencing also provides an opportunity to better contextualize and compare results from different systems and different studies. However, variation in methodological approaches, including in sample collection and bioinformatic procedures, can largely influence microbiome analyses (Clooney, Fouhy et al. 2016). Therefore, standardizing sampling and analytical pipelines is key to allowing for meaningful comparisons between systems and studies, which can only enhance our understanding of microbial communities, and help draw broader conclusions. Recent efforts at standardization, for example, the adoption of PCR and sequencing protocols associated with the Earth Microbiome Project (Thompson, Sanders et al. 2017), and the establishment of best practices in computation (Knight, Vrbanc et al. 2018), are helping to unify the field. However, there remains

considerable and healthy debate about certain analytical or statistical decisions (e.g., normalization methods, the use of rarefaction in comparing datasets), with a growing appreciation and tool kit for exploring data with different underlying characteristics (e.g., library and sample size, (Weiss, Xu et al. 2017)).

While studies have shown correlations between microbes and environmental variables that suggest important roles in ecosystem processes (Martiny, Bohannan et al. 2006), other studies show functional convergence without similar convergence in taxonomic profiles, which suggests a decoupling between microbial community taxonomic composition and function (Louca, Parfrey et al. 2016). Moreover, a large proportion of microbes within a community can be dormant (~90 %), and microbes can also modulate their gene expression (Locey 2010, Lennon and Jones 2011). This potential for variation in microbial activity underlines the need to complement taxonomic analysis with functional characterization if we want to understand microbial community processes and interactions. Community DNA and RNA sequencing (meta omics) provide further insight into microbial function, expression, and interactions (Muegge, Kuczynski et al. 2011). This information is particularly valuable as previous studies have shown that functional redundancy, rather than taxonomic redundancy, impacts resilience and adaptation capabilities at the community level, and affects host-microbiome interactions (Arnold, Roach et al. 2016). For example, gut microbiome metatranscriptomics showed that 50% of the genes expressed were primarily involved in enhancing host metabolism (Gosalbes, Durbán et al. 2011). In addition, transcriptome studies can help identify early effects of disturbance on microbiome function, before taxonomic changes occur. This feature can be particularly helpful for identifying early signs of dysbiosis, before a diseased state is established (El



Aidy and Kleerebezem 2013, Franzosa, Morgan et al. 2014). Metatranscriptomics can also be used to assess host cell activity and therefore bring insight into host-microbiome interactions, as research has shown that the microbiota can modulate host gene expression, and ultimately impact host health (Carding, Verbeke et al. 2015, Meisel, Sfyroera et al. 2018).

Studying gene expression can provide insight into microbe-microbe and host-microbe interactions. However, the mechanisms involved are still poorly understood. The increasing use of metabolomics, which allows us to track the release of microbial metabolites, can be helpful to understand metabolic processes, physiology, and the interplay between the environment, the host, and its microbiota (Bernini, Bertini et al. 2009, Wu, Compher et al. 2016). Indeed, most microbe-microbe and host-microbe interactions are chemically mediated. Therefore, establishing how the associated microbiota alter the host biogeochemical environment, ultimately affecting microbe-host interactions, host metabolism, physiology, and health, is key to identify specific mechanisms allowing to draw causality patterns when changes in microbiome are observed (Hay, Beatty et al. 2017). For example, a study by (Koeth, Wang et al. 2013), showed that individuals following a vegetarian to vegan diet had lower trimethylamine-N-oxide blood levels compared to omnivorous subjects, and this metabolite shift corresponded with lower proportions of bacteria involved in the catabolism of carnitine and trimethylamine (found in meat, dairy, energy drinks, and other dietary supplements). Moreover, the use of microscopy techniques, such as fluorescent in situ hybridization (FISH) that allows the visualization of specific genes or taxa, or nano-SIMS that allows the semi-quantification of molecule incorporation (Klitgaard, Bretó et al. 2013, Radziwill-Bienkowska, Talbot et

al. 2018), can provide further insight into microbial interactions or chemical cycling at more relevant resolution and spatial scales.

Metabolomics and microscopy-based methods are particularly useful for identifying the pathways involved in microbial interactions, or the spatial dynamics of these interactions. However, culturing the participants in these interactions is likely to provide the most insight into the mechanisms involved. While only a small fraction of microbes have been cultured (Torsvik and Øvreås 2002, Schmeisser, Steele et al. 2007), advances in culturing methods have greatly facilitated our understanding of microbiome processes in certain host systems. For example, the successful use of gnotobiotic mice and anaerobic cultivation techniques has allowed researchers to culture over 50% of the bacterial species in the human gut, most of which were only previously understood based on their 16S rRNA sequence (Faith, Rey et al. 2010, Goodman, Kallstrom et al. 2011). The use of gnotobiotic animals, which allows inoculation of the host individual with a specific set of microbes under semi-natural conditions, has allowed to identify the effects of specific cultured microbes or microbial consortia on host metabolism or health (Faith, Ahern et al. 2014) and to study how members from the gut microbial community are transferred throughout generations (Turnbaugh, Hamady et al. 2009). Culturing methods have also been enhanced by better reproducing natural conditions and isolating microbes more effectively. Such techniques include the isolation Chip (iChip) that uses individual cells to isolate microbes within a complex community, thereby allowing nutrients to permeate through (Nichols, Cahoon et al. 2010). The use of automated conditions has also facilitated the cultivation of many individual microbes from the same community. For example, microfluidic and fluorescence-activated cell sorting technologies allow the sorting and culturing of microbes

based on their production and consumption of certain metabolites (Wang, Ghaderi et al. 2014). Finally, *in vitro* systems that reconstruct specific environmental conditions allow the study of microbial interactions in a highly controlled yet very realistic environment (Possemiers, Verthé et al. 2004). Despite the high potential of these new culturing technologies, using these methods can be complex and expensive, while lacking the capacity to consider all interactions within a community (Arnold, Roach et al. 2016). Therefore, combining different technologies is necessary to fully understand microbial communities, taking into account taxonomic composition and functional potential, gene and protein expression, cell-to-cell interactions, and the mechanisms involved.

The complexity of host-associated microbial communities, the multi-factorial and partly stochastic nature of community assembly, and the intrinsic high inter-individual and inter-sample variability of these systems require the use of large datasets to establish strong, statistically significant patterns. Hence, the implementation of complementary technologies, particularly those allowing the processing and analysis of large multi-omic datasets in a high throughput fashion, coupled with systematic high replication and sampling efforts, are useful in microbiome studies (Arnold, Roach et al. 2016, Knight, Vrbanac et al. 2018). However, the unequal interest and number of microbiome studies that have focused on the gut of humans and terrestrial mammals, compared to other body sites and wild fauna, has skewed the development of new methodologies and statistical analysis to be optimal only in model systems. This can create additional challenges when applying these technologies to wild animal microbiomes. Indeed, the number of samples required to establish statistically robust patterns and associations is hard to estimate due to the limited sampling opportunities, challenges in sample preservation, and high inter-sample

variability. Therefore, large sample sets and replicates are often needed, increasing sample collection and processing costs (Hird 2017). Moreover, once samples are collected, the wet-lab and bioinformatic procedures required to characterize the community often present their own challenges. For instance, exploring the taxonomic structure of microbial communities using 16S rRNA sequencing, usually relies on a single portion of the gene, requires PCR amplification, produces relatively short fragments (Hird 2017), and relies on existing databases to assign taxonomy. This can be problematic for highly diverse and underrepresented wild microbiome samples that may contain large proportions of unknown microbes. Therefore, the increased application of established microbiome approaches to wild microbiomes is necessary to move the field forward and create a solid framework that would allow to accurately compare and draw strong overarching patterns from a variety of studies and systems.

## **1.6 Conclusion**

Microbial community assembly is driven by stochastic and deterministic processes, whose relative influence is variable and can be difficult to determine. Many of the same ecological and evolutionary processes that drive community assembly in free-living microbes also apply to host-associated systems. However, the action of the host and the variability associated with different body sites that are differentially exposed to the external environment and other microbial pools, can greatly influence the relative importance of such processes. It is now widely recognized that the associated microbiota has a profound effect on host metabolic processes, physiology, behavior, and health. As climate change and anthropogenic disturbances keep transforming ecosystems, causing habitat loss, and accelerating species extinction, studies focused on the microbiome of wild hosts are vital

to protect endangered species and preserve entire ecosystems. While captivity has been associated with microbiome changes, animals under these conditions are generally healthy, closely monitored, and their environment is highly controlled and often simpler compared to the wild. Therefore, they provide a unique opportunity to explore the microbiome of understudied fauna in environments with limited confounding factors, with access to key information on the host and its environment, and the possibility to collect large sample sets over extended periods of time. This type of comprehensive studies can facilitate the identification of microbial or environmental biomarkers that greatly influence host health, community assembly and succession, and disturbance resilience. This knowledge can ultimately be used to enhance conservation strategies in captive and wild populations, while advancing the understanding of host-microbiome interactions.

**CHAPTER 2.      MICROBIOME DIFFERENCES BETWEEN**  
**WILD AND CAPTIVE SPOTTED EAGLE RAYS**  
**(*AETOBATUS NARINARI*)**

Disclaimer: This chapter is currently in final manuscript form

## 2.1 Abstract

Animal-associated microbiomes can be influenced by both host and environmental factors. Comparing wild versus captive animals can help isolate the effects of host versus environmental factors, while also testing whether captive conditions foster a ‘natural’ microbiome. Focusing on an endangered and charismatic elasmobranch species – the spotted eagle ray *Aetobatus narinari* – we compared skin, gill, and cloaca microbiomes of wild individuals to those of captive individuals at Georgia Aquarium. Captive *A. narinari* microbiomes were also compared to those of cownose rays (*Rhinoptera bonasus*) in the same exhibit, allowing us to explore the effect of host identity on the ray microbiome. Long-term veterinary monitoring indicated that the captive rays did not have a history of disease and maintained health parameters consistent with that of wild individuals. None of the sampled rays appeared diseased or otherwise unhealthy. However, microbiome  $\alpha$ - and  $\beta$ -diversity differed between wild versus captive *A. narinari* at all body sites, with  $\alpha$ -diversity significantly higher in wild individuals. At each body site, we detected microbial taxa shared between wild and captive eagle rays, although the majority of these taxa were unclassified. Potentially pathogenic microbes were at low abundance in both wild and captive rays.  $\beta$ -diversity differences (wild versus captive) were greater for skin and gill microbiomes compared to those of the cloaca. The cloaca, skin and gill microbiomes of captive eagle rays differed from those of captive cownose rays and from the surrounding water. Captivity is associated with a significant restructuring of the eagle ray microbiome. This restructuring is not absolute, as the microbiome of captive rays shares members with that of wild counterparts and is distinct from that of a cohabitating ray species. Despite having microbiomes distinct from those of their wild counterparts, captive eagle rays at

Georgia Aquarium appear healthy, suggesting that their microbiomes are not associated with compromised host health. However, the ray microbiome is dynamic, differing with both environmental factors and host identity. Monitoring of captive ray microbiomes over time may identify taxonomic patterns that co-vary with host health.

## **2.2 Background**

It is now becoming widely accepted that host associated microbiomes play a critical role in controlling host metabolism, physiology, behavior, and overall health (Hooper, Littman et al. 2012, Brestoff and Artis 2013, Kamada, Chen et al. 2013, Archie and Tung 2015). Both environmental and host factors affect microbial community assembly (Benson, Kelly et al. 2010) and vary in their relative influence based on factors such as host species, and body site niche (Pratte et al., 2018b)(Ruiz-Rodríguez, Scheifler et al. 2020). In studying the effects of host species and environment on microbial community assembly, captive individuals can be particularly useful thanks to tightly controlled environmental factors. Moreover, captive environments are relatively simple, with fewer variables compared to the wild, and the health of captive animals is often rigorously monitored. Species comparisons can also prove useful, as different species within the same captive space are exposed to the same environmental conditions, removing environmental variables which is not possible in the wild. Therefore, captive animals provide an ideal framework for identifying microbial players that may be strongly related to host metabolism and health, and potentially important parameters influencing microbiome assembly such as environmental changes and species. Specifically, determining what characterizes a healthy versus dysbiotic state may help identify and address disease progression (Potter 2013), leading to information that can be



used to enhance protection and rconservation plans (Ainsworth and Gates 2016, Pace, Dipineto et al. 2019).

In marine systems, large predatory fish are sentinels of ecosystem health and are increasingly targeted as subjects for microbiome research due to their popularity in captivity, longer lifespans, key roles in food webs, propensity for accumulating toxins in tissues and fat, and potential for carrying pathogenic microbes that can affect both human and environmental health (Reddy, Dierauf et al. 2001, Wells, Rhinehart et al. 2004) (King, Hure et al. 2002, Ylitalo, Stein et al. 2005, Fackelmann and Sommer 2019). In particular, elasmobranchs are considered keystone species in many ecosystems in which they fill several roles within food chains as top- and meso- predators (Libralato, Christensen et al. 2006, Baum and Worm 2009), and declines in elasmobranch populations can have dramatic effects on ecosystem functioning (Sguotti, Lynam et al. 2016). While large sharks have received increased attention due to their prominent role as top predators (Stevens, Bonfil et al. 2000, Bascompte, Melián et al. 2005, Myers, Baum et al. 2007, Ferretti, Worm et al. 2010), mesopredators such as rays are far less studied.

Spotted eagle rays (*Aetobatus narinari*) are hard-prey specialist mesopredators that feed mainly on gastropods and other benthic mollusks (Ajemian, Powers et al. 2012, Serrano-Flores, Pérez-Jiménez et al. 2019), and also serve as prey for larger predators, including sharks (Chapman and Gruber 2002). Therefore, *Aetobatus narinari* plays a key role in tropical, warm-tempered waters food webs, filling an intermediate position where it acts as both predator and prey. Spotted eagle ray populations have largely declined due to overfishing and bycatch (Devadoss 1984, Trent, Parshley et al. 1997, Dubick 2000, Shepherd and Myers 2005, Cuevas-Zimbrón, Pérez-Jiménez et al. 2011, Tagliafico, Rago

et al. 2012), and the species is now considered near threatened by the IUCN. Despite the ecological importance of spotted eagle rays in maintaining food web structure and their current state of decline, studies on these animals remain scarce. However, they are common in public aquariums worldwide, presenting an ideal opportunity for comparing microbiomes of wild and captive individuals. Pairing captive and wild individuals provides a unique opportunity to identify potential changes in microbial structure associated with captivity and helps to characterize a potential core microbiome composed of microbial species conserved between captive and wild spotted eagle ray populations, despite environmental differences. In this study, we characterized the microbiome composition of the gills, skin, and cloaca of *Aetobatus narinari* from both wild (Sarasota Bay) and captive (Georgia Aquarium) populations using 16S rRNA gene sequencing. *Aetobatus narinari* microbial communities were also compared to those from captive cownose rays (*Rhinoptera bonasus*). Including cownose rays from the same exhibit as captive spotted eagle rays in this study enabled a cross-species comparison to capture the effect of phylogeny compared to differences in the microbiome of spotted eagle rays related to captivity status. We hypothesized that the spotted eagle ray microbiome would differ between captive and wild spotted eagle rays, and between captive spotted eagle rays and cownose rays, with the extent of the change varying according to body site niche.

## **2.3 Materials and methods**

### *2.3.1 Sample collection*

Microbiome swabs were collected (described below) from a total of 18 wild spotted eagle rays, 15 captive spotted eagle rays (*Aetobatus narinari*), and 7 captive cownose rays

(*Rhinoptera bonasus*) by Georgia Aquarium and Mote Marine Laboratory staff. Origin (captive vs. wild), date of sampling, sex, disc width, and weight for all individuals are given in Table 2.1 and Table A.1. Captive spotted eagle rays and cownose rays were sampled from the Ocean Voyager exhibit (OV) exhibit at Georgia Aquarium between 2018 and 2019, while the wild spotted eagle ray samples were collected in June 2018 and April 2019 from Sarasota Bay (27.4, -82.6). Captive spotted eagle rays had been retrieved from multiple locations near Florida, including Sarasota Bay, between 2009 and 2015 and transferred to Georgia Aquarium (OV) where they were kept until the time of sampling. Captive cownose rays were acquired for the exhibit between 2009 and 2018 from North Carolina waters.

**Table 2.1. Summary of the number of samples collected and the number of individuals sampled according to body site, ray species, and captivity status**

Sample type	Species	Origin	Number of samples	Number of individuals represented
Cloaca	<i>Aetobatus narinari</i>	Aquarium	16	14
Gill	<i>Aetobatus narinari</i>	Aquarium	15	13
Skin	<i>Aetobatus narinari</i>	Aquarium	17	13
Cloaca	<i>Aetobatus narinari</i>	Wild	11	11
Gill	<i>Aetobatus narinari</i>	Wild	19	19
Skin	<i>Aetobatus narinari</i>	Wild	19	19
Cloaca	<i>Rhinoptera bonasus</i>	Aquarium	7	7
Gill	<i>Rhinoptera bonasus</i>	Aquarium	7	7
Skin	<i>Rhinoptera bonasus</i>	Aquarium	7	7
Water		Aquarium	9	
Water		Wild	3	

Captive spotted eagle rays and cownose rays were housed in the Georgia Aquarium OV exhibit, a 6.3 million gallon artificial sea-water (Atlanta tap water mixed with Instant

Ocean, Blacksburg, VA, USA) tank containing thousands of fish (sharks, rays, and teleosts) representing over 50 species from the open ocean. The water from the exhibit was filtered through a complex filtering system composed of foam fractionators (protein skimmers), sand filters, ozone contact towers, countercurrent heat exchangers, sulfur-based denitrification vessels, and a deaeration tower, at a rate of 130,000 gallons per min, turning over the exhibit water of approximately 4 million gallons once per hour (Patin, Pratte et al. 2018). Physico-chemical parameters of the exhibit were kept within a tight range with a temperature of about 24 °C, and a salinity of about 33 ppt. Approximately 225 kg of food goes into OV daily, 75 kg of which is broadcast into the system, while the remaining 150 kg is target fed to specific individuals such as the spotted eagle rays. These rays were target fed a daily ration of 1.3-1.5% their body weight consisting of surf clam (*Spisula solidissima*), hard-shell clam (*Mercenaria mercenaria*), Jonah crab (*Cancer borealis*), knobbed whelk (*Busycon carica*), Atlantic sea scallops (*Placopecten magellanicus*), whiteleg shrimp (*Litopenaeus vannamei*) and blue mussels (*Mytilus edulis*). In contrast, cownose rays were fed from pumping a variety of food options (~ 40 kg) including capelin, Pacific herring, mackerel, surf clam, shrimp, and night smelt, into the bottom of the exhibit once or twice a day.

For wild spotted eagle ray sample collection, rays were circled with a net and brought on board the ship in a water bath to collect the samples. Samples were collected for captive individuals during routine veterinary examinations performed at least once a year or more frequently as veterinary or husbandry needs dictated. For these examinations, animals were transferred from the main exhibit into a small holding pool with oxygenated water. The rays were lightly restrained for the dorsal skin swab sampling and then placed

into tonic immobility for gill and cloacal swab collection. After examination, the rays were released into the main exhibit and often resumed feeding the same day. Because microbiome samples were collected during routine veterinary examinations, which frequency could vary between individuals, certain individuals were sampled more than once during the same sampling period.

Multiple body sites were swabbed for each captive and wild spotted eagle rays and captive cownose ray, including the gills, cloaca, and dorsal skin (Figure 1). For all rays, microbiome swabs were collected by gently rubbing sterile swabs along the gill, cloaca, or skin, making sure to accumulate material (mucus, skin sloughing and microbes) over the entire surface of the swab. Swabs were placed into 2 mL cryovials containing 1 mL of RNA/DNA stabilizing solution and stored at -80°C until lab processing. Water samples were also obtained from both the captive and wild environment. Water samples from the OV water column were collected by filtration through 0.2 µm Sterivex filters (as described in (Patin, Pratte et al. 2018), and were obtained as part of 3-year time series monitoring program involving biweekly collections; the water column samples analyzed here correspond to those collected nearest in time (within 2 weeks) to each animal sampling event. Water samples from the wild environment were collected at 3 locations in the same area where the animals were sampled. These water samples were filtrated through a 0.2 µm Isopore membrane filter (Millipore), as in (Pratte, Longo et al. 2018), and were only collected in 2018, at the same time as the spotted eagle ray sampling.

DNA was extracted from each swab by transferring the swabs directly into

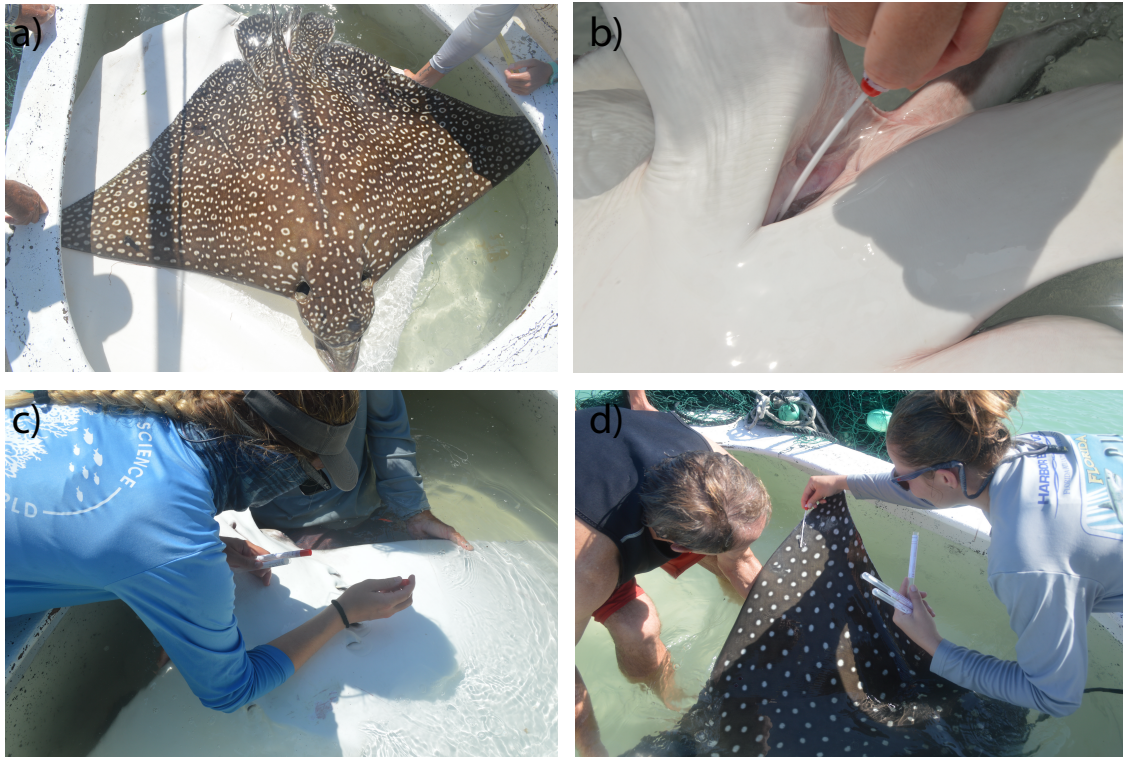


**Figure 2.1. Pictures demonstrating sample collection for wild spotted eagle rays (*Aetobatus narinari*):** a) a spotted eagle ray in the water bath after being brought on board the ship, b) cloaca sampling, c) gill sampling, d) skin sampling. All samples were collected by gently rubbing sterile swabs along the target body site.

Powerbead tubes from the Qiagen DNeasy PowerSoil DNA extraction kits and following the manufacturer's instructions. Extraction blanks (no swab or material added) were performed for each new kit. For each sample, the V3-V4 region of the 16S rRNA gene was amplified by polymerase chain reaction (PCR) using the primers F515 and R806 (Caporaso, Lauber et al. 2011), each appended with barcodes and Illumina-specific adapters as described previously (Kozich, Westcott et al. 2013). Reaction mixtures included 2 to 5  $\mu$ L DNA template, 12.5  $\mu$ L Hot Start Taq PCR MasterMix (VWR), 0.25  $\mu$ L (each) forward and reverse primers (20  $\mu$ M), and 0.5  $\mu$ L bovine serum albumin (BSA) (20 mg/ml; New England BioLabs Inc.). PCR conditions included an initial 1 min

denaturation at 94°C, followed by 30 cycles of denaturation at 94°C (1 min), primer annealing at 55°C (2 min), and primer extension at 72°C (90 s) and then a final extension at 72°C for 10 min. The amplicon products were pooled at equimolar concentrations and purified with Diffinity RapidTip2 PCR purification tips (Diffinity Genomics, NY). Amplicons were sequenced on an Illumina MiSeq machine across 4 different runs, using a V2 500-cycle kit (250 X 250 bp) with 5% PhiX to increase read diversity.

### 2.3.2 *Illumina data processing*

Sequence data were analyzed using DADA2 (Callahan, McMurdie et al. 2016) and QIIME 2 2019.4 (Bolyen, Rideout et al. 2019). Raw sequence data were demultiplexed, quality filtered, trimmed to 150 bp, and denoised following the DADA2 pipeline from (Callahan, McMurdie et al. 2016). Taxonomy was assigned to amplicon sequence variants (ASVs) using the SILVA-132 database. The resulting representative sequences, taxonomy and ASV tables, were imported into QIIME 2 2019.4 (Bolyen, Rideout et al. 2019). Sequences classified as *Chloroplast* or *Mitochondria* were removed from the dataset. Extraction blanks were processed following the same procedures, one of which was highly dominated by *Mollicutes*. As a result, all *Mollicutes* were removed from the entire dataset, and the contaminated kit was not used again.

### 2.3.3 *Statistical analysis*

All (ASVs) were aligned with Mafft (Katoh, Misawa et al. 2002), via q2-alignment, and used to construct a phylogeny with fasttree2 (Price, Dehal et al. 2010), via q2-phylogeny. Based on the variation of  $\alpha$ -diversity as a function of sampling depth (Shannon Diversity and Faith's phylogenetic Diversity (Faith 1992) computed using the q2-diversity

plugin in QIIME2), samples were rarefied (subsampling without replacement) to 1150 reads. Surface swabs of marine animals tend to produce low DNA yields which can result in higher stochasticity of data. To address this, our sample set contained some biological replicates (two separate samples taken from the same individual and body site at the same sampling event) and all samples had technical replicates (same sample either amplified twice, or sequenced twice). To identify outliers in our replicates, weighted UniFrac (Lozupone, Hamady et al. 2007) distances between replicates (biological and technical) from the same sample were calculated using the q2-diversity plugin. Weighted UniFrac distances from all samples with their replicates were then pooled and subsequently plotted in a boxplot. Values above Q3 were considered outliers and removed accordingly; this resulted in the removal of 1 sample with 4 replicates. After removing these outliers, replicates were merged for each sample to increase rarefaction depth to 1500. After quality control and merging replicates, 139 samples remained. A summary of the samples in the final dataset and the associated metadata can be found in Tables A.1 and A.2. All subsequent analyses were performed using this merged ASV table, unless specified.

$\alpha$ -diversity metrics (observed ASV number, Shannon, Pielou, and Faith's Phylogenetic Diversity indices) and a Kruskal-Wallis test were computed to identify significant differences between captive spotted eagle rays, wild spotted eagle rays, and captive cownose rays, for each body site.  $\beta$ -diversity dissimilarity matrices (Bray-Curtis, weighted and unweighted UniFrac distances) were calculated using q2-diversity plugin in QIIME2 and used to construct Principle Coordinate Analysis (PCoA) using Primer-e v.7 (Clarke 2015). PERMANOVA and PERMDISP tests were subsequently performed to identify significant differences in microbiome composition and the level of inter-individual



variability in microbiome composition between captive spotted eagle rays, wild spotted eagle rays, and captive cownose rays, for each body site.

To identify the proportion of ASVs shared between different microbial pools, four separate Venn diagrams were constructed in Python using the package `matplotlib-venn` 0.11.5, and the merged ASV table rarefied to 1500 sequences. Venn diagram calculations were performed to assess the number of ASVs shared with seawater. ASVs shared between seawater and host microbiomes were removed to assess the number of ASVs shared between body sites, animals from different environments (wild vs. captive), and species (spotted eagle ray vs. cownose ray). For each body site, we identified ASVs that differ in abundance between captive and wild individuals using the package `DESeq2` in R (Love, Huber et al. 2014) with the non-rarefied merged ASV table. For this analysis, we removed ASVs that were detected in both the host-associated and seawater microbiomes.

## **2.4 Results**

### *2.4.1 Differences in microbial composition according to captivity status*

Samples that were used for 16S rRNA gene sequencing included cloaca, gill and skin samples from captive spotted eagle rays and cownose rays at Georgia Aquarium, and from wild spotted eagle rays from Sarasota Bay, as well as samples from the surrounding water for both environments. After quality filtering, trimming, merging of replicates, and rarefaction, 139 samples remained in the final dataset (Table 2.1, Table A.1). From these, we detected a total of 5,398 ASVs. 1,916 ASVs were detected in captive spotted eagle rays (cloaca – 549; gills – 1188; skin – 1118); 1,694 ASVs were detected in captive cownose rays (cloaca – 738; gills – 1006; skin 803); 3,031 ASVs were detected in wild spotted eagle

rays (cloaca – 909; gills – 1785; skin - 2143). These ASV numbers include some ASVs shared between body sites, species, and environments (captive vs. wild).

For each body site, microbiomes of captive eagle rays were significantly less rich (observed ASVs) compared to those of wild individuals (Figure 2.2, Table A.2).

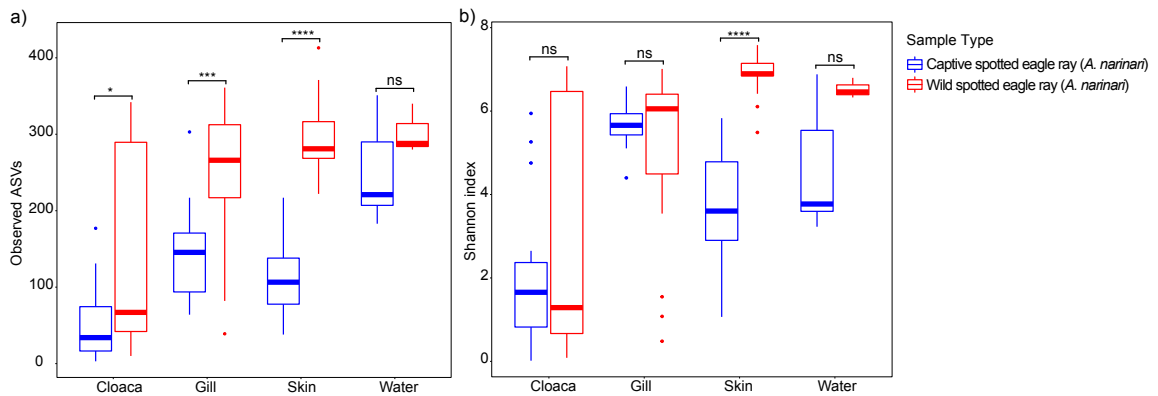


**Figure 2.2  $\alpha$ -diversity metrics** a) observed ASVs, and b) Shannon diversity index, for different body sites (cloaca, gill, and skin of captive and wild spotted eagle rays (*Aetobatus narinari*), along with their respective water samples. Captive spotted eagle rays have lower diversity for all body sites compared to wild spotted eagle rays.

The same general pattern was observed using various  $\alpha$ -diversity indexes, despite comparisons not always being statistically significant (Table A.2). Similarly, for each body site, spotted eagle ray microbiome composition ( $\beta$ -diversity) differed significantly between captive and wild individuals (Figure 2.3, Table A.3).

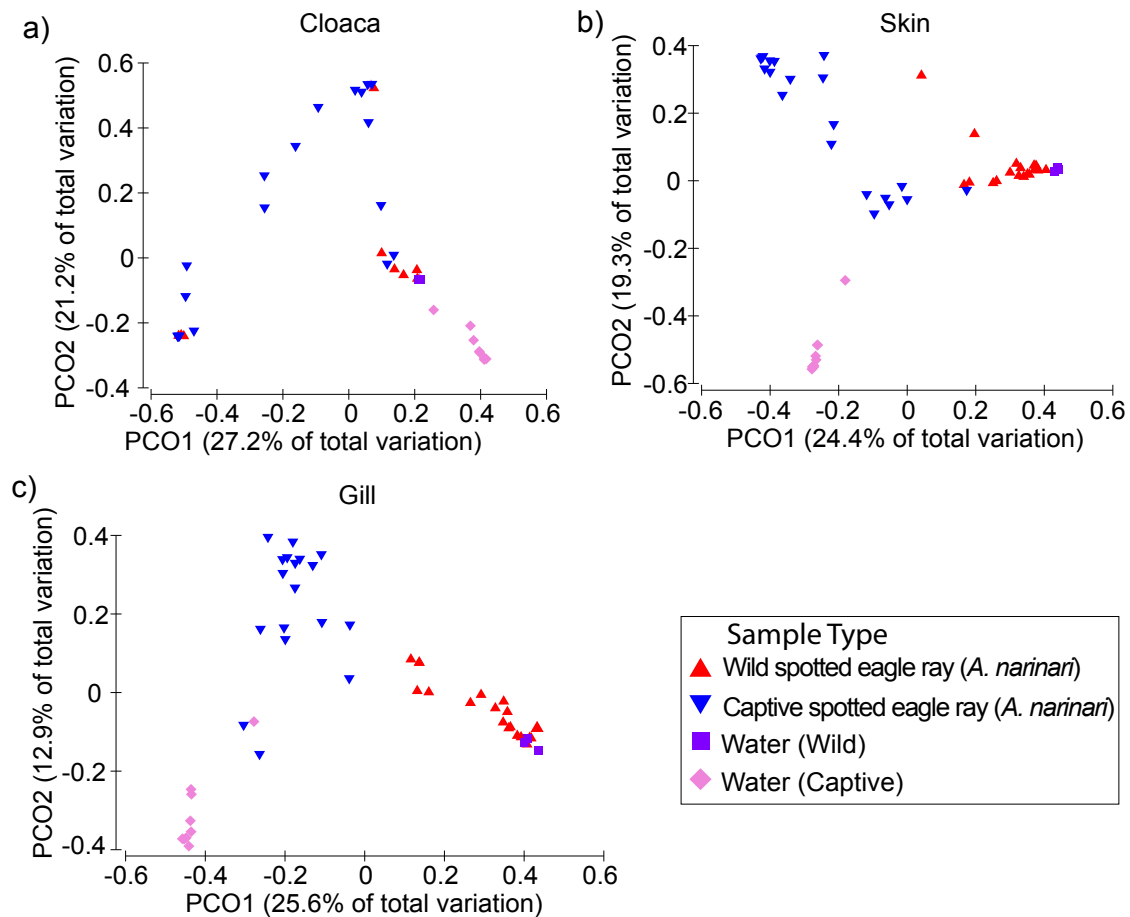


**Figure 2.3 Principal coordinate analysis (PCoA) of  $\beta$ -diversity comparison using Bray-Curtis distances between wild spotted eagle rays (*Aetobatus narinari*), and captive spotted eagle rays (*Aetobatus narinari*) for a) cloaca, b) gill, and c) skin samples. Note that wild spotted eagle rays harbor different microbial communities than captive spotted eagle rays, and both captive and wild spotted eagle rays harbor microbial communities that differ from the surrounding water for all body sites. Interestingly, cloaca samples show higher overlap, suggesting higher similarities compared to more external body sites (gill and skin)**

Cloaca microbial composition was more similar between captive and wild individuals compared to other body sites (Figure 2.3, Figure A.1), and this difference was not significant based on weighted UniFrac distances (Table A.3). Dispersion analyses measuring the level of inter-individual variability showed no significant differences in cloaca microbial community composition between captive and wild spotted eagle rays, while the significance of the change differed based on the metric used for gill and skin

microbiomes (Table A.4). For all body-sites, microbiomes of captive cownose rays clustered apart from those of captive and wild spotted eagle rays, while being more similar to those of captive spotted eagle rays (Figure A.2, Table A.3). Microbiome dispersion of captive cownose rays was also not significantly different from the one of captive eagle rays for all body sites (Table A.4).

#### 2.4.2 Differences in microbial composition according to body site niche

Using datasets partitioned based on ray species and captivity status (captive spotted eagle rays, wild spotted eagle rays, and captive cownose rays), we analyzed microbiome composition among body sites. For each ray group, cloaca microbiomes were significantly less diverse compared to those of other body sites, and seawater (Figure A.3, Table A.5). The microbial composition of spotted eagle ray microbiomes also varied among body sites (Figure 2.4, Table A.6); this was not true for cownose ray microbiomes (Figure A.4, Table A.6).

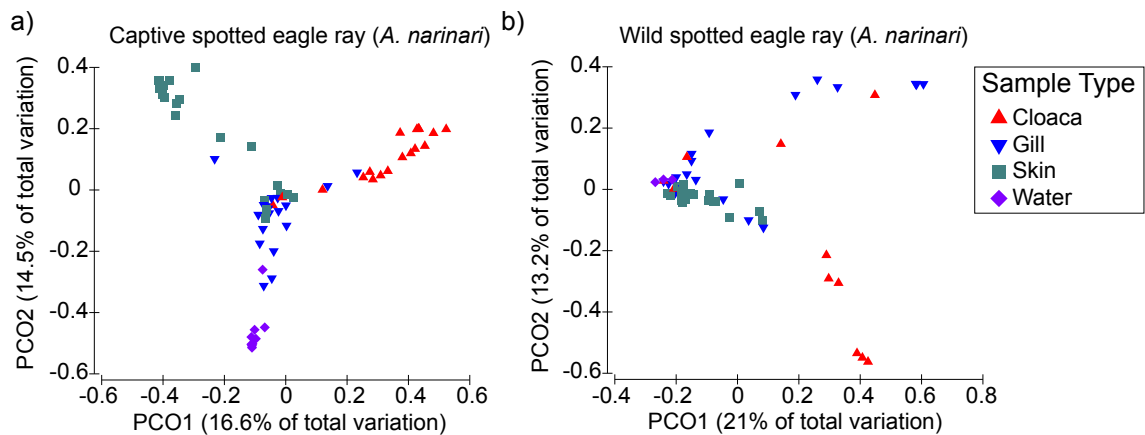


**Figure 2.4. Principal coordinate analysis (PCoA) based upon Bray-Curtis dissimilarity matrices between cloaca, gill, skin, and water for a) captive spotted eagle rays (*Aetobatus narinari*), and b) wild spotted eagle rays.** Note that different body sites have different microbial community structures that differ from the surrounding water, as indicated by the separate clustering. In captive spotted eagle rays, the gills appear more similar to the surrounding water, while the skin is more similar to the surrounding water in wild spotted eagle rays

For both eagle and cownose rays, the microbiome of gills and skin were more similar to the surrounding environment (Figure 2.4, Figure A.1, Figure A.5) but remained significantly distinct (Table A.6). Interestingly, the microbiome of wild spotted eagle rays was not always statistically distinct from seawater depending on the metric used (Table A.6). No significant compositional differences were associated with date of sampling, weight, disc width or sex, for either wild or captive rays.

While the proportion of ASVs shared between the cloacae of wild and captive spotted eagle rays was lower compared to that of ASVs shared among other body sites, these ASVs represented a fraction of the cloaca microbial community 3 to 11 times higher compared to ASVs shared between gills or skin of captive and wild individuals (Table A.7). In contrast, the fraction of the microbiome represented by ASVs shared with seawater was similar for all body sites in wild spotted eagle rays, while it was the lowest for the cloaca microbiome of captive spotted eagle rays (Table A.7). Interestingly, ASVs shared between the cloaca, gills, and skin microbiomes, represented the lowest proportions and relative abundances of the gill and skin microbiomes compared to the cloaca, for cownose and spotted eagle rays (Table A.8).

#### *2.4.3 Taxonomic composition of the microbiome of spotted eagle rays and cownose rays*

At the phyla level, cownose rays and spotted eagle rays shared a similar taxonomic composition, as all samples were dominated by *Proteobacteria*, *Bacteroidetes*, and *Firmicutes*. *Bacteroidetes* were abundant in the cloaca, while *Cyanobacteria* and *Actinobacteria* had higher proportions in the gills and skin where *Proteobacteria* were also more prevalent. At finer taxonomic levels, cownose rays' microbiome was distinct from

that of spotted eagle rays. Major differences were observed in the cloaca and skin microbiomes where an unclassified species from the genus *Kordiimonas*, and another one from the class *Rhodobacteraceae* were at least 2 times more abundant in cownose rays compared to spotted eagle rays, (Figure A.1).

A single ASV classified to bacterial species *Photobacterium damsela* and others from the Order *Flavobacteriales* were abundant in cloaca microbiomes of spotted eagle rays, constituting  $\sim 23\% \pm 31$  and  $\sim 34\% \pm 43\%$  of total sequences, respectively, across both captive and wild individuals.

Differential abundance analyses performed using DESeq2 showed that most microbial ASVs that differed significantly in frequency between wild and captive spotted eagle rays such as SAR11-clade Ia members, *Synechococcus*-CC9902, and *Tyzzarella* sp., more abundant in wild spotted eagle rays or *Helcococcus* sp., more abundant in captive rays (Figure A.1), were also found in the surrounding water (Figure A.5). After removing these ASVs, no cloaca ASVs were found to be differentially abundant between wild and captive eagle rays. Based on the gill data, only one ASV, identified as *Kistimonas* sp., was significantly enriched in wild versus captive spotted eagle ray microbiomes. This ASV was present in two wild individuals (at 12.5% and 34.3%) and was absent from all gill microbiomes from captive individuals. Based on the skin data, only one ASV, identified as *Alkanindiges illinoisensis*, was significantly enriched in captive versus wild spotted eagle ray microbiomes. This ASV was present in half of captive datasets, but at an average of only 0.3%; it was absent from all skin microbiomes from wild individuals.

#### 2.4.4 Potential spotted eagle rays' core microbiome

We defined a core microbiome as ASVs shared between captive and wild spotted eagle rays, excluding ASVs that were also found in seawater. Based on these criteria, no shared ASVs between captive and wild spotted eagle rays were shared by all individuals, and the proportion of individuals sharing a specific ASV also varied between captive and wild environments. We found 72, 216, and 306 ASVs identified as ‘core’ in the cloaca, gill, and skin microbiomes, respectively. The cloaca core microbiome was primarily composed of *Proteobacteria*, *Bacteroidetes*, and *Firmicutes*. An ASV classified in the Order *Flavobacteriales* represented an average of 39% and 26% of sequences in captive and wild cloacal datasets, respectively. Apart from this ASV, > 95% of the cloaca core ASVs had frequencies under 2%. Similarly, the gill and skin core microbiomes were primarily composed of *Proteobacteria*, *Firmicutes*, and *Bacteroidetes*, as well as *Actinobacteria*. An ASV classified in the Order *Betaproteobacteriales* represented an average of 1% and 24% of sequences in captive and wild gill datasets, respectively. None of the core ASVs of the gill represented over 3% of sequences in captive ray microbiomes. On the skin, an ASV identified as *Helcococcus* sp. represented an average of 32% and 2% of sequences in captive and wild datasets, respectively. A core skin ASV classified as ‘unknown bacterium’ represented 8% of skin sequences from captive rays. All other core skin ASVs had frequencies under 3%.

ASVs classified as genera containing known fish opportunistic pathogens were found in spotted eagle rays and cownose rays (Table A.9). While average proportions of the majority of these potential pathogens remained under 1% in captive and wild rays, members of the genus *Photobacterium*, and more specifically one ASV identified as *Photobacterium damsela* showed average relative abundances of up to 26% in cloaca

microbiomes where it dominated the microbial community and was more abundant in captive compared to wild individuals (Figure A.1). Moreover, the gill and skin core microbiomes also contained ASVs classified as genera containing opportunistic pathogens, including *Streptococcus*, *Clostridium*, and *Vibrio*, all at frequencies under 0.1%.

## 2.5 Discussion

### 2.5.1 Environmental influence (Captive vs. Wild)

In this study, we characterized the microbiome of the spotted eagle ray (*Aetobatus narinari*), focusing on differences between captive and wild individuals, and used microbiome data from captive cownose rays (*Rhinoptera bonasus*) to distinguish the relative influence of phylogeny and body site. Captive cownose ray microbial community was distinct from that of captive spotted eagle rays, demonstrating that the phylogeny and relatedness of hosts is an important factor shaping the microbiome, as has been observed in other animals (Chiarello, Auguet et al. 2018, Tarnecki, Brennan et al. 2019). The microbiome of spotted eagle rays also differed according to captivity status with the cloaca microbial communities being more similar between captive and wild individuals compared to those of the skin and gills, suggesting that the cloaca may be more influenced by gut microbes which are potentially more conserved compared to microbes from external body sites that are constantly exposed to the environment.

We also found significantly lower diversity estimates in captive spotted eagle ray samples. Previous studies on marine and terrestrial animals have shown decreases in  $\alpha$ -diversity associated with captivity (McKenzie, Song et al. 2017, Webster, Consuegra et al. 2018, Tarnecki, Brennan et al. 2019), reinforcing the idea that captivity can decrease



microbiome diversity in animals. In most captive animals, changes in  $\alpha$ -diversity are accompanied by shifts in the structure of the microbial community ( $\beta$ -diversity) (McKenzie, Song et al. 2017, Webster, Consuegra et al. 2018, Tarnecki, Brennan et al. 2019, Uren Webster, Rodriguez-Barreto et al. 2020). Such differences in  $\beta$ -diversity were observed in captive vs wild spotted eagle rays for both internal (cloaca) and external (skin and gills) body sites, suggesting that environmental and dietary changes may influence spotted eagle rays' microbiome composition. While there is concern that decreases or changes in microbiome diversity may cause shifts or losses in metabolic functions carried out by specific microbes (Amato, Yeoman et al. 2013) and may hinder the success of reintroduction efforts (Redford, Segre et al. 2012), these changes are often host species specific, and hard to link to host metabolism and health.

Differences in wild vs captive microbial community structure were accompanied by taxonomic differences for all body sites. Microbes often found in aquatic environments such as *Betaproteobacteriales*, SAR11, and *Synechococcus* were found in higher proportions in wild spotted eagle ray microbiomes at all body sites, suggesting that most of these microbes are transient and probably lost upon captivity. Specifically, *Tyzzereella* sp. had an average relative abundance over 300 times higher in the cloaca of captive vs wild spotted eagle rays. *Tyzzereella* sp. have been previously found in the gut microbiota of a variety of animals (Ijaz, Sivaloganathan et al. 2018, Shui, Yang et al. 2019, Shao and Zhu 2020), and have appeared to vary with dietary shifts (Shao and Zhu 2020, Zhang, Chen et al. 2020). Only one ASV identified as *Kistimonas* was significantly more abundant in the gills of wild spotted eagle rays compared to captive ones. *Kistimonas* and *Kistimonas*-like species have been previously identified as part of a several invertebrate's gill (Lim, Davis

et al. 2019) and skin (Choi, Kwon et al. 2010) microbiomes, and include potentially pathogenic species (Lee, Shin et al. 2012).

Previous studies have shown that fish external surfaces such as the skin can be majorly influenced by environmental and neutral processes (Chiarello, Paz-Vinas et al. 2019). For example, Krotman and collaborators showed that water pollution could cause dysbiosis in fish skin communities, highlighting the important effect of the environment on fish skin microbiomes (Krotman, Yergaliyev et al. 2020). Perhaps not surprisingly, the skin microbiota showed the strongest difference in taxonomic composition between captive and wild spotted eagle rays. *Helcococcus*, which was over 10 times more abundant in skin samples of captive spotted eagle rays, are known for colonizing diverse body sites in marine animals including the respiratory tract of dolphins (Godoy-Vitorino, Rodriguez-Hilario et al. 2017, Vendl, Nelson et al. 2020) and whales (Vendl, Slavich et al. 2020), and in the gut of *Cephalopholis urodeta*, a carnivorous coral reef fish (Gao, Zou et al. 2020). Despite its low abundance ( $< 0.5\%$ ), the only ASV significantly differentially abundant between the skin microbiome of captive and wild spotted eagle rays was *Alkanindiges illinoisensis*, which was only present in captive individuals. This microorganism is an alkane-degrading bacterium that has not been reported in marine ecosystems (Bogan, Sullivan et al. 2003, Rastogi, Sbodio et al. 2012, Williams and Marco 2014, Fuentes, Barra et al. 2016, Colvin DO and Fagg 2020, Yadav, Kim et al. 2020). However this ASV found on the skin of captive spotted eagle rays shared 100% sequence identity with an uncultured prokaryote (sequence ID: MT067094.1) found in the sediments of Lake Ohrid (Thomas, Francke et al. 2020), which suggests that this microbe can also be found in aquatic environments.

### 2.5.2 Species influence (*Eagle ray* vs. *cownose ray*)

Spotted eagle rays and cownose rays shared the same major taxonomic groups, and diversity pattern for each body site. In accordance with previous studies (Sylvain, Holland et al. 2020), the cloaca was less diverse compared to the gills and skin. Cloaca microbial communities showed low prevalence of *Proteobacteria* compared to skin and gills. This was accompanied by higher relative abundances of *Bacteroidetes* while *Cyanobacteria* and *Actinobacteria* showed lower relative abundances than in the gills or skin. In contrast, *Firmicutes* had higher relative abundances in skin samples. All these same patterns of abundance were recovered in a previous analysis of teleost fish-associated microbial communities (Ruiz-Rodríguez, Scheifler et al. 2020), suggesting these groups are widespread in fish.

Cownose rays' microbial communities were significantly different from those of spotted eagle rays for all body sites and from that of seawater, highlighting the effect of host species on microbiome assembly. The skin and gill microbiomes from these ray species were more similar compared to those from the cloaca, suggesting that the influence of phylogeny is more pronounced in the cloaca microbiome. In particular, an unidentified *Betaproteobacteriales-Incertae-Sedis* ASV was significantly more abundant in cownose rays' cloaca, while an ASV identified as *Tyzzrella* sp. was significantly more abundant in spotted eagle ray's cloaca and gill microbiome. No ASVs with a relative abundance above 1% were significantly differentially abundant between the skin microbiome of spotted eagle and cownose rays.

Interestingly, while spotted eagle rays' microbiome community structure ( $\beta$ -diversity) differed between different body sites, this was not the case for cownose rays.

This result could suggest that body site niche has a smaller influence on microbiome composition in this species compared to spotted eagle rays. The cownose ray sample size was low (7 individuals); additional studies may be needed to distinguish clear niche separation.

### 2.5.3 Physiology influence (*skin vs. gills vs. cloaca*)

The proportion of ASVs shared between the cloacae of wild and captive spotted eagle rays was smaller compared to the one shared between the cloacae and seawater, but was mostly composed of dominant members of the community, while the larger fraction shared by the cloaca and water samples included mostly rare members. These results suggest that fewer ASVs with higher relative abundances compose cloaca's core microbiome, while environmental ASVs may potentially remain transient. In the core cloaca microbiome, one unidentified *Flavobacteriales* was the most abundant, contributing up to 99% in certain samples. These microbes have been previously recognized as part of the intestinal microflora of trout (Kim, Brunt et al. 2007) and other marine fish (MacDonald, Stark et al. 1986, LeaMaster, Walsh et al. 1997). However, certain *Flavobacterium* species have also been associated with disease in fish (Ekman, Börjeson et al. 1999, Wahli and Madsen 2018). These results suggest that the constant contact of the cloaca to gut microbes influences cloaca microbiome composition. While the gut microbiome can be influenced by habitat modifications (Eichmiller, Hamilton et al. 2016, Hyde, Navas-Molina et al. 2016), this microbiome niche may be relatively stable compared to those of more external body sites. Host-intrinsic factors such as age and health status can also influence gut microbiome composition. The factors underlying stability differences among body sites are uncertain but it is hypothesized that host physiology and

diet may play a relatively stronger role in regulating microbiome composition in the gut, whereas environmental parameters play a relatively stronger role in regulating microbiome composition in more external body sites (Sylvain, Cheaib et al. 2016, Sylvain, Holland et al. 2020). Alternatively, the relative similarity in cloaca microbiomes between wild and captive individuals might suggest that the diet of captive animals (clams, crab, whelk, scallops, shrimp, and mussels) is either similar to that of wild individuals or host physiology prevents a major change in gut microbiome structure

On the other hand, gill and skin spotted eagle ray's microbiomes were more similar to that of the surrounding water. While the proportion of ASVs shared for these body sites between captive and wild spotted eagle rays was higher compared to those shared for the cloaca, they represented a smaller fraction of the microbial community. Moreover, ASVs shared with seawater represented a similar or larger fraction of the gill and skin microbiome compared to the cloaca, highlighting a stronger influence from the environment. However, the skin and gill microbiomes shared under 50 % of ASVs with any body site, which suggests an influence from the host in these external body sites. These probably harbor microbes that act as a protective barrier against potential environmental pathogens (Marshall and Bellamy 2010, Boutin, Audet et al. 2013, Peatman, Lange et al. 2015, Derome, Gauthier et al. 2016). Among the ASVs composing the gill core microbiome, one identified as a species of the order *Betaproteobacteriales* was particularly abundant in the gills of wild spotted eagle rays. These microbes have previously been found in various aquatic environments (van der Kooij, Veenendaal et al. 2018, Picazo, Rochera et al. 2019), and appear to be enriched in fish gill microbiomes (Pratte, Patin et al. 2018). Finally, as part of the skin core microbiome of spotted eagle rays, one ASV identified as *Helcococcus*

was particularly abundant on the skin of captive spotted eagle rays. This ASV had 98% identity with an uncultured bacterium clone from California sea lion rectal swabs (Bik, Costello et al. 2016), as well as with an uncultured bacterium from the skin of fur seals (Grosser, Sauer et al. 2019). The presence of multiple unclassified ASVs in the different body sites of spotted eagle rays, with low identity levels to previously described microorganisms, indicates a large uncharacterized fraction of the microbial community and opens the possibility to find novel organisms with metabolic adaptations that allow them to colonize and survive in the particular conditions associated with marine life.

#### 2.5.4 *Potential pathogens*

*Flavobacteriales* species and *Photobacterium damsela* dominated the gut microbial community of both wild and captive rays, although it is important to point out that *Photobacterium* harbor several copies of the 16S rRNA gene (Pei, Oberdorf et al. 2010), which may result on an overestimation of their proportion in the microbial community. Despite the potential pathogenicity of this microbe (Pedersen, Dalsgaard et al. 1997), rays appeared healthy based on medical assessments, which suggests that the strain found in these animals may not be pathogenic. Indeed, this bacterium has been identified as a common constituent of elasmobranch's skin and blood microbiome (Grimes, Brayton et al. 1985, Mylniczenko, Harris et al. 2007, Givens, Ransom et al. 2015). The Anna-Karenina principle relies on the idea that microbiome perturbations translate into a variety of unstable states, and not a single dysbiotic state (Zaneveld, McMinds et al. 2017), and might be relied upon to estimate animal health. No statistically significant differences in the level of inter-individual variability (dispersion) of the cloaca microbiome were observed, suggesting that captive individuals do not harbor a disturbed cloaca microbiome.

Moreover, the absence of clear outliers or high abundances of potentially pathogenic microbial species in either captive or wild individuals suggests that captive spotted eagle rays are not less healthy than their wild counterparts. While wild individuals appeared healthy, their health status was not medically determined, nor was their age, and these factors may contribute to some of the variation we observe in this study. However, it is unlikely that all animals sampled were the same age, suggesting that the patterns observed are majorly driven by other parameters such as changes in environmental conditions.

## **2.6 Conclusion**

This study is the first to characterize the microbiome of spotted eagle rays and compare captive versus wild individuals. We found that while captive individuals experienced lower diversity and a different microbiome composition than wild rays, the extent of the change was modulated by body site niche. The gut microbiome was more conserved between captive and wild spotted eagle rays compared to the gills and skin. However, the microbiome from all spotted eagle rays' body sites still remained different from the one of sea water and from those of cownose rays, highlighting the influence of host related factors in spotted eagle rays' microbial community assembly. The presence of multiple unclassified ASVs as part of spotted eagle rays' core microbiome underlines its uniqueness, and the need for future work to better characterize the structure and function of these microbial communities and their role in host health. Moreover, the low relative abundance of potential pathogens suggests that both captive and wild individuals were healthy, and that captivity had not impaired host health. Our findings lay down a framework to determine what a healthy microbiome looks like in spotted eagle rays, and the relative influence of environmental versus host specific factors in shaping this

microbiome. Future research considering microbial function and using larger sample sizes could help bridge the gap between microbiome composition and host health, and potentially find microbial markers of host and ecosystem health used to improve conservation strategies.



**CHAPTER 3. THE MICROBIOME OF THE AFRICAN  
PENGUIN (*SPHENISCUS DEMERSUS*) REFLECTS THEIR  
LIFESTYLE BETWEEN LAND AND SEA**

Disclaimer: This chapter is currently in final manuscript form

### 3.1 Abstract

Host associated microbiomes are tightly linked to host's physiology, metabolism, behavior and ecology. Establishing baselines for wild animals' microbiome, the relative influence of environmental factors and how it varies across different body sites, is particularly important to better understand species ecology and develop new conservation strategies. While captivity can alter animals' microbiota, the stability and strict monitoring of environmental factors, provides ideal conditions to explore these questions. In this study, we examined how variable the microbiome of African penguins (*Spheniscus demersus*) from Georgia Aquarium is between body sites and how these compare to environmental samples to determine the level of microbiome similarity with the environment relative to body site niche. Moreover, we compared the penguin oral and fecal microbiome to those of other vertebrate hosts, to determine the differential effect of phylogeny in structuring the microbiome of these two body sites. The oral and fecal penguin microbiomes were distinct from each other and environmental samples, while microbiomes from all other body sites were similar to the surrounding environment. Interestingly, the penguin oral microbiome was more similar to that of other marine mammals, while their cloaca microbiome was more similar to that of wild birds, which suggests that the particular lifestyle of penguins highly influences their oral microbial community, while host associated factors may play a larger role in the gut. The penguin microbiome also showed the highest proportions of unique sequences compared to other vertebrates, highlighting the specificity of penguin's associated microbial communities. Our results suggest that African penguins harbor unique microbial communities that reflect their specific lifestyle between land and sea, with variations according to body site niche. This study contributes

to establishing a baseline for penguin's microbiome, and provides a framework relating host associated and environmental factors to microbiome composition. Future studies can use this knowledge to identify biomarkers and link microbiome composition to host health.

### **3.2 Background**

It is now widely accepted that host associated microbes are a crucial component of vertebrate's digestion, organ development, immune system function, behavior, protection against pathogens, and overall health (Qin, Li et al. 2010, Heijtz, Wang et al. 2011, Al-Asmakh, Stukenberg et al. 2014). Because of its important role in organismal development and health, determining the diversity, function, and variability of the gut microbiome across different animal hosts has received increased attention. Indeed, while intra-specific variability in both microbial richness and abundance exists (Eckburg, Bik et al. 2005, Hird, Carstens et al. 2014), gut microbial communities appear more similar in closely related organisms and can affect processes that extend beyond the individual, such as mating and reproduction, but also pathogenic load, spread of disease or even the vectorization of antibiotic resistant genes (Sharon, Segal et al. 2010, Marcelino, Wille et al. 2018).

Despite the increasing body of work related to microbiomes, those of wild animals remain understudied. In particular, little is known about wild birds' microbial communities, how they compare to other vertebrate's microbiomes, and their potential effect on host health. Birds are a widespread, abundant and diverse lineage that encompasses a variety of morphologies, feeding preferences, life history traits, and ecological characteristics (Jenkins, Pimm et al. 2013). From previous research, we know that similarly to other vertebrates, birds' gut microbiota is composed of 4 major phyla including Firmicutes, Bacteroidetes, Actinobacteria, and Proteobacteria, with variable relative abundances

between species, and greater divergence in microbial richness and abundance at finer taxonomic levels (Grond, Sandercock et al. 2018). While phylogeny appears as the primary component differentiating gut microbiotas' composition (Dewar, Arnould et al. 2013, Waite and Taylor 2014, Hird, Sánchez et al. 2015, Kropáčková, Těšický et al. 2017), other extrinsic factors such as environmental conditions and social interactions, and intrinsic factors such as diet, age and gender, reproduction, gut physiology and host health have also been shown to influence the establishment and composition of birds' and other vertebrates' microbiota (Ley, Peterson et al. 2006, Banks, Cary et al. 2009, Wienemann, Schmitt-Wagner et al. 2011, Roggenbuck, Schnell et al. 2014, Ding, Cao et al. 2017, Jiang, Ma et al. 2017). For example, environmental parameters such as the nesting environment can shape birds microbiome and may be more important in shaping chicks' microbiota than genetic factors in penguins and Great tits (Lucas, Moureau et al. 2005, Dewar, Arnould et al. 2013, Barbosa, Balagué et al. 2016, Dewar, Arnould et al. 2017). However, the relative effect of these factors is not known and may vary depending on species, developmental stage, life history characteristics, and geographical location, among others. Moreover, because the collection of feces and cloacal swabs are relatively safe and non-invasive methods, most studies have solely relied on these types of samples, leaving other areas of the GIT (gastrointestinal tract) and other body sites unsampled, despite studies showing that different body sites harbor distinct microbial communities with different functional diversity and are differentially affected by both intrinsic and extrinsic factors (Grond, Sandercock et al. 2018).

In contrast to most sections of the GIT, the oral microbiome is largely exposed to external components including air and food which is then moved through the rest of the

gut. Because it is the first compartment of the GIT, microbes can be easily transferred from the oral cavity to other sections of the GIT, underlining the importance of the oral system as part of the digestive process but also as a potential reservoir and vector of pathogens and disease (Costalonga and Herzberg 2014, Blod, Schlichting et al. 2018, Philip, Suneja et al. 2018, Wasfi, Abd El-Rahman et al. 2018). Despite the importance of the oral cavity, fewer studies have explored its microbial composition, and most are focused on mammals with an emphasis on humans. The structure of the oral cavity varies among certain vertebrate lineages, affecting the specific environments inside the mouth, and potentially influencing the associated microbial communities. On the other hand, environmental factors such as diet have been shown to also influence the oral microbiome (Kato, Vasquez et al. 2017, Murtaza, Burke et al. 2019).

To our knowledge, no studies have explored the microbiome of the African penguin (*Spheniscus demersus*). Like other wild birds, it is now considered an endangered species; their population has decreased by ~70 % in 50 years, and is still decreasing (Paleczny, Hammill et al. 2015). Despite active conservation efforts including recovery plans, ex-situ conservation, protected areas, and education, the levels of breeding success have been considered insufficient to maintain the population which keeps decreasing. To tackle this, controlling other factors such as disease spread has been proposed to recover or at least stabilize population numbers (Cooper, Crawford et al. 2009). However, the implementation of such strategies requires baseline knowledge on what a healthy microbiome looks like.

In this study, we characterized the microbiome of African penguins from Georgia Aquarium using 16S rRNA amplicon sequencing. We mostly focused on the GIT, and more specifically on the oral and fecal microbiomes that we compared to other vertebrates in

order to identify the influence of phylogeny for these two body sites. In addition, we explored the microbial communities associated with different body sites including the skin, the preening gland, the brood pouch, and feathers as well as from environmental samples from the penguin exhibit to determine difference in microbial composition according to body site niche. While previous studies have shown that captivity alters the microbiome of wild animals, exploring this animal's microbiome in a highly controlled environment such as the exhibit from Georgia Aquarium, reduces the number of confounding variables usually present in the wild and provides a unique opportunity to compare the penguin microbiota to that of the surrounding environment.

### **3.3 Materials and methods**

#### *3.3.1 Sample collection*

Samples were obtained between November 2018 to March 2019 from various body sites of 36 captive African Penguins (*Spheniscus demersus*) kept at the Georgia Aquarium penguin facility (Atlanta, GA, USA). All sampled penguins were born in captivity either at Georgia Aquarium or at a different aquarium before being transferred to Georgia Aquarium. The Georgia Aquarium facility houses a total 55 penguins but the number of individuals occupying the exhibit fluctuates as chicks are born, animals are moved to other holding areas, or animals are transferred to other facilities for breeding. The penguin facility is an indoor, temperature-controlled 16,500 gallons exhibit that contains an artificial rocky environment, and 3 basins filled with artificial seawater 2 to 5 feet deep. All basins are connected and supplied from the aquarium life support system (LSS). The water from the entire exhibit is turned over every 37 mins using a filtration system

composed of two vertical sand filters, a protein fractionator (PSK), an ozone contactor (OZC), and a deaeration tower. Both the OZC and the PSK receive direct ozone gas injection. A waste water recovery system composed of dirty basin, a clean basin, and a recovery sand filter, PSK and OZC, allows to backwash and recover water from the main system sand filters to recycle dirty water that can then be sent back to the exhibit. A chemical dosing station and salt addition station allows to adjust the pH, alkalinity, and salinity as needed. The water temperature is maintained around 12°C, within the temperature range experienced by African penguins in the wild, which varies between 5 °C to 20 °C, using a Titanium plate heat exchanger. The penguins are fed ad libitum twice a day capelin, Pacific herring, squid (*Loligo* sp.), night smelt, and silversides. They do not feed during moult.

Penguin samples were collected while the birds were removed from the exhibit for routine health exams which take place annually or as needed to address medical concerns. No birds were sampled more than once. These exams also include bloodwork and radiographs. All microbiome samples were collected by gently rubbing sterile swabs along the region to sample including the cloaca, oral cavity (near the choana), brood pouch, uropygial (preening) gland, leg or back skin, making sure to accumulate enough material over the surface of the swab. For skin samples, feathers were parted to access the skin. Sample collection was approved by the IACUC ethics committee at Georgia Institute of Technology.

Swabs were also collected from surfaces within the exhibit, including dry rocks, wet rocks, the shoreline (rock constantly in contact with water from the basin), fresh and dry guano, and three different nests. Water microbiome samples from the exhibit basin

were collected by filtering water from the basin through a 0.2 µm Sterivex filter, as described in previous work (Patin, Pratte et al. 2018). Penguin food microbiome samples were collected by gently rubbing a sterile swab on the external surface of fish and other mollusks contained in a bucket of food to be delivered to the penguins. All environmental samples (water, surface and food swabs) were collected at a single time point in February 2019. Apart from environmental samples, all samples were collected by certified veterinarians. Samples were immediately preserved in an RNA/DNA preserving buffer (25 mM sodium citrate, 10 mM EDTA, 5.3 M ammonium sulfate, pH 5.2), and frozen at -80 C° until further processing. A summary of all samples is included in Table 3.1 and Table B.1. Data from extraction blanks (sterile swabs without biomass) were processed following the same procedures as for the rest of the samples.



**Table 3.1. Summary of the number of samples and ASVs associated with each sample type from the African penguin (*Spheniscus demersus*) and from the Georgia Aquarium penguin exhibit.** These ASV numbers include ASVs shared between body sites, and environmental samples.

Sample type	Number of samples	Number of ASVs
cloaca	33	815
oral cavity	35	650
brood pouch	18	1145
feather	3	444
uropygial gland	18	1067
dorsal skin	9	812
leg skin	20	1122
fecal*	2	223
dry rock	2	536
wet rock	2	262
water	2	824
shoreline	3	538
nest	4	416
dry guano**	2	200
food	8	595
fecal*: opportunistically collected from the floor during routine veterinary examinations		
dry guano**: dry fecal matter collected from rocks in the exhibit		

### 3.3.2 DNA extraction and sequencing

Total DNA was extracted from swabs using the PowerSoil DNA extraction kit (QIAGEN, Location, USA). Swabs were placed directly into PowerBead tubes and extracted according to the manufacturer's instructions. DNA from Sterivex filters was extracted following the protocol described in Padilla et al, 2017. For each sample, the V3-V4 region of the 16S rRNA gene was amplified by PCR using primers F515 and R806 (Caporaso, Lauber et al. 2011), each appended with barcodes and Illumina-specific adapters as described previously (Kozich, Westcott et al. 2013). Reaction mixtures included 2 to 5 µl DNA template, 12.5 µl Hot Start Taq PCR MasterMix (VWR), 0.27 µl (each) forward and reverse primers, and 0.5 µl bovine serum albumin (BSA) (20 mg/ml;

New England BioLabs Inc.). PCR conditions included an initial 1 min denaturation at 94°C, followed by 30 cycles of denaturation at 94°C (1 min), primer annealing at 55°C (2 min), and primer extension at 72°C (90 s) and then a final extension at 72°C for 10 min. Amplicon libraries were purified using Diffinity RapidTip PCR purification tips (Diffinity Genomics, NY), quantified fluorometrically on a Qubit (Life Technologies), and pooled at equimolar concentrations. Amplicons were sequenced on an Illumina MiSeq using a V2 500-cycle kit (250 × 250 bp) with 5% PhiX to increase read diversity.

### 3.3.3 *Illumina data processing*

Raw reads were quality checked using the DADA2 R-package (Callahan, McMurdie et al. 2016) and QIIME 2 2019.4 (Bolyen, Rideout et al. 2019). All forward reads were demultiplexed, quality filtered and trimmed to 175 bp following the DADA2 pipeline from (Callahan, McMurdie et al. 2016), while reverse reads were discarded due to lower quality. Taxonomy was assigned to amplicon sequence variants (ASVs) using the SILVA-132 database. The resulting representative sequences, taxonomy and ASV tables, were imported into QIIME 2 2019.4 (Bolyen, Rideout et al. 2019). Sequences classified as *Chloroplast*, and *Eukaryota* were removed from the dataset.

Penguin oral and cloaca samples were compared to other vertebrate oral and fecal or cloaca 16S rRNA gene datasets, respectively. To assess the relative influence of phylogeny in shaping the oral and cloaca penguin microbiomes, the datasets used for comparisons included terrestrial birds, reptiles and mammals (including marine mammals). If phylogeny were to play a more important role, penguin microbial communities would appear more similar to those of other birds. Due to the limited number of studies on oral microbiomes from diverse species, the sampling methods differed among the studies

included in both the oral and fecal comparisons. A summary of these datasets is included in Tables B.2 and B.3. Reads from these prior studies were trimmed to retain the same V3-V4 region amplified in this study. Datasets sequenced using Illumina technology were then pooled and processed through DADA2 using the same method as for the penguin dataset. Datasets sequenced using 454 technology were processed separately, and parameters were adjusted in the DADA2 algorithm to deal with such data by modifying denoising parameters, and filtering sequences by maximum length (Callahan, McMurdie et al. 2016). Final ASV tables issued from Illumina and 454 sequencing technologies were merged and taxonomy was assigned following the same method as for the penguin dataset.

#### 3.3.4 *Statistical analysis*

All amplicon sequence variants (ASVs) were aligned with Mafft (Katoh, Misawa et al. 2002), via q2-alignment, and used to construct a phylogeny with fasttree2 (Price, Dehal et al. 2010), via q2-phylogeny. Based on the variation of  $\alpha$ -diversity as a function of sampling depth (Shannon Diversity and Faith's phylogenetic Diversity (Faith 1992) computed using the q2-diversity plugin in QIIME2), samples were rarefied (subsampling without replacement) to 2500 reads, with the exception of the fecal microbiome comparisons, for which the data were rarefied to 2000 sequences. Data analyses were focused on characterizing the microbiome of the African penguin and identifying the relative influence of environmental versus host related factors in shaping this microbiome depending on the body site considered. These analyses included assessing differences in  $\alpha$  (Observed ASVs, and Shannon diversity index) and  $\beta$ -diversity (weighted and unweighted UniFrac, and Bray-Curtis distances) between different penguin body sites and

environmental samples, and between different animal classes (reptiles, birds, and mammals) and penguins when focusing on the oral and cloaca microbiomes. All analyses were performed using the rarefied ASV tables, unless otherwise specified. Both  $\alpha$  and  $\beta$ -diversity analyses were performed on the merged and rarefied ASV tables, and Kruskal-Wallis test were computed to identify significant differences in microbial community composition between penguin body sites, or between the oral and cloaca microbial communities of the different animal classes compared to those of the penguin.  $\beta$ -diversity was measured as weighted Unifrac dissimilarity calculated using q2-diversity plugin in QIIME2. Weighted Unifrac dissimilarity matrices were used to construct Principle Coordinate Analysis (PCoA) using Primer-e v.7 (Clarke 2015), and PERMANOVA tests were subsequently performed to identify significant differences in microbiome composition between penguin body sites and the environment, and between different animal classes when focusing on the cloaca and oral microbiome exclusively.

To determine if ASVs from the phylum Tenericutes present in the penguin food were the same found in the oral cavity and cloaca microbiome, a heatmap representing the relative abundances of these ASVs organized following Bray Curtis distances, with a hierarchical clustering of the samples was performed using the package Heatplus in R .

To identify ASVs potentially composing the core penguin microbiome, for each body site, we identified ASVs representing over 1 % of the microbial community, and present in 100 % of individuals, that differ in relative abundance between penguin samples and the environment (fresh feces on floor, dry feces on floor, dry rock, nest, wet rock, rock from the shoreline, water, and food), using the package DEseq2 in R (Love, Huber et al. 2014), with the non-rarefied merged ASV table.

### 3.4 Results

#### 3.4.1 *Microbiome samples*

176 penguin samples used for 16SrRNA sequencing span body sites including the cloaca, mouth, skin, brood pouch, and preening gland, as well as environmental samples including the exhibit water, surfaces in the exhibit, and the food. After quality filtering, trimming, and rarefaction, 161 samples constituting 3232 ASVs composed the final penguin dataset. The number of ASVs recovered for each sample type and sample number are summarized in Table 3.1. Penguin oral and cloaca microbiomes were also compared to those from other vertebrate species. After quality filtering, trimming, and rarefaction, a total of 162 samples constituting a total 6522 ASVs were recovered from the oral microbiome comparison, and 226 samples constituting 8795 ASVs were recovered from the fecal microbiome comparison. The number of ASVs recovered for each sample type and sample number are summarized in Tables B.2 and B.3, respectively. The ASV numbers include ASVs shared between different sample types (penguin body sites, animal species, or environmental samples). Sampling fecal matter from wild animals can be difficult, particularly for those that live in aquatic environments. Moreover, the samples used in this study needed to be issued from studies using 454 or Illumina sequencing technologies, targeting the V4-V5 portion of the 16S rRNA gene to make meaningful comparisons. Therefore, samples used in fecal comparisons included both fecal and cloaca samples (Table B.3).

#### 3.4.2 *The penguin oral microbiome is similar to those of marine mammals*

Richness and diversity estimated using the number of observed ASVs and the Shannon diversity index varied significantly among the oral microbiome of vertebrate species (Figure B.1, Kruskal-Wallis p-values <0.05). The Komodo dragon showed the highest richness and diversity, followed by the dolphin and the Great tit. In contrast, the prairie rattlesnake, the sea lion, and the hawk showed the lowest  $\alpha$ -diversities. Similarly, oral microbiome composition (based on weighted UniFrac distances) also varied significantly between vertebrate species (Figure 3.1, PERMANOVA, F=24.1, p=0.01), except between the Komodo dragon and the Gray's monitor (PERMANOVA, F=1.6, p=0.11). Despite tighter clustering within species, the oral microbiomes of marine vertebrates (penguin, sea lion, and dolphin) were more similar in composition compared to other vertebrate species and formed a distinct group (Figure 3.1). While this pattern was conserved when using unweighted UniFrac distances, it was lost when using Bray-Curtis distances.

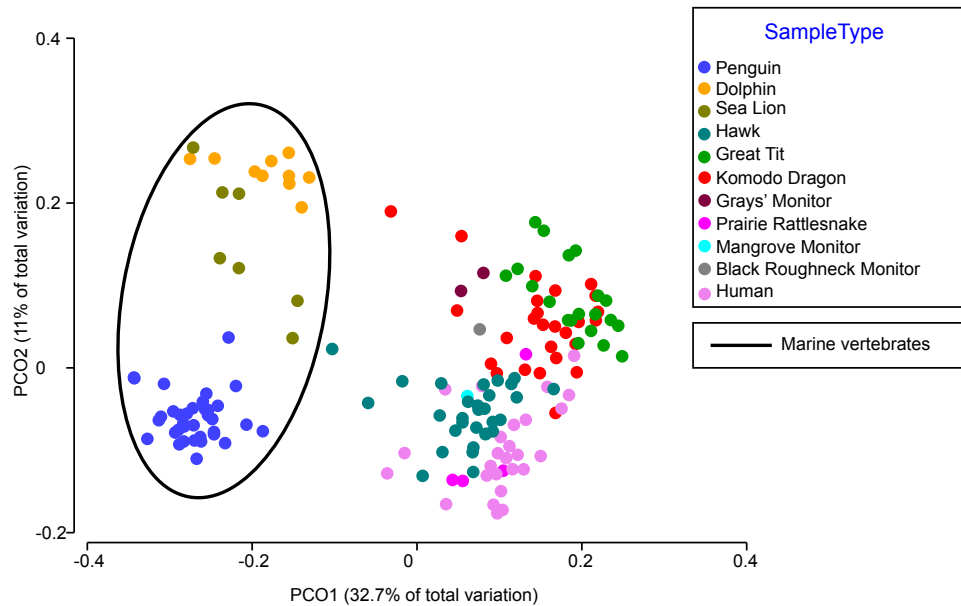


**Figure 3.1. Principal coordinate analysis (PCoA) of  $\beta$ -diversity comparisons using weighted Unifrac distances between the oral microbiome of various vertebrate hosts including birds, reptiles, and mammals. Penguin samples are from the current study**

Five bacterial phyla - Actinobacteria, Bacteroidetes, Proteobacteria, Firmicutes, and Fusobacteria - were shared among all host species (Figure 3.2A), with substantial variations in relative abundance between hosts. Interestingly, at the phyla level, marine vertebrates appeared more similar to each other compared to other vertebrate hosts, harboring the lowest relative abundances of Actinobacteria (< 2%) and Firmicutes (< 9 %), and the highest relative abundances of Bacteroidetes (> 34%).

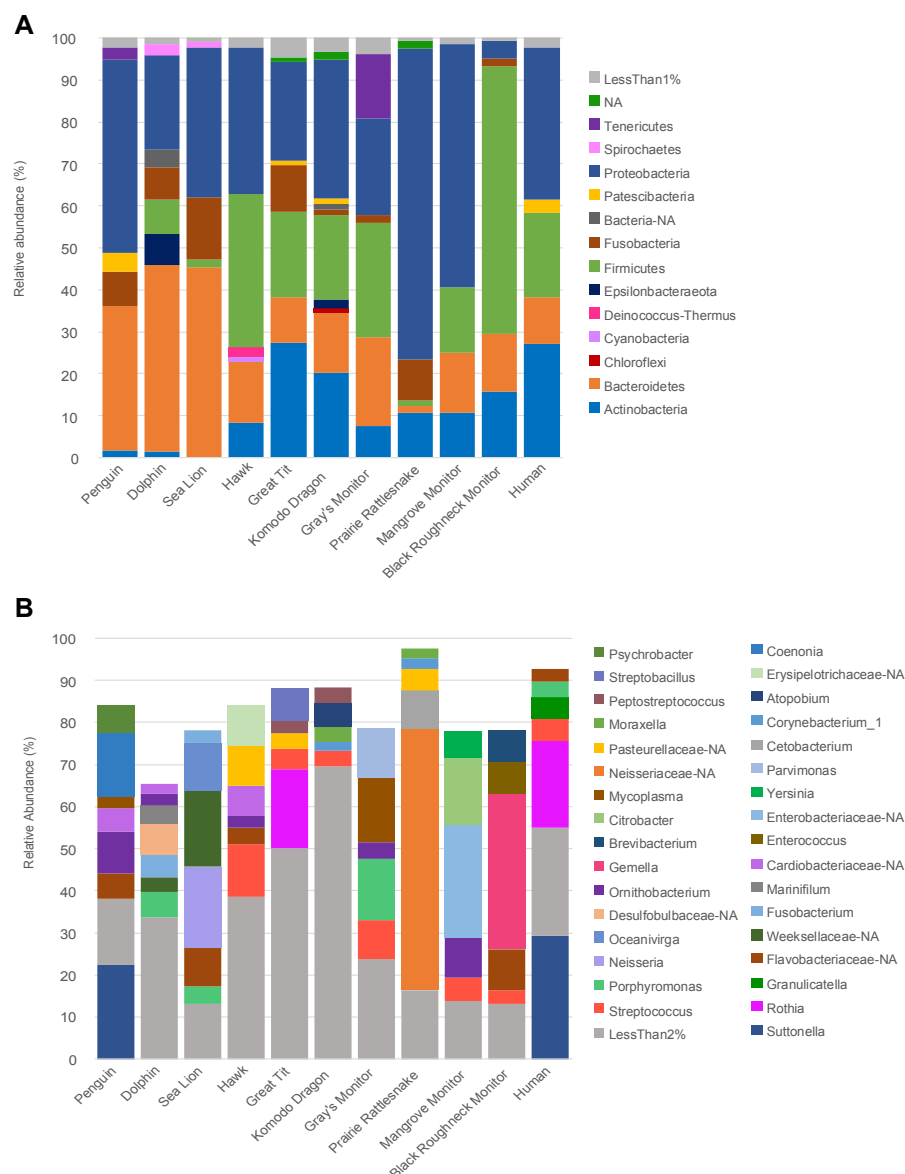


**Figure 3.2.** Bar plots indicating the average relative abundance of taxa composing the oral microbiome of various vertebrate hosts (birds, reptiles, and mammals). A) at the phyla level, B) at the genus level. Only the 4 most abundant genera for each host species are included

Only 4 unclassified genera – including members from *Chitinophagaceae*, *Lachnospiraceae*, *Rhodobacteraceae*, and *Gammaproteobacteria* – were shared by all animal species, despite strong inter-individual variability (Figure 3.2B). The genus *Proteiniphilum* was uniquely shared by all bird species, while marine vertebrates shared 4



unique genera including *Paludibacteraceae-unassigned*, *Tenacibaculum*, *Desulfobacteraceae-unassigned*, and *Desulfoplanes*. However, these ASVs represented small fractions of the oral microbial community (< 3 %) and were represented by different ASVs in each of the vertebrate species. Despite similarities with marine mammals' oral microbiome, the penguin oral microbiota still shared a larger number of taxa with those of other birds (66 genera with birds vs 26 with marine mammals).

The number of unassigned ASVs varied from 0.9 % (Gray's monitor) to 3.8% (bottlenose dolphin) and was highly variable between host species (Table 3.2). Interestingly, the penguin oral microbiome was composed of the highest percentage of unique ASVs (~92 %), followed by the microbiome of mammals, where percentages ranged from ~71 % (sea lion and human) to ~89 % (bottlenose dolphin; Table 3.4). Among penguin's unique ASVs, ~97% could not be assigned to the species level. Unique ASVs representing over 1% of the penguin's oral microbiota included *Suttonella* and other *Cardiobacteraceae*, *Flavobacteriaceae* such as *Coenonia*, *Moraxellaceae* such as *Suttonella* and *Psychrobacter*, *Ornithobacterium*, and *Mycoplasma* (Table B.4).

**Table 3.2. Summary of the proportion of each host species oral microbiome represented by unique or unassigned ASVs.** Unique ASVs corresponded to ASVs not shared with any other host species, and unassigned ASVs corresponded to ASVs that could not be classified beyond the kingdom level

Host species	Unique ASVs (%)	Unassigned ASVs (%)
African penguin	92.32	1.4
Urban Cooper's hawk	57.05	1.7
Great tit	47.52	2.7
Komodo dragon	69.94	5.1
Mangrove monitor	21.67	2.5
Gray's monitor	13.62	0.9
Black roughneck monitor lizard	13.33	2.2
Prairie rattlesnake	16.56	7.0
California sea lion	71.20	2.4
Bottlenose dolphin	88.52	3.8
Human	71.31	2.6

### 3.4.3 *The penguin fecal microbiome is most similar to those of other kids*

Richness and diversity, estimated using the number of observed ASVs and the Shannon diversity index varied significantly among the fecal microbiome of vertebrate species (Figure B.2, Kruskal-Wallis p-values <0.05 for all pairwise comparisons). The hen showed the highest richness and diversity, followed by the human and the Great tit. In contrast, the dolphin, showed the lowest  $\alpha$ -diversity. Similarly, fecal microbiome composition (based on weighted UniFrac distances) also varied significantly between vertebrate species (Figure 3.3, PERMANOVA,  $F=158.4$ ,  $p=0.001$ ). Interestingly, poultry samples were highly different from all other fecal microbiomes (Figure 3.3A). In contrast to the oral microbiome vertebrate comparisons, the penguin fecal microbiome clustered with those of other wild birds, while the marine mammal microbiomes (dolphin and sea lion) clustered with those of humans (Figure 3.3B).

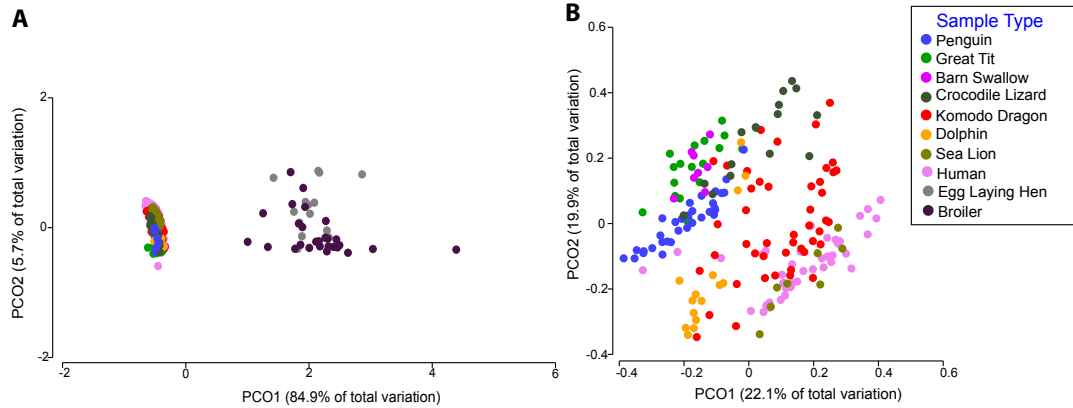


**Figure 3.3. Principal coordinate analysis (PCoA) of  $\beta$ -diversity comparisons using weighted Unifrac distances between the fecal microbiome of various vertebrate hosts including birds, reptiles, and mammals A) includes poultry samples, B) does not include poultry samples. Penguin samples are from the current study**

All vertebrate's fecal microbiome shared the same main phyla including Firmicutes, Proteobacteria, Bacteroidetes, and Actinobacteria, despite strong inter-species variability (Figure 3.4A). Mammals showed low proportions of Actinobacteria (< 0.1 %), while wild birds (penguin, barn swallow, and Great tit) showed the highest (> 13 %). Patescibacteria was almost exclusively present in wild birds, while Fusobacteria was almost exclusively shared by mammals and reptiles (Figure 3.4A). Poultry taxonomic composition was highly distinct compared to that of other vertebrates (Figure 3.4). This group did not share several phyla present in all other bird hosts, and was instead highly dominated by *Lactobacillus* (25 to 50 %), while this genus represented under 3 % of the fecal microbiome in all other vertebrates.

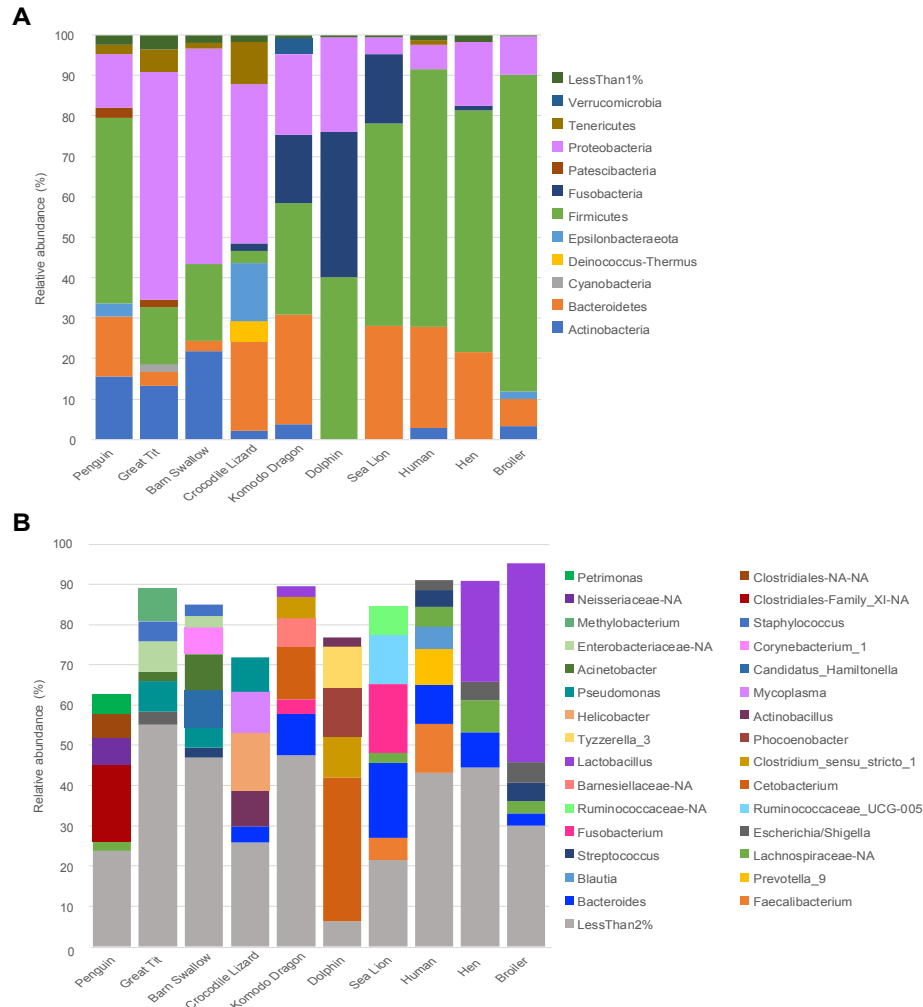


**Figure 3.4.** Bar plots indicating the average relative abundance of taxa composing the fecal microbiome of various vertebrate hosts (birds, reptiles, and mammals). A) at the phyla level, B) at the genus level. Only the 4 most abundant genera for each host species are included

Only 4 genera – including *Lactobacillus*, *Clostridium*, *Escherichia/Shigella*, and *Enterobacteriaceae*-unassigned – were shared by all animal species, despite strong inter-individual variability (Figure 3.4B). The genera *Corynebacteriaceae* and *Catellibacterium* were uniquely shared by all bird species' fecal microbiome. They represented a small fraction of the microbiome (< 1.5 %) and were primarily composed by different ASVs for each host species. In contrast to the oral microbiome, the penguin did not share any genera with marine mammals' fecal microbiota.

Interestingly, the number of unassigned and unique fecal ASVs was the highest in the penguin (~2.2 % and ~86 %, respectively), followed by that of the human microbiome (~1.8 % and ~83 % respectively; Table 3.3). Among penguin's unique ASVs, ~98% could not be assigned to the species level. Unique ASVs representing over 1% of the penguin's fecal microbiota, included members of the *Clostridiales*-Family XI such as *Ezakiella* and *Gallicola*, members of the family Neisseriaceae, and genera *Campylobacter*, *Actinomices*, *Petrimonas*, *Proteiniphilum*, and *Fastidiosipila* (Table B.5).

**Table 3.3. Summary of the proportion of each host species fecal microbiome represented by unique or unassigned ASVs.** Unique ASVs corresponded to ASVs not shared with any other host species, and unassigned ASVs corresponded to ASVs that could not be classified beyond the kingdom level

Host species	Unique ASVs (%)	Unassigned ASVS (%)
African penguin	85.920	2.155
Barn swallow	59.504	0.432
Great tit	55.776	0.550
Broiler	33.378	0.203
Hen	46.838	0.656
Crocodile lizard	66.754	0.982
Komodo dragon	79.442	1.804
California sea lion	51.020	0.000
Bottlenose dolphin	52.101	0.000
Human	82.738	1.758

#### 3.4.4 Penguin microbiomes from external body sites are similar to those of the environment

No significant differences in richness or diversity were observed between penguin body sites and environmental samples (Figure B.3, Kruskal-Wallis p-values >0.05). The penguin microbiome composition (based on a weighted UniFrac distances), showed a distinct grouping of cloaca and oral samples, while the more external penguin body sites

clustered with environmental samples (Figure 3.5). However, the microbial composition from the majority of these external body sites still appeared significantly different between body sites, and from the environment, except for dry rock, and feather samples (PERMANOVA, Table B.6).

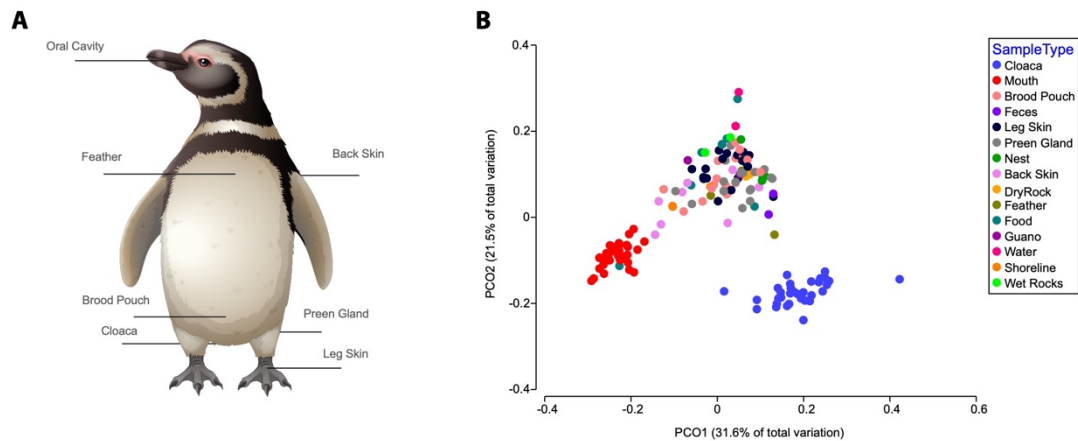


**Figure 3.5. A) Schematic of the penguin (*Spheniscus demersus*) body sites sampling locations and B) Principal coordinate analysis (PCoA) of  $\beta$ -diversity comparisons using weighted Unifrac distances between the microbiome of various penguin body sites and from environmental samples of the penguin exhibit**

All samples were mostly dominated by Proteobacteria, Firmicutes, Bacteroidetes, and Actinobacteria, and shared genera *Psychrobacter*, and *Oceanisphaera* (Figure 3.6).

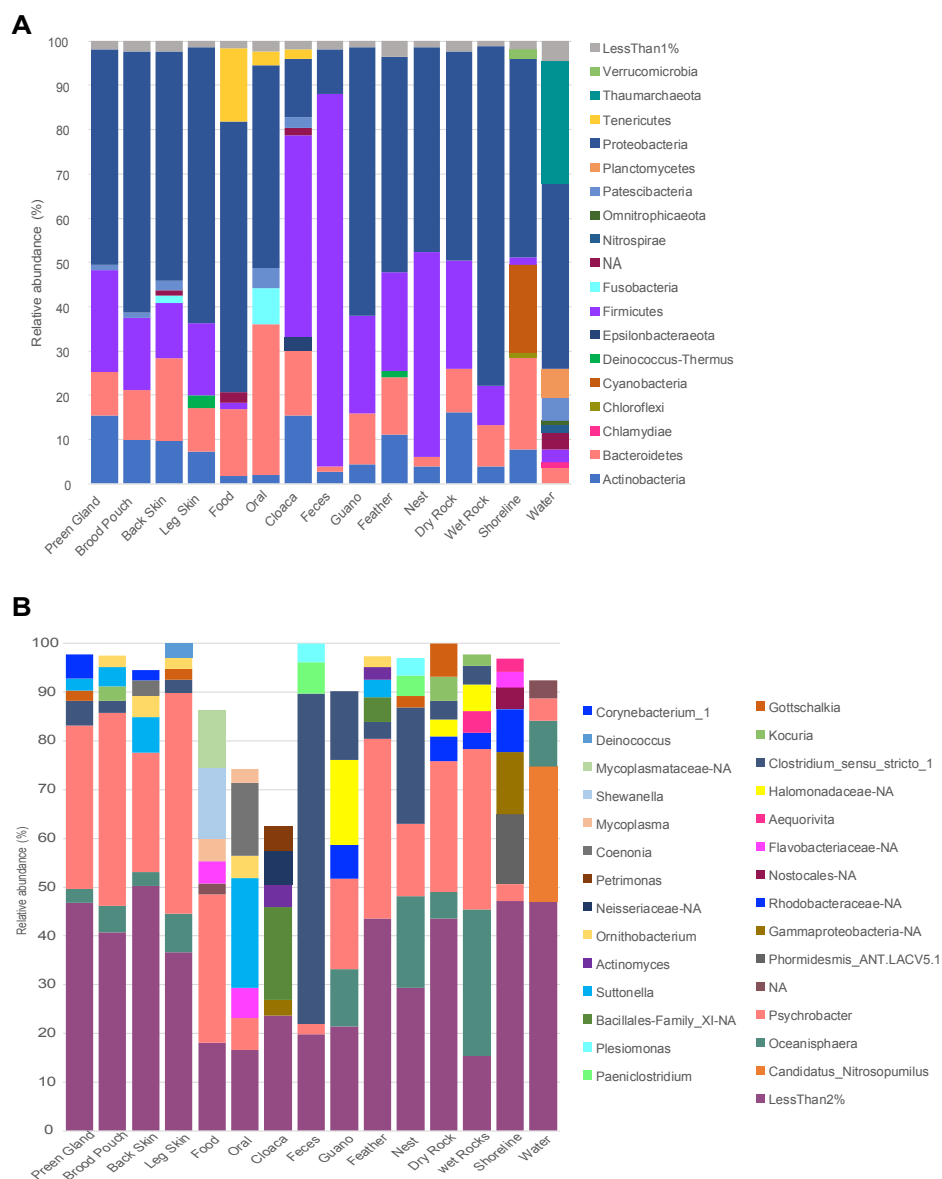


**Figure 3.6.** Bar plots indicating the average relative abundance of taxa composing the penguin (*Spheniscus demersus*) microbiome at different body sites and of environmental samples collected from the penguin exhibit . A) at the phyla level, B) at the genus level. Only the 4 most abundant genera for each host species are included

Interestingly, food, oral, and cloaca samples contained Tenericutes with higher relative abundance in the food. However few ASVs from this phylum were shared between these sample types (Figure B.4). Under 45 % of cloaca and oral ASVs were shared with environmental samples, while all other penguin samples shared over 60 % of their ASVs

with the environment. Moreover, the fraction of unique ASVs constituting the oral and cloaca microbiomes was also twice as high, compared to other body sites (Table B.7). Because ASVs unique to specific penguin body sites were often present in few individuals, with low (<1 %) proportions, we identified microbes differentially abundant from the environment, representing over 1 % of the microbiome, and present in 100 % of individuals for each body site, as potential members of the penguin core microbiome. These corresponded to ASVs identified as unassigned *Psychrobacter*, and *Suttonella*, which were significantly more abundant in penguin's microbiome at all body sites, except for the cloaca, compared to that of the environment. ASVs identified as unassigned *Ornithobacterium* and *Coenonia* composed the oral and back skin core microbiome, an ASV belonging to the genus *Kocuria* was identified as part of the brood pouch core microbiota, and an unassigned ASV belonging to the class *Oceanisphaera* belonged to the leg skin microbiome. ASVs including unassigned members of the genera *Gallicola*, *Actinomyces*, *Petrimonas*, *Campilobacter*, and *Fastidiosipila* composed the cloaca core microbiome (Table B.8). Among these, were some microbial species that are known to be potentially pathogenic (Table B.9).

Patterns in microbial composition related to metadata variables including age, sex, time since moult, reproductive status, use of a nest, use of specific medications and supplements, and antiseptic treatment for bumblefoot were also tested. However, small sample sizes did not allow us to find statistically significant patterns.

### 3.5 Discussion

#### 3.5.1 Influence of phylogeny (cloaca vs. oral cavity)



Based on previous research, phylogeny and diet appear as main factors shaping the microbiome of vertebrates (Groussin, Mazel et al. 2017, Pascoe, Hauffe et al. 2017, Youngblut, Reischer et al. 2019) with variations in their relative importance among host clades. Confirming these observations, cloaca and oral microbial communities clustered principally based on species, and differences in  $\alpha$ -diversity also appeared to be species specific. Interestingly, the penguin oral microbiome appeared more similar to that of other marine vertebrates (bottlenose dolphin and California sea lion). In accordance with previous studies highlighting the major role that diet plays in shaping the oral microbiota (Adler, Dobney et al. 2013, Kato, Vasquez et al. 2017), this result suggests that the marine lifestyle, and a potentially similar diet may explain the similarity between the penguin and marine mammals oral microbiome, despite strong differences in physiology. On the other hand, penguin's cloaca microbiota was more similar to that of other birds (barn swallow and Great tit), highlighting the effect of phylogeny as a main driver of bird's gut microbiome (Hird, Carstens et al. 2014, Waite and Taylor 2014, Kropáčková, Těšický et al. 2017). Interestingly, poultry fecal microbial composition was very different from that of any other vertebrates and was highly dominated by *Lactobacillus*. This suggests that while phylogeny plays a major role in structuring the bird gut microbiome, highly controlled environments such as those used in commercial farming through multiple generations, can cause drastic changes in microbiome composition.

All species oral and cloaca microbiomes were dominated by phyla that usually prevail in vertebrate microbiomes including Firmicutes, Bacteroidetes, Proteobacteria, and Actinobacteria (Marchesi 2011, Waite and Taylor 2014, Youngblut, Reischer et al. 2019), with proportions that were more similar between marine vertebrates oral microbial

communities (penguin, dolphin and sea lion). In contrast, few genera were shared by all host species, and corresponded to groups commonly found in the GIT including members of families *Chitinophagaceae*, *Lachnospiraceae*, *Rhodobacteraceae*, and *Gammaproteobacteria* for the oral microbiome, and members of *Lactobacillus*, *Clostridium*, *Escherichia/Shigella*, and *Enterobacteriaceae* for the fecal microbiome (Koren, Spor et al. 2011, Armingohar, Jørgensen et al. 2014, Kviatkovski and Minz 2015, Cassir, Benamar et al. 2016, Chen, Wu et al. 2018, Lu, Ren et al. 2019). A single genus identified as *Proteiniphilum*, previously found in hawks oral microbiome (Taylor, Mannan et al. 2019) was unique to the oral microbiome of birds, and 2 genera commonly found in birds' GIT, identified as *Corynebacteriaceae* (Yakimova, Kapustin et al. 2019), and *Catellibacoccus* (Sinigalliano, Ervin et al. 2013) were unique to birds' fecal microbiota.

Marine vertebrates' oral microbiome shared 4 genera unique to this group. These included sulfate reducers such as *Desulfoplanes* and *Desulfobacteraceae* found in aquatic environments and some host associated systems (Watanabe, Kojima et al. 2015, Bernasconi, Stat et al. 2019), as well as genera that have been previously identified as part of marine mammals microbiome such as *Paludibacteraceae* (D'Agnese, McLaughlin et al. 2020), and *Tenacibaculum* which has been found in the skin microbiome of humpback whales where it could provide benefits to the host (Apprill, Robbins et al. 2014). No genera were shared between the penguin's and marine mammals' fecal microbiota.

### 3.5.2 Differences in microbial composition according to body site niche

$\beta$ -diversity analyses showed that except for the cloaca and oral penguin microbiomes, the microbiota from all other body sites was similar to that of the surrounding environment. Moreover, while both environmental and penguin samples were mostly

dominated by the same phyla, and shared genera *Ocanisphaera* and *Psychrobacter*, which have been associated with both free (Xu, Zhang et al. 2014, Hurtado-Ortiz, Nazimoudine et al. 2017) and host-associated marine environments (Apprill, Robbins et al. 2014, Sung, Kim et al. 2018), cloaca and oral microbiomes still shared a lesser number of ASVs with the environment and contained the highest fraction of unique ASVs. Moreover, while the *Tenericutes* phylum was particularly present in GIT related samples with decreasing proportions from food, to oral, to cloaca samples, the ASVs present in each of these environments were mostly different, suggesting that each of these environments present specific microbial communities that are not just left over from the food. These results confirm the specificity of the penguin cloaca and oral microbiomes, while the higher similarity of other penguin body sites with the surrounding environment, suggests a higher level of transfer of microbes between these body sites and the environment. However, this pattern may be accentuated by captivity in an enclosed and constrained environment.

### 3.5.3 Uniqueness of the African penguin microbiome

Compared to other vertebrates, penguin oral and cloaca microbiomes were composed of the highest proportion of unique sequences among which > 95 % could not be identified to the species level, and the cloaca microbiota also presented the highest fraction of unassigned sequences that could potentially be novel microbes, highlighting the uniqueness of the penguin GIT microbiome. The most abundant ASVs (> 1%) unique to the penguin oral and cloaca microbiota, corresponded to taxonomic groups that are often found associated with the respiratory or GIT of birds but also contain potential pathogens. These included microbes from the families *Cardiobacteriaceae* (Mihaylova and Gomila 2014), *Flavobacteriaceae* (Grond, Sandercock et al. 2018), *Weeksellaceae*, *Moraxellaceae*

(Pearce, Hoover et al. 2017), and *Mycoplasmataceae* (Lierz, Hagen et al. 2008). Unique cloaca penguin ASVs with the highest proportions corresponded to members of the *Clostridiales*-Family XI (Chintoan-Uta, Wisedchanwet et al. 2020), *Neisseriaceae* (Liu, Tang et al. 2015), *Campylobacteraceae* (Pitkänen and Hänninen 2017), *Dysgonomonadaceae* (Sandri, Correa et al. 2020), *Ruminococcaceae* (Stanley, Hughes et al. 2016), and *Actinomcetaceae* (Kelly, Kennedy et al. 2015), also usually found in the GIT. Other body sites' core microbiome were also majorly composed by these same taxonomic groups, reinforcing the potential benefit they have on the host. Specific to the brood pouch core microbiome, an ASV was identified as an unclassified *Kocuria*, a microbial species recently found in the preening glands of wild birds (Braun, Wang et al. 2019). While the penguin microbiome contained a variety of microbe species that harbor some pathogenic strains with relative abundances of up to ~ 15% (*Coenonia* in the oral microbiome), penguins from Georgia Aquarium were healthy and are constantly monitored, which suggests that the ASVs recovered from these animals are more likely non pathogenic.

### 3.6 Conclusion

Our study showed that the oral microbiome of African penguins was more similar to that of other marine mammals while their fecal microbiota was more similar to that of other wild birds, reflecting differences in the effect of phylogeny in different sections of the GIT. While cloaca and oral penguin samples harbored distinct microbial communities, all other body sites appeared similar to environmental samples showing a tight connection with their habitat. Both cloaca and oral penguin samples also showed the highest number of unique sequences compared to other vertebrates, and most of these unique sequences could not be

assigned to the species level. These results emphasize the uniqueness of the penguin GIT microbiome and the need to further characterize these microbial communities and how they may influence host-health. Future studies would benefit from including wild animals to assess the influence of captivity on penguins' microbiome and identify potential biomarkers of host and ecosystem health.

**CHAPTER 4.      WATER COLUMN AND SEDIMENT CORE  
DEPTH DRIVE SPATIAL DECOUPLING OF SEDIMENT  
MICROBIAL COMMUNITIES IN THE NORTHERN GULF  
OF MEXICO**

Disclaimer: This chapter is currently in final manuscript form

## 4.1 Abstract

Biogeographic surveys of sediment microbial communities and their link to geochemical parameters as a function of depth on broad spatial scales across a region are relatively scarce. In this study, sequencing of 16S rRNA gene amplicons from both *Bacteria* and *Archaea* was used alongside high resolution depth profiles of the main redox species involved in carbon remineralization processes and nutrients to explore microbial diversity patterns in sediment cores from the continental shelf to the slope of the northern Gulf of Mexico. Both shelf and slope sediments were deprived of dissolved oxygen within 7 mm from the sediment-water interface and were therefore mostly anoxic. The shelf sediments were characterized by geochemical indicators of sulfate reduction with either dissolved  $\text{H}_2\text{S}$  or  $\text{FeS}_{\text{aq}}$  proxies for iron sulfide mineral precipitation, whereas the slope sediments were characteristic of intense nitrate- and metal-reducing conditions with strong nitrate gradients below the sediment-water interface and high dissolved manganese but relatively low dissolved iron concentrations. Canonical Correspondence Analysis (CCA) revealed that dissolved inorganic carbon, orthophosphate, and sulfide concentrations were the main drivers in shaping the microbial communities across the shelf communities, while  $\text{NO}_3^-$  appeared more important in shaping microbial communities along the slope ( $p\text{-value} \leq 0.01$ ). Specifically, dissimilatory sulfur metabolizing (oxidizing and reducing) microbes such as *Desulfobulbaceae*, *Desulfobacteriaecae*, *Thiohalorhabdaceae*, *Thioalkalispiraceae*, and *Ectothiorhodospiraceae* were enriched in continental shelf sediments, consistent with elevated dissolved sulfide in these cores. In contrast, sediments from the continental slope were enriched in aerobic ammonia oxidizing *Thaumarchaeota* and *Bacteria*, as well as anaerobic ammonia oxidizing *Brocadiales*, suggesting ammonia

consumption and nitrification as important microbial processes in slope sediments. Multivariate analyses of 16S rRNA gene amplicons and geochemical signals provided strong evidence that the composition of both the sediment bacterial and archaeal communities was linked to the depth of the overlying water column and proximity to shore. Vertical differences in composition were observed at centimeter resolution along the sediment depth profiles and were most pronounced in continental shelf sediments. Particularly on the shelf, *Bathyarchaeota* which have been implicated in sulfur and nitrogen reduction and methane cycling, showed some the highest increases in relative abundance with sediment core depth. Analysis of the *Archaea* community using domain-specific primers did not provide better estimates of diversity compared to conventional 16S rRNA gene survey primers. Overall, the data support the hypothesis that high organic matter deposition to shelf sediments significantly differentiates the resident microbial communities from those in deeper, continental slope environments, and may stimulate taxa involved in sulfur and methane cycling. Such studies are useful to identify geochemical features associated with unique microbial assemblages and, therefore, help clarify the functional roles of microbes in the environment.

## **4.2 Introduction**

Sedimentary processes in marine environments affect the overlying column and the global cycling of elements including carbon, nitrogen, iron, manganese, and sulfur (Snelgrove, Blackburn et al. 1997). Despite the importance of these environments, biogeographic surveys of sediment microbial communities and their link to geochemical parameters on broad spatial scales across a region are relatively scarce. This information is critical to better characterize sediment ecosystems and their impact on global processes



such as nutrient cycling (Forsberg 1989, Arrigo 2005), ocean acidification (Cai, Hu et al. 2011), and primary production (Johnson, Chavez et al. 1999).

Sediment microbial communities are estimated to represent at least half of the Earth's microbial biomass (Whitman, Coleman et al. 1998) but remain relatively under characterized. In addition to the lack of culturable representatives which can limit our understanding of microbial function, most studies have mainly focused on the bacterial fraction of the prokaryotic community. Archaea, however, also appear to be active, abundant, and widespread in marine sediments, particularly in the deep marine subsurface where they contribute to carbon degradation processes and nutrient cycling (Sturt, Summons et al. 2004, Schippers, Neretin et al. 2005, Biddle, Lipp et al. 2006). The lack of culturable representatives and the mutual exclusivity of lineages, as well as the fact that most PCR 16S rRNA universal primers are predominantly designed to target the bacterial fraction, can bias the estimates of abundance and phylogenetic diversity of archaeal members (Teske and Sørensen 2008, Raymann, Moeller et al. 2017). Therefore, better targeting this group may be particularly useful to better understand deep sedimentary processes, including the processes only conducted by archaea, such as the production and consumption of methane (Hinrichs, Hayes et al. 1999, Lloyd, Alperin et al. 2011, McGlynn 2017, Beulig, Røy et al. 2019).

The amount of organic and inorganic material reaching sediments mostly depends on the intensity of primary production in the overlying water column, water column depth, distance from shore, and riverine inputs (Hartnett, Keil et al. 1998, Wei, Rowe et al. 2010, Zinger, Amaral-Zettler et al. 2011, Bienhold, Zinger et al. 2016, Overholt, Schwing et al. 2019), and the amount of organic matter deposition structures sediment's chemical

environment. Near shore sediments are associated with higher loads of organic material from surface primary production and riverine sources, and as a result experience more biogeochemical variability than deep sea systems because of their stronger connection to terrestrial processes (Bauer, Cai et al. 2013). In these organic matter rich sediments, oxygen is rapidly depleted through aerobic respiration and reoxidation of reduced metabolites (Glud 2008), anaerobic processes using sulfate as the primary terminal electron acceptor (Jørgensen 1982) are found closer to the sediment-water interface, and geochemical gradients are sharper (Burdige 1993). Thus, higher abundances of microbial species associated with sulfur cycling are present in organic-rich marine sediments, followed by a fast and sharp increase in methane- or hydrocarbon-related microbial species in the deeper layers (Beulig, Røy et al. 2018), while gradients of physical and geochemical parameters such as pressure, temperature, salinity, and pH, which control microbial community composition and function, remain mostly consistent in deep sea sediments (Lozupone and Knight 2007, Bienhold, Boetius et al. 2012). In these environments, the input flux of organic carbon is so low that oxygen penetration depth reaches several centimeters (Glud, 2008), and are dominated by aerobic respiration, denitrification and manganese reduction (Jahnke, Reimers et al. 1990).

In continental slope sediments, riverine dissolved and particulate material eventually delivered to the ocean flocculates and aggregates into fine-grained material that settles into the benthic boundary layer (BBL) 0.1-2 m above the seabed and forms mobile muds, an ephemeral layer that is often remobilized by physical mixing generated by tidal currents or storms (Aller 1982, Aller 1998, McKee, Aller et al. 2004). These mobile muds are eventually deposited on continental shelves and slopes, with selective dispersal that

depends on particle size, density, morphology, or composition (McKee et al., 2004), and enhance carbon remineralization by exposing sediment to oxygenated bottom waters (Aller 1998, Hartnett, Keil et al. 1998, Blair and Aller 2012) and co-metabolizing fresh, planktonic organic carbon (Canfield 1994). As a result, sediment distribution across continental margins and their associated diagenetic processes may vary widely depending on the organic carbon and lithologic composition of the top sediment layers (Canfield 1994, Grégoire and Friedrich 2004, Taillefert, Beckler et al. 2017). Subsequently, sulfur cycling processes are more prevalent deeper into the sediment in the anoxic zones as a result of the depletion of more energetically favorable electron acceptors (Froelich, Klinkhammer et al. 1979). Finally, the low concentration of organic material in open ocean environments limits microbial diversity, while in organic rich sediments, the unavailability of electron donors and acceptors deeper within the sediment control microbial abundance and richness (D'Hondt, Rutherford et al. 2002, D'Hondt, Jørgensen et al. 2004).

The Louisiana continental shelf in the northern Gulf of Mexico is a dynamic system within close proximity of the Mississippi and Atchafalaya River system (MARS) which transports large amounts of freshwater and sediment material to the shelf (Dagg, Benner et al. 2004) and references therein). The high discharge of nutrients to the nGoM creates a seasonal hypoxic zones in the water column during the summer (May-August) (Rabalais, Turner et al. 2007). Hypoxic zone sediments can be classified in three geochemically distinct zones influenced by the sedimentology resulting from MARS discharge including regions where (1) metal oxide cycling dominates, (2) oxygen delivery into sediments exist from due to bioturbation, and (3) iron oxide limited sulfate reduction dominates (Devereux, Lehrter et al. 2019). Additionally, the continental slope and Mississippi canyon receive

terrestrial inputs from the shelf region, including organic (Bianchi, Allison et al. 2006) and inorganic material (Trefry and Presley 1982) (Owings et al., 2020) that influence microbial respiration processes. Therefore, continental slope sediments (>1,000 m water depth) of the nGoM could potentially be more microbially active than previously considered. The nGoM is a unique environment to study sediment microbial communities linked to geochemical parameters due to the proximity of geochemically distinct sedimentary regions corresponding to a range of bottom water oxygen concentrations as well as a range of organic carbon inputs due to the influence of the Mississippi River on the region. This study combined molecular and geochemical investigations to characterize the effect of a dominant riverine system (MARS) on the surrounding shelf and slope ecosystems during the hypoxic season and provide insights into the potential influence of sediment carbon remineralization pathways on the overlying water column.

### **4.3 Materials and methods**

#### *4.3.1 Station locations and core descriptions*

Sediments were collected for coupled molecular and geochemical analyses across the Louisiana continental shelf (LCS) in the northern Gulf of Mexico (nGoM) at stations across two transects (Figure 4.1) during July-August 2016 onboard the *R/V Pelican*. The first transect, referred to as the shelf transect, investigated geochemical and microbial processes across the hypoxic continental shelf. The shelf transect began at St. 6 (15 m water depth, located outside of Vermilion Bay, LA) and continued east toward the Mississippi River delta (St. 2, 67 m), including stations 5B, C6C, and MK (Figure 4.1, Table 4.1). The second transect, referred to as the slope transect, examined the molecular and geochemical

differences in the underlying sediment at four stations ranging in depths from 67 m (St. 2) on the hypoxic shelf to 1,230 m (St. 10) in the oxygenated waters of the continental slope (Figure 4.1, Table 4.1). At most stations, dissolved oxygen, conductivity, and temperature were measured as a function of depth in the water column with a Conductivity, Temperature and Depth (CTD) rosette (Sea-bird) equipped with oxygen sensor. To avoid disturbing the sediment, the rosette was lowered to about 1-2 m above the seafloor. CTD casts were not conducted at St. 5B, St. 2, and St. 3.

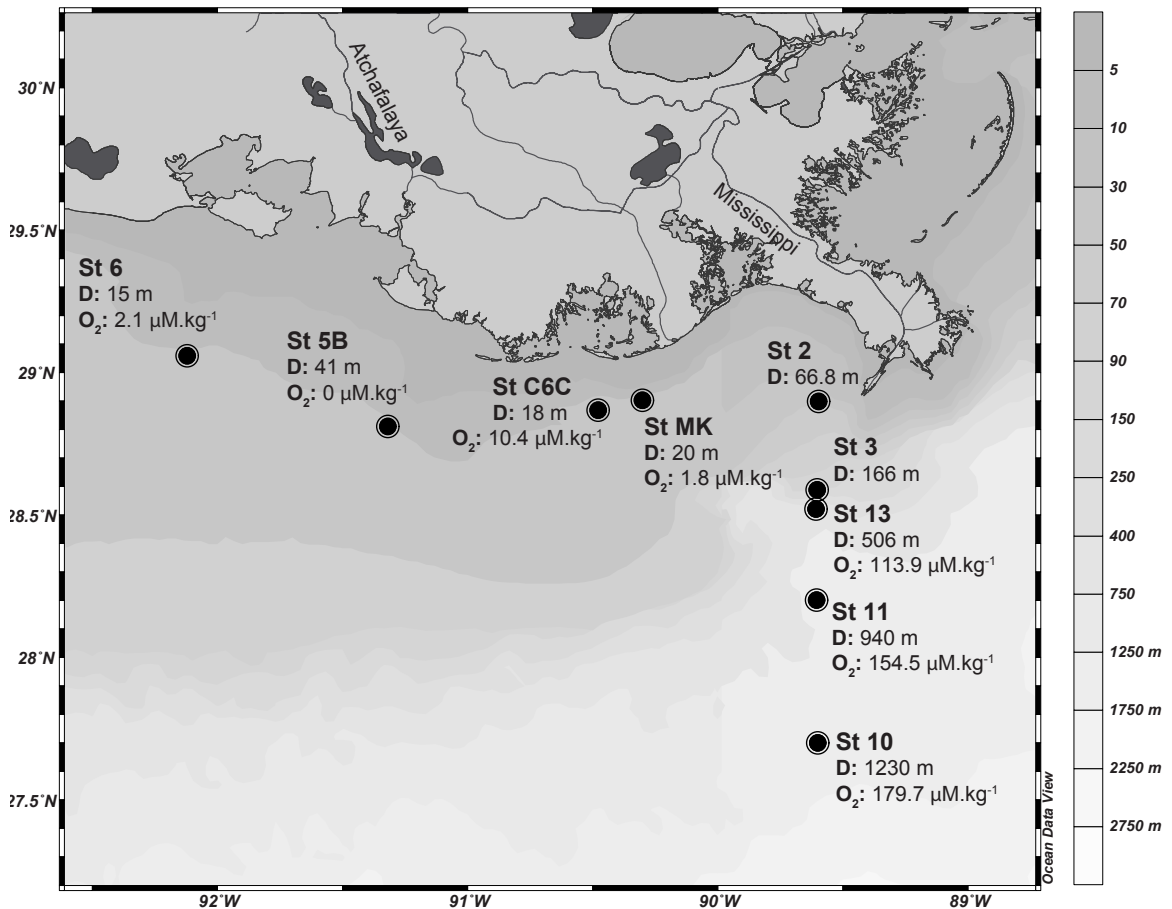


**Figure 4.1. Map of the locations across the Louisiana shelf and slope in the northern Gulf of Mexico where sediment cores were collected during a research cruise in late July- early August of 2016. Water depths (D, m) and bottom water oxygen concentrations measured from CTD profiles (O<sub>2</sub>, μM kg<sup>-1</sup>) are provided for reference. Depth contours (m) indicate ocean bathymetry. Mississippi and Atchafalaya Rivers are labeled.**

**Table 4.1 Station location, depth and corresponding bottom water oxygen concentrations, salinities and temperatures**

Transect	Station Name	Latitude (deg)	Longitude (deg)	Depth (m)	Oxygen, ( $\mu\text{mol/kg}$ ) <sup>a</sup>	Salinity (PSU) <sup>b</sup>	Temperature ( $^{\circ}\text{C}$ ) <sup>b</sup>
Shelf	6	29.060	-92.120	15	2.1	36	26.8
	5B	28.484	-91.199	41	< 63 $\mu\text{M}$ <sup>c</sup>	36	27.1
	C6C	28.868	-90.478	18	10.43	37	27.4
	MK	28.903	-90.301	20	3.26	37.5	27.6
	2	28.899	-89.595	66.8	114 <sup>d</sup>	38	22.6
Slope	3	28.590	-89.603	166	168 <sup>e</sup>	38	28.6
	13	28.308	-89.358	506	113.91	35	13.3
	11	28.121	-89.358	940	154.52	35	9.0
	10	27.420	-89.360	1230	179.68	38	13.4

<sup>a</sup>: Oxygen concentrations measured by CTD rosette

<sup>b</sup>: Salinity and temperature of overlying waters measured onboard with refractometer and thermocouple

<sup>c</sup>: averaged from 2015 and 2017 NOAA dead zone data at a nearby location (Rabalais and Turner, 2015, 2017)

<sup>d</sup>: data from Taillefert cruise 2017 (Owings et al., submitted)

<sup>e</sup>: data from June 2006 at a nearby station (Devereux et al., 2015)

#### 4.3.2 Sediment collection, voltammetric profiling, and pore water analyses

Sediment cores of approximately 20 cm in length and 9.6 cm inner diameter were collected using a MC-800 Multi-Corer (Ocean Instruments). After collection, the temperature and salinity of the overlying water of the core were measured using a thermocouple and refractometer. All cores were voltammetrically profiled immediately after collection except in the case of the sediment core from St. 3, which was collected in the evening, sealed, stored on deck, and analyzed 12 hours later. Voltammetric profiles detected redox active species, including oxygen ( $\text{O}_{2(\text{aq})}$ ), manganese(II)( $\text{Mn}^{2+}$ ), iron (II) ( $\text{Fe}^{2+}$ ), organic-Fe(III) complexes (org-Fe(III)),  $\text{FeS}_{\text{aq}}$ , and  $\Sigma\text{H}_2\text{S}$  (Taillefert, Luther et al. 2000, Luther, Glazer et al. 2008), using a three-electrode configuration including a silver/silver chloride (Ag/AgCl) reference electrode, a platinum (Pt) counter electrode, and a gold/mercury (Au/Hg) working electrode (Brendel and Luther 1995, Luther, Reimers et al. 1999, Beckler, Kiriazis et al. 2016). Profiles were conducted with less than 1 mm resolution using minimally invasive Au/Hg voltammetric microelectrodes connected to a

computer-controlled Analytical Instrument Systems, Inc. (AIS, Inc.) MAN-1 micromanipulator and measured with an AIS, Inc. DLK-70 potentiostat. A combination potentiometric minielectrode (1.6 mm diameter, Microelectrodes, Inc.) was used to measure pH at each depth along the profile. The pH minielectrode electrode was connected to the potentiostat and pH was calibrated externally using TRIS buffer in synthetic seawater (Dickson 1993). Dissolved oxygen was measured by linear sweep voltammetry (LSV) between -0.1 and -1.8 V including a preconditioning period of 10 s at -0.1 V and calibrated assuming the maximum peak amplitude measured in the overlying water corresponded to the bottom water oxygen concentration detected using the CTD oxygen sensors.  $\text{Mn}^{2+}$  and all other redox species were measured by cathodic square wave voltammetry (CSW) using at 200  $\text{mV s}^{-1}$  scan rate, and a preconditioning step of 10 s at -0.1 V. An additional preconditioning step consisting of 10 seconds at -0.9 V was added before the aforementioned -0.1 V conditioning step if organic-Fe(III) complexes or dissolved sulfide signals were detected to clean the electrode surface (Tercier-Waeber and Taillefert 2008). The resulting scans of current versus potential were analyzed to quantify peak height and surface area using a semi-automated VOLTINT software package (Bristow and Taillefert 2008). The working electrodes were calibrated with a  $\text{MnCl}_2$  solution (0-400  $\mu\text{M}$ ) in 0.54 M NaCl before profiling.  $\text{Fe}^{2+}$  and  $\Sigma\text{H}_2\text{S}$  concentrations in the pore waters were quantified using the pilot ion method with  $\text{Mn}^{2+}$  as pilot ion (Luther, Glazer et al. 2008). As the exact structures of the organic-Fe(III) and  $\text{FeS}_{\text{aq}}$  complexes are unknown, voltammetric signals are reported in peak current intensities normalized to the sensitivity of the manganese calibration for the respective core (Taillefert, Luther et al. 2000).

After voltammetric microprofiles were completed, the sediment cores were sectioned in approximately twenty 7-10 mm sections and pore waters extracted under N<sub>2</sub> atmosphere in a glove bag (Sigma-Aldrich). A pellet of less than 0.5 g of sediment from the top 2 sections and every other section afterward was added to RNeasy lysis buffer, flash frozen on dry ice, and stored at -20°C for 16S rRNA extraction at Georgia Tech. The sediment sections were then centrifuged for 10 minutes at 3000 rpm and the pore waters were filtered through 0.22 µm PES Puradisc syringe filters (Whatman) into polypropylene Falcon tubes (Nalgene). To minimize oxidation of the sample, pore waters were then immediately transferred to a secondary glove bag under N<sub>2</sub> atmosphere and split for subsequent analyses of dissolved Fe(II) (Fe<sup>2+</sup><sub>d</sub>) by the Ferrozine method (Stookey 1970), orthophosphates (ΣPO<sub>4</sub><sup>3-</sup>) by the methylene blue method (Murphy and Riley 1962), and dissolved inorganic carbon (DIC) via a flow-injection analysis (Hall and Aller 1992). Aliquots of pore water samples were also added to 0.2 M hydroxylamine at pH 1.0 and stored in the dark for 24 hours to quantify total dissolved iron (Fe<sub>tot</sub>) by the Ferrozine method and dissolved Fe(III) (Fe(III)<sub>d</sub>) by difference between Fe<sub>tot</sub> and Fe<sup>2+</sup> (Stookey 1970). Finally, aliquots were analyzed onboard for dissolved Mn (Mn<sub>d</sub>) by ligand exchange reaction with a porphyrin molecule [(α,β,γ,δ-tetrakis(4-carboxyphenyl)porphine (T(4-CP)P)] and absorbance measurement at 468 nm (Madison, Tebo et al. 2011) after correction for Fe<sup>2+</sup> interference by dilution (Owings et al., submitted). The leftover pore waters were frozen at -20°C until analysis of ammonium (NH<sub>4</sub><sup>+</sup>) by the indophenol blue method (Strickland and Parsons 1972) and anions by high performance liquid chromatography (HPLC) without suppression at Georgia Tech. Anion separation was achieved with a Waters 1525 pump and a 4.0 mm x 150 mm Metrosep Supp 5 anion exchange column (Metrohm) using either 3.2 mM NaCO<sub>3</sub>



/ 1.0 mM NaHCO<sub>3</sub> buffer bicarbonate (Cl<sup>-</sup>, Br<sup>-</sup>, SO<sub>4</sub><sup>2-</sup> in 30-fold diluted samples) or 54 mM sodium chloride (NO<sub>2</sub><sup>-</sup>, and NO<sub>3</sub><sup>-</sup> in undiluted samples) as mobile phase. The mobile phase was eluted through the column at a flow rate of 0.75 ml min<sup>-1</sup> and absorbance was measured at 210 nm with a Waters 2487 photodiode array detector (Beckler, Nuzzio et al. 2014). Error for dissolved components analysis was propagated from the calibration curves.

#### 4.3.3 *Nucleic acids extraction and Illumina sequencing*

Microbial communities were characterized at every station. In order to relate chemical changes within the sediment with potential changes in microbial community composition, 10 samples were taken from every core, down to approximately 135 mm, with a separation of 5 to about 20 mm between each sample. DNA was extracted using the MoBio Power Soil Kit<sup>TM</sup>. Approximately 0.3 grams of sediment was used for extraction, yielding approximately 20 ng/μL (in 50 μL) DNA. For Bacteria, 16S rRNA genes were amplified using primer pairs 505F and 806R, with PCR primers harboring sample specific adapters for de-multiplexing as described previously (Kozich, Westcott et al. 2013). PCR reactions were carried out in 25 μL total volume with 0.5μL of each forward and reverse primer at (0.2 μM final concentration) with GoTaq green master mix (12.5 μL per reaction), 1 μL of template, and 9.5 μL PCR-grade water. PCR reactions consisted of an initial denaturation step of 95 degrees C for 5 minutes, followed by 28 cycles of 95 degrees C for 1 minute, 55 degrees C annealing for 1 minute, 72 degrees C extension for 2 minutes, followed by a final 5 minute extension of 72 degrees. PCR products (5μL) were visualized by gel electrophoresis (1% agarose, 1% Gel Red). The remainder of the products (20 μL) were cleaned using the QIAQuick PCR clean-up kit, and eluted in 30 μL elution buffer. Cleaned PCR products were quantified using the broad range double stranded DNA

quantification kit (Thermo Scientific). PCR products were pooled, with each sample-PCR product representing 10ng. This pooled mixture was then diluted to 1.2 ng/μL and used for further sequencing analyses on an Illumina MiSeq, using a V2 500 cycle paired end mode kit.

Archaeal 16S rRNA gene amplifications were carried out using the same PCR-recipe as above, with PCR primers Arch516F (TGYCAGCCGCCGCGGTAHACCVGC) and 915R (GTGCTCCCCGCCAATTCCT) (Stahl 1991, Takai and Horikoshi 2000). These primers were amended with Illumina adapters specific for the forward and reverse primers, barcodes, primer pad, and primer linkers. The thermocycler protocol was similar, with one exception, 30 cycles were utilized rather than 28.

#### *4.3.4 Quality sequence processing analyses*

Amplicon sequences from both Bacterial and Archaeal data sets were analyzed in a similar fashion, using the DADA2 pipeline, with differences detailed below. Taxonomy was assigned to the representative ASVs from this pipeline using the SILVA rRNA gene database (version 132) through the naïve Bayesian classifier method of (Wang, Garrity et al. 2007). Sample-taxonomy tables were generated by ‘adding’ the taxonomy information for each representative ASV to sample-ASV tables in Qiime-2019.4. Sequences classified as chloroplasts or Eukaryota were removed from the final tables. Amplicons obtained using universal prokaryotic primers were rarefied to a depth of 50000 reads, while those obtained using the archaea specific primer set were rarefied to 1200 reads. Further diversity analyses including phylogenetic tree construction, and  $\alpha$ - and  $\beta$ -diversity metrics were conducted using Qiime-2019.4.

#### 4.3.5 *Phylogenetic inference*

In order to better characterize the Bathyarcheota group in our dataset, phylogenetic approximation of Bathyarchaeal ASVs were inferred by comparing those sequences to the Bathyarchaeota database from Zhou, Pan et al. (2018) using BLASTN (97 % similarity cutoff).

#### 4.3.6 *Multivariate analyses*

Canonical correspondence analyses (CCA) were performed in R (version 3.6) using the *vegan* package. Rarefied sample-ASV matrices, and the associated metadata (environmental parameters) were used. ASV relative abundances were square root transformed while sediment chemistry measurements were log transformed. To identify which environmental variables were significant, an ANOVA test was performed on those terms of the CCA.

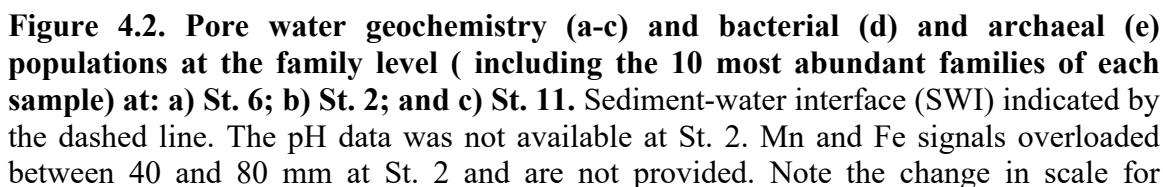
Co-occurrence network analysis was performed following the pipeline established by (Pylro, Roesch et al. 2014), which used SparCC to determine correlations between ASVs. This analysis was performed on the ASVs with a relative abundance  $\geq 0.002$  % from the ASV table obtained using the universal primer set. Only strong correlations with a p-value  $\leq 0.01$ , and imported into Cytoscape where and Markov clustering method (MCL) was applied based on betweenness centrality.

The Bathyarcheota heatmap was realized using R (version 3.6), package 'Heatplus'. Only Bathyarcheota ASVs retrieved from the ASV table obtained using the archaea specific primer set were used. For clarity and visibility, only ASVs with a relative abundance  $\geq 1.5$  % are presented.

## 4.4 Results

### 4.4.1 *Mississippi river discharge and visual sediment characteristics*

The Mississippi River discharge from Belle Chasse, LA monitoring station (29°51'25", 89°58'40") was  $418,556 \pm 22,875 \text{ cm}^3 \text{ s}^{-1}$  during this study (Figure C.1). Overall, the discharge pattern was transitioning from high discharge ( $1,330,000 \text{ cm}^3 \text{ s}^{-1}$  between January and March 2016) to low discharge ( $229,000 \text{ cm}^3 \text{ s}^{-1}$  in December 2016) (Figure C.1, USGS). Sediment cores collected varied in color depending on station location (Figure C.2). Across the shelf (St. 6, 5B, C6C and MK), sediments were a mix of gray to dark gray with patches of black (Figure C.2). A worm (approx. 6.5 cm long) was discovered while sectioning St. 6 sediment core, indicative of active bioturbation (not pictured). Interestingly, at St. MK a floc of black sediment was present in the top 7 cm (Figure C.2). Sediments from St. 2 and St. 3 were similar with a small band of brown sediments in the top few centimeters, followed by dark gray/black sediments to depth. At St. 11, sediments contained a thicker layer of brown sediments in the top 4 cm that was distinct from the remaining gray sediment below the brown layer (Figure C.2). The sediment core from St. 10 appeared to be homogenously distributed as brown/gray sediment throughout the core (Figure C.2). Station 6, Station 2 and station 10 were chosen as representative stations of the shelf, shelf-slope transition, and slope regions (Figure 4.2). The sediment biogeochemistry at these three stations are discussed in detail (Figure 4.2) in the results, however, the remainder of the stations are briefly discussed and figures for each data set at each station are found in the supplemental material.



voltammetric  $\text{Mn}^{2+}$ ,  $\text{Fe}^{2+}$  and org-Fe(III) measurements, as well as  $\text{Mn}_d$ ,  $\text{Fe}^{2+}$  (St. 6), and  $\Sigma\text{PO}_4^{3-}$  (St. 2) concentrations to better display trends at each station.

#### 4.4.2 *Bottom water oxygen concentrations and oxygen penetration depths in the sediment*

Bottom water oxygen concentrations along the shelf transect ranged from 2 to 11  $\mu\text{M}$  (Table 4.1), therefore falling under the defined conditions of hypoxic ( $< 63 \mu\text{M}$ ) (Rabalais, Díaz et al. 2010). Although not measured in the present study, St. 5B was in the hypoxic zone according to 2015 and 2017 historical data (Rabalais and Turner 2015, Rabalais and Turner 2017). In turn, bottom water oxygen concentrations at St. 2 were slightly below saturation at 114  $\mu\text{M}$  during the summer of 2017 (Owings et al., submitted) and close to saturation at 168  $\mu\text{M}$  in 2006 at a station (St. 201 29°0.117' N, 89° 32.258' W) near St. 2 and 3 was (Devereux, Mosher et al. 2015), suggesting that the hypoxic zone did not extend over the shelf. Indeed, bottom waters of the slope stations were oxic and fully saturated (Table 4.1). Correlating bottom oxygen concentrations, dissolved oxygen concentrations in the sediment core overlying waters were below detection limit of the voltammetric microelectrodes (Minimum Detection Limit: MDL  $\sim 5 \mu\text{M}$  (Luther, Glazer et al. 2008)) across the hypoxic shelf. In turn, overlying waters of the continental shelf ranged between 113 and 180  $\mu\text{M kg}^{-1}$  (Table 4.1), while oxygen penetration depths (OPDs) increased from 4 mm (St.2) to  $>10$  mm across the slope.

#### 4.4.3 *DIC, $\text{NH}_4^+$ , $\Sigma\text{PO}_4^{3-}$ and pH profiles*

Pore water DIC concentrations were generally higher across the hypoxic shelf than across the continental slope (Figure 4.3) and more elevated on the western and eastern ends of the hypoxic zone.

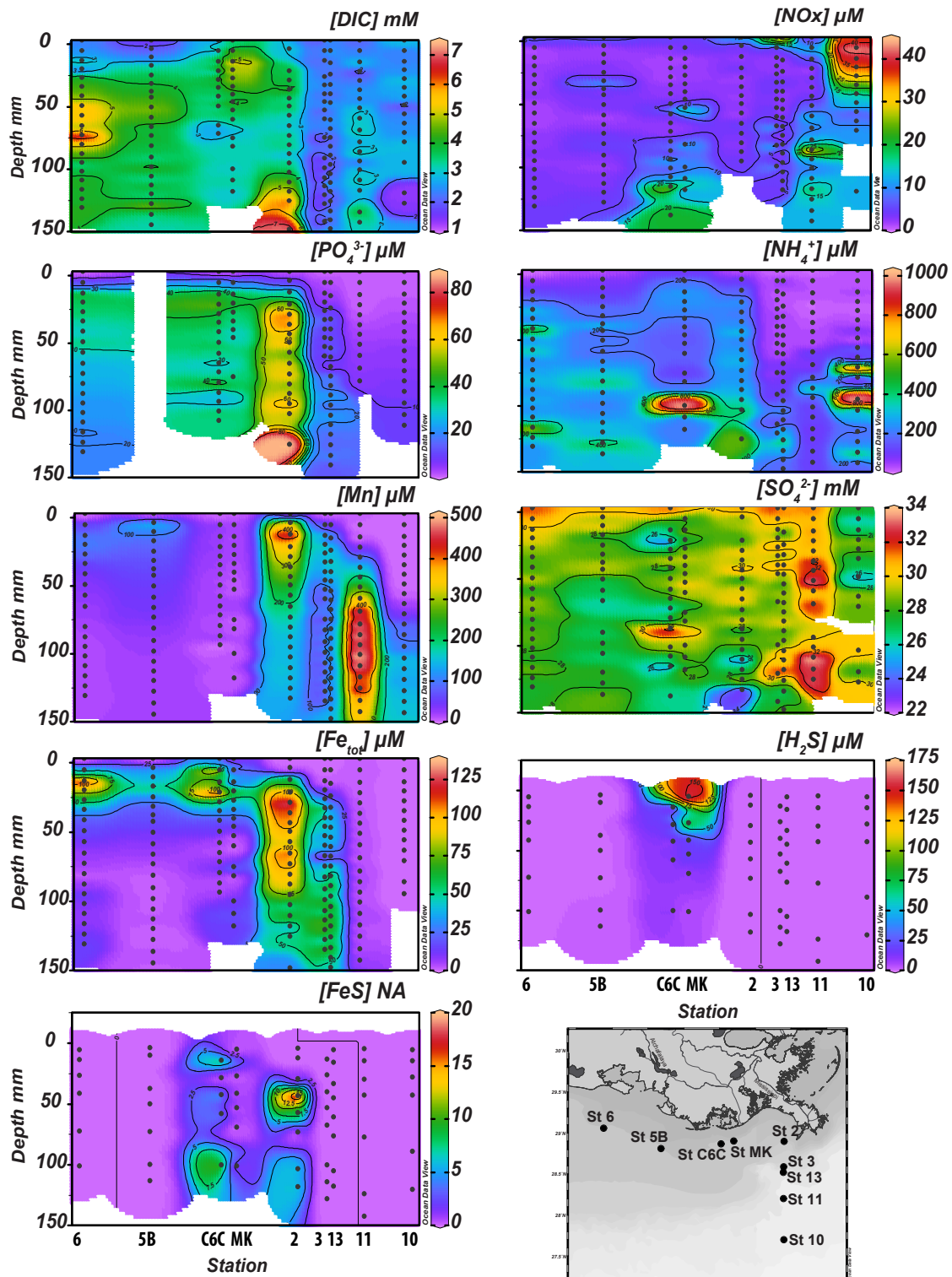


**Figure 4.3. Dissolved inorganic carbon (DIC, mM),  $\text{NO}_x = \text{NO}_2^- + \text{NO}_3^-$  ( $\mu\text{M}$ ), orthophosphate ( $\text{PO}_4^{3-}$ ,  $\mu\text{M}$ ), ammonium ( $\text{NH}_4^+$ ,  $\mu\text{M}$ ), total dissolved Mn ( $\text{Mn}_d$ ,  $\mu\text{M}$ ), sulfate ( $\text{SO}_4^{2-}$ , mM), and total dissolved Fe ( $\text{Fe}_d$ ,  $\mu\text{M}$ ) measured in the pore waters along with dissolved sulfide ( $\Sigma\text{H}_2\text{S}$ ,  $\mu\text{M}$ ) and aqueous FeS ( $\text{FeS}$ , nA) measured by voltammetric microelectrodes as a function of depth at each station using a heat map. The map of station locations is included for reference (bottom right). Black dots on each plot represent actual measurement locations. Color contours from red to purple represent high to low concentrations indicated by the scale to the right of each panel. Plots created in Ocean Data View (ODV) software.**

Bottom water DIC concentrations at the shelf stations were between 2-2.8 mM and pore water DIC concentrations increased to maximum concentrations of 4.3-5.5 mM at St. C6C (Figure C.3**Error! Reference source not found.**), St. 6 (Figure 4.2a), and St. 5B (Figure C.4) around 50 mm below the sediment water, however the peak at St. MK was more shallow at 13 mm (Figure C.5). Deeper, DIC concentrations generally decreased to 4.2, 3.0 or 2.3 mM at stations 6, 5B and MK respectively. DIC at St. 2 (closest to the Mississippi River delta) increased from 3.0 mM at 3 mm to 7.1 mM at 148 mm (Figure 4.2b). On the other hand, no variations in DIC concentrations (2.3-3.8 mM) were observed in the slope sediments (Figure 4.3). Simultaneously,  $\text{NH}_4^+$  concentrations increased constantly with depth from the sea water interface (SWI) to maximum concentrations at the bottom of the sediment cores and, similarly to DIC, reached higher maximum concentrations at the shelf stations (210-440  $\mu\text{M}$ ) than slope stations (113-160  $\mu\text{M}$ ) (Figure 4.3). A few stations displayed linear trends of about 200  $\mu\text{M}$  with slight oscillations at depth (St. MK, St. 13, St. 10). St. 11 maintained low concentrations (11-34  $\mu\text{M}$ ) until 51 mm, followed by higher concentrations of 93-149  $\mu\text{M}$  until depth (143 mm), with a peak to 360  $\mu\text{M}$  at 86 mm (Figure 4.2c). Similarly, St. 10 maintained low concentrations of  $\text{NH}_4^+$  within the first 48 mm (20-78  $\mu\text{M}$ ) followed by peaks in concentrations at 71 and 95 mm of 896 and 1,023  $\mu\text{M}$ , respectively before a return to concentrations between 144-444  $\mu\text{M}$



between depths 103-151 mm (Figure C.6).  $\text{NH}_4^+$  concentrations for St. C6C and  $\Sigma\text{PO}_4^{3-}$  concentrations for St. 5B were not analyzed due to limited sample size.  $\Sigma\text{PO}_4^{3-}$  concentrations in shelf sediments were low near the SWI ( $<30 \mu\text{M}$ ) and peaked to about 40-80  $\mu\text{M}$  around 20-40 mm and remained elevated through the remainder of the core (Figure 4.3, Figure 4.2a, Figure C.3, Figure C.5, Figure 4.2b). In contrast, the  $\Sigma\text{PO}_4^{3-}$  concentrations in the slope stations increased continuously with depth to maximum concentrations around 25  $\mu\text{M}$  (Figure 4.3, Figure C.6, Figure C.7, and Figure C.8).

The overlying water pH ranged between a minimum of 7.5 (St. 6, Figure 4.2a) and a maximum of 8.1 (St. C6C, Figure C.3) across the shelf stations and reached a maximum (approx. 0.1 units higher than overlying waters) around 3-5 mm below the SWI (Figure 4.2a,b, Figure C.3, Figure C.4, Figure C.5). Deeper, the pH decreased by about 0.5-0.7 units and remained constant between 7.2 (St. 6, Figure 4.2a) and 7.3 (St. C6C, Figure C.3) at depth. The overlying water pH of the continental slope stations was generally higher, ranging from 7.4 at St. 13 (Figure C.8) to 7.7-7.9 at St. 3, 11, and 10 (Figure C.7, Figure 4.2c, Figure C.6). pH data was not collected at St. 2. Interestingly, the pH of the continental slope stations did not produce a maximum below the SWI, instead the pH decreased moderately in comparison to the shelf stations from approximately 3-10 mm below the SWI to a pH minimum ranging between 7.1 and 7.6 (Figure C.7, Figure 4.2c, and Figure C.6).

#### 4.4.4 *Main sedimentary redox processes in the LCS*

$\text{NO}_2^-$  and  $\text{NO}_3^-$  concentrations (presented as  $\text{NO}_x = \text{NO}_2^- + \text{NO}_3^-$  in Figure 4.3) were generally low in most shelf and slope sediments with some subsurface maxima found in the middle of the shelf (St. C6C and MK) and at St. 3, 10, and 11 on the slope (Figure 4.3).

In contrast,  $\text{NO}_x$  concentrations were high at the sediment surface of most of the slope stations (St. 3, 13, and 10). At most stations (St.6, 5B, 2, and 13),  $\text{NO}_x$  decreased rapidly with depth and remained below 5  $\mu\text{M}$  and 1.8  $\mu\text{M}$  respectively within 20 mm from the SWI (Figure 4.2a, Figure C.4, Figure 4.2b, and Figure C.8). The profiles of the easternmost shelf stations, St. C6C and St. MK, however, revealed that both  $\text{NO}_2^-$  and  $\text{NO}_3^-$  concentrations increased at depth to maximums of 23  $\mu\text{M}$   $\text{NO}_3^-$  and 6.3  $\mu\text{M}$   $\text{NO}_2^-$  at 115 mm at station C6C (Figure C.3), and 11  $\mu\text{M}$   $\text{NO}_3^-$  and 3.9  $\mu\text{M}$   $\text{NO}_2^-$  at 108 mm at station MK (Figure C.5). Although  $\text{NO}_2^-$  concentrations remained constant below 2.3  $\mu\text{M}$  throughout the core at St. 3 (Figure C.7) and 11 (Figure 4.2c),  $\text{NO}_3^-$  concentrations decreased from 19  $\mu\text{M}$  at St. 3 and 3.8  $\mu\text{M}$  at St. 11 in the overlying waters to approx. 2  $\mu\text{M}$  at 20 mm, followed by a rebound to 12  $\mu\text{M}$  at 67 mm at St. 3 and between 8 and 13  $\mu\text{M}$  with depth at St. 11. In turn, St.10 displayed a broad subsurface  $\text{NO}_2^-$  peak of 23  $\mu\text{M}$  centered at 20 mm, while  $\text{NO}_3^-$  concentrations decreased from 37  $\mu\text{M}$  in the overlying waters to 9.8  $\mu\text{M}$  at 27 mm and remained stable around this concentration deeper in the sediment (Figure C.6).

Most stations on the shelf displayed generally low dissolved Mn and dissolved Fe concentrations with small peaks at shallow depths in the profiles (Figure 4.3). At St. 6,  $\text{Mn}_d$ ,  $\text{Fe}^{2+}$  and  $\text{Fe(III)}_d$  peaked at 20 mm to concentrations of 102, 36, and 46  $\mu\text{M}$  respectively (Figure 4.2a). Although slightly offset with depth, a broad  $\text{Mn}^{2+}$  peak (max. concentration of 98  $\mu\text{M}$  at 32 mm) was also observed in the voltammetric profile at St. 6, while all other redox species remained below detection limit (Figure 4.2a). Such differences between voltammetric and pore water measurements likely reflect the fact that voltammetric measurements are obtained at one point at each depth in the sediment, compared to the pore water measurements that are integrated over the entire slice of

sediment from which they are extracted. At St. 5B, a peak in  $Mn_d$  concentrations (145  $\mu M$ ) occurred immediately below the SWI (3.5 mm), followed by a peak in  $Fe^{2+}$  and  $Fe(III)_d$  (11 and 40  $\mu M$  respectively) at 17 mm. A  $Fe^{2+}$  peak in the voltammetry profile also mirrored the  $Fe^{2+}_d$  peak in the pore waters (Figure C.4). The pore water profile of St. C6C displayed a peak in  $Fe^{2+}$  and  $Fe(III)_d$  of equal concentrations (67-71  $\mu M$ ) at 21 mm and low  $Mn_d$  (< 35  $\mu M$ ) concentrations throughout the core (Figure C.3). The voltammetry profile at St. C6C detected  $Fe^{2+}$  throughout the core, except between 33 and 82 mm where  $Mn^{2+}$  was detected. Additionally, org-Fe(III) complexes were detected around 30 nA between 26-84 mm and at depth between 150-197 nA. At St. MK,  $Mn_d$  in the pore waters remained around 4-14  $\mu M$  throughout the core, and  $Fe(III)_d$  peaked at 20 mm (36  $\mu M$ ). Dissolved Mn and Fe species were below detection limit of the voltammetric measurements at St. MK.

In contrast, dissolved Mn and dissolved Fe concentrations were much higher in the slope station sediments (Figure 4.3), although the onset depth of these species in the pore waters increased progressively with water depth. As a result, dissolved metals were the most abundant at St. 2 compared to the other shelf stations: A broad  $Mn_d$  peak of 445  $\mu M$  centered at 12 mm that progressively decreased in concentration to 136  $\mu M$  at 132 mm (Figure 4.2b) was accompanied by a modest increase in  $Fe^{2+}$  (to 41  $\mu M$  at depth) and a broad peak in organic-Fe(III) voltammetric signals (between 20-70 mm) that was mirrored by the  $Fe(III)_d$  pore water measurements (Figure 4.2b). The  $Mn_d$  peak migrated progressively deeper in the sediment across the continental slope, whereas  $Fe_d$  concentrations generally decreased in the pore waters (Figure 4.3). At St. 3,  $Mn_d$  concentrations peaked to 181  $\mu M$  at 13 mm, decreased to 51  $\mu M$  at 75 mm, and remained

constant deeper in the sediment (Figure C.7).  $\text{Fe}^{2+}$  and  $\text{Fe(III)}_d$  species appeared around 26 mm and hovered around 9-40  $\mu\text{M}$  and 34- 62  $\mu\text{M}$  deeper, respectively (Figure C.7). Although slightly offset with depth and concentrations, the voltammetric profiles at St. 3 also revealed a  $\text{Mn}^{2+}$  peak (203  $\mu\text{M}$ ) at 31 mm before coinciding  $\text{Fe}^{2+}$  (433  $\mu\text{M}$ ) and org- $\text{Fe(III)}$  complexes (78 nA) peaks around 50 mm. At St. 13,  $\text{Mn}_d$  increased to a maximum concentration of 190  $\mu\text{M}$  at 32 mm, dipped to around 100  $\mu\text{M}$  at 60 mm, and remained constant deeper in the sediment.  $\text{Mn}^{2+}$  was not detected by voltammetry until 75 mm and remained relatively low around 25-63  $\mu\text{M}$  deeper in the same sediment. At St. 13, the onset of  $\text{Fe}^{2+}$  and  $\text{Fe(III)}_d$  production occurred simultaneously around 32 mm, and  $\text{Fe}^{2+}$  and  $\text{Fe(III)}_d$  concentrations increased up to 21 and 51  $\mu\text{M}$  with depth, although voltammetric  $\text{Fe}^{2+}$  remained below detection limit and org- $\text{Fe(III)}$  signals were small (Figure C.8).  $\text{Mn}_d$  concentrations at St. 11 increased from below detection limit at 20 mm to 600  $\mu\text{M}$  at 70 mm and remained elevated deeper (Figure 4.2c), whereas pore water  $\text{Fe}^{2+}$  remained below detection limit and  $\text{Fe(III)}_d$  concentrations were around 2  $\mu\text{M}$  (Figure 4.2). In turn, the voltammetry profile only showed  $\text{Mn}^{2+}$  production at 120 mm to a maximum concentration around 307  $\mu\text{M}$   $\text{Mn(II)}$  at 140 mm that remained constant deeper, whereas  $\text{Fe}^{2+}$  and org- $\text{Fe(III)}$  were not detected throughout the profile (Figure 4.2). Finally,  $\text{Mn}_d$  concentrations at St. 10 were below detection limit until 55 mm below the SWI and gradually increased with depth to 170  $\mu\text{M}$  at 151 mm, whereas pore water  $\text{Fe}^{2+}$  and  $\text{Fe(III)}_d$  remained below detection limit and  $\text{Mn}^{2+}$  and Fe species were not detected by voltammetry (Figure C.6).

$\text{SO}_4^{2-}$  concentrations across the shelf and slope ranged from 25-32 mM, with no significant decrease with depth at all stations (Figure 4.3), except at St. 2 where  $\text{SO}_4^{2-}$  decreased to 22.5 mM at 133 mm (Figure 4.2b). Despite no significant decrease in  $\text{SO}_4^{2-}$

concentrations,  $\Sigma\text{H}_2\text{S}$  was detected in all shelf station sediments (Figure 4.3) except for the westernmost St. 6 (Figure 4.2a).  $\Sigma\text{H}_2\text{S}$  concentrations were low ( $< 5 \mu\text{M}$ ) but present consistently below 25 mm at St. 5B (Figure C.4).  $\Sigma\text{H}_2\text{S}$  was detected in the overlying waters (26-31  $\mu\text{M}$ ) at St. MK (Figure C.5), formed a sharp peak around 181  $\mu\text{M}$  at 15 mm, and decreased progressively deeper (Figure C.5). A similarly sharp  $\Sigma\text{H}_2\text{S}$  peak was found below the SWI at St. C6C (41  $\mu\text{M}$  at 18mm) that was followed by another broader peak reaching 20  $\mu\text{M}$  between 74 and 116 mm that progressively decreased with depth (Figure C.3). Finally, the onset of sulfate reduction as revealed by the  $\Sigma\text{H}_2\text{S}$  depth profile, where  $\Sigma\text{H}_2\text{S}$  concentrations increased to approximately 20  $\mu\text{M}$  at 113 mm, remained constant until 170 mm, then progressively decreased in concentration with depth (Figure 4.2b). In contrast,  $\Sigma\text{H}_2\text{S}$  was detected generally in much lower levels at the slope stations (Figure 4.3), but decreased from the mid-slope stations (5-10  $\mu\text{M}$ ) at depth ( $> 80\text{mm}$ ) at St. 3 and St. 13 (Figure C.7 and Figure C.8) to below detection limit at the deep St. 11 and St.10 (Figure 4.2c and Figure C.6). Finally,  $\text{FeS}_{\text{aq}}$  was below detection limits at most stations, except on the eastern shelf and on the shelf break (Figure 4.3). Although detected in low current intensities ( $< 5 \text{ nA}$ ) throughout most of the profile at St. 6C6,  $\text{FeS}_{\text{aq}}$  formed a subsurface peak (2-20 nA) between 35-142 mm and hovered around 5 nA deeper at St. 2 (Figure 4.2b). Similarly,  $\text{FeS}_{\text{aq}}$  was produced below 80 mm at St. 3 and reached current intensities oscillating between 5 and 17 nA deeper (Figure 4.3).

#### 4.4.5 *Abiotic factors influencing microbial community structure in the Northern GoM*

$\beta$ - and  $\alpha$ -diversity analyses indicated that microbial communities varied with both water column and sediment core depth. Canonical correspondence analysis (CCA) on both

prokaryotic and archaea datasets separated microbial communities from shelf stations from those from slope stations (Figure 4.4).

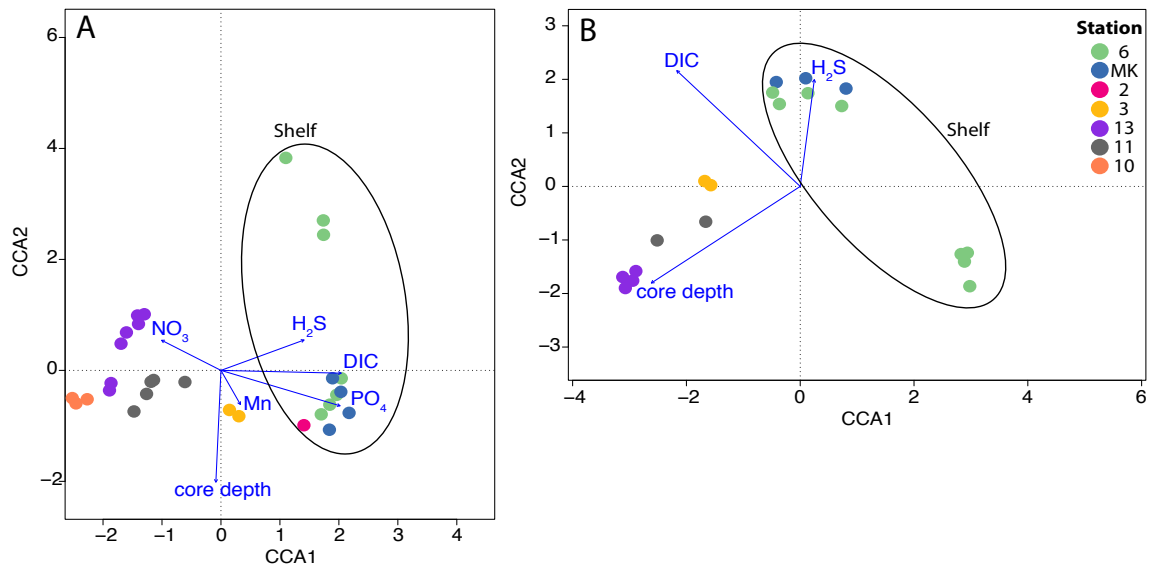


**Figure 4.4. Ordination plots of Canonical Correspondence Analysis (CCA) obtained with: a) universal primers; and b) archaeal specific primers to explore the relationship between prokaryotic communities at each station and significant environmental variables ( $p$ -value<0.01). Only samples with measurements of all geochemical parameters were included in analysis (i.e.  $\text{NH}_4^+$  data not available for C6C and  $\Sigma\text{PO}_4^{3-}$  data not available for 5B)**

Except for  $\text{NO}_2^-$  and org-Fe(III), most chemical species appeared to be significantly related to microbial community structure in the prokaryotic dataset (Table C.1a), whereas only DIC,  $\text{NH}_4^+$ ,  $\text{SO}_4^{2-}$ , and  $\Sigma\text{H}_2\text{S}$  appeared significantly related to the archaeal dataset (Table C.1b). Despite these features, the same trend appeared for both datasets with DIC,  $\Sigma\text{PO}_4^{3-}$ , and  $\Sigma\text{H}_2\text{S}$  as the main variables related to shelf microbial structure ( $p$ -value  $\leq 0.01$ ), whereas  $\text{NO}_3^-$  was the most related species to slope microbial assemblages ( $p$ -value  $\leq 0.01$ ) (Figure 4.4). Moreover, sediment core depth also appeared as a principal variable related to the microbial community composition of both datasets ( $p$ -value  $\leq 0.01$ ) (Figure 4.4). Interestingly, differences in  $\alpha$ -diversity were also observed with water column depth, as

well as within the sediment in both shelf and slope samples (Figure C.9). Richness measured by Faith-phylogenetic diversity index (Faith-pd) decreased between shelf and slope in both the prokaryotic (p-value = 0.006) and archaea (p-value = 9.00E-07) datasets, while diversity (Shannon index) did not appear to significantly change. On the shelf, richness (Faith- pd) of both the prokaryotic (p-value = 0.007) and archaea (p-value = 0.0008) showed an overall decrease with sediment core depth, whereas diversity (Shannon index) of both shelf (p-value = 0.0058) and slope (p-value = 0.05) stations increased with sediment core depth only for the archaea dataset.

#### 4.4.6 *Universal prokaryotic primers vs. Archaea specific primers*

Sediment samples used for microbial characterization were collected at all stations along with geochemical data. Microbial community composition in sediments was evaluated by sequencing 16S rRNA gene amplicons generated using both non-domain-specific primers that amplify all bacterial and some archaeal groups (Earth Microbiome Primers 505F and 806R; “bacterial” amplicons hereafter) as well as Archaea domain-specific primers that amplify the V4-V5 region of the 16S rRNA gene (516F/915R; “archaeal” amplicons hereafter). The initial microbial composition using universal prokaryotic primers revealed that a significant portion of the community was represented by archaea (15 %). Moreover, in accordance with previous research, MG-I *Thaumarchaeota* was the second most abundant class in our dataset (Learman, Henson et al. 2016, Overholt, Schwing et al. 2019), and earlier studies have shown that due to the larger proportion of bacteria compared to archaea in many environments, the use of universal primers is not enough to accurately capture the entire archaeal diversity (Teske and Sørensen 2008, Raymann, Moeller et al. 2017). Hence, in an attempt to better

characterize this archaeal diversity, archaea specific primers were used which had showed that over 90 % of the archaeal gut diversity in humans and apes was not captured using universal prokaryotic primers (Raymann, Moeller et al. 2017). Initial analyses were performed on sequence data partitioned at the level of amplicon sequence variant (ASVs) using DADA2. ASVs from the bacterial and archaeal datasets were compared against the SILVA rRNA gene database (version 132). Sequence counts corresponding to ASVs sharing identical taxonomic hierarchies were summed and the rank abundance of ASVs was compared among sites. 76 prokaryotic amplicon datasets were rarefied to 50000 sequences, yielding a total of 70332 ASVs, and 58 archaeal amplicon datasets were rarefied to 1200 sequences each, yielding 3999 ASVs.

In order to compare the specificity of both the universal and archaea specific primers in targeting the archaeal community, the bacterial reads from the prokaryotic dataset were removed, and all samples were rarefied to 1200 sequences. This new archaeal dataset derived from the prokaryotic dataset obtained using universal primers, yielded 77 samples with a total of 8053 ASVs. In order to see if the extra ASVs obtained using the universal primer set were due to the extra number of samples retrieved (77 vs 58), both the dataset obtained using universal primers and the one obtained using archaea specific primers were filtered to keep the exact same samples. The final archaea datasets contained 49 samples, and 6127 ASVs using the universal primer set versus 3922 ASVs using the archaea specific pair. Despite this difference in number of ASVs retrieved using either the universal primer pair or the archaea specific one, the overall trends remained unchanged.

#### *4.4.7 Microbial community composition along the Northern GoM shelf and slope*



The entire prokaryotic dataset was dominated by *Gammaproteobacteria* (19.4 %), and *Deltaproteobacteria* (18.5 %). *Nitrosphaeria* was the third most abundant class (5.3 %), followed by *Anaerolineae* (4.8 %) *Phycisphaerae* (4.2 %), *Bathyarchaeia* (3.4 %), *Alphaproteobacteria* (3.5 %), *Bacteroidia* (2.9 %), *Woesearchaeia* (2.4 %), and *Acidobacteria-Subgroup22* (1.8 %). Interestingly, most of these groups varied strongly in relative abundance and microbial composition at finer taxonomic resolution between shelf and slope stations. While samples for microbial and biochemical profiling were collected at every station and at different depths within the sediment core, 3 stations including St 6, St 2, and St 10 were chosen to represent the general trends observed on the shelf (St 6), on the slope (St 10), and on the transition between the two (St 2) (Figure 4.2). Among the groups that showed the largest differences between shelf and slope, *Bathyarchaeia* were 17 times more abundant on the shelf (Figure 4.2). Other classes that were among the 10 most abundant at shelf stations, such as *Thermoplasmata* (~ 3.5 times more abundant on the shelf) dominated by Marine Benthic Group D and DHVEG-1, and *Anaerolineae* (~ 2 times more abundant on the shelf) dominated by *Anaerolineaceae*, also showed higher relative abundances on the shelf compared to the slope (Figure 4.2). In contrast, *Brocadiae*, *Nitrososphaeria*, *Alphaproteobacteria*, and *Phycisphaerae* were 38, 6, 4 and 2 times more abundant on the slope, respectively (Figure 4.2). Moreover, a microbial network analysis conducted on the prokaryotic dataset (relative abundances > 0.0002) was able to partition the microbial diversity into several clusters which were composed by ASVs that were differentially abundant following water column or sediment depth gradients (Figure 4.5).

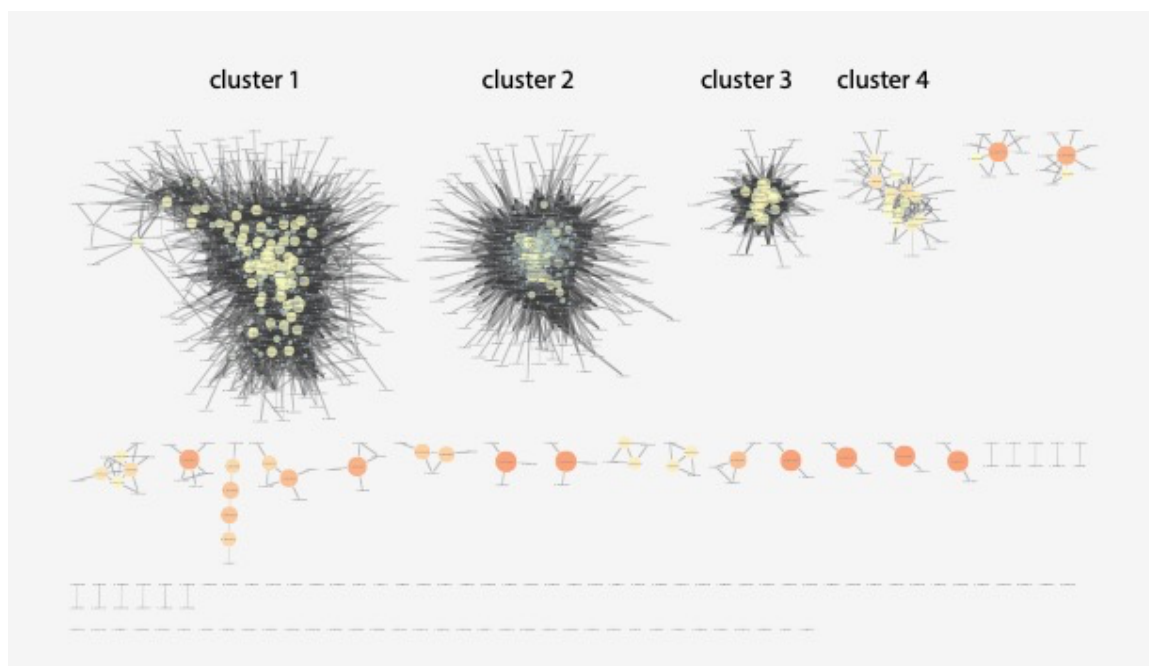


**Figure 4.5. Interaction networks of sediment microbial community members.** ASVs are depicted as circles, and sized and colored based on betweenness centrality values (the larger this value, the larger the size of the circle, and the warmer the color). Cluster 1 is composed by ASVs with higher relative abundances on the slope, cluster 2 is composed by ASVs with higher relative abundances on the shelf, and clusters 3 and 4 are composed by ASVs particularly abundant in deeper layers of the sediment. For this analysis, only ASVs with a relative abundance  $\geq 0.0002$  %, and only interactions with a  $p$ -value  $\leq 0.01$  were included.

Families including *Bathyarchaeia*-NA, *Desulfobacteraceae*, *Desulfobulbaceae*, *Anaerolineaceae*, *Haliaceae*, Marine Benthic group D and DHVEG-1, *Thiohalorhabdaceae*, *Thioalkalispiraceae*, *Ectothiorhodospiraceae*, *Lokiarchaeia*-NA, 4572-13 (Phycisphaerae-MSBL9), *Thiotrichaceae*, *Fusobacteriaceae*, *Methanofastidiosales*-NA, and *Methanosarcinaceae*, were part of a single cluster (cluster 2), which was primarily composed of microorganisms that showed higher relative abundances on the shelf (Figure 4.2, Figure 4.5). These particular groups represented about  $\sim 30$  % of the microbial community on the shelf compared to  $\sim 8$  % on the slope, and potentially play an important role in microbial community composition and function in

shelf sediments based on network analysis (Figure 4.5, Figure C.2). On the other hand, the slope was characterized by higher relative abundances of *Nitrosopumilaceae*, *Woeseiaceae*, *NB1-J-NA* (*Deltaproteobacteria*), *Kiloniellaceae*, *Acidobacteria* (Subgroup 21, 22), *Phycisphaerae-MSBL9* (*L21-RPul-D3*, *SG8-4*), *Scalinduaceae*, *Nitrosococcaceae*, *NC10* (*Methylomirabilaceae*), *Nitrospinaceae*, *Rhodobacteraceae*, *Methyloligellaceae*, *Nitrospiraceae*, and which also appeared as important nodes of a separate cluster (cluster 1) on the network analysis, representing slope microbial communities (Figure 4.2, Figure 4.5). These groups represented about 35 % of the microbial community on the slope, compared to ~ 11 % on the shelf (Figure 4.2).

Microbial community composition also varied with sediment core depth. On the shelf, *Bathyarchaeia* dramatically increased in relative abundance below ~ 10 cm, as it represented an average of ~ 5 % of the community on upper layers compared to ~ 53 % in sediments below 10 cm (Figure 4.2). A heat map of the most abundant *Bathyarchaeia* ASVs (> 1.5 % of the archaea dataset) revealed that this group presented strong spatial clustering between shelf and slope at the ASV level (Figure C.10). To better characterize the bathyarchaeal diversity in the present samples, bathyarchaeal sequences were compared to another bathyarchaeal database using BLASTN (Zhou, Pan et al. (2018)). This analysis showed that subgroup 8 dominated shelf communities, followed by subgroup 15, 12, 13, and 17, while subgroup 15 dominated slope communities followed by subgroup 2, 13, and 6 (Figure C.10, Table C.2). Other microbial groups such as *Anaerolineae-NA*, *Woesearchaeia*, *Sva0485* (*Deltaproteobacteria*), *SG8-4* (*Phycisphaerae-MSBL9*), *H3.93* (*Dehalococcoida*), *Methanofastidiosales*, *Methanosarcinales*, *Methanocellales*, *ANME-1(a, b)*, and *Methanomicrobiales* also increased with sediment core depth on the shelf and,

by forming clusters 3 and 4 in the network analysis (Figure 4.2, Figure 4.5), appeared important players in deeper layers of these sediments. Although less striking than shelf sediments, differences in microbial diversity associated with sediment core depth were also observed on the slope. For example, *NC10*, *Woesarchaeia*, and *Scalinduaceae* increased in relative abundance with sediment core depth (Figure 4.2).

## 4.5 Discussion

### 4.5.1 *Water column depth and sediment core depth represent major drivers of microbial community composition*

Both prokaryotic and archaeal datasets were primarily structured by water column depth and sediment core depth (Figure 4.2, Figure 4.4). Sediment communities from samples along the shelf (St 6 to St 2, < 100 m water column depth) were significantly different from sediment communities on the slope (St. 3 to St. 10, >100 m water column depth). In addition,  $\alpha$ -diversity decreased between shelf and slope stations, which appeared stronger in the archaeal dataset (Figure C.9). This decrease in microbial diversity may be related to a decrease in organic carbon availability at deep sea stations where inputs from both primary production and terrestrial sources may not be as strong compared to shelf stations. Interestingly, this result was significant using the Faith-pd index (Figure C9a) but not the Shannon index (Figure C.9c) for the prokaryotic dataset, which indicates a decrease in richness but not specifically in diversity. Richness (Faith-pd) decreased with sediment core depth on the shelf but appeared to stay constant or even increase in deeper layers of slope sediments, particularly for the archaea dataset (Figure C.9a,b). On the shelf, this result suggests a more constraining environment in deeper layers of the sediment, probably

related to a lack of electron donors and acceptors, which may limit microbial development (D'Hondt, Rutherford et al. 2002, D'Hondt, Jørgensen et al. 2004). The fact that diversity remained unchanged or showed a slight increase with sediment core depth in slope sediments, suggests that in contrast to other deep sea sediments, organic carbon may still be sufficient available in the deeper layers (between 66 mm and 130 mm) of these sediments to sustain a level of microbial diversity similar to the one observed in the upper layers. This result may in part be explained by the strong influence of the Atchafalaya and Mississippi rivers in this region (Owings et al., 2020), which could transport enough organic matter on the slope to maintain microbial diversity throughout the sediment. Interestingly, whereas archaeal richness (Faith-pd) decreased with sediment core depth on the shelf (Figure C.9), archaeal diversity (Shannon index) increased. In addition to the differentiation between shelf and slope stations,  $\beta$ -diversity analysis also revealed differences in microbial community structure with sediment core depth in accordance to previous studies (Hunter, Mills et al. 2006, Durbin and Teske 2011, Overholt, Schwing et al. 2019). This pattern had already been observed in the GoM (Overholt et al., 2019) where these factors not only stratified sediment microbial communities but also influenced niche diversification across geographically distant regions. In turn,  $\alpha$ -diversity in this past study appeared to be lower in shallower samples (<100 m water column depth) compared to deeper samples (> 400 m), whereas the opposite trend was observed in the present study (Figure C.9).

Similarly, to other sediment studies in the GoM (Reese, Mills et al. 2013, Overholt, Schwing et al. 2019), Proteobacteria dominated the entire prokaryotic dataset with an average relative abundance of about 42 % at both shelf and slope stations. This phylum

was largely dominated by Gammaproteobacteria (19.4 %) and Deltaproteobacteria (18.5 %) throughout both shelf and slope stations. Some archaeal classes were also particularly abundant including *Nitrososphaeria* (5.3 %), *Bathyarchaeia* (4 %), *Woesearchaeia* (2.4 %), and *Thermoplasmata* (1.8 %). The use of these primers in this specific system was not particularly useful in better characterizing this portion of the prokaryotic community. Indeed, patterns of diversity remained relatively unchanged using either universal or archaea specific primers, and the number of samples and archaea ASVs recovered was actually higher using the universal primer pair (77 samples versus 58, and 8053 versus 3999 ASVs). This result suggests that the effectiveness of these primers may be related to the environment studied and may not be particularly useful when characterizing sediment communities.

#### 4.5.2 *Shelf sediments are characterized by intense carbon remineralization and sulfur cycling*

The analysis of microbial community composition relative to the sediment geochemistry using Canonical Correspondence Analysis (CCA) revealed that DIC,  $\Sigma\text{PO}_4^{3-}$ , and  $\Sigma\text{H}_2\text{S}$  were the main variables controlling shelf communities ( $p\text{-value} \leq 0.01$ ) (Figure 4.4). Indeed, DIC,  $\text{NH}_4^+$ , and  $\Sigma\text{PO}_4^{3-}$  concentration increased with depth in the pore waters on the shelf, indicating that carbon remineralization processes were intensified with depth. However, overall concentrations of these species generally decreased eastward from St 6 to St C6C before increasing again, along with  $\Sigma\text{H}_2\text{S}$  and  $\text{FeS}_{\text{aq}}$ , across the eastern side of the shelf (St. MK to St. 2) (Figure 4.3). These two compounds are main indicators of  $\text{SO}_4^{2-}$  reduction and suggest increase in  $\text{SO}_4^{2-}$  reduction on the eastern shelf, despite undetectable  $\text{SO}_4^{2-}$  loss. In addition,  $\Sigma\text{H}_2\text{S}$  rapidly reduces organic-Fe(III) complexes (Taillefert, Hover

et al. 2002), Mn(IV/III) oxides, and Fe(III) oxides, and precipitates rapidly with  $\text{Fe}^{2+}$  to form  $\text{FeS}_{(s)}$  (Pyzik and Sommer 1981) but does not precipitate easily with  $\text{Mn}^{2+}$  (Luther 2005). Therefore, low dissolved  $\text{Fe}^{2+}$  and  $\text{Fe(III)}_d$  concentrations, lack of org-Fe(III) complexes, and the relatively high  $\text{Mn}_d$  concentrations (Figure 4.2a, Figure C.3, Figure C.4, and Figure C.5), along with the dark color of the sediment typical of  $\text{FeS}_{(s)}$  (Figure C.2) are all indicative of active  $\text{SO}_4^{2-}$  reduction on the continental shelf. In accordance with the geochemical data, microbes that are implicated in organic matter degradation, sulfur, and methane cycling were enriched at shelf stations. In order of relative contribution on the shelf, families such as *Bathyarchaeia-NA* (~ 7 %), *Desulfobulbaceae* (~ 5 %) , *Desulfobacteraceae* (~ 5 %), *Anaerolineaceae* (~ 3.5 %), *Woeseiaceae* (~ 3 %), *Haliaceae* (~ 2 %), Marine Benthic group D and DHVEG-1 (~ 1 %), *Thiohalorhabdaceae* (~ 1 %), *Thioalkalispiraceae* (~ 1 %), *Lokiarchaea-NA* (~ 0.7 %), *Thiotrichaceae* (~ 0.6 %), *Methanofastidiosales-NA* (~ 0.1 %), and *Methanosarcinaceae* (~ 0.03 %), among others, represented important members of the shelf microbial community (Figure 4.2, Figure 4.5). Following changes in redox potential and decreases in pH with increasing sediment core depth, shifts in shelf microbial community were also observed (Figure 4.2). Upper sediment layers were dominated by SRB including *Desulfobacteraceae*, and *Desulfobulbaceae* (Bahr, Crump et al. 2005, Kümmel, Herbst et al. 2015). Despite having relative abundances below 1.5 %, several members of the families *Thioalkalispiraceae*, *Ectothiorhodospiraceae*, *Rhodobacteraceae*, and *Thiotrichaceae*, among others, which have been related to sulfide oxidation (Cytryn, van Rijn et al. 2005, Franz, Lichtenberg et al. 2009, Sakurai, Ogawa et al. 2010, Montoya, Lozada-Chávez et al. 2011, Mori, Suzuki et al. 2011, Xu 2014, Devereux, Mosher et al. 2015, Lipsewiers 2017) were generally more

abundant in the upper layers of the sediment. Similarly, *Lokiarchaea* which have been implied in homoacetogenesis in sulfidic marine sediments (Orsi, Vuillemin et al. 2019), and *Halioglobus* and *Parahalaea* (*Haliaceae*) which are both aerobic bacteria implicated in denitrification processes (Jung, Jeong et al. 2017, Kim, Noh et al. 2017) were also more abundant in surficial sediments. Finally, *Woeseiaceae* also appeared as important contributor to the surface sediment structure on the shelf (Figure 4.2, Figure 4.5). This family seems to possess an incomplete denitrification pathway and be able to reduce nitrite and NO and produce N<sub>2</sub>O (Hinger, Pelikan et al. 2019), underlining that denitrification is a potentially significant process in these sediments.

In contrast, deeper sediment layers (below ~ 10 cm) harbored increasing proportions of microbes such as *Bathyarchaeia*, Marine Benthic group D and DHVEG-1, *Thermoplasmata*, *Desulfarculaceae*, *Syntrophobacteraceae*, and *Dehalococcoidia* (Figure 4.2). Although some of these microorganisms are also members of the SRB, including *Syntrophobacteraceae* and *Desulfarculaceae* (Julies Elsabé, Brüchert et al. 2012, Liu and Conrad 2017), *Thermoplasmata* contain uncultured members present in anoxic sediments (Lloyd, Schreiber et al. 2013) and co-occur with *Bathyarchaeia* (Bukin, Pavlova et al. 2016). In turn, Marine Benthic group D and DHVEG-1 are usually found in anoxic, organic and sulfide rich environments and some of their members are capable of conducting assimilatory sulfate reduction (Lazar, Baker et al. 2017), whereas *Dehalococcoidia* respire on organohalide (Wasmund, Schreiber et al. 2014). More importantly represented deep in these sediments, *Bathyarchaeia* have been linked to acetogenesis and sulfur and nitrogen reduction and appear to play a role in methane cycling, as they metabolize methane and interact with anaerobic methane-oxidizing archaea, acetoclastic methanogens,



and heterotrophic bacteria (Zhou, Pan et al. 2018). This group showed the largest increases, particularly at St 6 and St MK where it went from  $< 0.5\%$  to representing about  $50\%$  of the total microbial community, and showed micro diversity at the ASV level with a clear differentiation between ASVs present on the shelf relative to the slope, as well as with sediment core depth (Figure C.10). Interestingly, communities more closely related to members of subgroup 8 were the most frequent among the most abundant ASVs ( $>1.5\%$  from the archaea specific primer dataset) in the deep layers of the shelf stations. This subgroup has been implicated in methylotrophic methanogenesis and the degradation of lignin and aromatics (Evans, Parks et al. 2015), which suggests that methane cycling may be important in the deep sediment layers. Finally, several additional archaeal groups implicated in methane metabolism, including *Methanosarcinales*, *Methanofastidiosales*, *Methanocellales*, ANME-1(a, b), and *Methanomicrobiales* (Chen, Wang et al. 2020), while in low relative abundances (from  $5E-5$  to  $0.03\%$  on the shelf), were also more abundant in shelf sediments and increased with sediment depth. Other more abundant microbial groups linked to hydrocarbons, such as *Anaerolineaceae* (McIlroy, Kirkegaard et al. 2017), or associated with high organic matter content, a potentially symbiotic lifestyle, and methane cycling, such as *Woesarchaeia* (Castelle, Wrighton et al. 2015, Fan and Xing 2016, Liu, Klose et al. 2018), tended to increase with sediment core depth (Figure 4.2). In particular, *Woesearchaeia* which did not show strong changes in relative abundance between shelf and slope, increased with sediment core depth in both these regions. Based on network analysis, a subset of ASVs from these groups that were more abundant in shelf stations appeared as significant taxa structuring the microbial community in this region (Figure

4.5). Together with the higher abundance of methanogens, this observation reinforces the possibility of methane cycling taking place in the deep sediment layers of the shelf.

#### 4.5.3 *Slope sediments are characterized by metal reduction and nitrogen-related microbial processes*

Overall increases in dissolved Mn and Fe concentrations with depth, and below detection limit concentrations of FeS and  $\Sigma\text{H}_2\text{S}$ , suggest a transition from  $\text{SO}_4^{2-}$  reduction in shelf sediments to metal reduction in slope sediments (Figure 4.3) even though CCA revealed that  $\text{NO}_3^-$  appeared more important in shaping the microbial communities along the slope (Figure 4.4, Table C.1). Indeed,  $\text{NO}_x$  concentrations were much higher in continental slope sediments and generally decreased with depth (Figure 4.3), except at St. 11 where an increase in  $\text{NO}_x$  was evident (Figure 4.2c). These geochemical changes were accompanied by an increase in nitrogen cycling microbes. In order of relative contribution on the slope, these groups included *Nitrosopumilaceae* ( ~ 10 %), *Woeseiaceae* ( ~ 5 %), NB1-J-NA (Deltaproteobacteria) ( ~ 4 %), *Kiloniellaceae* ( ~ 3 %), *Scalinduaceae* ( ~ 2 %), *Acidobacteria* (Subgroup 21, 22; ~ 2 %), *Nitrosococcaceae* ( ~ 1 %), *NC10* ( ~ 0.8 %), *Nitrospinaceae* ( ~ 0.6 %), *Nitrospiraceae* ( ~ 0.4 %; Figure 4.2). Based on network analysis, these microbes also appeared as important members of the slope microbial community, with potentially important functions (Figure 4.5). In accordance with previous studies in the GoM, *Nitrosopumilaceae* was the most abundant family in the dataset, particularly in surficial sediments where it reached up to 34 % (Learman, Henson et al. 2016, Overholt, Schwing et al. 2019). As part of the *Thaumarchaeota* phylum, these organisms are known ammonia oxidizers that usually occupy oxic or suboxic sediment layers where either the quality or quantity of organic carbon has decreased (Durbin and

Teske 2011, Durbin and Teske 2012, Danovaro, Molari et al. 2016, Learman, Henson et al. 2016). *Nitrospiraceae* was dominated by *Nitrospira*, and *Nitrospinaceae* was dominated by *Nitrospina*. Although these groups are usually affiliated with nitrite oxidation, certain cultivated *Nitrospira* strains have recently been implicated in complete ammonia oxidation to nitrite and then to nitrate, so-called ‘comammox’ (Daims, Lebedeva et al. 2015, van Kessel, Speth et al. 2015). Whereas *Nitrospira* showed microdiversity at the ASV level between shelf and slope stations, the majority of *Nitrospira* ASVs from either shelf or slope sediments were not closely related with any of the subgroups or sublineages of previously reported comammox or nitrite-oxidizing organisms. In much lower abundance, *Nitrosococcaceae* are capable of ammonia oxidation (Ward, Johnston et al. 2019), *Acidobacteria* (Subgroup 21,22) are typical of sedimentary environments, have been correlated with higher nitrogen concentrations (Chaves, Silva et al. 2019), and are capable of both nitrite and nitrate reduction (Ward, Challacombe et al. 2009), whereas *Scalinduaceae* are usually related to anammox (van de Vossenberg, Woebken et al. 2013). Finally, *Woeseiaceae* possess an incomplete denitrification pathway and reduce nitrite and NO to produce N<sub>2</sub>O (Hinger, Pelikan et al. 2019), whereas *Kiloniellaceae* conduct denitrification (Imhoff and Wiese 2014). On the other hand, members of the NC10 group, which was dominated by *Methylospiraceae* (wb1-A12) are known to carry out nitrite dependent methane oxidation (He, Geng et al. 2015).

Similar to shelf stations, changes in microbial community composition were observed with changes in redox potential associated with sediment core depth in the slope stations (Figure 4.2). In particular, NC10, *Woesarchaeia*, and *Scalinduaceae*, which was only represented by *Candidatus-Scalindua* increased in relative abundance. Interestingly,

these changes were accompanied by a shift in the trend in Mn<sub>d</sub> distributions from the behavior of a sub-surface peak, to the rise to a maximum concentration at depth (Figure 4.3). This behavior could be due to reaching super saturation with respect to carbonate minerals in shelf-break and mid-slope sediments (Owings et al., 2020), or possibly a link between the nitrogen and manganese cycles at depth (Luther, Sundby et al. 1997). Moreover, NO<sub>2</sub><sup>-</sup> and NO<sub>3</sub><sup>-</sup> were produced at depth in slope sediments at St. 3, 11, and possibly 10 (Figure 4.2c, Figure C.6, and Figure C.7) and, coincidentally, at two shelf stations (St. C6C and MK). Anaerobic ammonium oxidation (anammox) to NO<sub>2</sub><sup>-</sup> or NO<sub>3</sub><sup>-</sup> linked to Mn(IV/III)O<sub>2</sub> reduction has been demonstrated in anoxic sediments (Anschutz, Sundby et al. 2000, Bartlett, Mortimer et al. 2007, Bartlett, Mortimer et al. 2008, Lin and Taillefert 2014). Although *Scalinduaceae* (Candidatus Scalindua) are usually linked to anammox using nitrite as electron acceptor (van de Vossenberg, Woebken et al. 2013), members of this particular genus are able to use Fe(III) and Mn(IV/III) oxides as terminal electron acceptors (van Niftrik and Jetten 2012, Bertrand, Bonin et al. 2018). Their increase in abundance in deeper layers of these sediments therefore suggests that they might be related to subsurface maxima in both NO<sub>x</sub> and dissolved Mn (Figure 4.2c, Figure C.6, and Figure C.7). The high relative abundances of microbes related to nitrogen cycling on the slope including nitrifying, denitrifying, and anammox bacteria, supports previous work showing that inorganic nitrogen species are an important source of electron acceptors and donors in these sediments (Glud, Thamdrup et al. 2009, Swan, Martinez-Garcia et al. 2011, Danovaro, Molari et al. 2016, Overholt, Schwing et al. 2019), which can ultimately affect global nitrogen budgets.

#### 4.5.4 Possible cryptic sulfur cycling in shelf and slope sediments

As described above, intense sulfur cycling was observed in both the geochemistry and microbial data on shelf stations. However, although the sediment pore water geochemistry showed a transition from  $\text{SO}_4^{2-}$  to metal reduction from the continental shelf to the slope, microbes potentially implicated in sulfur cycling persisted on the slope. Both SRB and SOB groups generally decreased in relative abundance moving from shelf to slope but remained relatively abundant on the slope, with SRB representing over 5 % of the microbial community in 55 % of slope samples (Figure 4.2). *Deltaproteobacteria* and *Gammaproteobacteria* dominated at all stations and included microbes that play an important role in  $\text{SO}_4^{2-}$  reduction (Figure 4.2). These organisms included *Desulfobacteraceae*, *Desulfobulbaceae*, *Desulfarculaceae*, and *Syntrophobacteraceae*, known SRB which were among the most abundant families of Deltaproteobacteria. While in lower relative abundance (from  $\sim 0.003$  % to  $\sim 0.7$  %), SOB including *Thioalkalispiraceae*, *Ectothiorhodospiraceae*, *Rhodobacteraceae*, *Thiotrichaceae*, *Hyphomicrobiaceae*, *Chromatiaceae*, *Burkholderiaceae*, and *Rhodospirillaceae*, (Cytryn, van Rijn et al. 2005, Franz, Lichtenberg et al. 2009, Sakurai, Ogawa et al. 2010, Montoya, Lozada-Chávez et al. 2011, Mori, Suzuki et al. 2011, Xu 2014, Devereux, Mosher et al. 2015, Lipsewiers 2017), were also present throughout both shelf and slope sediments. The high relative abundance and distribution of these taxa along the whole dataset indicate that sulfur cycling is a potentially important process in both shelf and slope stations, despite the lack of geochemical evidence of these processes occurring on the slope (Figure 4.2).

Interestingly, the fact that neither  $\text{SO}_4^{2-}$  loss nor intense dissolved sulfide production were clearly observed in the geochemical profiles at most stations suggests the existence of either a biological cryptic sulfur cycle, in which SRB and SOB are metabolically active, resulting in no dissolved sulfide accumulation, nor  $\text{SO}_4^{2-}$  loss, or a

geochemical cryptic cycle, in which SRB produces  $\Sigma\text{H}_2\text{S}$  but abiotic or biotic reduction of Fe(III) oxides simultaneously promotes the removal of  $\Sigma\text{H}_2\text{S}$  by precipitation of  $\text{FeS}_{(s)}$  (Reese, Mills et al. 2013, Reese, Witmer et al. 2014). In the present study, iron-reducing bacteria (FeRB) including *Geobacteraceae* ( ~ 0.05 %), *Shewanellaceae* ( ~ 0.02 %), and *Pseudomonadaceae* ( ~ 0.006 % ) (Balashova and Zavarzin 1979, Fredrickson and Gorby 1996, Hersman, Maurice et al. 1996, Lin, Braster et al. 2005) were present in both shelf and slope samples. However, FeRB showed low relative abundances compared to SOB, which were on average 10 times higher. Moreover, dissolved  $\text{Fe}^{2+}$  concentrations remained low throughout the transect, and the cores did not appear particularly black which would indicate the presence of FeS. These observations suggest that a biological rather than geochemical cryptic sulfur cycle may be going on in these sediments. Nevertheless, actual  $\text{SO}_4^{2-}$  reduction measurements, metagenomics or other analysis looking at microbial function should be performed to confirm and better characterize the presence of the sulfur cryptic cycle.

#### 4.6 Conclusions

This study reports extensive geochemical, bacterial, and archaeal data sets to characterize the main biogeochemical cycles in sediments of the northern Gulf of Mexico and understand the interplay between geochemical and microbial pathways in nutrient and carbon cycling. Results indicate different geochemical characteristics paired with distinct microbial communities across the shelf and slope. Shelf sediments provide geochemical evidence of sulfate reduction via detection of  $\Sigma\text{H}_2\text{S}$  and elevated DIC,  $\text{NH}_4^+$ , and  $\text{PO}_4^{3-}$  concentrations in the pore waters. In parallel, the dominant microbial communities across the shelf included sulfate-reducing bacteria and sulfur-oxidizing bacteria. In addition, slope

sediments display geochemical proxies indicative of increased nitrogen and metal cycling. In agreement, the dominant microbial communities include species affiliated with nitrogen cycling (including co-annamox) as well as communities capable of using iron and manganese as electron acceptors. In addition, indications of cryptic sulfur cycling were apparent in the slope sediments in the microbial populations despite the lack of sulfur cycling observed in the geochemical proxies. Both the shelf and slope sediment communities contained changes in microbial community composition with respect to depth, indicative of the change in community due to organic carbon source and availabilities of terminal electron acceptors. This study illustrates the importance of pairing microbial and geochemical techniques to characterize the relative importance of biogeochemical and abiotic pathways involved in carbon and nutrient cycling in sediments.

## **CHAPTER 5. CONCLUSIONS AND SUGGESTIONS**

The importance of microbes in free living and host-associated environments is now widely recognized, and studying the factors controlling microbial community assembly is necessary to assess ecosystem functioning and health. However, most studies have been conducted in terrestrial environments, on mammals or commercial species, and we remain naïve about the relative importance of microbiome assembly processes in aquatic environments. This is especially true for marine host-associated microbiomes such as those of elasmobranchs and marine birds, or those of sedimentary systems that experience high variability. In this dissertation, we used 16S rRNA gene sequencing to characterize the biogeography of the microbiome of spotted eagle rays, African penguins, and sediments from the GoM shelf and slope. Results revealed that microbial communities are differentially spatially distributed in host-associated and free-living systems due to the differential influence of processes driving microbial community assembly. These studies provide a starting point to establish a baseline for what a healthy/natural microbiome looks like for each of these systems and encourage future studies to potentially identify specific biomarkers to help bridge the gap between microbiome composition, host/ecosystem health, and enhance conservation strategies.

### **5.1 Effect of body site niche**

Results from Chapters 2 and 3 describe differences in microbiome composition across body sites for spotted eagle rays and African penguins. Microbial communities from all sampled body sites were distinct from each other and the surrounding environment,



which reflects the action of the host on establishing specific physico-chemical properties that act as filters for microbial colonization. Body sites in high contact with components from the GIT such as the cloaca or oral cavity microbiota were more distinct from the surrounding environment compared to those of other body sites, due perhaps to a larger proportion of microbes coming from more internal portions of the GIT in the cloaca and oral cavity that may be less affected by environmental factors.

Supporting this idea, results from Chapter 2 indicated that captivity was associated with modifications in the microbiome composition of skin, gills, and cloaca from spotted eagle rays. However, the cloaca microbiome structure was more conserved between captive and wild individuals compared to those of the gills and skin, perhaps due to the stronger influence from microbes of internal regions of the GIT. Despite not being able to establish causality, these results suggest that environmental change impacts microbial community assembly in these animals, an effect modulated by body site niche. In particular, body sites in connection with the GIT appeared more conserved compared to other body sites tested, which suggests that either the microbial composition of the GIT is more tightly regulated by the host, that the more internal nature of this system reduces the influence of external factors on microbial community assembly, or a combination of these possibilities.

Although differences in microbial community composition associated with captivity status and body site niche have already been observed in other animals, this is the first time these have been explored in spotted eagle rays and African penguins. These results provide an initial framework but future studies that monitor microbiome changes in captive animals over time are necessary to establish causality between environmental change and

microbiome composition and identify specific drivers of microbiome assembly in these animals.

## **5.2 Relative effect of phylogeny and uniqueness of the microbiome**

Results from Chapter 3 revealed that the microbiome of the African penguins' oral cavity was more similar to that of marine mammals, whereas the penguin's cloaca microbiome was more similar to that of other wild birds, which highlights a differential effect of phylogeny between these body sites, and the specific lifestyle of penguins between land and sea. However, the penguin microbiome still remained highly species specific with high proportions (> 95%) of ASVs not shared with any other host vertebrate used for comparison, and high proportions of unassigned sequences which could represent novel microbes. ASVs differentially abundant in penguins compared to the environment, representing over 1% of the penguin microbiome, and present in 100% of individuals for each body site, were identified as potential members of the penguin core microbiome. This core microbiome was mostly composed of taxa commonly found in birds including members of families *Cardiobacteriaceae*, *Weeksellaceae*, and *Moraxellaceae*, among others, which suggests that microbes from these groups are potentially beneficial to their bird hosts. Moreover, while taxa known for containing potential pathogens were identified as part of the penguin microbiota, long term monitoring of the animals confirms that they are healthy, which suggests that the strains identified are non-pathogenic. These results provide a starting point for establishing a baseline of what a healthy African penguin microbiome looks like. However, further studies including wild populations are needed to identify specific microbes and functions that may be related to host health.

### **5.3 Sediment biogeography**

Results from Chapter 4 indicate a strong spatial distinction in geochemical characteristics and microbial community composition between the GoM shelf and slope. Both geochemical proxies and microbial communities were indicative of stronger organic matter remineralization processes along with sulfur cycling in shelf sediments, while slope sediments were characterized by increased metal and nitrogen cycling. These results are potentially explained by the differential influence of the MARS which transports large amounts of freshwater and sediment material to the shelf. Both the shelf and slope sediment communities contained changes in microbial community composition with respect to depth, indicative of the change in community due to organic carbon source and availabilities of terminal electron acceptors. These results assess the effect of the MARS on the surrounding shelf and slope ecosystems during the hypoxic season and provide insights into the potential influence of sediment carbon remineralization pathways on the overlying water column. However, the effect of the MARS can be highly variable throughout the year, which highlights the need to study these sediment's microbial and geochemical processes over time. Moreover, the nGoM is subject to oil exploitation, converting it into a high-risk area for accidental oil releases, which reinforces the need to establish a baseline of the microbial diversity and ecology of these sediments.

### **5.4 Final remarks**

Microbiomes from free-living and host-associated systems are diverse and variable due to the combination effect of different drivers of microbial community assembly. However, parsing out the relative effect of these factors is often difficult, and requires

monitoring of the microbiome over space and time. For instance, the metagenomic analysis of time series samples of animals being transferred from wild to captive conditions would allow us to understand the rate of change from a wild microbiome to a captive state and help identify, in combination with metadata, major factors influencing this transition. On the other hand, establishing what a healthy microbiome looks like is essential to assess the effect disturbances on microbiome composition and function. Trends identified here provide a starting point for future studies to bridge the gap between microbiome composition and host/ecosystem health. For example, exploring changes in microbial function using metagenomics or proteomics, in addition to taxonomic changes, may be more informative when determining the impact of microbiome shifts associated with captivity on host metabolism and health. Moreover, searching for antibiotic resistant genes, which are potentially more abundant in captive individuals, could inform us on changes in microbiome resilience. Using shotgun metagenomics, we could also identify the level of genomic diversity in a more comprehensive way by assessing potential changes in genomospecies associated with hosts under captive conditions. This would help characterize the loss of genomic diversity at higher resolutions and identify specific functions that are selected under captivity. Finally, expanding the geographic range from where wild animals are sampled would help narrow down what microbes are beneficial to the host and part of the core microbiome.

**APPENDIX A. SUPPLEMENTARY INFORMATION FOR  
CHAPTER 2: MICROBIOME DIFFERENCES BETWEEN  
WILD AND CAPTIVE SPOTTED EAGLE RAYS  
(AETOBATUS NARINARI)**

**Table A.1. Metadata for all samples, including captive and wild spotted eagle rays, and cownose rays**

Elasmobranch name	Species	Origin	Year arrived in exhibit	Date collected	Sample type	Sex	Disc width (cm)	Weight (kg)	Medication
180424_T2	Aetobatus narinari	Wild		4/24/18	Cloaca	F	60-90	0-20	
180424_T2	Aetobatus narinari	Wild		4/24/18	Gill	F	60-90	0-20	
180424_T2	Aetobatus narinari	Wild		4/24/18	Skin	F	60-90	0-20	
180424_T3	Aetobatus narinari	Wild		4/24/18	Cloaca	F	150p	60p	
180424_T3	Aetobatus narinari	Wild		4/24/18	Gill	F	150p	60p	
180424_T3	Aetobatus narinari	Wild		4/24/18	Skin	F	150p	60p	
180424_TI	Aetobatus narinari	Wild		4/24/18	Gill	M	60-90	0-20	
180424_TI	Aetobatus narinari	Wild		4/24/18	Skin	M	60-90	0-20	
180426_T2M	Aetobatus narinari	Wild		4/26/18	Gill	M	150p	60p	
180426_T2M	Aetobatus narinari	Wild		4/26/18	Skin	M	150p	60p	
180426_TI	Aetobatus narinari	Wild		4/26/18	Cloaca	M	150p	60p	
180426_TI	Aetobatus narinari	Wild		4/26/18	Gill	M	150p	60p	
180426_TI	Aetobatus narinari	Wild		4/26/18	Skin	M	150p	60p	

Elasmobranch name	Species	Origin	Year arrived in exhibit	Date collected	Sample type	Sex	Disc width (cm)	Weight (kg)	Medication
180427_T1	Aetobatus narinari	Wild		4/27/18	Cloaca	F	90-120	20-40	
180427_T1	Aetobatus narinari	Wild		4/27/18	Gill	F	90-120	20-40	
180427_T1	Aetobatus narinari	Wild		4/27/18	Skin	F	90-120	20-40	
180501_TIF	Aetobatus narinari	Wild		5/1/18	Cloaca	F	60-90	0-20	
180501_TIF	Aetobatus narinari	Wild		5/1/18	Gill	F	60-90	0-20	
180501_TIF	Aetobatus narinari	Wild		5/1/18	Skin	F	60-90	0-20	
180503_T1	Aetobatus narinari	Wild		5/3/18	Gill	M	150p	40-60	
180503_T1	Aetobatus narinari	Wild		5/3/18	Skin	M	150p	40-60	
180503_T2	Aetobatus narinari	Wild		5/3/18	Cloaca	F	90-120	0-20	
180503_T2	Aetobatus narinari	Wild		5/3/18	Gill	F	90-120	0-20	
180503_T2	Aetobatus narinari	Wild		5/3/18	Skin	F	90-120	0-20	
180503_T3M	Aetobatus narinari	Wild		5/3/18	Gill	M	120-150	20-40	
180503_T3M	Aetobatus narinari	Wild		5/3/18	Skin	M	120-150	20-40	
180503_T4M	Aetobatus narinari	Wild		5/3/18	Cloaca	M	120-150	20-40	

Elasmobranch name	Species	Origin	Year arrived in exhibit	Date collected	Sample type	Sex	Disc width (cm)	Weight (kg)	Medication
180503_T4M	Aetobatus narinari	Wild		5/3/18	Gill	M	120-150	20-40	
180503_T4M	Aetobatus narinari	Wild		5/3/18	Skin	M	120-150	20-40	
180504_T2M	Aetobatus narinari	Wild		5/4/18	Cloaca	M	150p	40-60	
180504_T2M	Aetobatus narinari	Wild		5/4/18	Gill	M	150p	40-60	
180504_T2M	Aetobatus narinari	Wild		5/4/18	Skin	M	150p	40-60	
180504_T1F	Aetobatus narinari	Wild		5/4/18	Cloaca	M	150p	40-60	
180504_T1F	Aetobatus narinari	Wild		5/4/18	Gill	M	150p	40-60	
180504_T1F	Aetobatus narinari	Wild		5/4/18	Skin	M	150p	40-60	
20180509	Aetobatus narinari	Wild		5/9/18	Gill				
20180509	Aetobatus narinari	Wild		5/9/18	Skin				
T1F	Aetobatus narinari	Wild		4/25/19	Cloaca	F			
T1F	Aetobatus narinari	Wild		4/23/19	Gill	F			
T1F	Aetobatus narinari	Wild		4/25/19	Gill	F			
T1F	Aetobatus narinari	Wild		4/23/19	Skin	F			



Elasmobranch name	Species	Origin	Year arrived in exhibit	Date collected	Sample type	Sex	Disc width (cm)	Weight (kg)	Medication
T1F	Aetobatus narinari	Wild		4/25/19	Skin	F			
T2F	Aetobatus narinari	Wild		4/25/19	Gill	F			
T2F	Aetobatus narinari	Wild		4/25/19	Skin	F			
T2M	Aetobatus narinari	Wild		4/23/19	Cloaca	M			
T2M	Aetobatus narinari	Wild		4/23/19	Gill	M			
T2M	Aetobatus narinari	Wild		4/23/19	Skin	M			
T3M	Aetobatus narinari	Wild		4/25/19	Gill	M			
T3M	Aetobatus narinari	Wild		4/25/19	Skin	M			
Captain	Aetobatus narinari	Aquarium	2015	2/28/18	Cloaca	F	120-150	40-60	
Captain	Aetobatus narinari	Aquarium	2015	3/5/19	Cloaca	F	120-150	40-60	
Captain	Aetobatus narinari	Aquarium	2015	2/28/18	Gill	F	120-150	40-60	
Captain	Aetobatus narinari	Aquarium	2015	2/28/18	Skin	F	120-150	40-60	
Captain	Aetobatus narinari	Aquarium	2015	3/5/19	Skin	F	120-150	40-60	
Chex	Aetobatus narinari	Aquarium	2012	3/5/19	Cloaca				

Elasmobranch name	Species	Origin	Year arrived in exhibit	Date collected	Sample type	Sex	Disc width (cm)	Weight (kg)	Medication
Chex	Aetobatus narinari	Aquarium	2012	3/5/19	Gill				
Chex	Aetobatus narinari	Aquarium	2012	3/5/19	Skin				
Chunk	Aetobatus narinari	Aquarium	2013	3/1/18	Cloaca	M	120-150	20-40	
Chunk	Aetobatus narinari	Aquarium	2013	7/1/18	Cloaca	M	120-150	20-40	Died soon after sampling
Chunk	Aetobatus narinari	Aquarium	2013	3/1/18	Gill	M	120-150	20-40	
Chunk	Aetobatus narinari	Aquarium	2013	7/1/18	Gill	M	120-150	20-40	Died soon after sampling
Chunk	Aetobatus narinari	Aquarium	2013	3/1/18	Skin	M	120-150	20-40	
Chunk	Aetobatus narinari	Aquarium	2013	7/1/18	Skin	M	120-150	20-40	Died soon after sampling
Cookie	Aetobatus narinari	Aquarium	2012	3/1/18	Cloaca	M	120-150	20-40	
Cookie	Aetobatus narinari	Aquarium	2012	3/6/19	Cloaca	M	120-150	20-40	
Cookie	Aetobatus narinari	Aquarium	2012	3/1/18	Gill	M	120-150	20-40	
Cookie	Aetobatus narinari	Aquarium	2012	3/6/19	Gill	M	120-150	20-40	
Cookie	Aetobatus narinari	Aquarium	2012	3/1/18	Skin	M	120-150	20-40	
Cookie	Aetobatus narinari	Aquarium	2012	3/6/19	Skin	M	120-150	20-40	

Elasmobranch name	Species	Origin	Year arrived in exhibit	Date collected	Sample type	Sex	Disc width (cm)	Weight (kg)	Medication
Dan	Aetobatus narinari	Aquarium	2015	3/8/19	Cloaca	M	120-150	20-40	
Dan	Aetobatus narinari	Aquarium	2015	7/1/18	Cloaca	M	120-150	20-40	
Dan	Aetobatus narinari	Aquarium	2015	11/14/18	Gill	M	120-150	20-40	Prazi bath
Dan	Aetobatus narinari	Aquarium	2015	3/8/19	Gill	M	120-150	20-40	
Dan	Aetobatus narinari	Aquarium	2015	7/1/18	Gill	M	120-150	20-40	
Dan	Aetobatus narinari	Aquarium	2015	11/14/18	Skin	M	120-150	20-40	Prazi bath
Dan	Aetobatus narinari	Aquarium	2015	3/8/19	Skin	M	120-150	20-40	
Dan	Aetobatus narinari	Aquarium	2015	7/1/18	Skin	M	120-150	20-40	
GrapeNuts	Aetobatus narinari	Aquarium		3/7/19	Cloaca	M	120-150	20-40	
GrapeNuts	Aetobatus narinari	Aquarium		3/7/19	Gill	M	120-150	20-40	
GrapeNuts	Aetobatus narinari	Aquarium		3/7/19	Skin	M	120-150	20-40	
HoneyNut	Aetobatus narinari	Aquarium		3/7/19	Cloaca				
HoneyNut	Aetobatus narinari	Aquarium		3/7/19	Gill				
HoneyNut	Aetobatus narinari	Aquarium		3/7/19	Skin				

Elasmobranch name	Species	Origin	Year arrived in exhibit	Date collected	Sample type	Sex	Disc width (cm)	Weight (kg)	Medication
Kix	Aetobatus narinari	Aquarium	2009	3/6/19	Cloaca	M	120-150	20-40	
Kix	Aetobatus narinari	Aquarium	2009	3/6/19	Gill	M	120-150	20-40	
Kix	Aetobatus narinari	Aquarium	2009	3/6/19	Skin	M	120-150	20-40	
Magneto	Aetobatus narinari	Aquarium		3/7/19	Cloaca	M	90-120	20-40	
Magneto	Aetobatus narinari	Aquarium		3/7/19	Gill	M	90-120	20-40	
Magneto	Aetobatus narinari	Aquarium		3/7/19	Skin	M	90-120	20-40	
Miniwheat	Aetobatus narinari	Aquarium	2012	3/8/19	Cloaca	M	120-150	20-40	
Nightcrawler	Aetobatus narinari	Aquarium	2013	3/6/19	Cloaca	M	120-150	20-40	
Nightcrawler	Aetobatus narinari	Aquarium	2013	3/6/19	Gill	M	120-150	20-40	
Orion	Aetobatus narinari	Aquarium	2015	11/11/18	Cloaca	F	120-150	40-60	
Orion	Aetobatus narinari	Aquarium	2015	3/5/19	Cloaca	F	120-150	40-60	
Orion	Aetobatus narinari	Aquarium	2015	3/5/19	Gill	F	120-150	40-60	
Orion	Aetobatus narinari	Aquarium	2015	3/5/19	Skin	F	120-150	40-60	
Sloth	Aetobatus narinari	Aquarium	2013	3/7/19	Cloaca				

<b>Elasmobranch name</b>	<b>Species</b>	<b>Origin</b>	<b>Year arrived in exhibit</b>	<b>Date collected</b>	<b>Sample type</b>	<b>Sex</b>	<b>Disc width (cm)</b>	<b>Weight (kg)</b>	<b>Medication</b>
Sloth	Aetobatus narinari	Aquarium	2013	3/7/19	Gill				
Sloth	Aetobatus narinari	Aquarium	2013	3/7/19	Skin				
Squeak	Aetobatus narinari	Aquarium	2013	2/28/18	Cloaca	F	120-150	40-60	
Squeak	Aetobatus narinari	Aquarium	2013	2/28/18	Gill	F	120-150	40-60	
Squeak	Aetobatus narinari	Aquarium	2013	3/5/19	Gill	F	120-150	40-60	
Squeak	Aetobatus narinari	Aquarium	2013	2/28/18	Skin	F	120-150	40-60	
Squeak	Aetobatus narinari	Aquarium	2013	3/5/19	Skin	F	120-150	40-60	
Squishy	Aetobatus narinari	Aquarium	2013	3/6/19	Skin	F	150p	40-60	
Squishy	Aetobatus narinari	Aquarium	2013	6/27/18	Skin	F	150p	40-60	Prazi bath
Cow1	Rhinoptera bonasus	Aquarium	2009	7/3/18	Cloaca				
Cow1	Rhinoptera bonasus	Aquarium	2009	7/3/18	Gill				
Cow1	Rhinoptera bonasus	Aquarium	2009	7/3/18	Skin				
Cow2	Rhinoptera bonasus	Aquarium	2011	7/3/18	Cloaca				
Cow2	Rhinoptera bonasus	Aquarium	2011	7/3/18	Gill				

<b>Elasmobranch name</b>	<b>Species</b>	<b>Origin</b>	<b>Year arrived in exhibit</b>	<b>Date collected</b>	<b>Sample type</b>	<b>Sex</b>	<b>Disc width (cm)</b>	<b>Weight (kg)</b>	<b>Medication</b>
Cow2	Rhinoptera bonasus	Aquarium	2011	7/3/18	Skin				
Cow3	Rhinoptera bonasus	Aquarium	2016	7/3/18	Cloaca				
Cow3	Rhinoptera bonasus	Aquarium	2016	7/3/18	Gill				
Cow3	Rhinoptera bonasus	Aquarium	2016	7/3/18	Skin				
Cow4	Rhinoptera bonasus	Aquarium	2016	7/3/18	Cloaca				
Cow4	Rhinoptera bonasus	Aquarium	2016	7/3/18	Gill				
Cow4	Rhinoptera bonasus	Aquarium	2016	7/3/18	Skin				
Cow5	Rhinoptera bonasus	Aquarium	2016	7/3/18	Cloaca				
Cow5	Rhinoptera bonasus	Aquarium	2016	7/3/18	Gill				
Cow5	Rhinoptera bonasus	Aquarium	2016	7/3/18	Skin				
Cow6	Rhinoptera bonasus	Aquarium	2017	7/3/18	Cloaca				
Cow6	Rhinoptera bonasus	Aquarium	2017	7/3/18	Gill				
Cow6	Rhinoptera bonasus	Aquarium	2017	7/3/18	Skin				
Cow7	Rhinoptera bonasus	Aquarium	2018	7/3/18	Cloaca				

Elasmobranch name	Species	Origin	Year arrived in exhibit	Date collected	Sample type	Sex	Disc width (cm)	Weight (kg)	Medication
Cow7	Rhinoptera bonasus	Aquarium	2018	7/3/18	Gill				
Cow7	Rhinoptera bonasus	Aquarium	2018	7/3/18	Skin				
Longboard water	Wild water	Wild		5/3/18	Wild water				
Motedock water	Wild water	Wild		5/4/18	Wild water				
Redroof water	Wild water	Wild		5/4/18	Wild water				
Capt water	Capt water	Aquarium		2/26/18	Capt water				
Capt water	Capt water	Aquarium		2/28/19	Capt water				
Capt water	Capt water	Aquarium		3/14/19	Capt water				
Capt water	Capt water	Aquarium		3/15/18	Capt water				
Capt water	Capt water	Aquarium		3/30/18	Capt water				
Capt water	Capt water	Aquarium		6/21/18	Capt water				
Capt water	Capt water	Aquarium		7/5/18	Capt water				
Capt water	Capt water	Aquarium		11/10/18	Capt water				
Capt water	Capt water	Aquarium		11/29/18	Aquarium water				

**Table A.2. Pairwise results for a one way analysis of variance (Kruskal-Wallis) for all  $\alpha$ -diversity metrics between captive cownose (*Rhinoptera bonasus*) and spotted eagle (*Aetobatus narinari*) rays, and wild spotted eagle rays (*Aetobatus narinari*) for different body sites.** \* indicates a significant difference  $p \leq 0.05$ , \*\* indicates  $p \leq 0.01$ , \*\*\* indicates  $p \leq 0.001$ , \*\*\*\* indicates  $p \leq 0.0001$ , and NS indicates not significant ( $p > 0.05$ ). NA indicates no possible comparison.  $\alpha$ -diversity metrics include Observed ASVs, Shannon diversity index, Pielou's evenness, and Faith's Phylogenetic Diversity

Comparison	Diversity Index	Cloaca	Gill	Skin	Water
Captive spotted eagle ray (C)	Observed	* W > C	*** W > C	**** W > C	NS
	Shannon	NS	NS	**** W > C	NS
x Wild spotted eagle ray (W)	Evenness	NS	* C > W	*** W > C	NS
	Faith's	* W > C	** W > C	**** W > C	NS
Captive spotted eagle ray (C)	Observed	* Co > C	** Co > C	* Co > C	NA
	Shannon	* Co > C	* Co > C	*** Co > C	NA
x Captive cownose ray (Co)	Evenness	* Co > C	NS	** Co > C	NA
	Faith's	* Co > C	* Co > C	* Co > C	NA

**Table A.3. Pairwise results for all permutational multivariate analysis of variance (PERMANOVA) for all  $\beta$ -diversity metrics between captive cownose (*Rhinoptera bonasus*) and spotted eagle (*Aetobatus narinari*) rays, and wild spotted eagle rays (*Aetobatus narinari*) for different body sites.** \* indicates a significant difference  $p \leq 0.05$ , \*\* indicates  $p \leq 0.01$ , \*\*\* indicates  $p \leq 0.001$ , \*\*\*\* indicates  $p \leq 0.0001$ , and NS indicates not significant ( $p > 0.05$ ). NA indicates no possible.  $\beta$ -diversity metrics include Bray-Curtis, Weighted UniFrac, and Unweighted UniFrac

Comparison	Diversity Index	Cloaca	Gill	Skin	Water
Captive spotted eagle ray (C)	Bray-Curtis	NS	**	***	***
	Weighted	NS	**	**	***
x Wild spotted eagle ray (W)	Unweighted	**	***	***	***
Captive spotted eagle ray (C)	Bray-Curtis	NS	**	***	NA
	Weighted	*	*	**	NA
x Captive cownose ray (Co)	Unweighted	**	***	***	NA



**Table A.4. Pairwise results for all permutational multivariate analysis of dispersion (PERMDISP) for all  $\beta$ -diversity metrics and body sites for spotted eagle rays (*Aetobatus narinari*) and cownose rays (*Rhinoptera bonasus*). \*** indicates a significant difference  $p \leq 0.05$ , \*\* indicates  $p \leq 0.01$ , \*\*\* indicates  $p \leq 0.001$ , \*\*\*\* indicates  $p \leq 0.0001$ , and NS indicates not significant ( $p > 0.05$ ). NA indicates no possible comparison.  $\beta$ -diversity metrics include Bray-Curtis, Weighted UniFrac, and Unweighted UniFrac

Comparison	Diversity Index	Cloaca	Gill	Skin	Water
Captive spotted eagle ray (C) x Wild spotted eagle ray (W)	Bray-Curtis	NS	**	NS	NS
	Weighted	NS	NS	*	NS
	Unweighted	NS	NS	**	**
Captive spotted eagle ray (C) x Captive cownose ray (Co)	Bray-Curtis	NS	NS	NS	NA
	Weighted	NS	NS	NS	NA
	Unweighted	NS	NS	NS	NA

**Table A.5. Pairwise results for a one way analysis of variance (Kruskal-Wallis) for all  $\alpha$ -diversity metrics between different body sites for cownose (*Rhinoptera bonasus*), and captive and wild spotted eagle rays (*Aetobatus narinari*). \*** indicates a significant difference  $p \leq 0.05$ , \*\* indicates  $p \leq 0.01$ , \*\*\* indicates  $p \leq 0.001$ , \*\*\*\* indicates  $p \leq 0.0001$ , and NS indicates not significant ( $p > 0.05$ ). NA indicates no possible comparison.  $\alpha$ -diversity metrics include Observed ASVs, Shannon diversity index, Pielou's evenness, and Faith's Phylogenetic Diversity

Comparison	Diversity Index	Captive spotted eagle ray ( <i>A. narinari</i> )	Wild spotted eagle ray ( <i>A. narinari</i> )	Captive cownose ray ( <i>R. bonasus</i> )
Cloaca (C) x Gill (G)	Observed	*** G>C	NS	* G>C
	Shannon	**** G>C	NS	* G>C
	Evenness	**** G>C	NS	NS
	Faith's	*** G>C	NS	NS
Cloaca (C) x Skin (S)	Observed	** S>C	* S>C	NS
	Shannon	** S>C	** S>C	NS
	Evenness	* S>C	** S>C	* S>C
	Faith's	** S>C	NS	NS
Gill (G) x Skin (S)	Observed	NS	NS	* G>S
	Shannon	**** G>S	*** S>G	NS
	Evenness	*** G>S	**** S>G	NS
	Faith's	NS	NS	NS

**Table A.6. Pairwise results for all permutational multivariate analysis of variance (PERMANOVA) for all  $\beta$ -diversity metrics between different body sites for cownose (*Rhinoptera bonasus*), and captive and wild spotted eagle rays (*Aetobatus narinari*). \*** indicates a significant difference  $p \leq 0.05$ , \*\* indicates  $p \leq 0.01$ , \*\*\* indicates  $p \leq 0.001$ , \*\*\*\* indicates  $p \leq 0.0001$ , and NS indicates not significant ( $p > 0.05$ ). NA indicates not possible.  $\beta$ -diversity metrics include Bray-Curtis, Weighted UniFrac, and Unweighted UniFrac

Comparison	Diversity Index	Captive spotted eagle ray ( <i>A. narinari</i> )	Wild spotted eagle ray ( <i>A. narinari</i> )	Captive cownose ray ( <i>R. bonasus</i> )
Cloaca (C)	Bray-Curtis	***	**	NS
x	Weighted	***	**	NS
Gill (G)	Unweighted	***	**	NS
Cloaca (C)	Bray-Curtis	***	**	NS
x	Weighted	***	**	NS
Skin (S)	Unweighted	***	**	NS
Gill (G)	Bray-Curtis	***	**	NS
x	Weighted	***	**	NS
Skin (S)	Unweighted	***	**	NS
Cloaca (C)	Bray-Curtis	***	NS	**
x	Weighted	***	NS	**
Water (W)	Unweighted	***	NS	**
Gill (G)	Bray-Curtis	***	NS	**
x	Weighted	***	*	**
Water (W)	Unweighted	***	*	**
Skin (S)	Bray-Curtis	***	NS	**
x	Weighted	***	NS	**
Water (W)	Unweighted	***	**	**

**Table A.7. Number of ASVs shared between captive and wild spotted eagle rays (*Aetobatus narinari*), and captive cownose rays (*Rhinoptera bonasus*) for each body site.** Proportion refers to the percentage shared out of the total microbial community of each body site. Relative abundance refers to the average relative abundance represented by shared ASVs for each body site

	Body site	Number of shared ASVs	Wild spotted eagle ray ( <i>Aetobatus narinari</i> )	
			Proportion of shared ASVs (%)	Average relative abundance of shared ASVs (%)
Captive spotted eagle ray ( <i>A. narinari</i> ) x	cloaca	72	13.00	0.53
	gill	216	15.98	0.14
	skin	306	17.89	0.05
Wild spotted eagle ray ( <i>A. narinari</i> )				
Spotted eagle ray ( <i>A. narinari</i> ) x Water	cloaca	355	39.05	0.15
	gill	433	24.26	0.12
	skin	433	20.21	0.14
			Captive spotted eagle ray ( <i>Aetobatus narinari</i> )	
			Proportion of shared ASVs (%)	Average relative abundance of shared ASVs (%)
Captive spotted eagle ray ( <i>A. narinari</i> ) x	cloaca	72	16.90	0.64
	gill	216	24.74	0.12
	skin	306	34.77	0.20
Wild spotted eagle ray ( <i>A. narinari</i> )				
Captive spotted eagle ray ( <i>A. narinari</i> ) x	cloaca	80	14.57	0.55
	gill	196	16.5	0.1
	skin	185	16.55	0.06
Captive cownose ray ( <i>R. bonasus</i> )				
Spotted eagle ray ( <i>A. narinari</i> ) x Water	cloaca	123	22.40	0.03
	gill	315	26.52	0.16
	skin	238	21.29	0.09
			Captive cownose ray ( <i>R. bonasus</i> )	
			Proportion of shared ASVs (%)	Average relative abundance of shared ASVs (%)
Captive spotted eagle ray ( <i>A. narinari</i> ) x	cloaca	80.00	10.84	0.11
	gill	196.00	19.48	0.10
	skin	185.00	23.04	0.15
Captive cownose ray ( <i>R. bonasus</i> )				
Captive cownose ray ( <i>R. bonasus</i> ) x Water	cloaca	200.00	27.10	0.27
	gill	266.00	26.44	0.19
	skin	171.00	21.30	0.24

**Table A.8. Number of ASVs shared between different body sites for wild and captive spotted eagle rays (*Aetobatus narinari*), and captive cownose rays (*Rhinoptera bonasus*). Proportion refers to the percentage shared out of the total microbial community of each body site. Relative abundance refers to the average relative abundance represented by shared ASVs for each body site**

Wild spotted eagle ray ( <i>Aetobatus narinari</i> )				
		Number of shared ASVs	Proportion of shared ASVs (%)	Average relative abundance of shared ASVs (%)
Cloaca x Gill	Cloaca	300	54.15	0.14
	Gill		22.19	0.12
Cloaca x Skin	Cloaca	350	63.18	0.13
	Skin		20.47	0.05
Gill x Skin	Gill	662	48.96	0.06
	Skin		38.71	0.04
Cloaca x Gill x Skin	Cloaca	237	42.78	0.18
	Gill		17.53	0.15
	Skin		13.86	0.07
Captive spotted eagle ray ( <i>Aetobatus narinari</i> )				
		Number of shared ASVs	Proportion of shared ASVs (%)	Average relative abundance of shared ASVs (%)
Cloaca x Gill	Cloaca	217	50.94	0.23
	Gill		24.86	0.15
Cloaca x Skin	Cloaca	252	59.15	0.21
	Skin		28.64	0.21
Gill x Skin	Gill	376	43.07	0.09
	Skin		42.73	0.18
Cloaca x Gill x Skin	Cloaca	165	38.73	0.30
	Gill		18.90	0.16
	Skin		18.75	0.31
Captive cownose ray ( <i>R. bonasus</i> )				
		Number of shared ASVs	Proportion of shared ASVs (%)	Average relative abundance of shared ASVs (%)
Cloaca x Gill	Cloaca	275	51.115	0.136
	Gill		37.162	0.118
Cloaca x Skin	Cloaca	245	45.539	0.146
	Skin		38.766	0.143
Gill x Skin	Gill	287	38.784	0.115
	Skin		45.411	0.133
Cloaca x Gill x Skin	Cloaca	199	21.215	0.173
	Gill		15.645	0.145
	Skin		20.431	0.163

**Table A.9. List of common fish pathogens, and number of ASVs and average relative abundance of those found in wild and captive spotted eagle rays (*Aetobatus narinari*), and cownose rays (*Rhinoptera bonasus*)**

Species	# ASVs	Captive cownose ray ( <i>R. bonasus</i> )	Captive spotted eagle ray ( <i>A. narinari</i> )	Wild spotted eagle ray ( <i>A. narinari</i> )
<i>Aeromonas</i> (all species)	6	0.093	0.189	0.077
<i>A. caviae</i>	Not present			
<i>A. hydrophila</i>	Not present			
<i>A. jandaei</i>	Not present			
<i>A. salmonicida</i>	Not present			
<i>A. sobria</i>	Not present			
<i>A. veronii</i>	Not present			
<i>Aliivibrio</i> (all species)	1	0.029	0.044	0.001
<i>A. salmonicida</i>	Not present			
<i>Chryseobacterium</i> (all species)	9	0.014	0.014	0.002
<i>C. balustinum</i>	Not present			
<i>C. scophthalmum</i>	Not present			
<i>Citrobacter</i> (all species)	1	0.010	0.023	0.022
<i>C. freundii</i>	Not present			
<i>Columnaris</i> (all species)	Not present			
<i>Cytophaga</i> (all species)	3	0.004	0.001	0.000
<i>C. agar</i>	Not present			
<i>C. psychrophila</i>	Not present			
<i>Edwardsiella</i> (all species)	Not present			
<i>E. ictaluri</i>	Not present			
<i>E. piscicida</i>	Not present			
<i>E. tarda</i>	Not present			
<i>Eubacterium</i> (all species)	Not present			
<i>E. tarantellae</i>	Not present			
<i>Flavobacterium</i> (all species)	9	0.019	0.037	0.015
<i>F. columnare</i>	Not present			
<i>F. branchiophilum</i>	Not present			
<i>F. psychrophilum</i>	Not present			
<i>Fransicella</i> (all species)	Not present			
<i>Halomonadaceae</i> (all species)	23	0.036	0.048	0.007
<i>H. (Deleya)cupida</i>	Not present			
<i>Lactococcus</i> (all species)	2	0.021	0.009	0.005
<i>L. garvieae</i>	Not present			
<i>Moritella</i> (all species)	2	0.021	0.002	0.003

Species	# ASVs	Captive cownose ray ( <i>R. bonasus</i> )	Captive spotted eagle ray ( <i>A. narinari</i> )	Wild spotted eagle ray ( <i>A. narinari</i> )
<i>Moritella viscosa</i>	Not present			
<i>Mycobacterium (all species)</i>	9	0.017	0.014	0.000
<i>M. marinum</i>	Not present			
<i>M. chelonae subsp. piscarium</i>	Not present			
<i>M. fortuitum</i>	Not present			
<i>M. marinum</i>	Not present			
<i>M. neoaurum</i>	Not present			
<i>Myxobacteria (all species)</i>	Not present			
<i>Neorickettsia (all species)</i>	1	0.000	0.000	0.011
<i>N. helminthoeca</i>	Not present			
<i>Nocardia (all species)</i>	Not present			
<i>Pasteurellaceae (all species)</i>	4	0.037	0.010	0.010
<i>P. skyensis</i>	Not present			
<i>Photobacterium (all species)</i>	10	0.798	1.051	0.383
<i>P. damsela</i>	1	7.705	10.450	3.799
<i>Piscirickettsia (all species)</i>	Not present			
<i>P. salmonis</i>	Not present			
<i>Pseudomonadaceae (all species)</i>	28	0.037	0.046	0.009
<i>P. anguilliseptica</i>	Not present			
<i>Renibacterium (all species)</i>	Not present			
<i>R. salmoninarum</i>	Not present			
<i>Rhodococcus (all species)</i>	3	0.024	0.016	0.000
<i>Serratia (all species)</i>	Not present			
<i>S. liquefaciens</i>	Not present			
<i>Shewanella (all species)</i>	11	0.024	0.039	0.023
<i>S. putrefaciens</i>	Not present			
<i>Streptococcus (all species)</i>	8	0.065	0.021	0.012
<i>S. iniae</i>	Not present			
<i>S. parauberis</i>	Not present			
<i>S. phocae</i>	Not present			
<i>Tenacibaculum (all species)</i>	23	0.051	0.029	0.018
<i>T (Flexibacter). maritimus</i>	Not present			
<i>T (Flexibacter). ovolyticus</i>	Not present			
<i>T (Flexibacter). psychrophilus</i>	Not present			
<i>Vibrio (all species)</i>	33	0.041	0.068	0.100
<i>V. fischeri</i>	Not present			
<i>V. furnissii</i>	Not present			

Species	# ASVs	Captive cownose ray ( <i>R. bonasus</i> )	Captive spotted eagle ray ( <i>A. narinari</i> )	Wild spotted eagle ray ( <i>A. narinari</i> )
<i>V. ichthyenteri</i>	Not present			
<i>V. logei</i>	Not present			
<i>V. pelagius</i>	Not present			
<i>V. alginolyticus</i>	Not present			
<i>V. anguillarum</i>	Not present			
<i>V. cholerae</i>	Not present			
<i>V. anguillarum</i>	Not present			
<i>V. ordalii</i>	Not present			
<i>V. harveyi</i>	Not present			
<i>V. vulnificus</i>	Not present			
<i>V. splendidus</i>	Not present			
<i>Yersinia (all species)</i>	Not present			

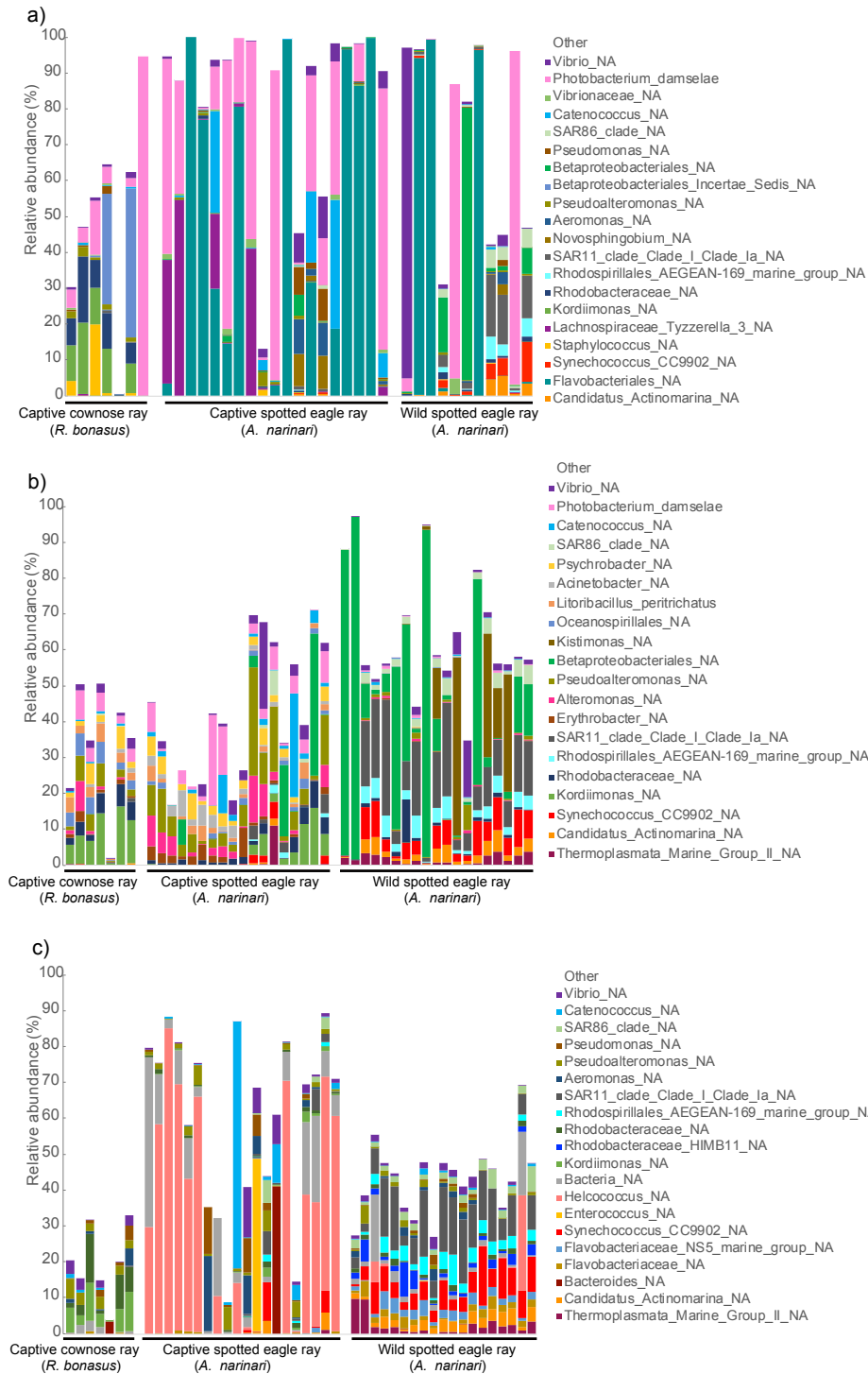


**Figure A.1. Bar plots representing the relative abundance of microbes associated with a) the cloaca, b) the gills, and c) the skin of captive cownose rays (*Rhinoptera bonasus*), captive spotted eagle rays (*Aetobatus narinari*), and wild spotted eagle rays. Skin communities appear highly distinct between captive and wild spotted eagle rays, while cloaca samples are more similar. Taxa are classified to the species level where possible**



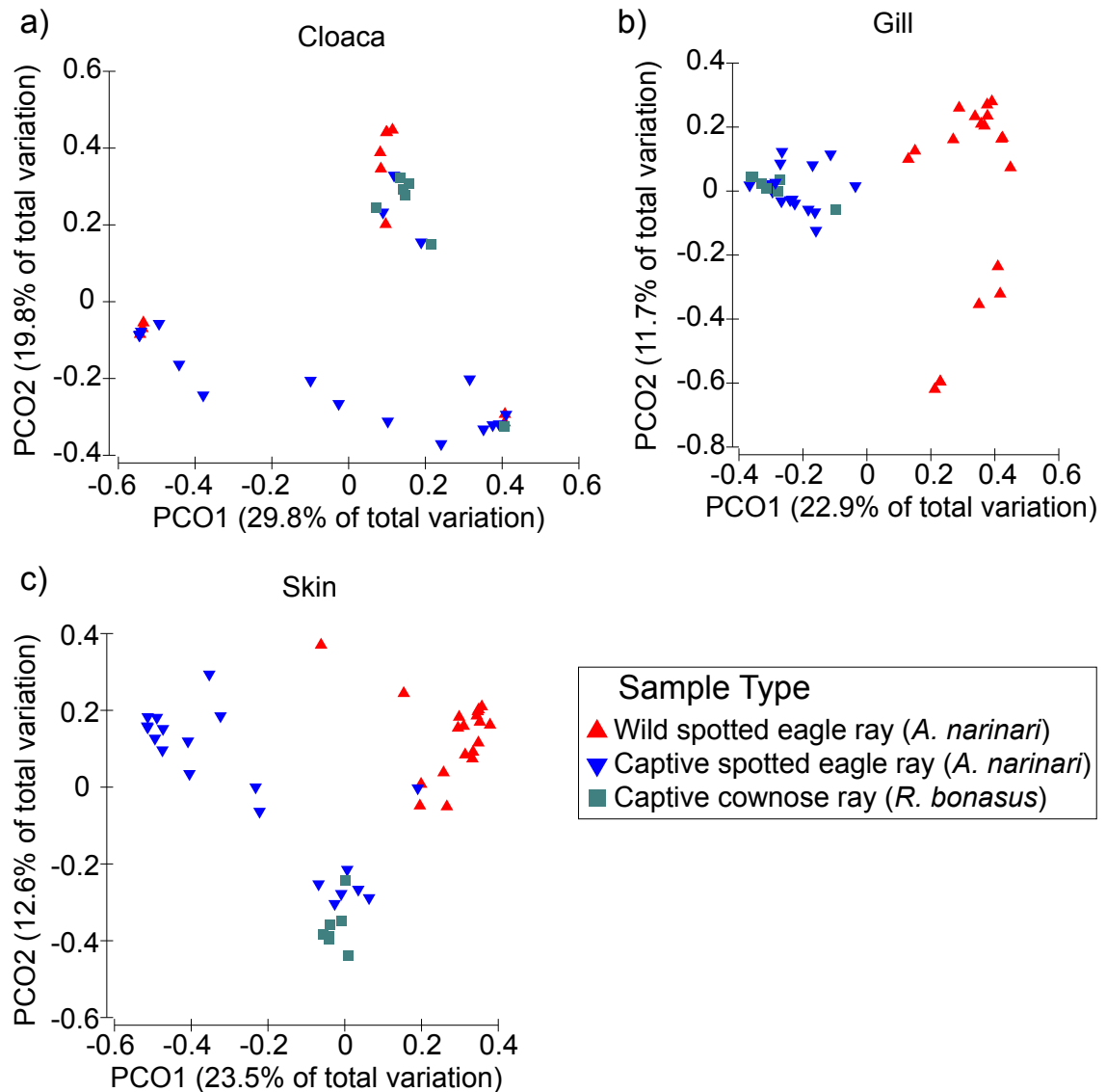


**Figure A.2. Principal coordinate analysis (PCoA) based upon a Bray-Curtis dissimilarity matrix between a) cloaca, b) gill, and c) skin samples for wild and captive spotted eagle rays (*Aetobatus narinari*) and captive cownose rays (*Rhinoptera bonasus*).** Wild spotted eagle rays harbor different microbial communities than captive spotted eagle rays, as indicated by the separate clustering, and microbial communities from cow-nose rays appear more similar to captive spotted eagle rays (as opposed those from the wild)

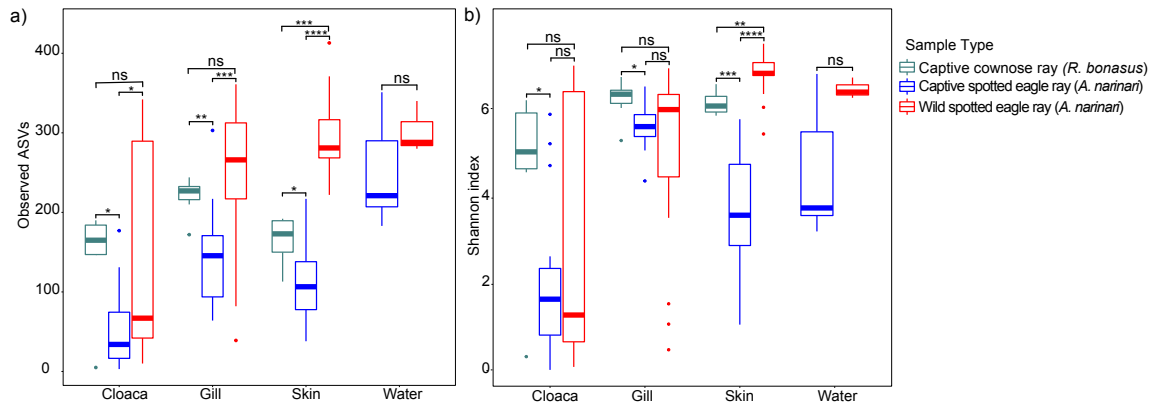


**Figure A.3.  $\alpha$ -diversity metrics a) observed amplicon sequence variants (ASVs), and b) Shannon diversity index, for all body sites (cloaca, gill, and skin) of captive cownose rays (*Rhinoptera bonasus*), captive and wild spotted eagle rays (*Aetobatus narinari*), as well as the surrounding water column. Cloaca microbiome had lower diversity compared to other body sites**

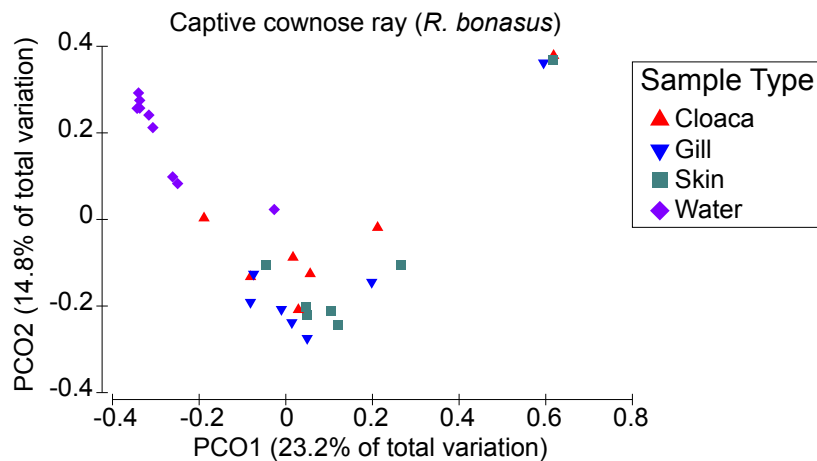


**Figure A.4. Principal coordinate analysis (PCoA) based upon a Bray-Curtis dissimilarity matrix between cloaca, gill, skin, and water samples for captive cownose rays (*Rhinoptera bonasus*). Microbial communities associated with all body sites cluster separately from the surrounding water, but do not differentiate according to body site**

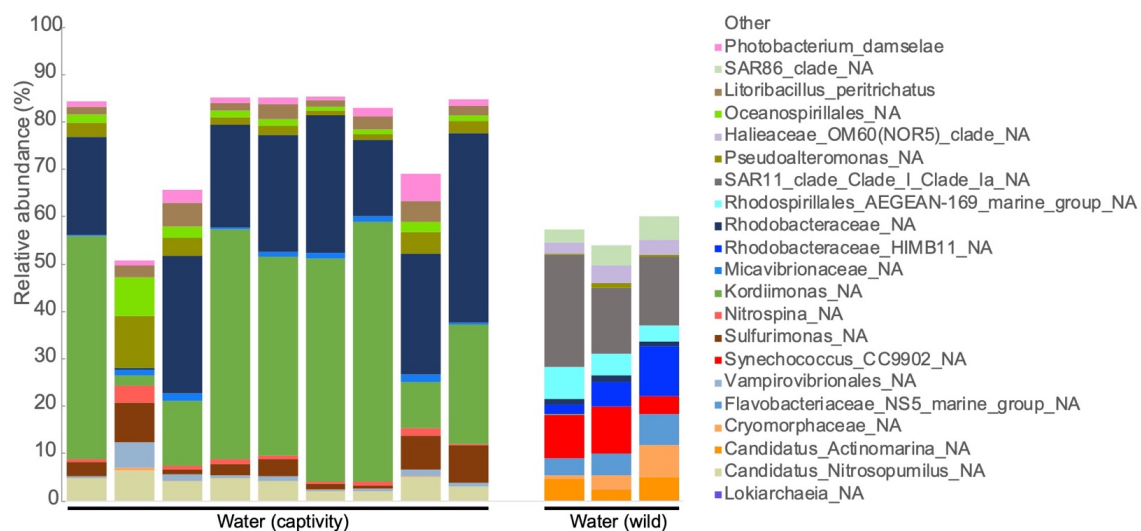


**Figure A.5. Bar plots representing the relative abundance of microbes associated with the surrounding water of the wild and captive environments. Taxa are classified to the species level where possible**

**APPENDIX B. SUPPLEMENTARY INFORMATION FOR  
CHAPTER 3: THE MICROBIOME OF THE AFRICAN  
PENGUIN (*SPHENISCUS DEMERSUS*) REFLECTS ITS  
LIFESTYLE BETWEEN LAND AND SEA**

**Table B.1. Metadata for all samples collected, including penguin (*Spheniscus demersus*) and environmental samples**

Sample Type	Penguin name	DOB	Moult date	Sex	Other
Brood pouch	Akila	1_15_16	7_25_18	F	Lameness_VaccineReaction
Cloaca	Akila	1_15_16	7_25_18	F	Lameness_VaccineReaction
Fecal floor	Akila	1_15_16	7_25_18	F	Lameness_VaccineReaction
Oral cavity	Akila	1_15_16	7_25_18	F	Lameness_VaccineReaction
Leg skin	Akila	1_15_16	7_25_18	F	Lameness_VaccineReaction
Gland	Akila	1_15_16	7_25_18	F	Lameness_VaccineReaction
Brood pouch	Bernie	3_10_09	6_19_18	M	NA
Oral cavity	Bernie	3_10_09	6_19_18	M	NA
Leg skin	Bernie	3_10_09	6_19_18	M	NA
Gland	Bernie	3_10_09	6_19_18	M	NA
Nest	NA	NA	NA	NA	NA
Brood pouch	Dapper	1_16_15	7_13_18	M	VaccineReaction
Cloaca	Dapper	1_16_15	7_13_18	M	VaccineReaction
Oral cavity	Dapper	1_16_15	7_13_18	M	VaccineReaction
Dorsal skin	Dapper	1_16_15	7_13_18	M	VaccineReaction
Leg skin	Dapper	1_16_15	7_13_18	M	VaccineReaction
Gland	Dapper	1_16_15	7_13_18	M	VaccineReaction
Dry rock	NA	NA	NA	NA	NA
Dry rock	NA	NA	NA	NA	NA
Brood pouch	Etana	6_18_09	5_25_18	F	ChronicFeatherLoss
Cloaca	Etana	6_18_09	5_25_18	F	ChronicFeatherLoss
Feather	Etana	6_18_09	5_25_18	F	ChronicFeatherLoss
Leg skin	Etana	6_18_09	5_25_18	F	ChronicFeatherLoss
Oral cavity	Etana	6_18_09	5_25_18	F	ChronicFeatherLoss
Gland	Etana	6_18_09	5_25_18	F	ChronicFeatherLoss
Brood pouch	Jackie	3_11_09	8_29_18	F	NoLongerMed
Brood pouch	Freya	1_09_14	8_17_18	F	NoLongerMed
Cloaca	Freya	1_09_14	8_17_18	F	NoLongerMed
Oral cavity	Freya	1_09_14	8_17_18	F	NoLongerMed
Leg skin	Freya	1_09_14	8_17_18	F	NoLongerMed

Sample Type	Penguin name	DOB	Moult date	Sex	Other
Gland	Freya	1_09_14	8_17_18	F	NoLongerMed
Dry guano	NA	NA	NA	NA	NA
Dry guano	NA	NA	NA	NA	NA
Brood pouch	Guja	7_7_09	5_8_18	M	No
Cloaca	Guja	7_7_09	5_8_18	M	No
Dorsal skin	Guja	7_7_09	5_8_18	M	No
Oral cavity	Guja	7_7_09	5_8_18	M	No
Dorsal skin	Guja	7_7_09	5_8_18	M	No
Gland	Guja	7_7_09	5_8_18	M	No
Water	NA	NA	NA	NA	NA
Water	NA	NA	NA	NA	NA
Cloaca	Idili	6_20_09	1_24_19	M	PeriodicPoor Feather
Leg skin	Idili	6_20_09	1_24_19	M	PeriodicPoor Feather
Oral cavity	Idili	6_20_09	1_24_19	M	PeriodicPoor Feather
Gland	Idili	6_20_09	1_24_19	M	PeriodicPoor Feather
Brood pouch	Idili	6_20_09	1_24_19	M	PeriodicPoor Feather
Feather	Idili	6_20_09	1_24_19	M	PeriodicPoor Feather
Cloaca	Jackie	3_11_09	8_29_18	F	NoLongerMed
Feather	Jackie	3_11_09	8_29_18	F	NoLongerMed
Leg skin	Jackie	3_11_09	8_29_18	F	NoLongerMed
Oral cavity	Jackie	3_11_09	8_29_18	F	NoLongerMed
Gland	Jackie	3_11_09	8_29_18	F	NoLongerMed
Brood pouch	Kakeena	2_28_15	7_3_18	F	No
Cloaca	Kakeena	2_28_15	7_3_18	F	No
Oral cavity	Kakeena	2_28_15	7_3_18	F	No
Dorsal skin	Kakeena	2_28_15	7_3_18	F	No
Leg skin	Kakeena	2_28_15	7_3_18	F	No
Gland	Kakeena	2_28_15	7_3_18	F	No
Cloaca	Klipper	8_10_09_0	6_26_18	F	No
Gland	Klipper	8_10_09_0	6_26_18	F	No
Fecal floor	Klipper	8_10_09_0	6_26_18	F	No
Oral cavity	Klipper	8_10_09_0	6_26_18	F	No

Sample Type	Penguin name	DOB	Moult date	Sex	Other
Brood pouch	Klipper	10_09_08	6_26_18	F	No
Leg skin	Klipper	10_09_08	6_26_18	F	No
Dorsal skin	Kymia	1_14_14	5_4_18	M	No
Brood pouch	Kymia	1_14_14	5_4_18	M	No
Cloaca	Kymia	1_14_14	5_4_18	M	No
Leg skin	Kymia	1_14_14	5_4_18	M	No
Oral cavity	Kymia	1_14_14	5_4_18	M	No
Gland	Kymia	1_14_14	5_4_18	M	No
Brood pouch	Lila	1_15_13	12_8_18	F	No
Cloaca	Lila	1_15_13	12_8_18	F	No
Oral cavity	Lila	1_15_13	12_8_18	F	No
Dorsal skin	Lila	1_15_13	12_8_18	F	No
Leg skin	Lila	1_15_13	12_8_18	F	No
Gland	Lila	1_15_13	12_8_18	F	No
Brood pouch	Manu	2_2_05	6_16_18	M	No
Cloaca	Manu	2_2_05	6_16_18	M	No
Oral cavity	Manu	2_2_05	6_16_18	M	No
Leg skin	Manu	2_2_05	6_16_18	M	No
Gland	Manu	2_2_05	6_16_18	M	No
Nest	NA	NA	NA	NA	NA
Brood pouch	Snap	NA	NA	M	NA
Cloaca	Snap	NA	NA	M	NA
Oral cavity	Snap	NA	NA	M	NA
Dorsal skin	Snap	NA	NA	M	NA
Leg skin	Snap	NA	NA	M	NA
Gland	Snap	NA	NA	M	NA
Nest	NA	NA	NA	NA	NA
Cloaca	Pepsi	3_2_09	4_26_18	M	No
Oral cavity	Pepsi	3_2_09	4_26_18	M	No
Dorsal skin	Pepsi	3_2_09	4_26_18	M	No
Leg skin	Pepsi	3_2_09	4_26_18	M	No
Gland	Pepsi	3_2_09	4_26_18	M	No

Sample Type	Penguin name	DOB	Moult date	Sex	Other
Brood pouch	QT	10_12_08	11_1_18	F	HistoryAbnormalEggLaying
Cloaca	QT	10_12_08	11_1_18	F	HistoryAbnormalEggLaying
Oral cavity	QT	10_12_08	11_1_18	F	HistoryAbnormalEggLaying
Dorsal skin	QT	10_12_08	11_1_18	F	HistoryAbnormalEggLaying
Leg skin	QT	10_12_08	11_1_18	F	HistoryAbnormalEggLaying
Gland	QT	10_12_08	11_1_18	F	HistoryAbnormalEggLaying
Brood pouch	Scari	7_10_09	6_2_18	F	On loan
Cloaca	Scari	7_10_09	6_2_18	F	On loan
Oral cavity	Scari	7_10_09	6_2_18	F	On loan
Gland	Scari	7_10_09	6_2_18	F	On loan
Shoreline	NA	NA	NA	NA	NA
Shoreline	NA	NA	NA	NA	NA
Shoreline	NA	NA	NA	NA	NA
Nest	NA	NA	NA	NA	NA
Brood pouch	Tweak	10_23_08	6_8_17	M	SingleItemDiet
Cloaca	Tweak	10_23_08	6_8_17	M	SingleItemDiet
Oral cavity	Tweak	10_23_08	6_8_17	M	SingleItemDiet
Gland	Tweak	10_23_08	6_8_17	M	SingleItemDiet
Wet rock	NA	NA	NA	NA	NA
Wet rock	NA	NA	NA	NA	NA
Brood pouch	Zola	3_2_15	6_29_18	F	No
Cloaca	Zola	3_2_15	6_29_18	F	No
Oral cavity	Zola	3_2_15	6_29_18	F	No
Leg skin	Zola	3_2_15	6_29_18	F	No
Gland	Zola	3_2_15	6_29_18	F	No
Cloaca	Agulhas	6_2_15	9_12_18	F	No
Oral cavity	Agulhas	6_2_15	9_12_18	F	No
Cloaca	Bacari	1_9_18	NA	M	AssistHatch
Oral cavity	Bacari	1_9_18	NA	M	AssistHatch
Cloaca	Bat	10_14_04	4_18_2018	F	No
Leg skin	Bat	10_14_04	4_18_2018	F	No



Sample Type	Penguin name	DOB	Moult date	Sex	Other
Oral cavity	Bat	10_14_04	4_18_2018	F	No
Cloaca	Chiku	12_29_17	NA	F	No
Oral cavity	Chiku	12_29_17	NA	F	No
Cloaca	Divo	1_30_15	5_16_15	M	No
Oral cavity	Divo	1_30_15	5_16_15	M	No
Cloaca	Keni	4_13_09	6_16_18	F	ChronicPoorFeather
Oral cavity	Keni	4_13_09	6_16_18	F	ChronicPoorFeather
Cloaca	Kidogo	3_3_15	3_29_19	M	No
Cloaca	Kumi	1_9_16	11_1_18	M	ChronicBumblefoot_OpenMouthRespiration_possibleStenoticNares
Leg skin	Kumi	1_9_16	11_1_18	M	ChronicBumblefoot_OpenMouthRespiration_possibleStenoticNares
Oral cavity	Kumi	1_9_16	11_1_18	M	ChronicBumblefoot_OpenMouthRespiration_possibleStenoticNares
Cloaca	Kyan	1_1_14	6_29_18	M	ChronicBumblefoot
Oral cavity	Kyan	1_1_14	6_29_18	M	ChronicBumblefoot
Oral cavity	Lizzy	3_6_87	6_23_18	F	PoorFeather
Cloaca	Matu	1_19_16	3_4_19	M	3_2019_Bumblefoot
Leg skin	Matu	1_19_16	3_4_19	M	3_2019_Bumblefoot
Oral cavity	Matu	1_19_16	3_4_19	M	3_2019_Bumblefoot
Cloaca	Mosi	1_28_18	NA	F	
Oral cavity	Mosi	1_28_18	NA	F	
Cloaca	Obi	3_3_15	11_9_18	M	
Oral cavity	Obi	3_3_15	11_9_18	M	
Oral cavity	Rafiki	1_12_18	3_29_19	M	
Cloaca	Tamu	3_5_15	6_21_18	M	
Oral cavity	Tamu	3_5_15	6_21_18	M	
Cloaca	Tau	2_6_14	7_1_18	M	2_2019_Bumblefoot_HistoryHeartMurmur
Oral cavity	Tau	2_6_14	7_1_18	M	2_2019_Bumblefoot_HistoryHeartMurmur
Cloaca	Trinity	4_8_09	6_1_18	F	HistorySeizures_ChronicPoorFeather_VitDdeficiency_SingleDietItem
Oral cavity	Trinity	4_8_09	6_1_18	F	HistorySeizures_ChronicPoorFeather_VitDdeficiency_SingleDietItem
Food	NA	NA	NA	NA	NA
Food	NA	NA	NA	NA	NA
Food	NA	NA	NA	NA	NA
Food	NA	NA	NA	NA	NA
Food	NA	NA	NA	NA	NA

Sample Type	Penguin name	DOB	Moult date	Sex	Other
Food	NA	NA	NA	NA	NA
Food	NA	NA	NA	NA	NA
Food	NA	NA	NA	NA	NA

**Table B.2. Summary of the number of samples and ASVs associated with the oral microbiome for each host species.** These ASV numbers include ASVs shared between body sites, and environmental samples

Host species	Scientific name	Origin of the data	Number of samples	Number of ASVs
African penguin	<i>Spheniscus demersus</i>	The present study	35	625
Urban Cooper's hawk	<i>Accipiter cooperii</i>	Taylor et al., 2019	30	298
Great tit	<i>Parus major</i>	Kropáčková et al., 2017	20	1711
Komodo dragon	<i>Varanus komodoensis</i>	Hyde et al., 2016	26	3912
Mangrove monitor	<i>Varanus indicus</i>	Hyde et al., 2016	1	120
Gray's monitor	<i>Varanus olivaceus</i>	Hyde et al., 2016	2	213
Balck roughneck monitor lizard	<i>Varanus rudicollis</i>	Hyde et al., 2016	1	91
Prairie rattlesnake	<i>Crotalus viridis</i>	Hyde et al., 2016	4	302
California sea lion	<i>Zalophus californianus</i>	Bik et al., 2016	7	125
Bottlenose dolphin	<i>Tursiops truncatus</i>	Bik et al., 2016	10	392
Human	<i>Homo sapiens</i>	Džunková et al., 2018	26	4956

**Table B.3. Summary of the number of samples and ASVs associated with the fecal microbiome for each host species.** These ASV numbers include ASVs shared between body sites, and environmental samples

Host species	Scientific name	Origin of the data	Type of sample	Number of samples	Number of ASVs
African penguin	<i>Spheniscus demersus</i>	The present study	cloaca	33	700
Barn swallow	<i>Hirundo rustica</i>	Kreisinger et al., 2015	cloaca	8	463
Great tit	<i>Parus major</i>	Kropačková et al., 2017	feces	17	1240
Broiler	<i>Gallus gallus domesticus</i>	Videnska et al 2014	feces	27	1480
Hen	<i>Gallus gallus domesticus</i>	Videnska et al 2014	feces	15	1738
Crocodile lizard	<i>Shinisaurus crocodilurus</i>	Jiang et al., 2017	cloaca	16	1528
Komodo dragon	<i>Varanus komodoensis</i>	Hyde et al., 2016	feces	46	1829
California sea lion	<i>Zalophus californianus</i>	Bik et al., 2016	cloaca	8	196
Bottlenose dolphin	<i>Tursiops truncatus</i>	Bik et al., 2016	cloaca	15	119
Human	<i>Homo sapiens</i>	Yarsunenko et al., 2012	feces	41	1877

**Table B.4. Summary of penguin's oral microbiome unique sequences (ASVs not shared with any other vertebrate host) with a relative abundance > 1 %**

<b>Taxonomy</b>	<b>Average relative abundance (%)</b>
Cardiobacteriaceae-Suttonella-NA	13.890
Flavobacteriaceae-Coenonia-NA	5.990
Weeksellaceae-Ornithobacterium-NA	5.358
Cardiobacteriaceae-Cardiobacterium-NA	4.673
Leptotrichiaceae-NA-NA	4.4285
Flavobacteriaceae-Coenonia-anatina	3.804
Flavobacteriaceae-Coenonia-NA	3.605
Flavobacteriaceae-NA-NA	3.411
Weeksellaceae-Ornithobacterium-NA	2.738
Cardiobacteriaceae-NA-NA	2.411
Cardiobacteriaceae-Suttonella-NA	2.244
Mycoplasmataceae-Mycoplasma-NA	2.218
Flavobacteriaceae-NA-NA	2.177
Cardiobacteriaceae-Suttonella-NA	2.04
Moraxellaceae-Psychrobacter-NA	1.752
Moraxellaceae-NA-NA	1.621
Moraxellaceae-Psychrobacter-NA	1.541
Cardiobacteriaceae-Suttonella-NA	1.537
Moraxellaceae-Moraxella-NA	1.450
Cardiobacteriaceae-NA-NA	1.384
Flavobacteriaceae-Coenonia-NA	1.363
Cardiobacteriaceae-Suttonella-NA	1.173
Weeksellaceae-Ornithobacterium-NA	1.032

**Table B.5. Summary of penguin's fecal microbiome unique sequences (ASVs not shared with any other vertebrate host) with a relative abundance > 1 %**

Taxonomy	Average relative abundance (%)
Clostridiales-Family_XI-NA	9.852
Clostridiales-Family_XI-NA	5.252
Neisseriaceae-NA	3.633
Neisseriaceae-NA	3.344
Campylobacteraceae-Campylobacter-NA	3.148
Clostridiales-NA	3.077
Actinomycetaceae-NA	2.597
Family_XI-Ezakiella-NA	2.450
Dysgonomonadaceae-NA	2.356
Gammaproteobacteria-NA	2.171
Firmicutes-NA	2.048
Actinobacteria-NA	1.968
Dysgonomonadaceae-Petrimonas-NA	1.955
Dysgonomonadaceae-Petrimonas-NA	1.844
Clostridiales-Family_XI-Ezakiella-NA	1.844
Ruminococcaceae-Fastidiosipila-NA	1.785
Clostridiales-Family_XI-Gallicola-NA	1.679
Clostridiales-Family_XI-NA	1.576
Lachnospiraceae-NA	1.450
Dysgonomonadaceae-Proteiniphilum-NA	1.302
Gracilibacteria-NA	1.227
Bacteroidia-NA	1.211

**Table B.6. Pairwise results for all permutational multivariate analysis of variance (PERMANOVA) for weighted UniFrac distances between penguin body sites and environmental samples.** \* indicates  $p \leq 0.05$ , and NS indicates not significant

Comparison	p-value
Cloaca x DryRock	*
Cloaca x Feather	*
Cloaca x FecalFloor	*
Cloaca x Food	*
Cloaca x Gland	*
Cloaca x GuanoFloor	*
Cloaca x Mouth	*
Cloaca x Nest	*
Cloaca x Pouch	*
Cloaca x Shoreline	*
Cloaca x SkinBack	*
Cloaca x SkinLeg	*
Cloaca x WetRocks	*
Cloaca x water	*
DryRock x Feather	NS
DryRock x FecalFloor	NS
DryRock x Food	NS
DryRock x Gland	NS
DryRock x GuanoFloor	NS
DryRock x Mouth	*
DryRock x Nest	NS
DryRock x Pouch	NS
DryRock x Shoreline	NS
DryRock x SkinBack	NS
DryRock x SkinLeg	NS
DryRock x WetRocks	NS
DryRock x water	NS
Feather x FecalFloor	NS
Feather x Food	NS
Feather x Gland	NS
Feather x GuanoFloor	NS
Feather x Mouth	*
Feather x Nest	*
Feather x Pouch	NS
Feather x Shoreline	NS

Comparison	p-value
Feather x SkinBack	NS
Feather x SkinLeg	NS
Feather x WetRocks	NS
Feather x water	NS
FecalFloor x Food	NS
FecalFloor x Gland	*
FecalFloor x GuanoFloor	NS
FecalFloor x Mouth	*
FecalFloor x Nest	NS
FecalFloor x Pouch	*
FecalFloor x Shoreline	NS
FecalFloor x SkinBack	*
FecalFloor x SkinLeg	*
FecalFloor x WetRocks	NS
FecalFloor x water	NS
Food x Gland	*
Food x GuanoFloor	NS
Food x Mouth	*
Food x Nest	*
Food x Pouch	*
Food x Shoreline	*
Food x SkinBack	*
Food x SkinLeg	*
Food x WetRocks	NS
Food x water	*
Gland x GuanoFloor	*
Gland x Mouth	*
Gland x Nest	*
Gland x Pouch	NS
Gland x Shoreline	*
Gland x SkinBack	*
Gland x SkinLeg	*
Gland x WetRocks	*
Gland x water	*
GuanoFloor x Mouth	*
GuanoFloor x Nest	NS
GuanoFloor x Pouch	*
GuanoFloor x Shoreline	NS
GuanoFloor x SkinBack	NS

Comparison	p-value
GuanoFloor x SkinLeg	*
GuanoFloor x WetRocks	NS
GuanoFloor x water	NS
Mouth x Nest	*
Mouth x Pouch	*
Mouth x Shoreline	*
Mouth x SkinBack	*
Mouth x SkinLeg	*
Mouth x WetRocks	*
Mouth x water	*
Nest x Pouch	*
Nest x Shoreline	
Nest x SkinBack	*
Nest x SkinLeg	*
Nest x WetRocks	NS
Nest x water	NS
Pouch x Shoreline	*
Pouch x SkinBack	*
Pouch x SkinLeg	NS
Pouch x WetRocks	*
Pouch x water	*
Shoreline x SkinBack	*
Shoreline x SkinLeg	*
Shoreline x WetRocks	NS
Shoreline x water	NS
SkinBack x SkinLeg	*
SkinBack x WetRocks	*
SkinBack x water	*
SkinLeg x WetRocks	*
SkinLeg x water	*
WetRocks x water	NS



**Table B.7. Summary of the number of ASVs shared between each penguin (*Spheniscus demersus*) body site and the environment, and of the number of unique ASVs (not shared with environmental samples) for each penguin body site, as well as their associated proportion**

Body site	number of ASVs shared with environment	proportion represented by ASVs shared with the environment	number of unique ASVs	proportion represented by unique ASVs
cloaca	336	41.227	182	22.331
oral cavity	291	44.769	120	18.462
brood pouch	709	61.921	103	8.996
feather	290	65.315	12	2.703
uropygial gland	674	63.168	75	7.029
dorsal skin	511	62.931	52	6.404
leg skin	724	64.528	92	8.200

**Table B.8. Summary of the number of ASVs unique to each penguin (*Spheniscus demersus*) body sites, including the taxonomic assignment.** Unique ASVs correspond to ASVs only present in one body site and not shared with either other penguin body sites or environmental samples of the penguin exhibit

Body site	Taxonomy	Number of ASVs
Cloaca	Dysgonomonadaceae-NA	1
	Clostridiales-Family_XI-NA	1
	Campylobacter-NA	1
	Petrimonas-NA	1
	Actinomycetaceae-NA	1
	Actinomyces-NA	1
	Actinobacteria-NA	1
	Clostridiales-Family_XI-Gallicola-NA	1
	Fastidiosipila-NA	1
Oral cavity	Cardiobacteriaceae-NA	1
	Suttonella-NA	5
	Coenonia-NA	2
	Coenonia-anatina	1
	Flavobacteriaceae-NA	1
	Cardiobacterium-NA	1
	Weeksellaceae-NA	1
	Ornithobacterium-NA	2
	Psychrobacter-NA	2
	Leptotrichiaceae-NA	1
Preening gland	Psychrobacter-NA	4
	Psychrobacter-phenylpyruvicus	1
Brood pouch	Psychrobacter-NA	3
	Suttonella-NA	1
	Kocuria-NA	1
Skin back	Coenonia-anatina	1
	Ornithobacterium-NA	1
	Suttonella-NA	2
	Psychrobacter-NA	3
SkinLeg	Oceanisphaera-NA	1
Feather	Psychrobacter-NA	6
	Ornithobacterium-NA	1
	Suttonella-NA	2
	Actinobacteria-NA	1
	Clostridiales-Family_XI-NA	2
	Neisseriaceae-NA	1

**Table B.9. List of pathogens, number of ASVs, and relative abundance (%) present in penguin body sites**

Pathogen	# ASVs	Cloaca	Oral	Preen Gland	Brood Pouch	Back Skin	Leg Skin	Feather
Escherichia/Shigella	1	0.067	0.003	0.491	0.449	3.151	0.206	0.987
Pseudomonas	29	0.006	0.005	0.227	0.311	0.111	0.662	0.04
Streptococcus	9	0.023	0.002	0.562	0.049	0.396	0.216	0.053
Enterococcus	2	0.006	0	0.004	0.007	0.102	0.006	0
Staphylococcus	9	0.021	0.019	1.738	0.676	0.8	1.016	0.4
Campylobacter	7	3.024	0.8	0.196	0.064	0.222	0.074	0.173
Clostridium	10	0.573	0.006	5.087	2.509	0.996	2.804	3.427
Mycoplasma	23	0.264	2.934	0.038	0.056	0.32	0.028	0.04
Mycobacterium	5	0.001	0	0.013	0.013	0.027	0.006	0
Ornithobacterium		0.56	4.653	1.022	2.427	4.244	2.252	2.293
Coenonia		0.361	14.905	1	0.709	3.253	0.22	0.933
Prevotella		0	0	0.022	0.007	0	0.006	0
Erysipelothrix		0.015	0.007	1.291	0.973	0.507	1.166	0.2
Salmonella	Not present							
Klebsiella	Not present							
Yersinia	Not present							
Pasteurella	Not present							
Listeria	Not present							
Chlamydia	Not present							
Borrelia	Not present							
Anaplasma	Not present							
Riemerella	Not present							

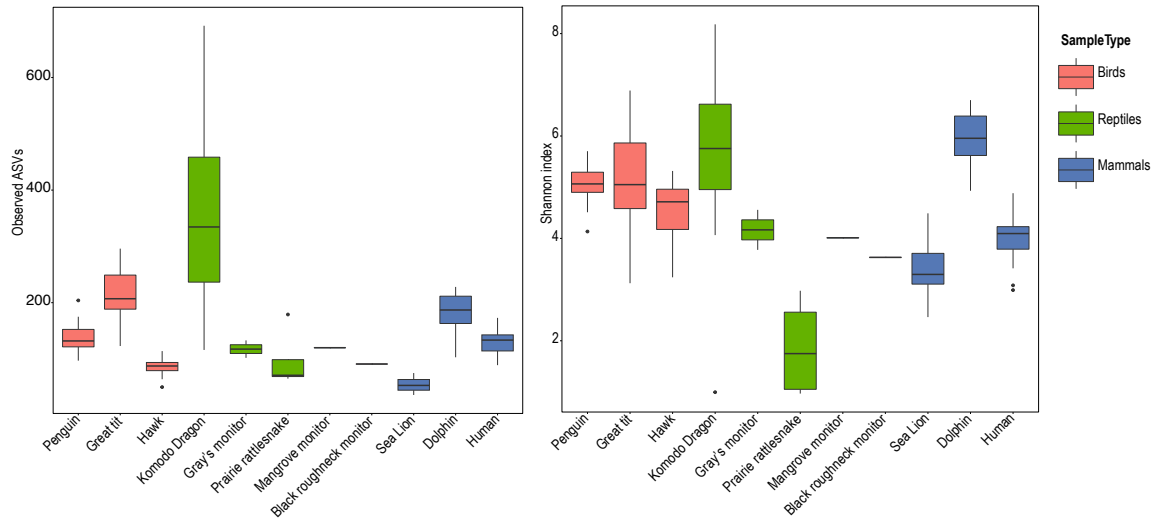


**Figure B.1. Box plots representing differences in  $\alpha$ -diversity (Observed ASVs, and the Shannon index) between the oral microbiome of various vertebrate hosts including birds, reptiles, and mammals**

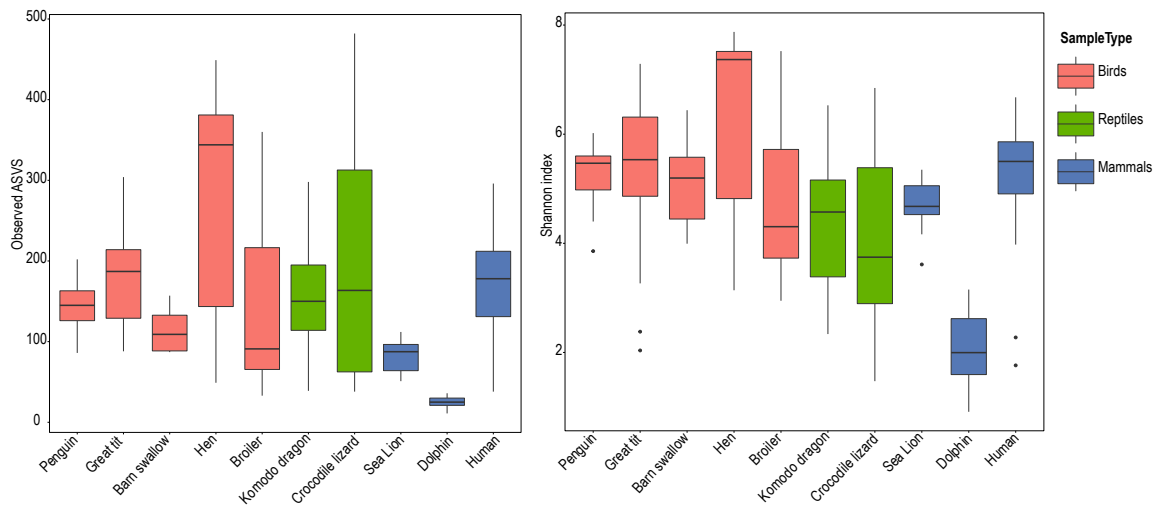


**Figure B.2. Box plots representing differences in  $\alpha$ -diversity (Observed ASVs, and the Shannon index) between the fecal microbiome of various vertebrate hosts including birds, reptiles, and mammals**

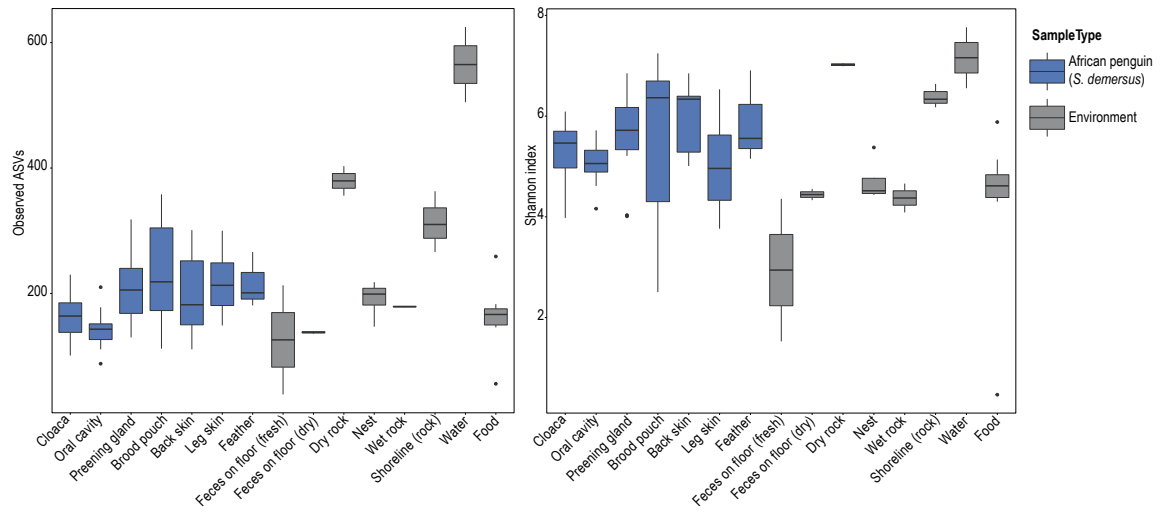


**Figure B.3. Box plots representing differences in  $\alpha$ -diversity (Observed ASVs, and the Shannon index) between different penguin (*Spheniscus demersus*) body sites and environmental samples from their exhibit**



**APPENDIX C. SUPPLEMENTARY INFORMATION FOR**  
**CHAPTER 4: WATER COLUMN AND SEDIMENT CORE**  
**DEPTH DRIVE SPATIAL DECOUPLING OF SEDIMENT**  
**MICROBIAL COMMUNITIES IN THE NORTHERN GULF OF**  
**MEXICO**

**Table C.1. Results of test of significance of environmental variables for Canonical Correspondence Analysis on both the prokaryotic and Archaea specific datasets.** \* indicates a significant difference  $p \leq 0.05$ , \*\* indicates  $p \leq 0.01$ , \*\*\* indicates  $p \leq 0.001$ , \*\*\*\* indicates  $p \leq 0.0001$ , and NS indicates not significant ( $p > 0.05$ )

Parameter	p-value	
	Prokaryotic data set	Archaea dataset
DIC (mM)	***	***
PO4 (uM)	***	NS
Mntot (uM)	**	NS
Fetot (uM)	*	NS
NH4 uM)	*	*
NO3 (uM)	**	NS
NO2 (uM)	NS	NS
SO4 (uM)	*	*
H2S (uM)	**	**
FeIII-L (nA)	NS	NS
depth (mm)	***	**



**Table C.2. Phylogenetic approximation of Bathyarchaeal ASVs inferred by comparing those sequences to the Bathyarchaeota database from Zhou, Pan et al. (2018) using BLASTN (97 % similarity cutoff). ASVs included correspond to those presented in the heatmap (Figure C.10)**

Sediment region	ASV	Ref_Name	Subgroup
shelf	Bathy_356	MCG-15_FR695318.1	15
shelf	Bathy_27	KC925875.1.915_1	15
shelf	Bathy_396	MCG-15_AB301865.1	15
shelf	Bathy_397	MCG-15_AB301865.1	15
shelf	Bathy_1190	KC925912.1.915_1	8
shelf	Bathy_40	KC925875.1.915_1	15
shelf	Bathy_1059	MCG-8_DQ363807.1	8
shelf	Bathy_1230	KC003572.1.884_1	1
shelf	Bathy_319	MCG-15_DQ641883.1	15
shelf	Bathy_661	MCG-12_GQ848385.1	12
shelf	Bathy_574	EF203596.1.898_1	13
shelf	Bathy_937	MCG-12_GQ848385.1	12
shelf	Bathy_20	KC925875.1.915_1	15
shelf	Bathy_938	MCG-12_GQ848385.1	12
shelf	Bathy_901	MCG-8_DQ363807.1	8
shelf	Bathy_196	MCG-17_FJ404037.1	17
shelf	Bathy_1012	KX077312.1.914_1	8
shelf	Bathy_943	MCG-12_GQ848385.1	12
shelf	Bathy_943	MCG-12_GQ848385.1	12
shelf	Bathy_1011	MCG-8_DQ363807.1	8
shelf	Bathy_823	AB213058.1.1549_1	8
shelf	Bathy_930	****	8
shelf	Bathy_1213	KC925912.1.915_1	8
shelf	Bathy_825	AB213058.1.1549_1	8
shelf	Bathy_1211	KC925912.1.915_1	8
shelf	Bathy_720	JX492958.1.890_1	13
shelf	Bathy_941	MCG-12_GQ848385.1	12
shelf	Bathy_1055	MCG-8_DQ363807.1	8
shelf	Bathy_751	GQ927628.1.918_1	8
shelf	Bathy_757	GQ927628.1.918_1	8
shelf	Bathy_848	MCG-12_GQ848385.1	12
slope	Bathy_209	MCG-17_FJ264803.1	17
slope	Bathy_334	AB797651.1.1428_1	15
slope	Bathy_355	MCG-15_FR695318.1	15
slope	Bathy_414	MCG-15_EU385859.1	15

Sediment region	ASV	Ref_Name	Subgroup
slope	Bathy_1253	DQ302018.1.863_1	13
slope	Bathy_795	MCG-6_FJ264555.1	6
slope	Bathy_202	MCG-17_FJ264803.1	17
slope	Bathy_345	MCG-15_EU385859.1	15
**** : Candidatus_Bathyarchaeota_archaeon_BA2_GCA_001399795.1_16S_1			

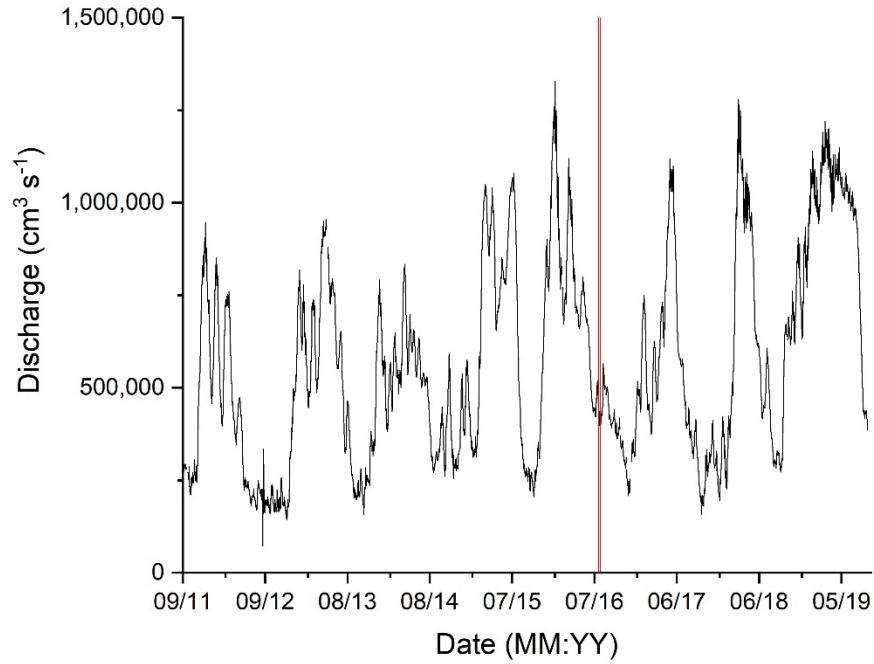


**Figure C.1. Mississippi River Discharge data (cm<sup>3</sup> s<sup>-1</sup>) at the Belle Chasse, LA monitoring station (USGS Station #07374525). Date in Month: Year format (MM:YY)**

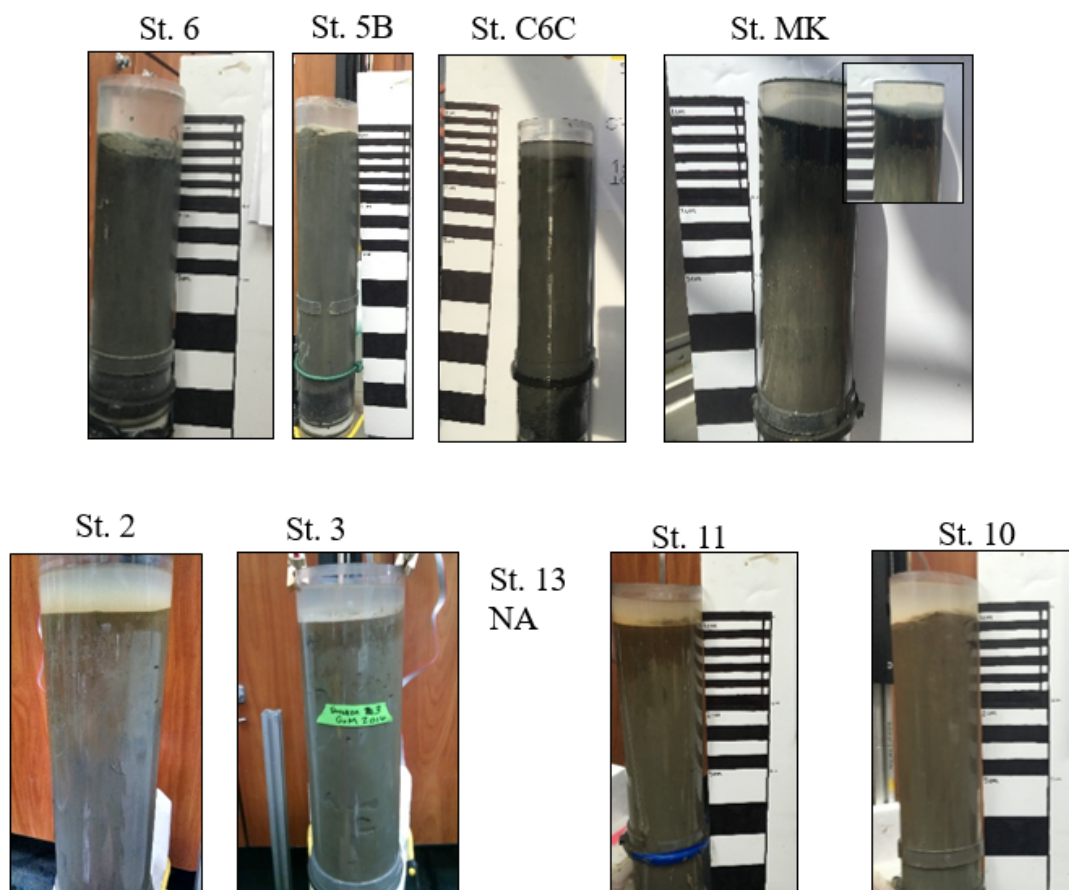


**Figure C.2. Pictures of the cores showing variations in sediment color and stratification at the different locations. Thin, medium, and thick white and black lines represent depth intervals of 1, 2, and 5 cm respectively. The inset picture of the St. MK sediment core provides a better contrast of the top 14 cm. A picture of the sediment core from St. 13 was not available (NA)**

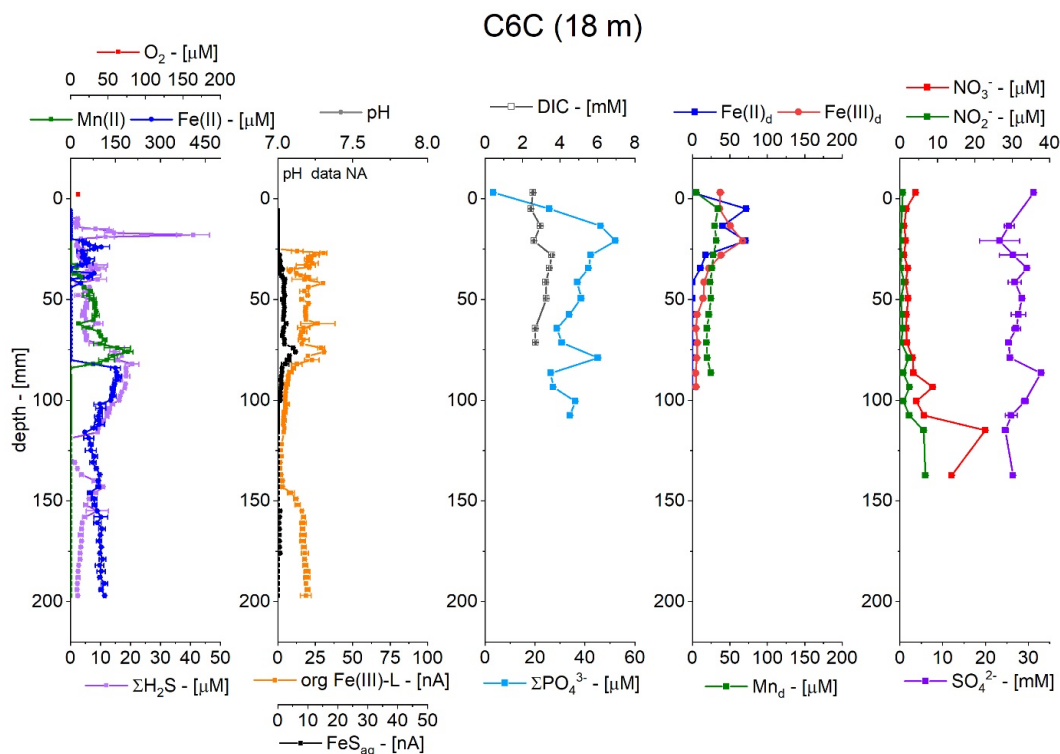


**Figure C.3. Depth microprofiles at St. C6C of  $O_2$ ,  $Mn^{2+}$ ,  $Fe^{2+}$ ,  $H_2S$ ,  $org-Fe(III)$  complexes and  $FeS_{aq}$  (first and second panel) as well as pH (second panel) obtained with voltammetric and potentiometric microelectrodes. Depth profiles of pore water species DIC,  $NH_4^+$  (third panel),  $Fe^{2+}$ ,  $Fe(III)_d$ ,  $Mn_d$  (fourth panel),  $NO_3^-$ ,  $NO_2^-$ , and  $SO_4^{2-}$  (fifth panel). pH and  $NH_4^+$  data were not available (NA)**

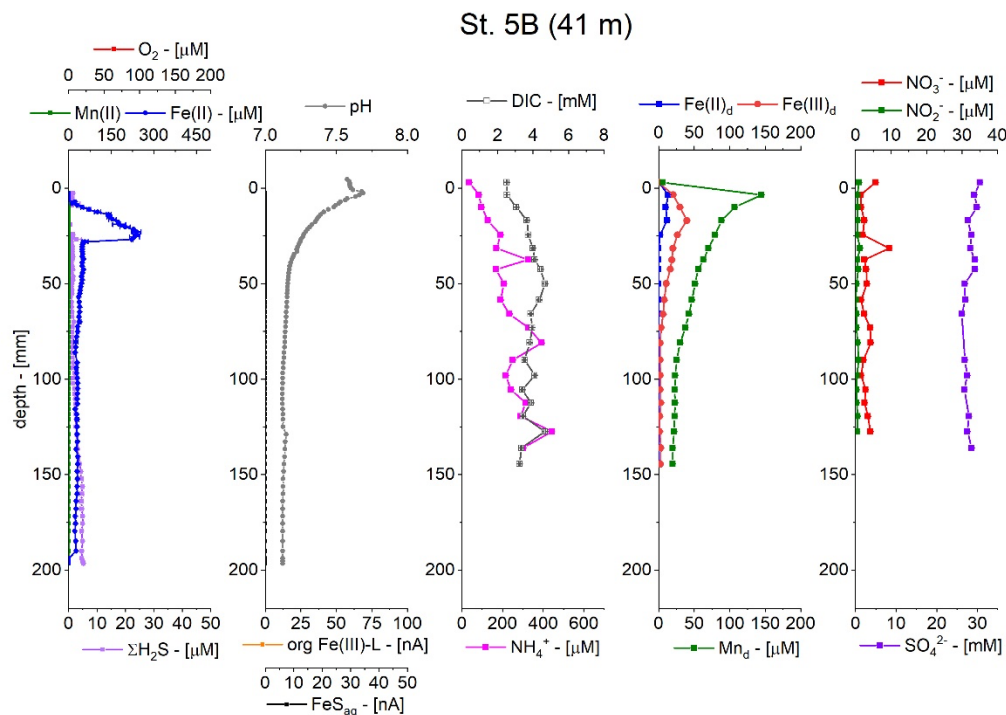


**Figure C.4. Depth microprofiles at St. 5B of  $\text{O}_2$ ,  $\text{Mn}^{2+}$ ,  $\text{Fe}^{2+}$ ,  $\text{H}_2\text{S}$ , org-Fe(III) complexes and  $\text{FeS}_{\text{aq}}$  (first and second panel) as well as pH (second panel) obtained with voltammetric and potentiometric microelectrodes. Depth profiles of pore water species DIC,  $\text{NH}_4^+$  (third panel),  $\text{Fe}^{2+}$ ,  $\text{Fe(III)}_{\text{d}}$ ,  $\text{Mn}_{\text{d}}$  (fourth panel),  $\text{NO}_3^-$ ,  $\text{NO}_2^-$ , and  $\text{SO}_4^{2-}$  (fifth panel).  $\Sigma\text{PO}_4^{3-}$  data were not available (NA)**

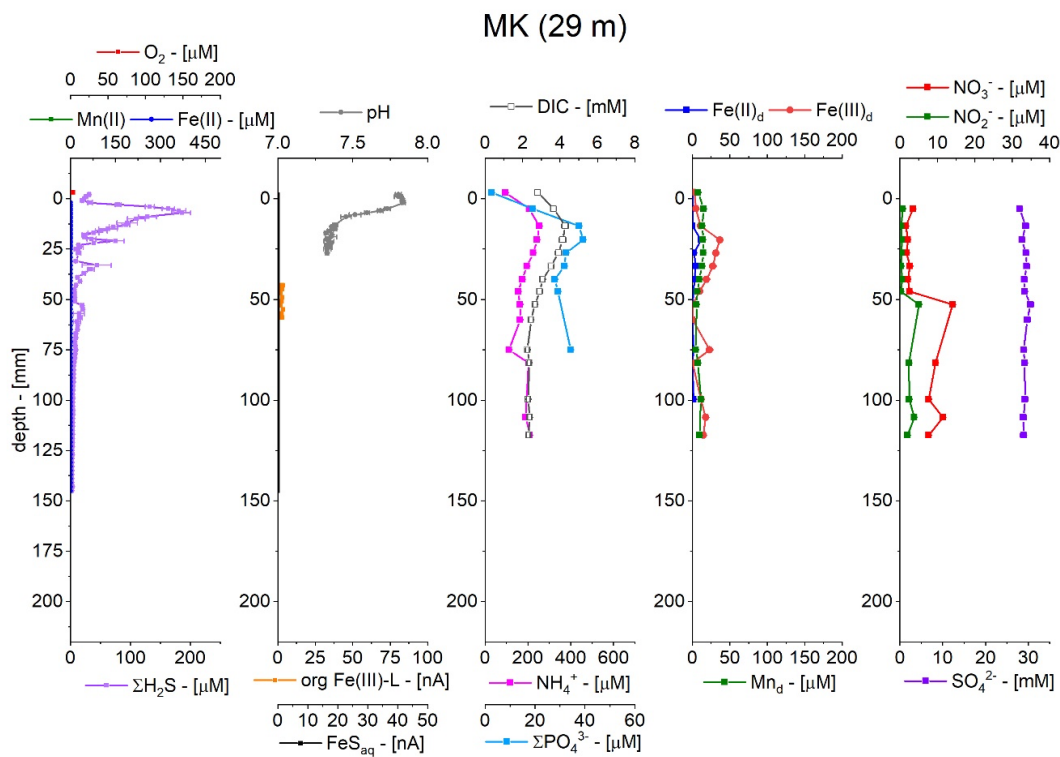


**Figure C.5. Depth microprofiles at St. MK of  $O_2$ ,  $Mn^{2+}$ ,  $Fe^{2+}$ ,  $H_2S$ , org-Fe(III) complexes and  $FeS_{aq}$  (first and second panel) as well as pH (second panel) obtained with voltammetric and potentiometric microelectrodes. Depth profiles of pore water species  $DIC$ ,  $NH_4^+$  (third panel),  $Fe^{2+}$ ,  $Fe(III)_d$ ,  $Mn_d$  (fourth panel),  $NO_3^-$ ,  $NO_2^-$ , and  $SO_4^{2-}$  (fifth panel)**

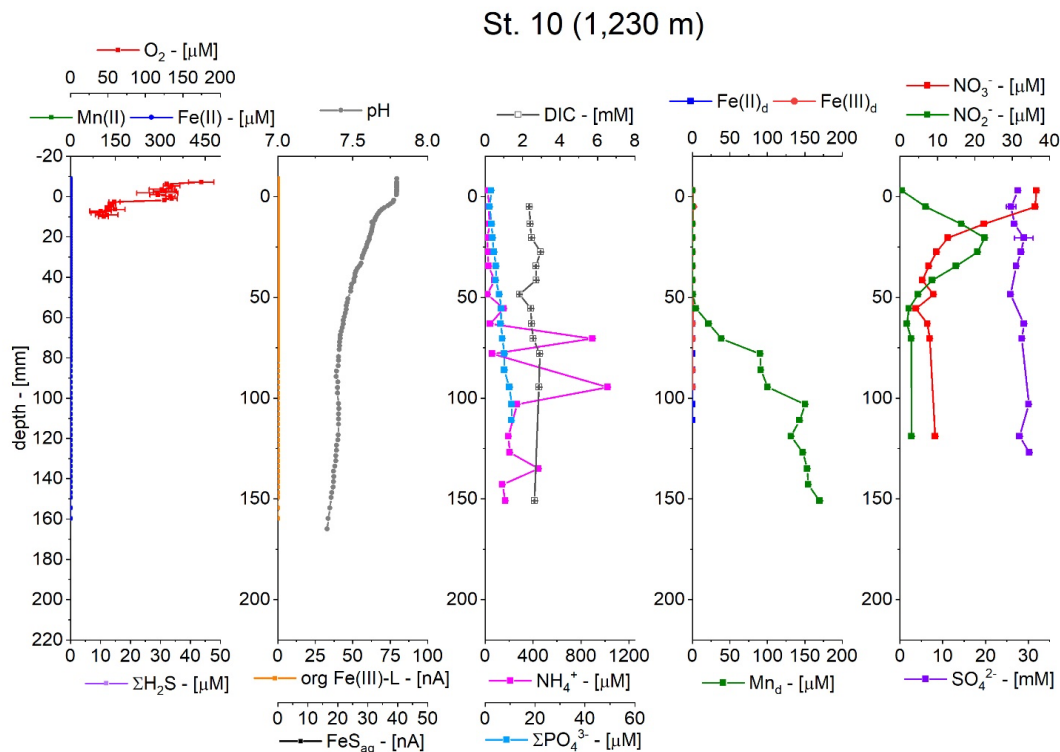


**Figure C.6. Depth microprofiles at St. 10 of  $Mn^{2+}$ ,  $Fe^{2+}$ ,  $H_2S$ ,  $S_2O_3^{2-}$ , org- $Fe(III)$  complexes and  $FeS_{aq}$  (first and second panel) as well as pH (second panel) obtained with voltammetric and potentiometric microelectrodes. Depth profiles of pore water species DIC,  $NH_4^+$  (third panel),  $Fe^{2+}$ ,  $Fe(III)_d$ ,  $Mn_d$  (fourth panel),  $NO_3^-$ ,  $NO_2^-$ , and  $SO_4^{2-}$  (fifth panel). Voltammetric  $O_2$  profiles were not available (NA)**



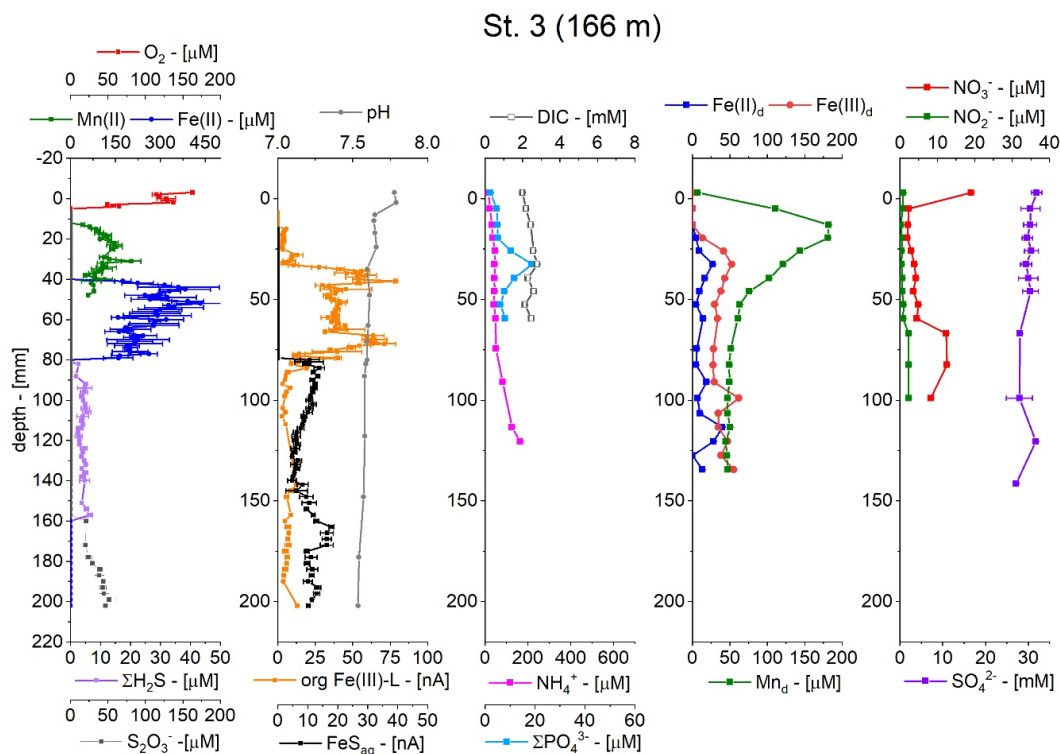


**Figure C.7. Depth microprofiles at St. 3 of O<sub>2</sub>, Mn<sup>2+</sup>, Fe<sup>2+</sup>, H<sub>2</sub>S, org-Fe(III) complexes and FeS<sub>aq</sub> (first and second panel) as well as pH (second panel) obtained with voltammetric and potentiometric microelectrodes. Depth profiles of pore water species DIC, NH<sub>4</sub><sup>+</sup> (third panel), Fe<sup>2+</sup>, Fe(III)<sub>d</sub>, Mn<sub>d</sub> (fourth panel), NO<sub>3</sub><sup>-</sup>, NO<sub>2</sub><sup>-</sup>, and SO<sub>4</sub><sup>2-</sup> (fifth panel)**

# St. 13 (506 m)

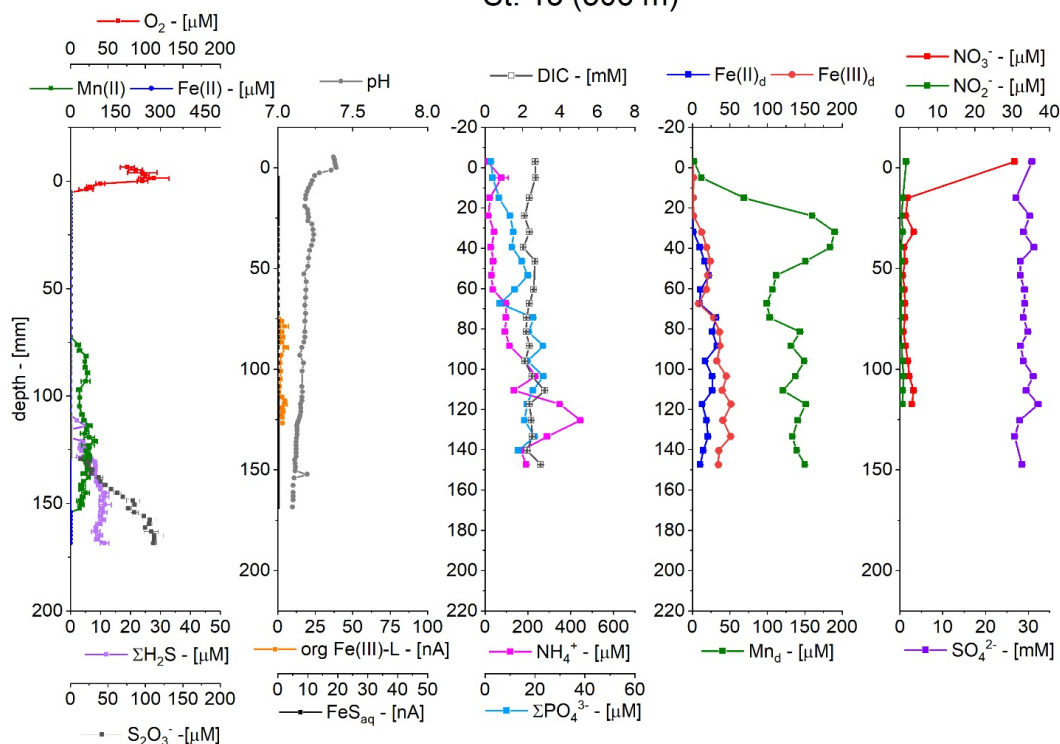


**Figure C.8. Depth microprofiles at St. 13 of  $O_2$ ,  $Mn^{2+}$ ,  $Fe^{2+}$ ,  $H_2S$ ,  $S_2O_3^{2-}$ ,  $org\text{-}Fe(III)$  complexes and  $FeS_{aq}$  (first and second panel) as well as  $pH$  (second panel) obtained with voltammetric and potentiometric microelectrodes. Depth profiles of pore water species  $DIC$ ,  $NH_4^+$  (third panel),  $Fe^{2+}$ ,  $Fe(III)_d$ ,  $Mn_d$  (fourth panel),  $NO_3^-$ ,  $NO_2^-$ , and  $SO_4^{2-}$  (fifth panel).  $\Sigma PO_4^{3-}$  data were not available (NA)**

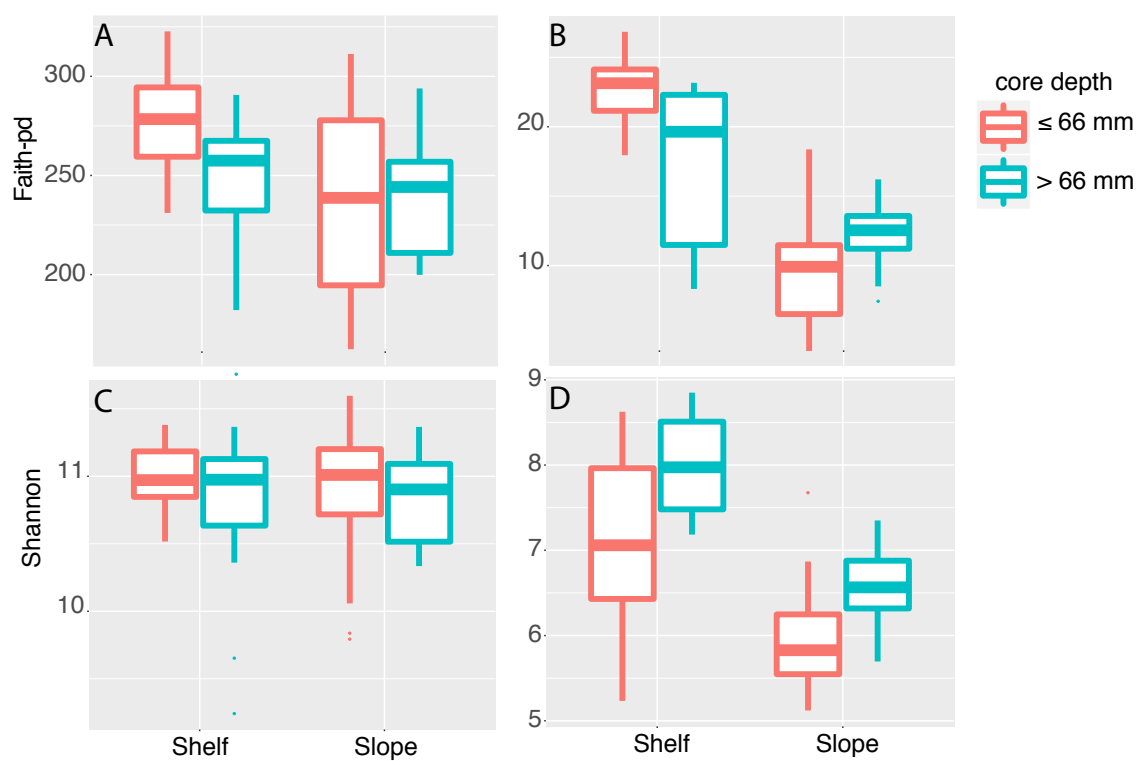


**Figure C.9.  $\alpha$ -diversity metrics A) and B) Faith phylogenetic index (Faith-pd), and C) and D) Shannon diversity index, of shelf and slope sediments according to sediment core depth.**

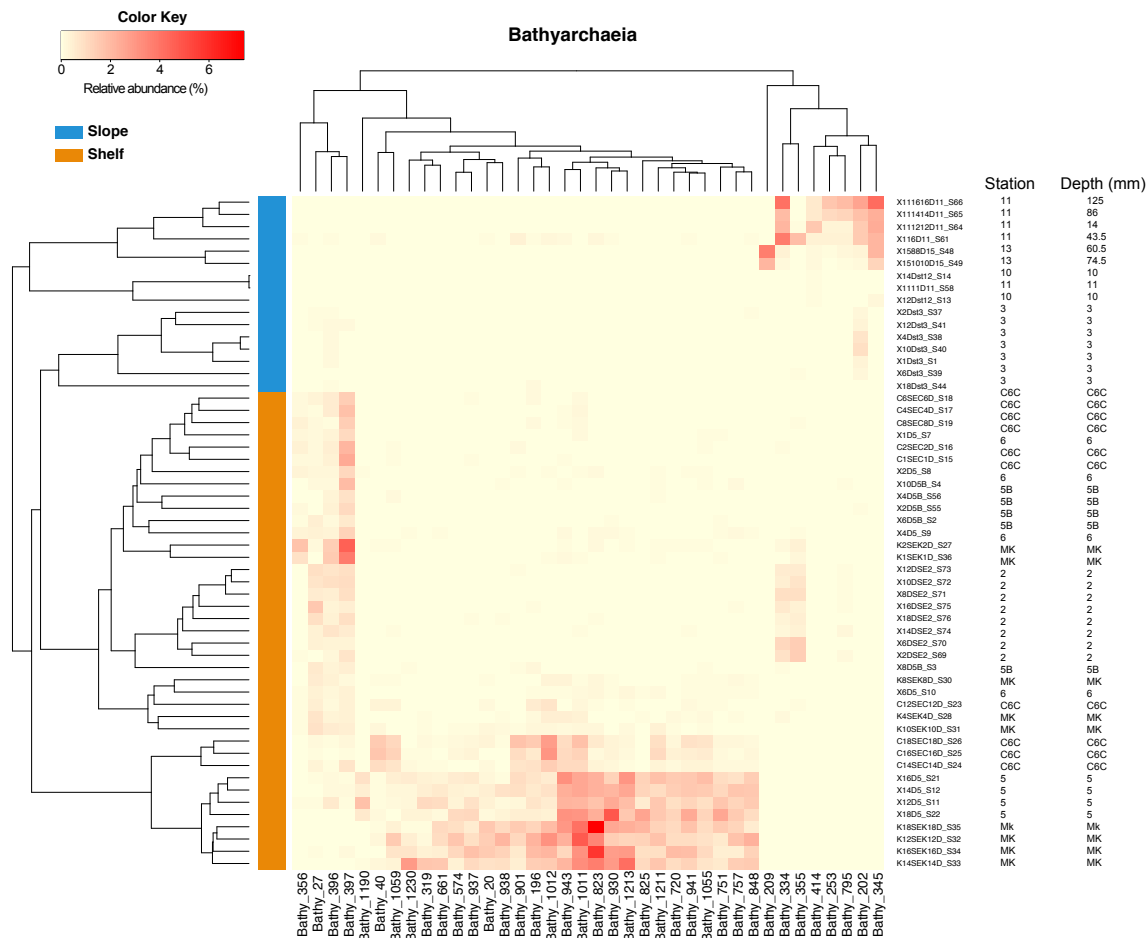


**Figure C.10.** Heat map showing the relative abundances of Bathyarchaeota in shelf and slope sediments. Hierarchical clustering of the samples is represented by the dendrogram on the left, while ASVs are organized following Bray Curtis distances

## REFERENCES

- Achtman, M. and M. Wagner (2008). "Microbial diversity and the genetic nature of microbial species." *Nature Reviews Microbiology* **6**(6): 431-440.
- Adair, K. L. and A. E. Douglas (2017). "Making a microbiome: the many determinants of host-associated microbial community composition." *Current Opinion in Microbiology* **35**: 23-29.
- Adler, C. J., K. Dobney, L. S. Weyrich, J. Kaidonis, A. W. Walker, W. Haak, C. J. Bradshaw, G. Townsend, A. Soltysiak and K. W. Alt (2013). "Sequencing ancient calcified dental plaque shows changes in oral microbiota with dietary shifts of the Neolithic and Industrial revolutions." *Nature genetics* **45**(4): 450.
- Adler, P. B. and W. K. Lauenroth (2003). "The power of time: spatiotemporal scaling of species diversity." *Ecology letters* **6**(8): 749-756.
- Ainsworth, E. A. and S. P. Long (2005). "What have we learned from 15 years of free-air CO<sub>2</sub> enrichment (FACE)? A meta-analytic review of the responses of photosynthesis, canopy properties and plant production to rising CO<sub>2</sub>." *New phytologist* **165**(2): 351-372.
- Ainsworth, T. D. and R. D. Gates (2016). "Corals' microbial sentinels." *Science* **352**(6293): 1518-1519.
- Ainsworth, T. D., L. Krause, T. Bridge, G. Torda, J.-B. Raina, M. Zakrzewski, R. D. Gates, J. L. Padilla-Gamiño, H. L. Spalding and C. Smith (2015). "The coral core microbiome identifies rare bacterial taxa as ubiquitous endosymbionts." *The ISME journal* **9**(10): 2261-2274.
- Ainsworth, T. D., R. V. Thurber and R. D. Gates (2010). "The future of coral reefs: a microbial perspective." *Trends in Ecology & Evolution* **25**(4): 233-240.
- Ajemian, M. J., S. P. Powers and T. J. Murdoch (2012). "Estimating the potential impacts of large mesopredators on benthic resources: integrative assessment of spotted eagle ray foraging ecology in Bermuda." *PloS one* **7**(7): e40227.
- Al-Asmakh, M., J.-B. Stukenborg, A. Reda, F. Anuar, M.-L. Strand, L. Hedin, S. Pettersson and O. Söder (2014). "The gut microbiota and developmental programming of the testis in mice." *PLoS One* **9**(8): e103809.
- Alfano, N., A. Courtiol, H. Vielgrader, P. Timms, A. L. Roca and A. D. Greenwood (2015). "Variation in koala microbiomes within and between individuals: effect of body region and captivity status." *Scientific reports* **5**: 10189.
- Aller, R. C. (1982). "Carbonate Dissolution in Nearshore Terrigenous Muds: The Role of Physical and Biological Reworking." *The Journal of Geology* **90**(1): 79-95.
- Aller, R. C. (1998). "Mobile deltaic and continental shelf muds as suboxic, fluidized bed reactors." *Marine Chemistry* **61**(3): 143-155.
- Amato, K. R., J. L. Metcalf, S. J. Song, V. L. Hale, J. Clayton, G. Ackermann, G. Humphrey, K. Niu, D. Cui and H. Zhao (2016). "Using the gut microbiota as a novel tool for examining colobine primate GI health." *Global Ecology and Conservation* **7**: 225-237.
- Amato, K. R., C. J. Yeoman, A. Kent, N. Righini, F. Carbonero, A. Estrada, H. R. Gaskins, R. M. Stumpf, S. Yildirim and M. Torralba (2013). "Habitat degradation impacts black howler

- monkey (*Alouatta pigra*) gastrointestinal microbiomes." The ISME journal **7**(7): 1344-1353.
- Anschutz, P., B. Sundby, L. Lefrancois, G. W. Luther and A. Mucci (2000). "Interactions between metal oxides and species of nitrogen and iodine in bioturbated marine sediments." Geochimica Et Cosmochimica Acta **64**(16): 2751-2763.
- Antwis, R. E., R. L. Haworth, D. J. Engelmoer, V. Ogilvy, A. L. Fidgett and R. F. Preziosi (2014). "Ex situ diet influences the bacterial community associated with the skin of red-eyed tree frogs (*Agalychnis callidryas*)." PloS one **9**(1): e85563.
- Apprill, A., J. Robbins, A. M. Eren, A. A. Pack, J. Reveillaud, D. Mattila, M. Moore, M. Niemeyer, K. M. Moore and T. J. Mincer (2014). "Humpback whale populations share a core skin bacterial community: towards a health index for marine mammals?" PLoS One **9**(3): e90785.
- Archie, E. A. and J. Tung (2015). "Social behavior and the microbiome." Current opinion in behavioral sciences **6**: 28-34.
- Armingohar, Z., J. J. Jørgensen, A. K. Kristoffersen, E. Abesha-Belay and I. Olsen (2014). "Bacteria and bacterial DNA in atherosclerotic plaque and aneurysmal wall biopsies from patients with and without periodontitis." Journal of oral microbiology **6**(1): 23408.
- Arnold, J. W., J. Roach and M. A. Azcarate-Peril (2016). "Emerging Technologies for Gut Microbiome Research." Trends in Microbiology **24**(11): 887-901.
- Arrigo, K. R. (2005). "Marine microorganisms and global nutrient cycles (vol 437, pg 349, 2005)." Nature **438**(7064): 122-122.
- Astorga, A., J. Oksanen, M. Luoto, J. Soininen, R. Virtanen and T. Muotka (2012). "Distance decay of similarity in freshwater communities: do macro-and microorganisms follow the same rules?" Global Ecology and Biogeography **21**(3): 365-375.
- Baas-Becking, L. G. M. (1934). Geobiologie; of inleiding tot de milieukunde, WP Van Stockum & Zoon NV.
- Bahr, M., B. C. Crump, V. Klepac-Ceraj, A. Teske, M. L. Sogin and J. E. Hobbie (2005). "Molecular characterization of sulfate-reducing bacteria in a New England salt marsh." Environmental Microbiology **7**(8): 1175-1185.
- Balashova, V. and G. Zavarzin (1979). "Anaerobic reduction of ferric iron by hydrogen bacteria." Mikrobiologiya **48**(5): 773-778.
- Banerjee, A., J. Cornejo and R. Bandopadhyay (2020). "Emergent climate change impact throughout the world: call for "Microbiome Conservation" before it's too late." Biodiversity and Conservation **29**(1): 345-348.
- Banks, J. C., S. C. Cary and I. D. Hogg (2009). "The phylogeography of Adelie penguin faecal flora." Environmental microbiology **11**(3): 577-588.
- Barbosa, A., V. Balagué, F. Valera, A. Martínez, J. Benzal, M. Motas, J. I. Diaz, A. Mira and C. Pedrós-Alió (2016). "Age-related differences in the gastrointestinal microbiota of chinstrap penguins (*Pygoscelis antarctica*)." PloS one **11**(4): e0153215.
- Bartlett, R., R. J. G. Mortimer and K. Morris (2008). "Anoxic nitrification: Evidence from Humber Estuary sediments (UK)." Chemical Geology **250**(1-4): 29-39.
- Bartlett, R., R. J. G. Mortimer and K. M. Morris (2007). "The biogeochemistry of a manganese-rich Scottish sea loch: Implications for the study of anoxic nitrification." Continental Shelf Research **27**(10-11): 1501-1509.

- Bascompte, J., C. J. Melián and E. Sala (2005). "Interaction strength combinations and the overfishing of a marine food web." Proceedings of the National Academy of Sciences **102**(15): 5443-5447.
- Bauer, J. E., W.-J. Cai, P. A. Raymond, T. S. Bianchi, C. S. Hopkinson and P. A. Regnier (2013). "The changing carbon cycle of the coastal ocean." Nature **504**(7478): 61-70.
- Baum, J. K. and B. Worm (2009). "Cascading top-down effects of changing oceanic predator abundances." Journal of Animal Ecology **78**(4): 699-714.
- Becker, M. H., C. L. Richards-Zawacki, B. Gratwicke and L. K. Belden (2014). "The effect of captivity on the cutaneous bacterial community of the critically endangered Panamanian golden frog (*Atelopus zeteki*)." Biological Conservation **176**: 199-206.
- Beckler, J. S., N. Kiriazis, C. Rabouille, F. J. Stewart and M. Tallefert (2016). "Importance of microbial iron reduction in deep sediments of river-dominated continental-margins." Marine Chemistry **178**: 22-34.
- Beckler, J. S., D. B. Nuzzio and M. Tallefert (2014). "Development of single-step liquid chromatography methods with ultraviolet detection for the measurement of inorganic anions in marine waters." Limnology and Oceanography: Methods **12**(8): 563-576.
- Belizário, J. E., J. Faintuch and M. Garay-Malpartida (2018). "Gut microbiome dysbiosis and immunometabolism: new frontiers for treatment of metabolic diseases." Mediators of inflammation **2018**.
- Bellwood, D. R., T. P. Hughes, C. Folke and M. Nyström (2004). "Confronting the coral reef crisis." Nature **429**(6994): 827-833.
- Benson, A. K., S. A. Kelly, R. Legge, F. Ma, S. J. Low, J. Kim, M. Zhang, P. L. Oh, D. Nehrenberg and K. Hua (2010). "Individuality in gut microbiota composition is a complex polygenic trait shaped by multiple environmental and host genetic factors." Proceedings of the National Academy of Sciences **107**(44): 18933-18938.
- Bernasconi, R., M. Stat, A. Koenders, A. Paparini, M. Bunce and M. J. Huggett (2019). "Establishment of Coral-Bacteria Symbioses Reveal Changes in the Core Bacterial Community With Host Ontogeny." Frontiers in Microbiology **10**(1529).
- Bernini, P., I. Bertini, C. Luchinat, S. Nepi, E. Saccenti, H. Schäfer, B. Schütz, M. Spraul and L. Tenori (2009). "Individual Human Phenotypes in Metabolic Space and Time." Journal of Proteome Research **8**(9): 4264-4271.
- Bertagnolli, A. D. and F. J. Stewart (2018). "Microbial niches in marine oxygen minimum zones." Nature Reviews Microbiology **16**(12): 723-729.
- Bertrand, J.-C., P. Bonin, B. Ollivier, K. Alain, A. Godfroy, N. Pradel and P. Normand (2018). Evolutionary success of prokaryotes. Prokaryotes and Evolution, Springer: 131-240.
- Beulig, F., H. Røy, C. Glombitza and B. B. Jørgensen (2018). "Control on rate and pathway of anaerobic organic carbon degradation in the seabed." Proceedings of the National Academy of Sciences **115**(2): 367.
- Beulig, F., H. Røy, S. McGlynn and B. Jørgensen (2019). "Cryptic CH<sub>4</sub> cycling in the sulfate–methane transition of marine sediments apparently mediated by ANME-1 archaea." The ISME journal **13**(2): 250-262.
- Biagi, E., C. Franceschi, S. Rampelli, M. Severgnini, R. Ostan, S. Turrone, C. Consolandi, S. Quercia, M. Scurti and D. Monti (2016). "Gut microbiota and extreme longevity." Current Biology **26**(11): 1480-1485.

- Bianchi, T. S., M. A. Allison, E. A. Canuel, D. R. Corbett, B. A. McKee, T. P. Sampere, S. G. Wakeham and E. Waterson (2006). "Rapid export of organic matter to the Mississippi Canyon." Eos, Transactions American Geophysical Union **87**(50): 565-573.
- Biddle, A. S., S. J. Black and J. L. Blanchard (2013). "An in vitro model of the horse gut microbiome enables identification of lactate-utilizing bacteria that differentially respond to starch induction." PloS one **8**(10).
- Biddle, J. F., J. S. Lipp, M. A. Lever, K. G. Lloyd, K. B. Sørensen, R. Anderson, H. F. Fredricks, M. Elvert, T. J. Kelly and D. P. Schrag (2006). "Heterotrophic Archaea dominate sedimentary subsurface ecosystems off Peru." Proceedings of the National Academy of Sciences **103**(10): 3846-3851.
- Bienhold, C., A. Boetius and A. Ramette (2012). "The energy–diversity relationship of complex bacterial communities in Arctic deep-sea sediments." The ISME journal **6**(4): 724-732.
- Bienhold, C., L. Zinger, A. Boetius and A. Ramette (2016). "Diversity and biogeography of bathyal and abyssal seafloor bacteria." PLoS One **11**(1).
- Bik, E. M., E. K. Costello, A. D. Switzer, B. J. Callahan, S. P. Holmes, R. S. Wells, K. P. Carlin, E. D. Jensen, S. Venn-Watson and D. A. Relman (2016). "Marine mammals harbor unique microbiotas shaped by and yet distinct from the sea." Nature Communications **7**(1): 10516.
- Blackall, L. L., B. Wilson and M. J. van Oppen (2015). "Coral—the world's most diverse symbiotic ecosystem." Molecular Ecology **24**(21): 5330-5347.
- Blagodatskaya, E. and Y. Kuzyakov (2008). "Mechanisms of real and apparent priming effects and their dependence on soil microbial biomass and community structure: critical review." Biology and Fertility of Soils **45**(2): 115-131.
- Blair, N. E. and R. C. Aller (2012). "The Fate of Terrestrial Organic Carbon in the Marine Environment." Annual Review of Marine Science **4**(1): 401-423.
- Blaut, M., M. Collins, G. Welling, J. Dore, J. Van Loo and W. de Vos (2002). "Molecular biological methods for studying the gut microbiota: the EU human gut flora project." British Journal of Nutrition **87**(S2): S203-S211.
- Bletz, M. C., M. Vences, J. Sabino-Pinto, Y. Taguchi, N. Shimizu, K. Nishikawa and A. Kurabayashi (2017). "Cutaneous microbiota of the Japanese giant salamander (*Andrias japonicus*), a representative of an ancient amphibian clade." Hydrobiologia **795**(1): 153-167.
- Blod, C., N. Schlichting, S. Schülin, A. Suttikus, N. Peukert, C. S. Stingu, C. Hirsch, W. Elger, M. Lacher and U. Bühligen (2018). "The oral microbiome—the relevant reservoir for acute pediatric appendicitis?" International journal of colorectal disease **33**(2): 209-218.
- Bogan, B. W., W. R. Sullivan, K. J. Kayser, K. Derr, H. C. Aldrich and J. R. Paterek (2003). "Alkanindiges illinoisensis gen. nov., sp. nov., an obligately hydrocarbonoclastic, aerobic squalane-degrading bacterium isolated from oilfield soils." Journal of Medical Microbiology **53**(5): 1389-1395.
- Bolyen, E., J. R. Rideout, M. R. Dillon, N. A. Bokulich, C. C. Abnet, G. A. Al-Ghalith, H. Alexander, E. J. Alm, M. Arumugam and F. Asnicar (2019). "Reproducible, interactive, scalable and extensible microbiome data science using QIIME 2." Nature biotechnology **37**(8): 852-857.
- Borbón-García, A., A. Reyes, M. Vives-Flórez and S. Caballero (2017). "Captivity shapes the gut microbiota of Andean bears: insights into health surveillance." Frontiers in microbiology **8**: 1316.



- Bourne, D., Y. Iida, S. Uthicke and C. Smith-Keune (2008). "Changes in coral-associated microbial communities during a bleaching event." The ISME journal **2**(4): 350-363.
- Bourne, D. G., K. M. Morrow and N. S. Webster (2016). "Insights into the coral microbiome: underpinning the health and resilience of reef ecosystems." Annual Review of Microbiology **70**: 317-340.
- Boutin, S., C. Audet and N. Derome (2013). "Probiotic treatment by indigenous bacteria decreases mortality without disturbing the natural microbiota of *Salvelinus fontinalis*." Canadian Journal of Microbiology **59**(10): 662-670.
- Braun, M. S., E. Wang, S. Zimmermann, H. Wagner and M. Wink (2019). "*Kocuria tytonis* sp. nov., isolated from the uropygial gland of an American barn owl (*Tyto furcata*)."
- International journal of systematic and evolutionary microbiology **69**(2): 447-451.
- Brendel, P. J. and G. W. Luther, III (1995). "Development of a Gold Amalgam Voltammetric Microelectrode for the Determination of Dissolved Fe, Mn, O<sub>2</sub>, and S(-II) in Porewaters of Marine and Freshwater Sediments." Environmental Science & Technology **29**(3): 751-761.
- Brestoff, J. R. and D. Artis (2013). "Commensal bacteria at the interface of host metabolism and the immune system." Nature immunology **14**(7): 676-684.
- Bright, M. and S. Bulgheresi (2010). "A complex journey: transmission of microbial symbionts." Nature Reviews Microbiology **8**(3): 218-230.
- Bristow, G. and M. Tallefert (2008). "VOLTINT: A Matlab®-based program for semi-automated processing of geochemical data acquired by voltammetry." Computers & Geosciences **34**(2): 153-162.
- Bryant, J. A., C. Lamanna, H. Morlon, A. J. Kerkhoff, B. J. Enquist and J. L. Green (2008). "Microbes on mountainsides: contrasting elevational patterns of bacterial and plant diversity." Proceedings of the National Academy of Sciences **105**(Supplement 1): 11505-11511.
- Bukin, S. V., O. N. Pavlova, A. Y. Manakov, E. A. Kostyreva, S. M. Chernitsyna, E. V. Mamaeva, T. V. Pogodaeva and T. I. Zemskaya (2016). "The ability of microbial community of Lake Baikal bottom sediments associated with gas discharge to carry out the transformation of organic matter under thermobaric conditions." Frontiers in microbiology **7**: 690.
- Burdige, D. J. (1993). "The biogeochemistry of manganese and iron reduction in marine sediments." Earth-Science Reviews **35**(3): 249-284.
- Burke, C., P. Steinberg, D. Rusch, S. Kjelleberg and T. Thomas (2011). "Bacterial community assembly based on functional genes rather than species." Proceedings of the National Academy of Sciences **108**(34): 14288-14293.
- Burns, A. R., E. Miller, M. Agarwal, A. S. Rolig, K. Milligan-Myhre, S. Seredick, K. Guillemin and B. J. M. Bohannan (2017). "Interhost dispersal alters microbiome assembly and can overwhelm host innate immunity in an experimental zebrafish model." Proceedings of the National Academy of Sciences **114**(42): 11181-11186.
- Cai, W.-J., X. Hu, W.-J. Huang, M. C. Murrell, J. C. Lehrter, S. E. Lohrenz, W.-C. Chou, W. Zhai, J. T. Hollibaugh, Y. Wang, P. Zhao, X. Guo, K. Gundersen, M. Dai and G.-C. Gong (2011). "Acidification of subsurface coastal waters enhanced by eutrophication." Nature Geoscience **4**: 766.
- Callahan, B. J., P. J. McMurdie, M. J. Rosen, A. W. Han, A. J. A. Johnson and S. P. Holmes (2016). "DADA2: High-resolution sample inference from Illumina amplicon data." Nature Methods **13**(7): 581-583.

- Canfield, D. E. (1994). "Factors influencing organic matter preservation in marine sediments." Chemical Geology **114**(3-4): 315-329.
- Caporaso, J. G., C. L. Lauber, W. A. Walters, D. Berg-Lyons, C. A. Lozupone, P. J. Turnbaugh, N. Fierer and R. Knight (2011). "Global patterns of 16S rRNA diversity at a depth of millions of sequences per sample." Proceedings of the national academy of sciences **108**(Supplement 1): 4516-4522.
- Carding, S., K. Verbeke, D. T. Vipond, B. M. Corfe and L. J. Owen (2015). "Dysbiosis of the gut microbiota in disease." Microbial ecology in health and disease **26**(1): 26191.
- Cassir, N., S. Benamar and B. La Scola (2016). "Clostridium butyricum: from beneficial to a new emerging pathogen." Clinical Microbiology and Infection **22**(1): 37-45.
- Castelle, C. J., K. C. Wrighton, B. C. Thomas, L. A. Hug, C. T. Brown, M. J. Wilkins, K. R. Frischkorn, S. G. Tringe, A. Singh and L. M. Markillie (2015). "Genomic expansion of domain archaea highlights roles for organisms from new phyla in anaerobic carbon cycling." Current biology **25**(6): 690-701.
- Chapman, D. and S. Gruber (2002). "Habitat use by *Dasyatis americana* in a south-western Atlantic oceanic island." Bulletin of Marine Science(70): 947-952.
- Chaves, M. G. d., G. G. Z. Silva, R. Rossetto, R. A. Edwards, S. M. Tsai and A. A. Navarrete (2019). "Acidobacteria subgroups and their metabolic potential for carbon degradation in sugarcane soil amended with vinasse and nitrogen fertilizers." Frontiers in microbiology **10**: 1680.
- Chen, H., H. Wu, B. Yan, H. Zhao, F. Liu, H. Zhang, Q. Sheng, F. Miao and Z. Liang (2018). "Core Microbiome of Medicinal Plant *Salvia miltiorrhiza* Seed: A Rich Reservoir of Beneficial Microbes for Secondary Metabolism?" International Journal of Molecular Sciences **19**(3): 672.
- Chen, S., P. Wang, H. Liu, W. Xie, X. S. Wan, S.-J. Kao, T. J. Phelps and C. Zhang (2020). "Population dynamics of methanogens and methanotrophs along the salinity gradient in Pearl River Estuary: implications for methane metabolism." Applied Microbiology and Biotechnology **104**(3): 1331-1346.
- Chiarello, M., J.-C. Auguet, Y. Bettarel, C. Bouvier, T. Claverie, N. A. Graham, F. Rieuvilleneuve, E. Sucré, T. Bouvier and S. Villéger (2018). "Skin microbiome of coral reef fish is highly variable and driven by host phylogeny and diet." Microbiome **6**(1): 1-14.
- Chiarello, M., I. Paz-Vinas, C. Veyssière, F. Santoul, G. Loot, J. Ferriol and S. Boulêtreau (2019). "Environmental conditions and neutral processes shape the skin microbiome of European catfish (*Silurus glanis*) populations of Southwestern France." Environmental microbiology reports **11**(4): 605-614.
- Chiarello, M., S. Villéger, C. Bouvier, J. C. Auguet and T. Bouvier (2017). "Captive bottlenose dolphins and killer whales harbor a species-specific skin microbiota that varies among individuals." Scientific Reports **7**(1): 15269.
- Chintoan-Uta, C., T. Wisedchanwet, L. Glendinning, A. Bremner, A. Psifidi, L. Vervelde, K. Watson, M. Watson and M. P. Stevens (2020). "Role of cecal microbiota in the differential resistance of inbred chicken lines to colonization by *Campylobacter jejuni*." Applied and environmental microbiology **86**(7).
- Choi, E. J., H. C. Kwon, Y. C. Sohn and H. O. Yang (2010). "Kistimonas asteriae gen. nov., sp. nov., a gammaproteobacterium isolated from *Asterias amurensis*." International journal of systematic and evolutionary microbiology **60**(4): 938-943.
- Clarke, K. R. a. G., R.N. (2015). "PRIMER v7: User Manual/Tutoria." PRIMER-E Plymouth.

- Clayton, J. B., P. Vangay, H. Huang, T. Ward, B. M. Hillmann, G. A. Al-Ghalith, D. A. Travis, H. T. Long, B. Van Tuan and V. Van Minh (2016). "Captivity humanizes the primate microbiome." Proceedings of the National Academy of Sciences **113**(37): 10376-10381.
- Clooney, A. G., F. Fouhy, R. D. Sleator, A. O'Driscoll, C. Stanton, P. D. Cotter and M. J. Claesson (2016). "Comparing apples and oranges?: next generation sequencing and its impact on microbiome analysis." PloS one **11**(2): e0148028.
- Colvin DO, L. D. and C. Fagg (2020). "A Novel Case of Bacterial Meningitis in a Patient with Loeys-Dietz."
- Cooper, J., R. J. Crawford, M. S. De Villiers, B. M. Dyer, G. G. Hofmeyr and A. Jonker (2009). "Disease outbreaks among penguins at sub-Antarctic Marion Island: a conservation concern." Marine Ornithology **37**: 193-196.
- Costalonga, M. and M. C. Herzberg (2014). "The oral microbiome and the immunobiology of periodontal disease and caries." Immunology letters **162**(2): 22-38.
- Costello, E. K., C. L. Lauber, M. Hamady, N. Fierer, J. I. Gordon and R. Knight (2009). "Bacterial community variation in human body habitats across space and time." Science **326**(5960): 1694-1697.
- Costello, E. K., K. Stagaman, L. Dethlefsen, B. J. Bohannan and D. A. Relman (2012). "The application of ecological theory toward an understanding of the human microbiome." Science **336**(6086): 1255-1262.
- Cuevas-Zimbrón, E., J. C. Pérez-Jiménez and I. Méndez-Loeza (2011). "Spatial and seasonal variation in a target fishery for spotted eagle ray *Aetobatus narinari* in the southern Gulf of Mexico." Fisheries Science **77**(5): 723.
- Cytryn, E., J. van Rijn, A. Schramm, A. Gieseke, D. de Beer and D. Minz (2005). "Identification of bacteria potentially responsible for oxic and anoxic sulfide oxidation in biofilters of a recirculating mariculture system." Appl. Environ. Microbiol. **71**(10): 6134-6141.
- D'Agnesse, E., R. McLaughlin, M.-A. Lea, E. Soto, W. Smith and J. Bowman (2020). "Comparative microbial community analysis of fur seals and salmon aquaculture in Tasmania." Authorea Preprints.
- D'Hondt, S., B. B. Jørgensen, D. J. Miller, A. Batzke, R. Blake, B. A. Cragg, H. Cypionka, G. R. Dickens, T. Ferdelman and K.-U. Hinrichs (2004). "Distributions of microbial activities in deep subseafloor sediments." Science **306**(5705): 2216-2221.
- D'Hondt, S., S. Rutherford and A. J. Spivack (2002). "Metabolic activity of subsurface life in deep-sea sediments." Science **295**(5562): 2067-2070.
- Dagg, M., R. Benner, S. Lohrenz and D. Lawrence (2004). "Transformation of dissolved and particulate materials on continental shelves influenced by large rivers: plume processes." Continental Shelf Research **24**(7): 833-858.
- Dahlhausen, K. E., L. Doroud, A. J. Firl, A. Polkinghorne and J. A. Eisen (2018). "Characterization of shifts of koala (*Phascolarctos cinereus*) intestinal microbial communities associated with antibiotic treatment." PeerJ **6**: e4452.
- Daims, H., E. V. Lebedeva, P. Pjevac, P. Han, C. Herbold, M. Albertsen, N. Jehmlich, M. Palatinszky, J. Vierheilig and A. Bulaev (2015). "Complete nitrification by *Nitrospira* bacteria." Nature **528**(7583): 504.
- Danovaro, R., M. Molari, C. Corinaldesi and A. Dell'Anno (2016). "Macroecological drivers of archaea and bacteria in benthic deep-sea ecosystems." Science advances **2**(4): e1500961.
- Das, S., P. Lyla and S. A. Khan (2006). "Marine microbial diversity and ecology: importance and future perspectives." Current science: 1325-1335.

- De Vries, F. and A. Shade (2013). "Controls on soil microbial community stability under climate change." Frontiers in Microbiology **4**(265).
- Delpont, T. C., R. G. Harcourt, L. J. Beaumont, K. N. Webster and M. L. Power (2015). "Molecular detection of antibiotic-resistance determinants in *Escherichia coli* isolated from the endangered Australian sea lion (*Neophoca cinerea*)."  
Journal of wildlife diseases **51**(3): 555-563.
- Delpont, T. C., M. L. Power, R. G. Harcourt, K. N. Webster and S. G. Tetu (2016). "Colony location and captivity influence the gut microbial community composition of the Australian sea lion (*Neophoca cinerea*)."  
Appl. Environ. Microbiol. **82**(12): 3440-3449.
- Derome, N., J. Gauthier, S. Boutin and M. Llewellyn (2016). Bacterial opportunistic pathogens of fish. The Rasputin effect: When commensals and symbionts become parasitic, Springer: 81-108.
- Devadoss, P. (1984). "On the incidental fishery of skates and rays off Calicut." Indian Journal of Fisheries **31**(2): 285-292.
- Devereux, R., J. C. Lehrter, G. Cicchetti, D. L. Beddick, D. F. Yates, B. M. Jarvis, J. Aukamp and M. D. Hoglund (2019). "Spatially variable bioturbation and physical mixing drive the sedimentary biogeochemical seascape in the Louisiana continental shelf hypoxic zone." Biogeochemistry **143**(2): 151-169.
- Devereux, R., J. J. Mosher, T. A. Vishnivetskaya, S. D. Brown, D. L. Beddick, D. F. Yates and A. V. Palumbo (2015). "Changes in northern Gulf of Mexico sediment bacterial and archaeal communities exposed to hypoxia." Geobiology **13**(5): 478-493.
- Dewar, M. L., J. P. Arnould, T. R. Allnutt, T. Crowley, L. Krause, J. Reynolds, P. Dann and S. C. Smith (2017). "Microbiota of little penguins and short-tailed shearwaters during development." PLoS One **12**(8): e0183117.
- Dewar, M. L., J. P. Arnould, P. Dann, P. Trathan, R. Groscolas and S. Smith (2013). "Interspecific variations in the gastrointestinal microbiota in penguins." Microbiologyopen **2**(1): 195-204.
- Dhanasiri, A. K., L. Brunvold, M. F. Brinchmann, K. Korsnes, Ø. Bergh and V. Kiron (2011). "Changes in the intestinal microbiota of wild Atlantic cod *Gadus morhua* L. upon captive rearing." Microbial ecology **61**(1): 20-30.
- Dickson, A. G. (1993). "pH buffers for sea water media based on the total hydrogen ion concentration scale." Deep Sea Research Part I: Oceanographic Research Papers **40**(1): 107-118.
- Ding, Z., M. Cao, X. Zhu, G. Xu and R. Wang (2017). "Changes in the gut microbiome of the Chinese mitten crab (*Eriocheir sinensis*) in response to White spot syndrome virus (WSSV) infection." Journal of fish diseases **40**(11): 1561-1571.
- Dinsdale, E. A., R. A. Edwards, D. Hall, F. Angly, M. Breitbart, J. M. Brulc, M. Furlan, C. Desnues, M. Haynes and L. Li (2008). "Functional metagenomic profiling of nine biomes." Nature **452**(7187): 629-632.
- Doney, S. C., M. Ruckelshaus, J. E. Duffy, J. P. Barry, F. Chan, C. A. English, H. M. Galindo, J. M. Grebmeier, A. B. Hollowed and N. Knowlton (2011). "Climate change impacts on marine ecosystems."
- Dubick, J. (2000). Age and growth of the spotted eagle ray, *Aetobatus narinari* (Euphrasen, 1790), from southwest Puerto Rico with notes on its biology and life history., Univ. Puerto Rico.

- Dunne, J. A. and R. J. Williams (2009). "Cascading extinctions and community collapse in model food webs." Philosophical Transactions of the Royal Society B: Biological Sciences **364**(1524): 1711-1723.
- Durbin, A. M. and A. Teske (2011). "Microbial diversity and stratification of South Pacific abyssal marine sediments." Environmental Microbiology **13**(12): 3219-3234.
- Durbin, A. M. and A. Teske (2012). "Archaea in organic-lean and organic-rich marine subsurface sediments: an environmental gradient reflected in distinct phylogenetic lineages." Frontiers in microbiology **3**: 168.
- Eckburg, P. B., E. M. Bik, C. N. Bernstein, E. Purdom, L. Dethlefsen, M. Sargent, S. R. Gill, K. E. Nelson and D. A. Relman (2005). "Diversity of the human intestinal microbial flora." science **308**(5728): 1635-1638.
- Eichmiller, J. J., M. J. Hamilton, C. Staley, M. J. Sadowsky and P. W. Sorensen (2016). "Environment shapes the fecal microbiome of invasive carp species." Microbiome **4**(1): 44.
- Eigeland, K. A., J. M. Lanyon, D. J. Trott, D. Ouwerkerk, W. Blanshard, G. J. Milinovich, L.-M. Gulino, E. Martinez, S. Merson and A. V. Klieve (2012). "Bacterial community structure in the hindgut of wild and captive dugongs (Dugong dugon)." Aquatic Mammals **38**(4): 402.
- Ekman, E., H. Börjeson and N. Johansson (1999). "Flavobacterium psychrophilum in Baltic salmon *Salmo salar* brood fish and their offspring." Diseases of aquatic organisms **37**(3): 159-163.
- El Aidy, S. and M. Kleerebezem (2013). "Molecular signatures for the dynamic process of establishing intestinal host–microbial homeostasis: potential for disease diagnostics?" Current Opinion in Gastroenterology **29**(6): 621-627.
- Evans, C. C., K. J. LePard, J. W. Kwak, M. C. Stancukas, S. Laskowski, J. Dougherty, L. Moulton, A. Glawe, Y. Wang and V. Leone (2014). "Exercise prevents weight gain and alters the gut microbiota in a mouse model of high fat diet-induced obesity." PloS one **9**(3).
- Evans, P. N., D. H. Parks, G. L. Chadwick, S. J. Robbins, V. J. Orphan, S. D. Golding and G. W. Tyson (2015). "Methane metabolism in the archaeal phylum Bathyarchaeota revealed by genome-centric metagenomics." Science **350**(6259): 434-438.
- Fackelmann, G. and S. Sommer (2019). "Microplastics and the gut microbiome: how chronically exposed species may suffer from gut dysbiosis." Marine pollution bulletin **143**: 193-203.
- Faith, D. P. (1992). "Conservation evaluation and phylogenetic diversity." Biological conservation **61**(1): 1-10.
- Faith, J. J., P. P. Ahern, V. K. Ridaura, J. Cheng and J. I. Gordon (2014). "Identifying gut microbe–host phenotype relationships using combinatorial communities in gnotobiotic mice." Science translational medicine **6**(220): 220ra211-220ra211.
- Faith, J. J., F. E. Rey, D. O'donnell, M. Karlsson, N. P. McNulty, G. Kallstrom, A. L. Goodman and J. I. Gordon (2010). "Creating and characterizing communities of human gut microbes in gnotobiotic mice." The ISME journal **4**(9): 1094-1098.
- Fan, X. and P. Xing (2016). "Differences in the composition of archaeal communities in sediments from contrasting zones of Lake Taihu." Frontiers in microbiology **7**: 1510.
- Fenchel, T. and B. J. Finlay (2004). "The ubiquity of small species: patterns of local and global diversity." Bioscience **54**(8): 777-784.
- Ferretti, F., B. Worm, G. L. Britten, M. R. Heithaus and H. K. Lotze (2010). "Patterns and ecosystem consequences of shark declines in the ocean." Ecology letters **13**(8): 1055-1071.

- Finlay, B. J. (2002). "Global dispersal of free-living microbial eukaryote species." Science **296**(5570): 1061-1063.
- Finlay, B. J. and K. J. Clarke (1999). "Ubiquitous dispersal of microbial species." Nature **400**(6747): 828-828.
- Flechas, S. V., A. Blasco-Zúñiga, A. Merino-Viteri, V. Ramírez-Castañeda, M. Rivera and A. Amézquita (2017). "The effect of captivity on the skin microbial symbionts in three *Atelopus* species from the lowlands of Colombia and Ecuador." PeerJ **5**: e3594.
- Flint, H. J., K. P. Scott, P. Louis and S. H. Duncan (2012). "The role of the gut microbiota in nutrition and health." Nature reviews Gastroenterology & hepatology **9**(10): 577.
- Forsberg, C. (1989). "IMPORTANCE OF SEDIMENTS IN UNDERSTANDING NUTRIENT CYCLINGS IN LAKES." Hydrobiologia **176**: 263-277.
- Foster, K. R., J. Schluter, K. Z. Coyte and S. Rakoff-Nahoum (2017). "The evolution of the host microbiome as an ecosystem on a leash." Nature **548**(7665): 43-51.
- Franz, B., H. Lichtenberg, C. Dahl, J. Hormes and A. Prange (2009). Utilization of elemental sulfur by different phototrophic sulfur bacteria (Chromatiaceae, Ectothiorhodospiraceae): A sulfur K-edge XANES spectroscopy study. Journal of Physics: Conference Series, IOP Publishing.
- Franzosa, E. A., X. C. Morgan, N. Segata, L. Waldron, J. Reyes, A. M. Earl, G. Giannoukos, M. R. Boylan, D. Ciulla and D. Gevers (2014). "Relating the metatranscriptome and metagenome of the human gut." Proceedings of the National Academy of Sciences **111**(22): E2329-E2338.
- Fredrickson, J. K. and Y. A. Gorby (1996). "Environmental processes mediated by iron-reducing bacteria." Current opinion in biotechnology **7**(3): 287-294.
- Frieler, K., M. Meinshausen, A. Golly, M. Mengel, K. Lebek, S. D. Donner and O. Hoegh-Guldberg (2013). "Limiting global warming to 2 degrees C is unlikely to save most coral reefs." Nature Climate Change **3**(2): 165-170.
- Froelich, P. N., G. P. Klinkhammer, M. L. Bender, N. A. Luedtke, G. R. Heath, D. Cullen, P. Dauphin, D. Hammond, B. Hartman and V. Maynard (1979). "Early oxidation of organic matter in pelagic sediments of the eastern equatorial Atlantic: suboxic diagenesis." Geochimica et Cosmochimica Acta **43**(7): 1075-1090.
- Fuentes, S., B. Barra, J. G. Caporaso and M. Seeger (2016). "From rare to dominant: a fine-tuned soil bacterial bloom during petroleum hydrocarbon bioremediation." Applied and environmental microbiology **82**(3): 888-896.
- Fukami, T., H. J. Beaumont, X.-X. Zhang and P. B. Rainey (2007). "Immigration history controls diversification in experimental adaptive radiation." Nature **446**(7134): 436-439.
- Gao, Y.-M., K.-S. Zou, L. Zhou, X.-D. Huang, Y.-Y. Li, X.-Y. Gao, X. Chen and X.-Y. Zhang (2020). "Deep Insights into Gut Microbiota in Four Carnivorous Coral Reef Fishes from the South China Sea." Microorganisms **8**(3): 426.
- Garren, M. and F. Azam (2012). "Corals shed bacteria as a potential mechanism of resilience to organic matter enrichment." The ISME journal **6**(6): 1159-1165.
- Gibbons, R., S. Socransky, W. De Araujo and J. Van Houte (1964). "Studies of the predominant cultivable microbiota of dental plaque." Archives of oral biology **9**(3): 365-370.
- Givens, C. E., B. Ransom, N. Bano and J. T. Hollibaugh (2015). "Comparison of the gut microbiomes of 12 bony fish and 3 shark species." Marine Ecology Progress Series **518**: 209-223.

- Glud, R. N. (2008). "Oxygen dynamics of marine sediments." Marine Biology Research **4**(4): 243-289.
- Glud, R. N., B. Thamdrup, H. Stahl, F. Wenzhoefer, A. Glud, H. Nomaki, K. Oguri, N. P. Revsbech and H. Kitazato (2009). "Nitrogen cycling in a deep ocean margin sediment (Sagami Bay, Japan)." Limnology and Oceanography **54**(3): 723-734.
- Godoy-Vitorino, F., A. Rodriguez-Hilario, A. L. Alves, F. Gonçalves, B. Cabrera-Colon, C. S. Mesquita, P. Soares-Castro, M. Ferreira, A. Marçalo and J. Vingada (2017). "The microbiome of a striped dolphin (*Stenella coeruleoalba*) stranded in Portugal." Research in microbiology **168**(1): 85-93.
- Gomez de Agüero, M., S. C. Ganai-Vonarburg, T. Fuhrer, S. Rupp, Y. Uchimura, H. Li, A. Steinert, M. Heikenwalder, S. Hapfelmeier, U. Sauer, K. D. McCoy and A. J. Macpherson (2016). "The maternal microbiota drives early postnatal innate immune development." Science **351**(6279): 1296-1302.
- Goodman, A. L., G. Kallstrom, J. J. Faith, A. Reyes, A. Moore, G. Dantas and J. I. Gordon (2011). "Extensive personal human gut microbiota culture collections characterized and manipulated in gnotobiotic mice." Proceedings of the National Academy of Sciences **108**(15): 6252-6257.
- Gosalbes, M. J., A. Durbán, M. Pignatelli, J. J. Abellan, N. Jiménez-Hernández, A. E. Pérez-Cobas, A. Latorre and A. Moya (2011). "Metatranscriptomic approach to analyze the functional human gut microbiota." PloS one **6**(3): e17447.
- Green, J. and B. J. Bohannan (2006). "Spatial scaling of microbial biodiversity." Trends in ecology & evolution **21**(9): 501-507.
- Green, J. L., A. J. Holmes, M. Westoby, I. Oliver, D. Briscoe, M. Dangerfield, M. Gillings and A. J. Beattie (2004). "Spatial scaling of microbial eukaryote diversity." Nature **432**(7018): 747-750.
- Grégoire, M. and J. Friedrich (2004). "Nitrogen budget of the northwestern Black Sea shelf inferred from modeling studies and in situ benthic measurements." Marine Ecology Progress Series **270**: 15-39.
- Griffin, J. S. and G. F. Wells (2017). "Regional synchrony in full-scale activated sludge bioreactors due to deterministic microbial community assembly." The ISME journal **11**(2): 500-511.
- Grimes, D. J., P. Brayton, R. R. Colwell and S. H. Gruber (1985). "Vibrios as Autochthonous Flora of Neritic Sharks." Systematic and Applied Microbiology **6**(2): 221-226.
- Grond, K., B. K. Sandercock, A. Jumpponen and L. H. Zeglin (2018). "The avian gut microbiota: community, physiology and function in wild birds." Journal of Avian Biology **49**(11): e01788.
- Grosser, S., J. Sauer, A. J. Paijmans, B. A. Caspers, J. Forcada, J. B. W. Wolf and J. I. Hoffman (2019). "Fur seal microbiota are shaped by the social and physical environment, show mother-offspring similarities and are associated with host genetic quality." Molecular Ecology **28**(9): 2406-2422.
- Groussin, M., F. Mazel, J. G. Sanders, C. S. Smillie, S. Lavergne, W. Thuiller and E. J. Alm (2017). "Unraveling the processes shaping mammalian gut microbiomes over evolutionary time." Nature Communications **8**(1): 1-12.
- Hale, V. L., C. L. Tan, K. Niu, Y. Yang, R. Knight, Q. Zhang, D. Cui and K. R. Amato (2018). "Diet versus phylogeny: a comparison of gut microbiota in captive colobine monkey species." Microbial ecology **75**(2): 515-527.

- Hall, P. J. and R. C. Aller (1992). "Rapid, small-volume, flow injection analysis for SCO<sub>2</sub>, and NH<sub>4</sub><sup>+</sup> in marine and freshwaters." Limnology and Oceanography **37**(5): 1113-1119.
- Hao, Y.-Q., X.-F. Zhao and D.-Y. Zhang (2016). "Field experimental evidence that stochastic processes predominate in the initial assembly of bacterial communities." Environmental Microbiology **18**(6): 1730-1739.
- Hartnett, H. E., R. G. Keil, J. I. Hedges and A. H. Devol (1998). "Influence of oxygen exposure time on organic carbon preservation in continental margin sediments." Nature **391**(6667): 572-575.
- Hay, M. E., D. S. Beatty and F. J. Stewart (2017). Chemical Ecology: The Language of Microbiomes. The Chemistry of Microbiomes: Proceedings of a Seminar Series, National Academies Press.
- He, Z., S. Geng, C. Cai, S. Liu, Y. Liu, Y. Pan, L. Lou, P. Zheng, X. Xu and B. Hu (2015). "Anaerobic oxidation of methane coupled to nitrite reduction by halophilic marine NC10 bacteria." Appl. Environ. Microbiol. **81**(16): 5538-5545.
- Heijtz, R. D., S. Wang, F. Anuar, Y. Qian, B. Björkholm, A. Samuelsson, M. L. Hibberd, H. Forssberg and S. Pettersson (2011). "Normal gut microbiota modulates brain development and behavior." Proceedings of the National Academy of Sciences **108**(7): 3047-3052.
- Hernandez-Agreda, A., R. D. Gates and T. D. Ainsworth (2017). "Defining the core microbiome in corals' microbial soup." Trends in Microbiology **25**(2): 125-140.
- Hersman, L., P. Maurice and G. Sposito (1996). "Iron acquisition from hydrous Fe (III)-oxides by an aerobic *Pseudomonas* sp." Chemical Geology **132**(1-4): 25-31.
- Hess, S., A. S. Wenger, T. D. Ainsworth and J. L. Rummer (2015). "Exposure of clownfish larvae to suspended sediment levels found on the Great Barrier Reef: impacts on gill structure and microbiome." Scientific reports **5**: 10561.
- Hinger, I., C. Pelikan and M. Mußmann (2019). Role of the ubiquitous bacterial family Woeseiaceae for N<sub>2</sub>O production in marine sediments. Geophysical Research Abstracts.
- Hinrichs, K.-U., J. M. Hayes, S. P. Sylva, P. G. Brewer and E. F. DeLong (1999). "Methane-consuming archaeobacteria in marine sediments." Nature **398**(6730): 802-805.
- Hird, S. M. (2017). "Evolutionary biology needs wild microbiomes." Frontiers in microbiology **8**: 725.
- Hird, S. M., B. C. Carstens, S. W. Cardiff, D. L. Dittmann and R. T. Brumfield (2014). "Sampling locality is more detectable than taxonomy or ecology in the gut microbiota of the brood-parasitic Brown-headed Cowbird (*Molothrus ater*)." PeerJ **2**: e321.
- Hird, S. M., C. Sánchez, B. C. Carstens and R. T. Brumfield (2015). "Comparative gut microbiota of 59 neotropical bird species." Frontiers in microbiology **6**: 1403.
- Hooper, L. V., D. R. Littman and A. J. Macpherson (2012). "Interactions Between the Microbiota and the Immune System." Science **336**(6086): 1268-1273.
- Horner-Devine, M. C. and B. J. Bohannan (2006). "Phylogenetic clustering and overdispersion in bacterial communities." Ecology **87**(sp7): S100-S108.
- Horner-Devine, M. C., M. Lage, J. B. Hughes and B. J. Bohannan (2004). "A taxa–area relationship for bacteria." Nature **432**(7018): 750-753.
- Hubbell, S. P. (2001). The unified neutral theory of biodiversity and biogeography (MPB-32), Princeton University Press.
- Huber, J. A., D. B. Mark Welch, H. G. Morrison, S. M. Huse, P. R. Neal, D. A. Butterfield and M. L. Sogin (2007). "Microbial Population Structures in the Deep Marine Biosphere." Science **318**(5847): 97.



- Hubert, C., A. Loy, M. Nickel, C. Arnosti, C. Baranyi, V. Brüchert, T. Ferdelman, K. Finster, F. M. Christensen, J. Rosa de Rezende, V. Vandieken and B. B. Jørgensen (2009). "A Constant Flux of Diverse Thermophilic Bacteria into the Cold Arctic Seabed." Science **325**(5947): 1541-1544.
- Hughes, T. P., J. T. Kerry, M. Álvarez-Noriega, J. G. Álvarez-Romero, K. D. Anderson, A. H. Baird, R. C. Babcock, M. Beger, D. R. Bellwood and R. Berkelmans (2017). "Global warming and recurrent mass bleaching of corals." Nature **543**(7645): 373-377.
- Hughes, T. P., J. T. Kerry, A. H. Baird, S. R. Connolly, A. Dietzel, C. M. Eakin, S. F. Heron, A. S. Hoey, M. O. Hoogenboom and G. Liu (2018). "Global warming transforms coral reef assemblages." Nature **556**(7702): 492-496.
- Hunter, E. M., H. J. Mills and J. E. Kostka (2006). "Microbial Community Diversity Associated with Carbon and Nitrogen Cycling in Permeable Shelf Sediments." Applied and Environmental Microbiology **72**(9): 5689-5701.
- Hurtado-Ortiz, R., A. Nazimoudine, A. Criscuolo, P. Hugon, D. Mornico, S. Brisse, C. Bizet and D. Clermont (2017). "Psychrobacter pasteurii and Psychrobacter piechaudii sp. nov., two novel species within the genus Psychrobacter." International journal of systematic and evolutionary microbiology **67**(9): 3192-3197.
- Huttenhower, C., D. Gevers, R. Knight, S. Abubucker, J. H. Badger, A. T. Chinwalla, H. H. Creasy, A. M. Earl, M. G. FitzGerald and R. S. Fulton (2012). "Structure, function and diversity of the healthy human microbiome." nature **486**(7402): 207.
- Hyde, E. R., J. A. Navas-Molina, S. J. Song, J. G. Kueneman, G. Ackermann, C. Cardona, G. Humphrey, D. Boyer, T. Weaver and J. R. Mendelson (2016). "The oral and skin microbiomes of captive komodo dragons are significantly shared with their habitat." Msystems **1**(4).
- Ijaz, U. Z., L. Sivaloganathan, A. McKenna, A. Richmond, C. Kelly, M. Linton, A. C. Stratakis, U. Lavery, A. Elmi and B. W. Wren (2018). "Comprehensive longitudinal microbiome analysis of the chicken cecum reveals a shift from competitive to environmental drivers and a window of opportunity for Campylobacter." Frontiers in microbiology **9**: 2452.
- Imhoff, J. F. and J. Wiese (2014). The order Kiloniellales, Springer.
- IUCN. (2019). "The IUCN Red List of Threatened Species."
- Jahnke, R. A., C. E. Reimers and D. B. Craven (1990). "Intensification of recycling of organic matter at the sea floor near ocean margins." Nature **348**(6296): 50-54.
- Jenkins, C. N., S. L. Pimm and L. N. Joppa (2013). "Global patterns of terrestrial vertebrate diversity and conservation." Proceedings of the National Academy of Sciences **110**(28): E2602-E2610.
- Jia, T., S. Zhao, K. Knott, X. Li, Y. Liu, Y. Li, Y. Chen, M. Yang, Y. Lu and J. Wu (2018). "The gastrointestinal tract microbiota of northern white-cheeked gibbons (Nomascus leucogenys) varies with age and captive condition." Scientific reports **8**(1): 1-14.
- Jiang, H.-Y., J.-E. Ma, J. Li, X.-J. Zhang, L.-M. Li, N. He, H.-Y. Liu, S.-Y. Luo, Z.-J. Wu and R.-C. Han (2017). "Diets alter the gut microbiome of crocodile lizards." Frontiers in Microbiology **8**: 2073.
- Jiang, H.-Y., J.-E. Ma, J. Li, X.-J. Zhang, L.-M. Li, N. He, H.-Y. Liu, S.-Y. Luo, Z.-J. Wu, R.-C. Han and J.-P. Chen (2017). "Diets Alter the Gut Microbiome of Crocodile Lizards." Frontiers in Microbiology **8**(2073).

- Jiménez, R. R. and S. Sommer (2017). "The amphibian microbiome: natural range of variation, pathogenic dysbiosis, and role in conservation." Biodiversity and Conservation **26**(4): 763-786.
- Johnson, K. S., F. P. Chavez and G. E. Friederich (1999). "Continental-shelf sediment as a primary source of iron for coastal phytoplankton." Nature **398**(6729): 697-700.
- Jørgensen, B. B. (1982). "Mineralization of organic matter in the sea bed—the role of sulphate reduction." Nature **296**(5858): 643-645.
- Julies Elsabé, M., V. Brüchert and B. M. Fuchs (2012). "Vertical shifts in the microbial community structure of organic-rich Namibian shelf sediments." African Journal of Microbiology Research **6**(17): 3887-3897.
- Jung, H. S., S. E. Jeong, K. H. Kim and C. O. Jeon (2017). "Parahaliea aestuarii sp. nov., isolated from the Asan Bay estuary." International journal of systematic and evolutionary microbiology **67**(5): 1431-1435.
- Kamada, N., G. Y. Chen, N. Inohara and G. Núñez (2013). "Control of pathogens and pathobionts by the gut microbiota." Nature immunology **14**(7): 685.
- Kato, I., A. Vasquez, G. Moyerbrailean, S. Land, Z. Djuric, J. Sun, H.-S. Lin and J. L. Ram (2017). "Nutritional Correlates of Human Oral Microbiome." Journal of the American College of Nutrition **36**(2): 88-98.
- Katoh, K., K. Misawa, K. i. Kuma and T. Miyata (2002). "MAFFT: a novel method for rapid multiple sequence alignment based on fast Fourier transform." Nucleic acids research **30**(14): 3059-3066.
- Kelly, J. R., P. J. Kennedy, J. F. Cryan, T. G. Dinan, G. Clarke and N. P. Hyland (2015). "Breaking down the barriers: the gut microbiome, intestinal permeability and stress-related psychiatric disorders." Frontiers in cellular neuroscience **9**: 392.
- Kelly, L. W., G. J. Williams, K. L. Barott, C. A. Carlson, E. A. Dinsdale, R. A. Edwards, A. F. Haas, M. Haynes, Y. W. Lim and T. McDole (2014). "Local genomic adaptation of coral reef-associated microbiomes to gradients of natural variability and anthropogenic stressors." Proceedings of the National Academy of Sciences **111**(28): 10227-10232.
- Khachatryan, Z. A., Z. A. Ktsoyan, G. P. Manukyan, D. Kelly, K. A. Ghazaryan and R. I. Aminov (2008). "Predominant role of host genetics in controlling the composition of gut microbiota." PloS one **3**(8): e3064.
- Khan, R. U. and S. Naz (2013). "The applications of probiotics in poultry production." World's Poultry Science Journal **69**(3): 621-632.
- Kim, D. H., J. Brunt and B. Austin (2007). "Microbial diversity of intestinal contents and mucus in rainbow trout (*Oncorhynchus mykiss*)." Journal of applied microbiology **102**(6): 1654-1664.
- Kim, K. K., J.-S. Lee and D. A. Stevens (2013). "Microbiology and epidemiology of *Halomonas* species." Future microbiology **8**(12): 1559-1573.
- Kim, Y.-S., E. S. Noh, D.-E. Lee and K.-H. Kim (2017). "Complete genome of a denitrifying *Halioglobus* sp. RR3-57 isolated from a seawater recirculating aquaculture system." 미생물학회지 **53**(1): 58-60.
- King, A. J., K. R. Freeman, K. F. McCormick, R. C. Lynch, C. Lozupone, R. Knight and S. K. Schmidt (2010). "Biogeography and habitat modelling of high-alpine bacteria." Nature communications **1**(1): 1-6.
- King, D. P., M. C. Hure, T. Goldstein, B. M. Aldridge, F. M. Gulland, J. T. Saliki, E. L. Buckles, L. J. Lowenstine and J. L. Stott (2002). "Otarine herpesvirus-1: a novel gammaherpesvirus

- associated with urogenital carcinoma in California sea lions (*Zalophus californianus*).  
Veterinary microbiology **86**(1-2): 131-137.
- Klitgaard, K., A. F. Bretó, M. Boye and T. K. Jensen (2013). "Targeting the treponemal microbiome of digital dermatitis infections by high-resolution phylogenetic analyses and comparison with fluorescent in situ hybridization." Journal of clinical microbiology **51**(7): 2212-2219.
- Knight, R., A. Vrbanac, B. C. Taylor, A. Aksenov, C. Callewaert, J. Debelius, A. Gonzalez, T. Kosciulek, L.-I. McCall, D. McDonald, A. V. Melnik, J. T. Morton, J. Navas, R. A. Quinn, J. G. Sanders, A. D. Swafford, L. R. Thompson, A. Tripathi, Z. Z. Xu, J. R. Zaneveld, Q. Zhu, J. G. Caporaso and P. C. Dorrestein (2018). "Best practices for analysing microbiomes." Nature Reviews Microbiology **16**(7): 410-422.
- Koenig, J. E., A. Spor, N. Scalfone, A. D. Fricker, J. Stombaugh, R. Knight, L. T. Angenent and R. E. Ley (2011). "Succession of microbial consortia in the developing infant gut microbiome." Proceedings of the National Academy of Sciences **108**(Supplement 1): 4578-4585.
- Koeth, R. A., Z. Wang, B. S. Levison, J. A. Buffa, E. Org, B. T. Sheehy, E. B. Britt, X. Fu, Y. Wu and L. Li (2013). "Intestinal microbiota metabolism of L-carnitine, a nutrient in red meat, promotes atherosclerosis." Nature medicine **19**(5): 576-585.
- Koren, O., A. Spor, J. Felin, F. Fåk, J. Stombaugh, V. Tremaroli, C. J. Behre, R. Knight, B. Fagerberg and R. E. Ley (2011). "Human oral, gut, and plaque microbiota in patients with atherosclerosis." Proceedings of the National Academy of Sciences **108**(Supplement 1): 4592-4598.
- Kowalchuk, G. A., S. E. Jones and L. L. Blackall (2008). "Microbes orchestrate life on Earth." The ISME Journal **2**(8): 795-796.
- Kozich, J. J., S. L. Westcott, N. T. Baxter, S. K. Highlander and P. D. Schloss (2013). "Development of a Dual-Index Sequencing Strategy and Curation Pipeline for Analyzing Amplicon Sequence Data on the MiSeq Illumina Sequencing Platform." Applied and Environmental Microbiology **79**(17): 5112-5120.
- Kropáčková, L., M. Těšický, T. Albrecht, J. Kubovčíak, D. Čížková, O. Tomášek, J. F. Martin, L. Bobek, T. Králová and P. Procházka (2017). "Codiversification of gastrointestinal microbiota and phylogeny in passerines is not explained by ecological divergence." Molecular Ecology **26**(19): 5292-5304.
- Krotman, Y., T. M. Yergaliyev, R. A. Shani, Y. Avrahami and A. Szitenberg (2020). "Dissecting the factors shaping fish skin microbiomes in a heterogeneous inland water system." Microbiome **8**(1): 9.
- Kubasova, T., L. Davidova-Gerzova, E. Merlot, M. Medvecký, O. Polansky, D. Gardan-Salmon, H. Quesnel and I. Rychlik (2017). "Housing systems influence gut microbiota composition of sows but not of their piglets." PLoS One **12**(1).
- Kueneman, J. G., D. C. Woodhams, R. Harris, H. M. Archer, R. Knight and V. J. McKenzie (2016). "Probiotic treatment restores protection against lethal fungal infection lost during amphibian captivity." Proceedings of the Royal Society B: Biological Sciences **283**(1839): 20161553.
- Kümmel, S., F.-A. Herbst, A. Bahr, M. Duarte, D. H. Pieper, N. Jehmlich, J. Seifert, M. von Bergen, P. Bombach and H. H. Richnow (2015). "Anaerobic naphthalene degradation by sulfate-reducing Desulfobacteraceae from various anoxic aquifers." FEMS microbiology ecology **91**(3).

- Kviatkovski, I. and D. Minz (2015). "A member of the Rhodobacteraceae promotes initial biofilm formation via the secretion of extracellular factor/s." Aquatic Microbial Ecology **75**.
- Lange, K., M. Buerger, A. Stallmach and T. Bruns (2016). "Effects of Antibiotics on Gut Microbiota." Digestive Diseases **34**(3): 260-268.
- Lazar, C. S., B. J. Baker, K. W. Seitz and A. P. Teske (2017). "Genomic reconstruction of multiple lineages of uncultured benthic archaea suggests distinct biogeochemical roles and ecological niches." The ISME journal **11**(5): 1118-1129.
- LeaMaster, B., W. Walsh, J. Brock and R. Fujioka (1997). "Cold stress-induced changes in the aerobic heterotrophic gastrointestinal tract bacterial flora of red hybrid tilapia." Journal of Fish Biology **50**(4): 770-780.
- Learman, D. R., M. W. Henson, J. C. Thrash, B. Temperton, P. M. Brannock, S. R. Santos, A. R. Mahon and K. M. Halanych (2016). "Biogeochemical and microbial variation across 5500 km of Antarctic surface sediment implicates organic matter as a driver of benthic community structure." Frontiers in Microbiology **7**: 284.
- Lee, J., N.-R. Shin, H.-W. Lee, S. W. Roh, M.-S. Kim, Y.-O. Kim and J.-W. Bae (2012). "Kistimonas scapharcae sp. nov., isolated from a dead ark clam (*Scapharca broughtonii*), and emended description of the genus *Kistimonas*." International journal of systematic and evolutionary microbiology **62**(12): 2865-2869.
- Leibold, M. A., M. Holyoak, N. Mouquet, P. Amarasekare, J. M. Chase, M. F. Hoopes, R. D. Holt, J. B. Shurin, R. Law and D. Tilman (2004). "The metacommunity concept: a framework for multi-scale community ecology." Ecology letters **7**(7): 601-613.
- Lennon, J. T. and S. E. Jones (2011). "Microbial seed banks: the ecological and evolutionary implications of dormancy." Nature reviews microbiology **9**(2): 119-130.
- Levy, M., C. A. Thaiss and E. Elinav (2015). "Metagenomic cross-talk: the regulatory interplay between immunogenomics and the microbiome." Genome Medicine **7**(1): 120.
- Lewis, J. D., E. Z. Chen, R. N. Baldassano, A. R. Otley, A. M. Griffiths, D. Lee, K. Bittinger, A. Bailey, E. S. Friedman and C. Hoffmann (2015). "Inflammation, antibiotics, and diet as environmental stressors of the gut microbiome in pediatric Crohn's disease." Cell host & microbe **18**(4): 489-500.
- Ley, R. E., D. A. Peterson and J. I. Gordon (2006). "Ecological and evolutionary forces shaping microbial diversity in the human intestine." Cell **124**(4): 837-848.
- Li, L. and Z. Ma (2016). "Testing the Neutral Theory of Biodiversity with Human Microbiome Datasets." Scientific Reports **6**(1): 31448.
- Libralato, S., V. Christensen and D. Pauly (2006). "A method for identifying keystone species in food web models." ecological modelling **195**(3-4): 153-171.
- Lierz, M., N. Hagen, S. Hernandez-Divers and H. Hafez (2008). "Occurrence of mycoplasmas in free-ranging birds of prey in Germany." Journal of Wildlife Diseases **44**(4): 845-850.
- Lim, S. J., B. G. Davis, D. E. Gill, J. Walton, E. Nachman, A. S. Engel, L. C. Anderson and B. J. Campbell (2019). "Taxonomic and functional heterogeneity of the gill microbiome in a symbiotic coastal mangrove lucinid species." The ISME journal **13**(4): 902-920.
- Lin, B., M. Braster, B. M. van Breukelen, H. W. van Verseveld, H. V. Westerhoff and W. F. Röling (2005). "Geobacteraceae community composition is related to hydrochemistry and biodegradation in an iron-reducing aquifer polluted by a neighboring landfill." Appl. Environ. Microbiol. **71**(10): 5983-5991.
- Lin, H. and M. Taillefert (2014). "Key geochemical factors regulating Mn(IV)-catalyzed anaerobic nitrification in coastal marine sediments." Geochimica et Cosmochimica Acta **133**: 17-33.

- Lindström, E. S. and Ö. Östman (2011). "The importance of dispersal for bacterial community composition and functioning." PloS one **6**(10).
- Lipsewiers, Y. A. (2017). Role of chemolithoautotrophic microorganisms involved in nitrogen and sulfur cycling in coastal marine sediments, Utrecht University.
- Littman, R., B. L. Willis and D. G. Bourne (2011). "Metagenomic analysis of the coral holobiont during a natural bleaching event on the Great Barrier Reef." Environmental Microbiology Reports **3**(6): 651-660.
- Liu, G., C. M. Tang and R. M. Exley (2015). "Non-pathogenic Neisseria: members of an abundant, multi-habitat, diverse genus." Microbiology **161**(7): 1297-1312.
- Liu, P. and R. Conrad (2017). "Syntrophobacteraceae-affiliated species are major propionate-degrading sulfate reducers in paddy soil." Environmental microbiology **19**(4): 1669-1686.
- Liu, P., M. Klose and R. Conrad (2018). "Temperature effects on structure and function of the methanogenic microbial communities in two paddy soils and one desert soil." Soil Biology and Biochemistry **124**: 236-244.
- Lloyd, K. G., M. J. Alperin and A. Teske (2011). "Environmental evidence for net methane production and oxidation in putative ANaerobic MEthanotrophic (ANME) archaea." Environmental Microbiology **13**(9): 2548-2564.
- Lloyd, K. G., L. Schreiber, D. G. Petersen, K. U. Kjeldsen, M. A. Lever, A. D. Steen, R. Stepanauskas, M. Richter, S. Kleindienst and S. Lenk (2013). "Predominant archaea in marine sediments degrade detrital proteins." Nature **496**(7444): 215-218.
- Locey, K. J. (2010). "Synthesizing traditional biogeography with microbial ecology: the importance of dormancy." Journal of biogeography **37**(10): 1835-1841.
- Louca, S., L. W. Parfrey and M. Doebeli (2016). "Decoupling function and taxonomy in the global ocean microbiome." Science **353**(6305): 1272-1277.
- Loudon, A. H., D. C. Woodhams, L. W. Parfrey, H. Archer, R. Knight, V. McKenzie and R. N. Harris (2014). "Microbial community dynamics and effect of environmental microbial reservoirs on red-backed salamanders (*Plethodon cinereus*)." The ISME journal **8**(4): 830-840.
- Love, M. I., W. Huber and S. Anders (2014). "Moderated estimation of fold change and dispersion for RNA-seq data with DESeq2." Genome biology **15**(12): 550.
- Lozupone, C. A., M. Hamady, S. T. Kelley and R. Knight (2007). "Quantitative and qualitative  $\beta$  diversity measures lead to different insights into factors that structure microbial communities." Applied and environmental microbiology **73**(5): 1576-1585.
- Lozupone, C. A. and R. Knight (2007). "Global patterns in bacterial diversity." Proceedings of the National Academy of Sciences **104**(27): 11436-11440.
- Lu, H.-F., Z.-G. Ren, A. Li, H. Zhang, S.-Y. Xu, J.-W. Jiang, L. Zhou, Q. Ling, B.-H. Wang, G.-Y. Cui, X.-H. Chen, S.-S. Zheng and L.-J. Li (2019). "Fecal Microbiome Data Distinguish Liver Recipients With Normal and Abnormal Liver Function From Healthy Controls." Frontiers in Microbiology **10**(1518).
- Lucas, F. S. and P. Heeb (2005). "Environmental factors shape cloacal bacterial assemblages in great tit *Parus major* and blue tit *P. caeruleus* nestlings." Journal of Avian Biology **36**(6): 510-516.
- Lucas, F. S., B. Moureau, V. Jourdie and P. Heeb (2005). "Brood size modifications affect plumage bacterial assemblages of European starlings." Molecular Ecology **14**(2): 639-646.

- Luther, G. W. (2005). "Manganese(II) Oxidation and Mn(IV) Reduction in the Environment—Two One-Electron Transfer Steps Versus a Single Two-Electron Step." Geomicrobiology Journal **22**: 195-203.
- Luther, G. W., B. T. Glazer, S. Ma, R. E. Trouwborst, T. S. Moore, E. Metzger, C. Kraiya, T. J. Waite, G. Druschel, B. Sundby, M. Taillefert, D. B. Nuzzio, T. M. Shank, B. L. Lewis and P. J. Brendel (2008). "Use of voltammetric solid-state (micro)electrodes for studying biogeochemical processes: Laboratory measurements to real time measurements with an in situ electrochemical analyzer (ISEA)." Marine Chemistry **108**(3): 221-235.
- Luther, G. W., C. E. Reimers, D. B. Nuzzio and D. Lovalvo (1999). "In Situ Deployment of Voltammetric, Potentiometric, and Amperometric Microelectrodes from a ROV To Determine Dissolved O<sub>2</sub>, Mn, Fe, S(−2), and pH in Porewaters." Environmental Science & Technology **33**(23): 4352-4356.
- Luther, G. W., B. Sundby, B. L. Lewis, P. J. Brendel and N. Silverberg (1997). "Interactions of manganese with the nitrogen cycle: Alternative pathways to dinitrogen." Geochimica et Cosmochimica Acta **61**(19): 4043-4052.
- MacDonald, N., J. Stark and B. Austin (1986). "Bacterial microflora in the gastro-intestinal tract of Dover sole (*Solea solea* L.), with emphasis on the possible role of bacteria in the nutrition of the host." FEMS Microbiology Letters **35**(1): 107-111.
- Madison, A. S., B. M. Tebo and G. W. Luther (2011). "Simultaneous determination of soluble manganese(III), manganese(II) and total manganese in natural (pore)waters." Talanta **84**(2): 374-381.
- Marcelino, V. R., M. Wille, A. C. Hurt, D. González-Acuña, M. Klaassen, J.-S. Eden, M. Shi, J. R. Iredell, T. C. Sorrell and E. C. Holmes (2018). "High levels of antibiotic resistance gene expression among birds living in a wastewater treatment plant." BioRxiv: 462366.
- Marchesi, J. R. (2011). "Human distal gut microbiome." Environmental microbiology **13**(12): 3088-3102.
- Marshall, W. S. and D. Bellamy (2010). "The 50 year evolution of in vitro systems to reveal salt transport functions of teleost fish gills." Comparative Biochemistry and Physiology Part A: Molecular & Integrative Physiology **155**(3): 275-280.
- Martiny, J. B. H., B. J. Bohannan, J. H. Brown, R. K. Colwell, J. A. Fuhrman, J. L. Green, M. C. Horner-Devine, M. Kane, J. A. Krumins and C. R. Kuske (2006). "Microbial biogeography: putting microorganisms on the map." Nature Reviews Microbiology **4**(2): 102-112.
- Marzinelli, E. M., A. H. Campbell, E. Zozaya Valdes, A. Vergés, S. Nielsen, T. Wernberg, T. De Bettignies, S. Bennett, J. G. Caporaso and T. Thomas (2015). "Continental-scale variation in seaweed host-associated bacterial communities is a function of host condition, not geography." Environmental microbiology **17**(10): 4078-4088.
- McGill, B. J., R. S. Etienne, J. S. Gray, D. Alonso, M. J. Anderson, H. K. Benecha, M. Dornelas, B. J. Enquist, J. L. Green and F. He (2007). "Species abundance distributions: moving beyond single prediction theories to integration within an ecological framework." Ecology letters **10**(10): 995-1015.
- McGlynn, S. E. (2017). "Energy metabolism during anaerobic methane oxidation in ANME archaea." Microbes and environments: ME16166.
- McIlroy, S. J., R. H. Kirkegaard, M. S. Dueholm, E. Fernando, S. M. Karst, M. Albertsen and P. H. Nielsen (2017). "Culture-independent analyses reveal novel anaerolineaceae as

- abundant primary fermenters in anaerobic digesters treating waste activated sludge." Frontiers in microbiology **8**: 1134.
- McKee, B. A., R. C. Aller, M. A. Allison, T. S. Bianchi and G. C. Kineke (2004). "Transport and transformation of dissolved and particulate materials on continental margins influenced by major rivers: benthic boundary layer and seabed processes." Continental Shelf Research **24**(7): 899-926.
- McKenney, E. A., K. Koelle, R. R. Dunn and A. D. Yoder (2018). "The ecosystem services of animal microbiomes." Molecular Ecology **27**(8): 2164-2172.
- McKenzie, V. J., S. J. Song, F. Delsuc, T. L. Prest, A. M. Oliverio, T. M. Korpita, A. Alexiev, K. R. Amato, J. L. Metcalf and M. Kowalewski (2017). "The effects of captivity on the mammalian gut microbiome." Integrative and comparative biology **57**(4): 690-704.
- Meisel, J. S., G. Sfyroera, C. Bartow-McKenney, C. Gimblet, J. Bugayev, J. Horwinski, B. Kim, J. R. Brestoff, A. S. Tyldsley, Q. Zheng, B. P. Hodkinson, D. Artis and E. A. Grice (2018). "Commensal microbiota modulate gene expression in the skin." Microbiome **6**(1): 20.
- Menke, S., J. Melzheimer, S. Thalwitzer, S. Heinrich, B. Wachter and S. Sommer (2017). "Gut microbiomes of free-ranging and captive Namibian cheetahs: Diversity, putative functions and occurrence of potential pathogens." Molecular ecology **26**(20): 5515-5527.
- Meron, D., E. Atias, L. I. Kruh, H. Elifantz, D. Minz, M. Fine and E. Banin (2011). "The impact of reduced pH on the microbial community of the coral *Acropora eurystroma*." The ISME journal **5**(1): 51-60.
- Metcalf, J. L., S. J. Song, J. T. Morton, S. Weiss, A. Seguin-Orlando, F. Joly, C. Feh, P. Taberlet, E. Coissac and A. Amir (2017). "Evaluating the impact of domestication and captivity on the horse gut microbiome." Scientific reports **7**(1): 1-9.
- Mihaylova, E. R. M. S. A. and M. Gomila (2014). "7 The Family Cardiobacteriaceae."
- Moberg, F. and C. Folke (1999). "Ecological goods and services of coral reef ecosystems." Ecological economics **29**(2): 215-233.
- Montoya, L., I. Lozada-Chávez, R. Amils, N. Rodriguez and I. Marín (2011). "The sulfate-rich and extreme saline sediment of the ephemeral tirez lagoon: a biotope for acetoclastic sulfate-reducing bacteria and hydrogenotrophic methanogenic archaea." International journal of microbiology **2011**.
- Mori, K., K.-i. Suzuki, T. Urabe, M. Sugihara, K. Tanaka, M. Hamada and S. Hanada (2011). "Thiopfundum hispidum sp. nov., an obligately chemolithoautotrophic sulfur-oxidizing gammaproteobacterium isolated from the hydrothermal field on Suiyo Seamount, and proposal of Thioalkalspiraceae fam. nov. in the order Chromatiales." International journal of systematic and evolutionary microbiology **61**(10): 2412-2418.
- Morrow, K. M., D. G. Bourne, C. Humphrey, E. S. Botté, P. Laffy, J. Zaneveld, S. Uthicke, K. E. Fabricius and N. S. Webster (2015). "Natural volcanic CO<sub>2</sub> seeps reveal future trajectories for host-microbial associations in corals and sponges." The ISME journal **9**(4): 894-908.
- Morrow, K. M., A. G. Moss, N. E. Chadwick and M. R. Liles (2012). "Bacterial associates of two Caribbean coral species reveal species-specific distribution and geographic variability." Appl. Environ. Microbiol. **78**(18): 6438-6449.
- Mouchka, M. E., I. Hewson and C. D. Harvell (2010). "Coral-associated bacterial assemblages: current knowledge and the potential for climate-driven impacts." Integrative and comparative biology **50**(4): 662-674.

- Muegge, B. D., J. Kuczynski, D. Knights, J. C. Clemente, A. González, L. Fontana, B. Henrissat, R. Knight and J. I. Gordon (2011). "Diet Drives Convergence in Gut Microbiome Functions Across Mammalian Phylogeny and Within Humans." Science **332**(6032): 970.
- Murphy, D. and F. Oshin (2015). "Reptile-associated salmonellosis in children aged under 5 years in South West England." Archives of disease in childhood **100**(4): 364-365.
- Murphy, J. and J. P. Riley (1962). "A modified single solution method for the determination of phosphate in natural waters." Analytica Chimica Acta **27**: 31-36.
- Murtaza, N., L. M. Burke, N. Vlahovich, B. Charlessen, H. M. O'Neill, M. L. Ross, K. L. Campbell, L. Krause and M. Morrison (2019). "Analysis of the Effects of Dietary Pattern on the Oral Microbiome of Elite Endurance Athletes." Nutrients **11**(3).
- Myers, R. A., J. K. Baum, T. D. Shepherd, S. P. Powers and C. H. Peterson (2007). "Cascading effects of the loss of apex predatory sharks from a coastal ocean." Science **315**(5820): 1846-1850.
- Myles, I. A., N. J. Earland, E. D. Anderson, I. N. Moore, M. D. Kieh, K. W. Williams, A. Saleem, N. M. Fontecilla, P. A. Welch and D. A. Darnell (2018). "First-in-human topical microbiome transplantation with *Roseomonas mucosa* for atopic dermatitis." JCI insight **3**(9).
- Mylniczenko, N. D., B. Harris, R. E. Wilborn and F. A. Young (2007). "Blood Culture Results from Healthy Captive and Free-Ranging Elasmobranchs." Journal of Aquatic Animal Health **19**(3): 159-167.
- Nelson, C. E., S. J. Goldberg, L. W. Kelly, A. F. Haas, J. E. Smith, F. Rohwer and C. A. Carlson (2013). "Coral and macroalgal exudates vary in neutral sugar composition and differentially enrich reef bacterioplankton lineages." The ISME journal **7**(5): 962-979.
- Nemergut, D. R., S. K. Schmidt, T. Fukami, S. P. O'Neill, T. M. Bilinski, L. F. Stanish, J. E. Knelman, J. L. Darcy, R. C. Lynch and P. Wickey (2013). "Patterns and processes of microbial community assembly." Microbiol. Mol. Biol. Rev. **77**(3): 342-356.
- Nichols, D., N. Cahoon, E. Trakhtenberg, L. Pham, A. Mehta, A. Belanger, T. Kanigan, K. Lewis and S. Epstein (2010). "Use of ichip for high-throughput in situ cultivation of "uncultivable" microbial species." Applied and environmental microbiology **76**(8): 2445-2450.
- Ochman, H., J. G. Lawrence and E. A. Groisman (2000). "Lateral gene transfer and the nature of bacterial innovation." nature **405**(6784): 299.
- Orcutt, R., F. Gianni and R. Judge (1987). "Development of an "Altered Schaedler Flora" for NCI gnotobiotic rodents." Microecol Ther **17**: 59.
- Ormerod, K. L., D. L. Wood, N. Lachner, S. L. Gellatly, J. N. Daly, J. D. Parsons, C. G. Dal'Molin, R. W. Palfreyman, L. K. Nielsen and M. A. Cooper (2016). "Genomic characterization of the uncultured Bacteroidales family S24-7 inhabiting the guts of homeothermic animals." Microbiome **4**(1): 36.
- Orsi, W. D., A. Vuillemin, P. Rodriguez, Ö. K. Coskun, G. V. Gomez-Saez, G. Lavik, V. Morholz and T. G. Ferdelman (2019). "Metabolic activity analyses demonstrate that *Lokiarchaeon* exhibits homoacetogenesis in sulfidic marine sediments." Nature Microbiology: 1-8.
- Overholt, W. A., P. Schwing, K. M. Raz, D. Hastings, D. J. Hollander and J. E. Kostka (2019). "The core seafloor microbiome in the Gulf of Mexico is remarkably consistent and shows evidence of recovery from disturbance caused by major oil spills." Environmental microbiology **21**(11): 4316-4329.



- Pace, A., L. Dipineto, A. Fioretti and S. Hochscheid (2019). "Loggerhead sea turtles as sentinels in the western Mediterranean: antibiotic resistance and environment-related modifications of Gram-negative bacteria." Marine pollution bulletin **149**: 110575.
- Paleczny, M., E. Hammill, V. Karpouzi and D. Pauly (2015). "Population trend of the world's monitored seabirds, 1950-2010." PloS one **10**(6): e0129342.
- Pandolfi, J. M., S. R. Connolly, D. J. Marshall and A. L. Cohen (2011). "The Future of Coral Reefs Response." Science **334**(6062): 1495-1496.
- Parker, R. and M. Snyder (1961). "Interactions of the Oral Microbiota I. A System for the Defined Study of Mixed Cultures." Proceedings of the Society for Experimental Biology and Medicine **108**(3): 749-752.
- Pascoe, E. L., H. C. Hauffe, J. R. Marchesi and S. E. Perkins (2017). "Network analysis of gut microbiota literature: an overview of the research landscape in non-human animal studies." The ISME journal **11**(12): 2644-2651.
- Patin, N. V., Z. A. Pratte, M. Regensburger, E. Hall, K. Gilde, A. D. Dove and F. J. Stewart (2018). "Microbiome dynamics in a large artificial seawater aquarium." Applied and environmental microbiology **84**(10).
- Pearce, D. S., B. A. Hoover, S. Jennings, G. A. Nevitt and K. M. Docherty (2017). "Morphological and genetic factors shape the microbiome of a seabird species (*Oceanodroma leucorhoa*) more than environmental and social factors." Microbiome **5**(1): 1-16.
- Peatman, E., M. Lange, H. Zhao and B. H. Beck (2015). "Physiology and immunology of mucosal barriers in catfish (*Ictalurus spp.*)." Tissue barriers **3**(4): e1068907.
- Pedersen, K., I. Dalsgaard and J. L. Larsen (1997). "Vibrio damsela associated with diseased fish in Denmark." Applied and environmental microbiology **63**(9): 3711-3715.
- Pei, A. Y., W. E. Oberdorf, C. W. Nossa, A. Agarwal, P. Chokshi, E. A. Gerz, Z. Jin, P. Lee, L. Yang, M. Poles, S. M. Brown, S. Sotero, T. DeSantis, E. Brodie, K. Nelson and Z. Pei (2010). "Diversity of 16S rRNA Genes within Individual Prokaryotic Genomes." Applied and Environmental Microbiology **76**(12): 3886-3897.
- Philip, N., B. Suneja and L. Walsh (2018). "Beyond Streptococcus mutans: clinical implications of the evolving dental caries aetiological paradigms and its associated microbiome." British dental journal **224**(4): 219-225.
- Philippot, L., S. G. Andersson, T. J. Battin, J. I. Prosser, J. P. Schimel, W. B. Whitman and S. Hallin (2010). "The ecological coherence of high bacterial taxonomic ranks." Nature Reviews Microbiology **8**(7): 523-529.
- Picazo, A., C. Rochera, J. A. Villaescusa, J. Miralles-Lorenzo, D. Velázquez, A. Quesada and A. Camacho (2019). "Bacterioplankton Community Composition Along Environmental Gradients in Lakes From Byers Peninsula (Maritime Antarctica) as Determined by Next-Generation Sequencing." Frontiers in Microbiology **10**(908).
- Pitkänen, T. and M.-L. Hänninen (2017). "Members of the family Campylobacteraceae: Campylobacter jejuni, Campylobacter coli." Global Water Pathogens Project. <http://www.waterpathogens.org> Part 3 Specific excreted pathogens: environmental and epidemiology aspects <http://www.waterpathogens.org/book/campylobacter>.
- Possemiers, S., K. Verthé, S. Uyttendaele and W. Verstraete (2004). "PCR-DGGE-based quantification of stability of the microbial community in a simulator of the human intestinal microbial ecosystem." FEMS Microbiology Ecology **49**(3): 495-507.
- Potter, S. L. (2013). Antimicrobial Resistance in Orcinus orca Scat: Using Marine Sentinels as Indicators of Pharmaceutical Pollution in the Salish Sea, Evergreen State College.

- Power, M. L., S. Emery and M. R. Gillings (2013). "Into the wild: dissemination of antibiotic resistance determinants via a species recovery program." *PLoS One* **8**(5).
- Pratte, Z. A., G. O. Longo, A. S. Burns, M. E. Hay and F. J. Stewart (2018). "Contact with turf algae alters the coral microbiome: contact versus systemic impacts." *Coral Reefs* **37**(1): 1-13.
- Pratte, Z. A., N. V. Patin, M. E. McWhirt, A. M. Caughman, D. J. Parris and F. J. Stewart (2018). "Association with a sea anemone alters the skin microbiome of clownfish." *Coral Reefs* **37**(4): 1119-1125.
- Price, M. N., P. S. Dehal and A. P. Arkin (2010). "FastTree 2—approximately maximum-likelihood trees for large alignments." *PloS one* **5**(3): e9490.
- Pyro, V. S., L. F. W. Roesch, J. M. Ortega, A. M. do Amaral, M. R. Tótola, P. R. Hirsch, A. S. Rosado, A. Góes-Neto, A. L. d. C. da Silva and C. A. Rosa (2014). "Brazilian microbiome project: revealing the unexplored microbial diversity—challenges and prospects." *Microbial ecology* **67**(2): 237-241.
- Pyzik, A. J. and S. E. Sommer (1981). "Sedimentary iron monosulfides: Kinetics and mechanism of formation." *Geochimica et Cosmochimica Acta* **45**(5): 687-698.
- Qin, J., R. Li, J. Raes, M. Arumugam, K. S. Burgdorf, C. Manichanh, T. Nielsen, N. Pons, F. Levenez and T. Yamada (2010). "A human gut microbial gene catalogue established by metagenomic sequencing." *nature* **464**(7285): 59-65.
- Qiu, Z., M. A. Coleman, E. Provost, A. H. Campbell, B. P. Kelaher, S. J. Dalton, T. Thomas, P. D. Steinberg and E. M. Marzinelli (2019). "Future climate change is predicted to affect the microbiome and condition of habitat-forming kelp." *Proceedings of the Royal Society B* **286**(1896): 20181887.
- Rabalais, N. N., R. J. Díaz, L. A. Levin, R. E. Turner, D. Gilbert and J. Zhang (2010). "Dynamics and distribution of natural and human-caused hypoxia." *Biogeosciences* **7**(2): 585-619.
- Rabalais, N. N. and R. E. Turner (2015). Press release. *Bottom water dissolved oxygen-2015*.
- Rabalais, N. N. and R. E. Turner (2017). Summary of 2017 Research Cruise Press release.
- Rabalais, N. N., R. E. Turner, B. K. Sen Gupta, D. F. Boesch, P. Chapman and M. C. Murrell (2007). "Hypoxia in the northern Gulf of Mexico: Does the science support the Plan to Reduce, Mitigate, and Control Hypoxia?" *Estuaries and Coasts* **30**(5): 753-772.
- Radziwill-Bienkowska, J. M., P. Talbot, J. B. Kamphuis, V. Robert, C. Cartier, I. Fourquaux, E. Lentzen, J.-N. Audinot, F. Jamme and M. Réfrégiers (2018). "Toxicity of food-grade TiO<sub>2</sub> to commensal intestinal and transient food-borne bacteria: new insights using nano-SIMS and synchrotron UV fluorescence imaging." *Frontiers in microbiology* **9**: 794.
- Rahbek, C. (1993). "Captive breeding—a useful tool in the preservation of biodiversity?" *Biodiversity & Conservation* **2**(4): 426-437.
- Rainey, P. B. and M. Travisano (1998). "Adaptive radiation in a heterogeneous environment." *Nature* **394**(6688): 69-72.
- Ramsey, M. M., M. O. Freire, R. A. Gabriliska, K. P. Rumbaugh and K. P. Lemon (2016). "Staphylococcus aureus shifts toward commensalism in response to Corynebacterium species." *Frontiers in microbiology* **7**: 1230.
- Rastogi, G., A. Sbodio, J. J. Tech, T. V. Suslow, G. L. Coaker and J. H. Leveau (2012). "Leaf microbiota in an agroecosystem: spatiotemporal variation in bacterial community composition on field-grown lettuce." *The ISME journal* **6**(10): 1812-1822.
- Raymann, K., A. H. Moeller, A. L. Goodman and H. Ochman (2017). "Unexplored Archaeal Diversity in the Great Ape Gut Microbiome." *mSphere* **2**(1): e00026-00017.

- Reddy, M., L. Dierauf and F. Gulland (2001). "Marine mammals as sentinels of ocean health." Marine mammal medicine: 3-13.
- Redford, K. H., J. A. Segre, N. Salafsky, C. M. del Rio and D. McAloose (2012). "Conservation and the microbiome." Conservation Biology **26**(2): 195-197.
- Reese, B. K., H. J. Mills, S. E. Dowd and J. W. Morse (2013). "Linking molecular microbial ecology to geochemistry in a coastal hypoxic zone." Geomicrobiology Journal **30**(2): 160-172.
- Reese, B. K., A. D. Witmer, S. Moller, J. W. Morse and H. J. Mills (2014). "Molecular assays advance understanding of sulfate reduction despite cryptic cycles." Biogeochemistry **118**(1-3): 307-319.
- Rhodes, A., J. Urbance, H. Youga, H. Corlew-Newman, C. Reddy, M. Klug, J. Tiedje and D. Fisher (1998). "Identification of bacterial isolates obtained from intestinal contents associated with 12,000-year-old mastodon remains." Applied and environmental microbiology **64**(2): 651-658.
- Roggenbuck, M., I. B. Schnell, N. Blom, J. Bælum, M. F. Bertelsen, T. Sicheritz-Pontén, S. J. Sørensen, M. T. P. Gilbert, G. R. Graves and L. H. Hansen (2014). "The microbiome of New World vultures." Nature Communications **5**(1): 1-8.
- Rohwer, F., V. Seguritan, F. Azam and N. Knowlton (2002). "Diversity and distribution of coral-associated bacteria." Marine Ecology Progress Series **243**: 1-10.
- Rosenberg, E., O. Koren, L. Reshef, R. Efrony and I. Zilber-Rosenberg (2007). "The role of microorganisms in coral health, disease and evolution." Nature Reviews Microbiology **5**(5): 355-362.
- Ruiz-Rodríguez, M., M. Scheifler, S. Sanchez-Brosseau, E. Magnanou, N. West, M. Suzuki, S. Duperron and Y. Desdevises (2020). "Host species and body site explain the variation in the microbiota associated to wild sympatric Mediterranean teleost fishes." Microbial Ecology: 1-11.
- Ruiz-Rodríguez, M., M. Scheifler, S. Sanchez-Brosseau, E. Magnanou, N. West, M. Suzuki, S. Duperron and Y. Desdevises (2020). "Host Species and Body Site Explain the Variation in the Microbiota Associated to Wild Sympatric Mediterranean Teleost Fishes." Microbial Ecology **80**(1): 212-222.
- Sakurai, H., T. Ogawa, M. Shiga and K. Inoue (2010). "Inorganic sulfur oxidizing system in green sulfur bacteria." Photosynthesis research **104**(2-3): 163-176.
- Sandri, C., F. Correa, C. Spiezio, P. Trevisi, D. Luise, M. Modesto, S. Remy, M.-M. Muzungaile, A. Checcucci and C. A. Zaborra (2020). "Fecal Microbiota Characterization of Seychelles Giant Tortoises (*Aldabrachelys gigantea*) Living in Both Wild and Controlled Environments." Frontiers in microbiology **11**: 2474.
- Sayer, E. J., M. S. Heard, H. K. Grant, T. R. Marthews and E. V. Tanner (2011). "Soil carbon release enhanced by increased tropical forest litterfall." Nature Climate Change **1**(6): 304-307.
- Schippers, A., L. N. Neretin, J. Kallmeyer, T. G. Ferdelman, B. A. Cragg, R. J. Parkes and B. B. Jørgensen (2005). "Prokaryotic cells of the deep sub-seafloor biosphere identified as living bacteria." Nature **433**(7028): 861-864.
- Schmeisser, C., H. Steele and W. R. Streit (2007). "Metagenomics, biotechnology with non-culturable microbes." Applied Microbiology and Biotechnology **75**(5): 955-962.
- Schofield, B. J., N. Lachner, O. T. Le, D. M. McNeill, P. Dart, D. Ouwerkerk, P. Hugenholtz and A. V. Klieve (2018). "Beneficial changes in rumen bacterial community profile in sheep

- and dairy calves as a result of feeding the probiotic *Bacillus amyloliquefaciens* H57." Journal of applied microbiology **124**(3): 855-866.
- Sebens, K. P. (1994). "Biodiversity of coral reefs: what are we losing and why?" American zoologist **34**(1): 115-133.
- Seekatz, A. M., J. Aas, C. E. Gessert, T. A. Rubin, D. M. Saman, J. S. Bakken and V. B. Young (2014). "Recovery of the gut microbiome following fecal microbiota transplantation." MBio **5**(3).
- Serino, M., E. Luche, S. Gres, A. Baylac, M. Bergé, C. Cenac, A. Waget, P. Klopp, J. Iacovoni and C. Klopp (2012). "Metabolic adaptation to a high-fat diet is associated with a change in the gut microbiota." Gut **61**(4): 543-553.
- Serrano-Flores, F., J. Pérez-Jiménez, I. Méndez-Loeza, K. Bassos-Hull and M. Ajemian (2019). "Comparison between the feeding habits of spotted eagle ray (*Aetobatus narinari*) and their potential prey in the southern Gulf of Mexico." Journal of the Marine Biological Association of the United Kingdom **99**(3): 661-672.
- Sguotti, C., C. P. Lynam, B. García-Carreras, J. R. Ellis and G. H. Engelhard (2016). "Distribution of skates and sharks in the North Sea: 112 years of change." Global change biology **22**(8): 2729-2743.
- Shafquat, A., R. Joice, S. L. Simmons and C. Huttenhower (2014). "Functional and phylogenetic assembly of microbial communities in the human microbiome." Trends in Microbiology **22**(5): 261-266.
- Shao, M. and Y. Zhu (2020). "Long-term metal exposure changes gut microbiota of residents surrounding a mining and smelting area." Scientific reports **10**(1): 1-9.
- Shapiro, B. J., J. Friedman, O. X. Cordero, S. P. Preheim, S. C. Timberlake, G. Szabó, M. F. Polz and E. J. Alm (2012). "Population genomics of early events in the ecological differentiation of bacteria." science **336**(6077): 48-51.
- Sharon, G., D. Segal, J. M. Ringo, A. Hefetz, I. Zilber-Rosenberg and E. Rosenberg (2010). "Commensal bacteria play a role in mating preference of *Drosophila melanogaster*." Proceedings of the National Academy of Sciences **107**(46): 20051-20056.
- Shepherd, T. D. and R. A. Myers (2005). "Direct and indirect fishery effects on small coastal elasmobranchs in the northern Gulf of Mexico." Ecology Letters **8**(10): 1095-1104.
- Shui, L., X. Yang, J. Li, C. Yi, Q. Sun and H. Zhu (2019). "Gut microbiome as a potential factor for modulating resistance to cancer immunotherapy." Frontiers in Immunology **10**.
- Signat, B., C. Roques, P. Poulet and D. Duffaut (2011). "Role of *Fusobacterium nucleatum* in periodontal health and disease." Curr Issues Mol Biol **13**(2): 25-36.
- Sinha, R., C. C. Abnet, O. White, R. Knight and C. Huttenhower (2015). "The microbiome quality control project: baseline study design and future directions." Genome Biology **16**(1): 276.
- Sinigalliano, C. D., J. S. Ervin, L. C. Van De Werfhorst, B. D. Badgley, E. Ballesté, J. Bartkowiak, A. B. Boehm, M. Byappanahalli, K. D. Goodwin, M. Gourmelon, J. Griffith, P. A. Holden, J. Jay, B. Layton, C. Lee, J. Lee, W. G. Meijer, R. Noble, M. Raith, H. Ryu, M. J. Sadowsky, A. Schriewer, D. Wang, D. Wanless, R. Whitman, S. Wuertz and J. W. Santo Domingo (2013). "Multi-laboratory evaluations of the performance of *Catellibacoccus marimammalius* PCR assays developed to target gull fecal sources." Water Research **47**(18): 6883-6896.
- Smillie, C. S., M. B. Smith, J. Friedman, O. X. Cordero, L. A. David and E. J. Alm (2011). "Ecology drives a global network of gene exchange connecting the human microbiome." Nature **480**(7376): 241-244.

- Snelgrove, P., T. H. Blackburn, P. A. Hutchings, D. M. Alongi, J. F. Grassle, H. Hummel, G. King, I. Koike, P. J. D. Lamshead, N. B. Ramsing and V. Solis-Weiss (1997). "The importance of marine sediment biodiversity in ecosystem processes." Ambio **26**(8): 578-583.
- Sogin, M. L., H. G. Morrison, J. A. Huber, D. M. Welch, S. M. Huse, P. R. Neal, J. M. Arrieta and G. J. Herndl (2006). "Microbial diversity in the deep sea and the underexplored "rare biosphere"." Proceedings of the National Academy of Sciences **103**(32): 12115.
- Song, C., B. Wang, J. Tan, L. Zhu, D. Lou and X. Cen (2017). "Comparative analysis of the gut microbiota of black bears in China using high-throughput sequencing." Molecular genetics and genomics **292**(2): 407-414.
- Spor, A., O. Koren and R. Ley (2011). "Unravelling the effects of the environment and host genotype on the gut microbiome." Nature Reviews Microbiology **9**(4): 279-290.
- Stahl, D. (1991). "Nucleic acid techniques in bacterial systematics." Development and application of nucleic acid probes: 205-248.
- Stanley, D., R. J. Hughes, M. S. Geier and R. J. Moore (2016). "Bacteria within the gastrointestinal tract microbiota correlated with improved growth and feed conversion: challenges presented for the identification of performance enhancing probiotic bacteria." Frontiers in microbiology **7**: 187.
- Steffan, S. A., Y. Chikaraishi, C. R. Currie, H. Horn, H. R. Gaines-Day, J. N. Pauli, J. E. Zalapa and N. Ohkouchi (2015). "Microbes are trophic analogs of animals." Proceedings of the National Academy of Sciences **112**(49): 15119-15124.
- Stegen, J. C., X. Lin, J. K. Fredrickson, X. Chen, D. W. Kennedy, C. J. Murray, M. L. Rockhold and A. Konopka (2013). "Quantifying community assembly processes and identifying features that impose them." The ISME journal **7**(11): 2069-2079.
- Sternbach, H. and R. State (1997). "Antibiotics: neuropsychiatric effects and psychotropic interactions." Harvard review of psychiatry **5**(4): 214-226.
- Stevens, J., R. Bonfil, N. Dulvy and P. Walker (2000). "The effects of fishing on sharks, rays, and chimaeras (chondrichthyans), and the implications for marine ecosystems." ICES Journal of Marine Science **57**(3): 476-494.
- Stewart, J. S. (1990). "Anaerobic bacterial infections in reptiles." Journal of Zoo and Wildlife Medicine: 180-184.
- Stookey, L. L. (1970). "Ferrozine- A New Spectrophotometric Reagent for Iron." Analytical Chemistry **42**(7): 779-781.
- Strickland, J. D. H. and T. R. Parsons (1972). A practical handbook of sea-water analysis.
- Stumpf, R. M., A. Gomez, K. R. Amato, C. J. Yeoman, J. Polk, B. A. Wilson, K. E. Nelson, B. White and S. R. Leigh (2016). "Microbiomes, metagenomics, and primate conservation: New strategies, tools, and applications." Biological Conservation **199**: 56-66.
- Sturt, H. F., R. E. Summons, K. Smith, M. Elvert and K. U. Hinrichs (2004). "Intact polar membrane lipids in prokaryotes and sediments deciphered by high-performance liquid chromatography/electrospray ionization multistage mass spectrometry—new biomarkers for biogeochemistry and microbial ecology." Rapid Communications in Mass Spectrometry **18**(6): 617-628.
- Sunagawa, S., C. M. Woodley and M. Medina (2010). "Threatened corals provide underexplored microbial habitats." PloS one **5**(3).
- Sung, H., H. S. Kim, J.-Y. Lee, W. Kang, P. S. Kim, D.-W. Hyun, E. J. Tak, M.-J. Jung, J.-H. Yun and M.-S. Kim (2018). "Oceanisphaera avium sp. nov., isolated from the gut of the

- cinereous vulture, *Aegypius monachus*." International journal of systematic and evolutionary microbiology **68**(6): 2068-2073.
- Swan, B. K., M. Martinez-Garcia, C. M. Preston, A. Sczyrba, T. Woyke, D. Lamy, T. Reinthaler, N. J. Poulton, E. D. P. Masland and M. L. Gomez (2011). "Potential for chemolithoautotrophy among ubiquitous bacteria lineages in the dark ocean." Science **333**(6047): 1296-1300.
- Sylvain, F.-É., B. Cheaib, M. Llewellyn, T. G. Correia, D. B. Fagundes, A. L. Val and N. Derome (2016). "pH drop impacts differentially skin and gut microbiota of the Amazonian fish tambaqui (*Colossoma macropomum*)." Scientific reports **6**(1): 1-10.
- Sylvain, F.-É., A. Holland, S. Bouslama, É. Audet-Gilbert, C. Lavoie, A. L. Val and N. Derome (2020). "Fish skin and gut microbiomes show contrasting signatures of host species and habitat." Applied and Environmental Microbiology.
- Szabó, K. É., P. O. Itor, S. Bertilsson, L. Tranvik and A. Eiler (2007). "Importance of rare and abundant populations for the structure and functional potential of freshwater bacterial communities." Aquatic microbial ecology **47**(1): 1-10.
- Tagliafico, A., N. Rago, S. Rangel and J. Mendoza (2012). "Exploitation and reproduction of the spotted eagle ray (*Aetobatus narinari*) in the Los Frailes Archipelago, Venezuela." Fishery Bulletin **110**(3): 307-316.
- Taillefert, M., J. S. Beckler, C. Cathalot, P. Michalopoulos, R. Corvaisier, N. Kiriazis, J.-C. Caprais, L. Pastor and C. Rabouille (2017). "Early diagenesis in the sediments of the Congo deep-sea fan dominated by massive terrigenous deposits: Part II – Iron–sulfur coupling." Deep Sea Research Part II: Topical Studies in Oceanography **142**: 151-166.
- Taillefert, M., V. C. Hover, T. F. Rozan, S. M. Theberge and G. W. Luther (2002). "The influence of sulfides on soluble organic-Fe(III) in anoxic sediment porewaters." Estuaries **25**(6): 1088-1096.
- Taillefert, M., G. W. Luther and D. B. Nuzzio (2000). "The Application of Electrochemical Tools for In Situ Measurements in Aquatic Systems." Electroanalysis **12**(6): 401-412.
- Takai, K. and K. Horikoshi (2000). "Rapid detection and quantification of members of the archaeal community by quantitative PCR using fluorogenic probes." Appl. Environ. Microbiol. **66**(11): 5066-5072.
- Tarnecki, A. M., N. P. Brennan, R. W. Schloesser and N. R. Rhody (2019). "Shifts in the skin-associated microbiota of hatchery-reared common snook *Centropomus undecimalis* during acclimation to the wild." Microbial ecology **77**(3): 770-781.
- Taylor, M. J., R. W. Mannan, J. M. U'Ren, N. P. Garber, R. E. Gallery and A. E. Arnold (2019). "Age-related variation in the oral microbiome of urban Cooper's hawks (*Accipiter cooperii*)." BMC Microbiology **19**(1): 47.
- Tercier-Waeber, M.-L. and M. Taillefert (2008). "Remote in situ voltammetric techniques to characterize the biogeochemical cycling of trace metals in aquatic systems." Journal of Environmental Monitoring **10**(1): 30-54.
- Terio, K., L. Munson, L. Marker, B. Aldridge and J. V. Solnick (2005). "Comparison of *Helicobacter* spp. in cheetahs (*Acinonyx jubatus*) with and without gastritis." Journal of clinical microbiology **43**(1): 229-234.
- Teske, A. and K. B. Sørensen (2008). "Uncultured archaea in deep marine subsurface sediments: have we caught them all?" The ISME journal **2**(1): 3-18.

- Thomas, C., A. Francke, H. Vogel, B. Wagner and D. Ariztegui (2020). "Weak Influence of Paleoenvironmental Conditions on the Subsurface Biosphere of Lake Ohrid over the Last 515 ka." Microorganisms **8**(11): 1736.
- Thompson, L. R., J. G. Sanders, D. McDonald, A. Amir, J. Ladau, K. J. Locey, R. J. Prill, A. Tripathi, S. M. Gibbons and G. Ackermann (2017). "A communal catalogue reveals Earth's multiscale microbial diversity." Nature **551**(7681): 457-463.
- Thurber, R. V., D. Willner-Hall, B. Rodriguez-Mueller, C. Desnues, R. A. Edwards, F. Angly, E. Dinsdale, L. Kelly and F. Rohwer (2009). "Metagenomic analysis of stressed coral holobionts." Environmental microbiology **11**(8): 2148-2163.
- Torsvik, V. and L. Øvreås (2002). "Microbial diversity and function in soil: from genes to ecosystems." Current Opinion in Microbiology **5**(3): 240-245.
- Trefry, J. H. and B. J. Presley (1982). "Manganese fluxes from Mississippi Delta sediments." Geochimica et Cosmochimica Acta **46**(10): 1715-1726.
- Trent, L., D. Parshley and J. Carlson (1997). "Catch and bycatch in the shark drift gillnet fishery off Georgia and east Florida." Marine Fisheries Review **59**(1): 19-28.
- Trevelline, B. K., S. S. Fontaine, B. K. Hartup and K. D. Kohl (2019). "Conservation biology needs a microbial renaissance: a call for the consideration of host-associated microbiota in wildlife management practices." Proceedings of the Royal Society B: Biological Sciences **286**(1895): 20182448.
- Troussellier, M., A. Escalas, T. Bouvier and D. Mouillot (2017). "Sustaining rare marine microorganisms: macroorganisms as repositories and dispersal agents of microbial diversity." Frontiers in microbiology **8**: 947.
- Tsuchida, S., S. Kakooza, P. P. Mbehang Nguema, E. M. Wampande and K. Ushida (2018). "Characteristics of gorilla-specific *Lactobacillus* isolated from captive and wild gorillas." Microorganisms **6**(3): 86.
- Turnbaugh, P. J., M. Hamady, T. Yatsunenko, B. L. Cantarel, A. Duncan, R. E. Ley, M. L. Sogin, W. J. Jones, B. A. Roe and J. P. Affourtit (2009). "A core gut microbiome in obese and lean twins." nature **457**(7228): 480-484.
- Ulloa, O., D. E. Canfield, E. F. DeLong, R. M. Letelier and F. J. Stewart (2012). "Microbial oceanography of anoxic oxygen minimum zones." Proceedings of the National Academy of Sciences **109**(40): 15996-16003.
- Urban, M. C., M. A. Leibold, P. Amarasekare, L. De Meester, R. Gomulkiewicz, M. E. Hochberg, C. A. Klausmeier, N. Loeuille, C. de Mazancourt, J. Norberg, J. H. Pantel, S. Y. Strauss, M. Vellend and M. J. Wade (2008). "The evolutionary ecology of metacommunities." Trends in Ecology & Evolution **23**(6): 311-317.
- Uren Webster, T. M., D. Rodriguez-Barreto, G. Castaldo, P. Gough, S. Consuegra and C. Garcia de Leaniz (2020). "Environmental plasticity and colonisation history in the Atlantic salmon microbiome: a translocation experiment." Molecular ecology **29**(5): 886-898.
- van de Vossenberg, J., D. Woebken, W. J. Maalcke, H. J. Wessels, B. E. Dutilh, B. Kartal, E. M. Janssen-Megens, G. Roeselers, J. Yan and D. Speth (2013). "The metagenome of the marine anammox bacterium '*Candidatus Scalindua profunda*' illustrates the versatility of this globally important nitrogen cycle bacterium." Environmental microbiology **15**(5): 1275-1289.
- Van Der Heijden, M. G., R. D. Bardgett and N. M. Van Straalen (2008). "The unseen majority: soil microbes as drivers of plant diversity and productivity in terrestrial ecosystems." Ecology letters **11**(3): 296-310.

- van der Kooij, D., H. R. Veenendaal, R. Italiaander, E. J. van der Mark and M. Dignum (2018). "Primary Colonizing *Betaproteobacteriales* Play a Key Role in the Growth of *Legionella pneumophila* in Biofilms on Surfaces Exposed to Drinking Water Treated by Slow Sand Filtration." *Applied and Environmental Microbiology* **84**(24): e01732-01718.
- van Kessel, M. A., D. R. Speth, M. Albertsen, P. H. Nielsen, H. J. O. den Camp, B. Kartal, M. S. Jetten and S. L  cker (2015). "Complete nitrification by a single microorganism." *Nature* **528**(7583): 555-559.
- van Niftrik, L. and M. S. Jetten (2012). "Anaerobic ammonium-oxidizing bacteria: unique microorganisms with exceptional properties." *Microbiol. Mol. Biol. Rev.* **76**(3): 585-596.
- van Oppen, M. J. and L. L. Blackall (2019). "Coral microbiome dynamics, functions and design in a changing world." *Nature Reviews Microbiology* **17**(9): 557-567.
- Vellend, M. (2010). "Conceptual synthesis in community ecology." *The Quarterly review of biology* **85**(2): 183-206.
- Vendl, C., T. M. Nelson, B. Ferrari, T. Thomas and T. Rogers (2020). "Highly abundant core taxa in the blow within and across captive bottlenose dolphins provide evidence for a temporally stable airway microbiota."
- Vendl, C., E. Slavich, B. Wemheuer, T. Nelson, B. Ferrari, T. Thomas and T. Rogers (2020). "Respiratory microbiota of humpback whales may be reduced in diversity and richness the longer they fast." *Scientific reports* **10**(1): 1-13.
- Vitousek, P. M., J. D. Aber, R. W. Howarth, G. E. Likens, P. A. Matson, D. W. Schindler, W. H. Schlesinger and D. G. Tilman (1997). "Human alteration of the global nitrogen cycle: sources and consequences." *Ecological applications* **7**(3): 737-750.
- Wahli, T. and L. Madsen (2018). "Flavobacteria, a never ending threat for fish: a review." *Current Clinical Microbiology Reports* **5**(1): 26-37.
- Waite, D. W. and M. W. Taylor (2014). "Characterizing the avian gut microbiota: membership, driving influences, and potential function." *Frontiers in microbiology* **5**: 223.
- Wallenstein, M. D. and E. K. Hall (2012). "A trait-based framework for predicting when and where microbial adaptation to climate change will affect ecosystem functioning." *Biogeochemistry* **109**(1-3): 35-47.
- Wan, X., R. Ruan, R. W. McLaughlin, Y. Hao, J. Zheng and D. Wang (2016). "Fecal bacterial composition of the endangered Yangtze finless porpoises living under captive and semi-natural conditions." *Current microbiology* **72**(3): 306-314.
- Wang, B. L., A. Ghaderi, H. Zhou, J. Agresti, D. A. Weitz, G. R. Fink and G. Stephanopoulos (2014). "Microfluidic high-throughput culturing of single cells for selection based on extracellular metabolite production or consumption." *Nature biotechnology* **32**(5): 473.
- Wang, J., Y. Gao and F. Zhao (2016). "Phage–bacteria interaction network in human oral microbiome." *Environmental microbiology* **18**(7): 2143-2158.
- Wang, J., S. Meier, J. Soininen, E. O. Casamayor, F. Pan, X. Tang, X. Yang, Y. Zhang, Q. Wu and J. Zhou (2017). "Regional and global elevational patterns of microbial species richness and evenness." *Ecography* **40**(3): 393-402.
- Wang, Q., G. M. Garrity, J. M. Tiedje and J. R. Cole (2007). "Naive Bayesian classifier for rapid assignment of rRNA sequences into the new bacterial taxonomy." *Appl Environ Microbiol* **73**(16): 5261-5267.
- Ward, L. M., D. Johnston and P. M. Shih (2019). "Phanerozoic Radiation of Ammonia Oxidizing Bacteria." *bioRxiv*: 655399.



- Ward, N. L., J. F. Challacombe, P. H. Janssen, B. Henrissat, P. M. Coutinho, M. Wu, G. Xie, D. H. Haft, M. Sait and J. Badger (2009). "Three genomes from the phylum Acidobacteria provide insight into the lifestyles of these microorganisms in soils." Appl. Environ. Microbiol. **75**(7): 2046-2056.
- Wasfi, R., O. A. Abd El-Rahman, M. M. Zafer and H. M. Ashour (2018). "Probiotic *Lactobacillus* sp. inhibit growth, biofilm formation and gene expression of caries-inducing *Streptococcus mutans*." Journal of cellular and molecular medicine **22**(3): 1972-1983.
- Wasmund, K., L. Schreiber, K. G. Lloyd, D. G. Petersen, A. Schramm, R. Stepanauskas, B. B. Jørgensen and L. Adrian (2014). "Genome sequencing of a single cell of the widely distributed marine subsurface Dehalococcoidia, phylum Chloroflexi." The ISME journal **8**(2): 383-397.
- Watanabe, M., H. Kojima and M. Fukui (2015). "Desulfoplanes formicivorans gen. nov., sp. nov., a novel sulfate-reducing bacterium isolated from a blackish meromictic lake, and emended description of the family Desulfomicrobiaceae." International Journal of Systematic and Evolutionary Microbiology **65**(Pt\_6): 1902-1907.
- Weber, M., D. De Beer, C. Lott, L. Polerecky, K. Kohls, R. M. Abed, T. G. Ferdelman and K. E. Fabricius (2012). "Mechanisms of damage to corals exposed to sedimentation." Proceedings of the National Academy of Sciences **109**(24): E1558-E1567.
- Webster, T. M. U., S. Consuegra, M. Hitchings and C. G. de Leaniz (2018). "Interpopulation variation in the Atlantic salmon microbiome reflects environmental and genetic diversity." Applied and Environmental Microbiology **84**(16).
- Wei, C.-L., G. T. Rowe, E. Escobar-Briones, A. Boetius, T. Soltwedel, M. J. Caley, Y. Soliman, F. Huettmann, F. Qu and Z. Yu (2010). "Global patterns and predictions of seafloor biomass using random forests." PloS one **5**(12).
- Weiss, S., Z. Z. Xu, S. Peddada, A. Amir, K. Bittinger, A. Gonzalez, C. Lozupone, J. R. Zaneveld, Y. Vázquez-Baeza, A. Birmingham, E. R. Hyde and R. Knight (2017). "Normalization and microbial differential abundance strategies depend upon data characteristics." Microbiome **5**(1): 27.
- Wells, R. S., H. L. Rhinehart, L. J. Hansen, J. C. Sweeney, F. I. Townsend, R. Stone, D. R. Casper, M. D. Scott, A. A. Hohn and T. K. Rowles (2004). "Bottlenose dolphins as marine ecosystem sentinels: developing a health monitoring system." EcoHealth **1**(3): 246-254.
- Wen, L., R. E. Ley, P. Y. Volchkov, P. B. Stranges, L. Avanesyan, A. C. Stonebraker, C. Hu, F. S. Wong, G. L. Szot and J. A. Bluestone (2008). "Innate immunity and intestinal microbiota in the development of Type 1 diabetes." Nature **455**(7216): 1109-1113.
- West, A. G., D. W. Waite, P. Deines, D. G. Bourne, A. Digby, V. J. McKenzie and M. W. Taylor (2019). "The microbiome in threatened species conservation." Biological conservation **229**: 85-98.
- Whitman, W. B., D. C. Coleman and W. J. Wiebe (1998). "Prokaryotes: the unseen majority." Proceedings of the National Academy of Sciences **95**(12): 6578-6583.
- Wienemann, T., D. Schmitt-Wagner, K. Meuser, G. Segelbacher, B. Schink, A. Brune and P. Berthold (2011). "The bacterial microbiota in the ceca of Capercaillie (*Tetrao urogallus*) differs between wild and captive birds." Systematic and Applied Microbiology **34**(7): 542-551.
- Wilkinson, D. M., S. Koumoutsaris, E. A. Mitchell and I. Bey (2012). "Modelling the effect of size on the aerial dispersal of microorganisms." Journal of biogeography **39**(1): 89-97.

- Williams, T. R. and M. L. Marco (2014). "Phyllosphere microbiota composition and microbial community transplantation on lettuce plants grown indoors." MBio **5**(4).
- Wooldridge, S. A. (2013). "Breakdown of the coral-algae symbiosis: towards formalising a linkage between warm-water bleaching thresholds and the growth rate of the intracellular zooxanthellae." Biogeosciences **10**(3).
- Wu, G. D., J. Chen, C. Hoffmann, K. Bittinger, Y.-Y. Chen, S. A. Keilbaugh, M. Bewtra, D. Knights, W. A. Walters and R. Knight (2011). "Linking long-term dietary patterns with gut microbial enterotypes." Science **334**(6052): 105-108.
- Wu, G. D., C. Compher, E. Z. Chen, S. A. Smith, R. D. Shah, K. Bittinger, C. Chehoud, L. G. Albenberg, L. Nessel and E. Gilroy (2016). "Comparative metabolomics in vegans and omnivores reveal constraints on diet-dependent gut microbiota metabolite production." Gut **65**(1): 63-72.
- Xie, Y., P. Xia, H. Wang, H. Yu, J. P. Giesy, Y. Zhang, M. A. Mora and X. Zhang (2016). "Effects of captivity and artificial breeding on microbiota in feces of the red-crowned crane (*Grus japonensis*)." Scientific reports **6**: 33350.
- Xu, A. O. X.-W. (2014). "11 The Family Hyphomicrobiaceae."
- Xu, Z., X.-Y. Zhang, H.-N. Su, Z.-C. Yu, C. Liu, H. Li, X.-L. Chen, X.-Y. Song, B.-B. Xie and Q.-L. Qin (2014). "Oceanisphaera profunda sp. nov., a marine bacterium isolated from deep-sea sediment, and emended description of the genus Oceanisphaera." International journal of systematic and evolutionary microbiology **64**(4): 1252-1256.
- Yadav, S., J.-S. Kim and S.-S. Lee (2020). "Alkanindiges hydrocarbonoclasticus sp. nov. Isolated From Crude Oil Contaminated Sands and Emended Description of the Genus Alkanindiges." Current Microbiology: 1-5.
- Yakimova, E., A. Kapustin, D. Smirnov, V. Savinov, A. Laishevtcev and S. Plygun (2019). "THE PARTICIPATION OF WILD MIGRATORY BIRDS IN THE SPREAD OF RIEMERELLOSIS AND THE MICROBIAL BIOGENESIS OF THE WILD DUCKS." Russian Journal of Agricultural and Socio-Economic Sciences **93**(9).
- Ylitalo, G. M., J. E. Stein, T. Hom, L. L. Johnson, K. L. Tilbury, A. J. Hall, T. Rowles, D. Greig, L. J. Lowenstine and F. M. Gulland (2005). "The role of organochlorines in cancer-associated mortality in California sea lions (*Zalophus californianus*)." Marine Pollution Bulletin **50**(1): 30-39.
- Youngblut, N. D., G. H. Reischer, W. Walters, N. Schuster, C. Walzer, G. Stalder, R. E. Ley and A. H. Farnleitner (2019). "Host diet and evolutionary history explain different aspects of gut microbiome diversity among vertebrate clades." Nature communications **10**(1): 1-15.
- Zaneveld, J. R., R. McMinds and R. Vega Thurber (2017). "Stress and stability: applying the Anna Karenina principle to animal microbiomes." Nature Microbiology **2**(9): 17121.
- Zhang, C., M. Derrien, F. Levenez, R. Brazeilles, S. A. Ballal, J. Kim, M.-C. Degivry, G. Quéré, P. Garault and J. E. van Hylckama Vlieg (2016). "Ecological robustness of the gut microbiota in response to ingestion of transient food-borne microbes." The ISME journal **10**(9): 2235-2245.
- Zhang, M., H. Chen, L. Liu, L. Xu, X. Wang, L. Chang, Q. Chang, G. Lu, J. Jiang and L. Zhu (2020). "The changes in the frog gut microbiome and its putative oxygen-related phenotypes accompanying the development of gastrointestinal complexity and dietary shift." Frontiers in Microbiology **11**: 162.
- Zhou, Y., H. Gao, K. A. Mihindukulasuriya, P. S. La Rosa, K. M. Wylie, T. Vishnivetskaya, M. Podar, B. Warner, P. I. Tarr, D. E. Nelson, J. D. Fortenberry, M. J. Holland, S. E. Burr, W.

- D. Shannon, E. Sodergren and G. M. Weinstock (2013). "Biogeography of the ecosystems of the healthy human body." Genome Biology **14**(1): R1.
- Zhou, Z., J. Pan, F. Wang, J.-D. Gu and M. Li (2018). "Bathyarchaeota: globally distributed metabolic generalists in anoxic environments." FEMS Microbiology Reviews **42**(5): 639-655.
- Zinger, L., L. A. Amaral-Zettler, J. A. Fuhrman, M. C. Horner-Devine, S. M. Huse, D. B. M. Welch, J. B. Martiny, M. Sogin, A. Boetius and A. Ramette (2011). "Global patterns of bacterial beta-diversity in seafloor and seawater ecosystems." PloS one **6**(9).